



Characterization of the MT1-MMP/invadopodia axis during breast cancer cells invasion in type I collagen

Robin Ferrari

► To cite this version:

Robin Ferrari. Characterization of the MT1-MMP/invadopodia axis during breast cancer cells invasion in type I collagen. Cellular Biology. Sorbonne Université, 2019. English. NNT : 2019SORUS098 . tel-03141340

HAL Id: tel-03141340

<https://theses.hal.science/tel-03141340>

Submitted on 15 Feb 2021

HAL is a multi-disciplinary open access archive for the deposit and dissemination of scientific research documents, whether they are published or not. The documents may come from teaching and research institutions in France or abroad, or from public or private research centers.

L'archive ouverte pluridisciplinaire **HAL**, est destinée au dépôt et à la diffusion de documents scientifiques de niveau recherche, publiés ou non, émanant des établissements d'enseignement et de recherche français ou étrangers, des laboratoires publics ou privés.

Sorbonne Université

Ecole doctorale Complexité du Vivant (ED 515)

*Laboratoire : UMR 144 Biologie cellulaire et cancer / Equipe : Dynamique de la membrane
et du cytosquelette*

Characterization of the MT1-MMP/invadopodia axis during breast cancer cells invasion in type I collagen

Par Robin Ferrari

Thèse de doctorat de Biologie cellulaire

Dirigée par Philippe Chavrier

Présentée et soutenue publiquement le 26 Juin 2019

Devant un jury composé de :

Corinne Albigès-Rizo, Directrice de Recherche – Rapportrice

Guillaume Montagnac, Chargé de Recherche – Rapporteur

Michel Labouesse, Directeur de Recherche – Président du Jury

Elisabeth Génot, Directrice de Recherche – Examinatrice

Alessandra Cambi, Full Professor – Examinatrice

Philippe Chavrier, Directeur de Recherche – Directeur de thèse



Except where otherwise noted, this work is licensed under
<http://creativecommons.org/licenses/by-nc-nd/3.0/>

Acknowledgements

First, I would like to deeply thank **Alessandra Cambi**, **Elisabeth Génot**, **Michel Labouesse**, **Corinne Albiges-Rizo** and **Guillaume Montagnac** who agreed to be part of my thesis jury as scientific experts to read my thesis manuscript, listen to my defense and review my PhD work. I am looking forward to hear about their comments and participate to interesting discussions about these 4 years of work.

I would like to particularly acknowledge **Michel Labouesse** who accepted to be the President of my jury. Michel followed my work all along these 4 years as a member of my thesis comitee and I am very pleased of his presence to see the final and global picture of my efforts.

More specifically, I would like to express my gratitude to **Corinne Albiges-Rizo** and **Guillaume Montagnac** for their role in revising my thesis manuscript. I know what a great amount of work it represents and I would like to thank them for their supportive comments on my manuscript.

Dans un second temps, c'est dans ma langue maternelle, le français, que je souhaite ici exprimer ma reconnaissance envers celles et ceux qui m'ont côtoyé, de près ou de loin, au cours de ces quatre années de thèse.

À **Philippe Chavier**, mon directeur de thèse, je tiens à exprimer ma gratitude pour m'avoir accueilli dans son laboratoire et accompagné tout au long de mon projet doctoral. Exigeant, rigoureux, mais aussi passionné par sa recherche et la « bonne » science en général. Bonne par le côté novateur et inédit, bonne par la rigueur technique et expérimentale, bonne enfin par la fiabilité et la précision de l'analyse, j'ai beaucoup appris à ses côtés et l'en remercie.

Je souhaiterais remercier nos proches collaborateurs avec lesquels j'ai pris beaucoup de plaisir à travailler et qui m'ont permis de combiner plusieurs approches pour faire de mon travail de thèse un projet pluridisciplinaire. En particulier, je souhaite adresser un immense merci à **Stéphane Vassilopoulos** pour avoir mis son expertise en microscopie électronique au service de notre projet, ainsi que pour son soutien enthousiaste tant lors des expériences que nous avons menées ensemble, que lors des phases de rédaction et de soumission du manuscrit. Un grand merci à **Raphaël Voituriez** pour sa contribution essentielle à la partie modélisation du projet où il a su faire preuve de pédagogie et de patience pour m'initier à la biophysique théorique et

me faire comprendre et m'approprier le modèle physique développé. Je tiens également à remercier **Oya Tagit** pour son aide et son savoir-faire précieux lors de la réalisation et l'analyse des expériences de microscopie à force atomique.

Enfin c'est à mes collègues de bureau et de laboratoire, qui sont parfois devenus bien plus que cela, que j'adresse ces quelques mots de remerciements. Ce sont les moments partagés avec eux, au quotidien ou ponctuellement, au laboratoire comme ailleurs, et leur soutien dans de nombreuses situations tant professionnelles que personnelles, qui me viendront en premier à l'esprit dans le futur au moment d'évoquer mes années de thèse.

En premier lieu, c'est à l'*Italian connection* que je souhaiterais dédier mes remerciements. À **Elvira Infante** avec qui j'ai travaillé en étroite collaboration au cours de mon Master 2 et mes premiers mois de thèse et qui m'a initié aux arcanes de la biologie cellulaire, du collagène et des premières expériences de microscopie. À **Alessia Castagnino**, la *mamma*, qui a eu un apport scientifique considérable au sein du premier projet présenté dans ma thèse. Je retiendrai aussi son excellent tiramisu, ses innombrables expressions italiennes fleuries, ainsi que, malgré son farouche démenti, sa francisation progressive avec un taux de ronchonneries qui n'avait plus rien à envier aux Parisiens à son départ du laboratoire. À **Valentina Marchesin** mais aussi **Pedro Monteiro** (mi-italien par alliance), représentants de la génération précédente de doctorants, qui m'ont accueilli et ont prodigué leurs conseils sur le déroulement de la thèse au laboratoire. **Pedro** m'a aussi familiarisé avec celui qui aura été mon fidèle compagnon de route (et de galère) pendant ces quatre années, mon microscope fétiche, le Spinning 4. Je lui en passe à nouveau la garde et le flambeau puisqu'il n'en avait visiblement pas eu assez de ses propres années de thèse !

Par la suite, j'ai moi-même été amené à encadrer et former des étudiants d'horizons divers et variés au cours de ma thèse. Je tiens à les remercier pour l'implication, la motivation et la bonne volonté dont ils ont fait preuve. Cela m'a sensiblement aidé à transmettre mes connaissances techniques et théoriques dans les meilleures conditions et j'espère qu'ils ont pu en tirer profit pour la suite de leurs études. Merci donc à **Prune Tricaud**, **Kathy Tian**, **Clément Binet-Moussy** et **Noémie Lacour**. Je tiens en outre à saluer **François Tyckaert**, un master 2 belge qui a su conjuguer travail et amusement avec un équilibre remarquable. Nos franches parties de rigolades resteront pour moi des moments marquants de ces quatre dernières années.

Je salue aussi les anciens membres du laboratoire, que j'ai connu et qui sont partis vers d'autres cieux pendant mes années de thèse. Je retiendrai notamment les blagues étranges et les vidéos

loufoques d'**Alan Guichard**, les conversations aussi intéressantes qu'originales de **Sonia Aguerra-Gonzalez**, ainsi qu'une partie de Times'up mémorable avec **Catalina Lodillinsky** entre autres. Un grand merci aussi à **Anna Zagryazhskaya-Masson**, avec qui j'ai eu d'intéressantes discussions sur de nombreux sujets, mais aussi beaucoup de bons moments de rires et de joies. Nous avons aussi partagé nos doutes et inquiétudes sur nos carrières respectives, et j'espère qu'elle trouvera rapidement sa voie dans le monde professionnel.

Les membres actuels du laboratoire ne sont pas en reste et je tiens tout particulièrement à remercier **Cecilia Colombero**, **Carine Rossé**, **Amulya Priya**, **David Remy**, **Sandra Antoine**, **Fiona Routet** et **Cecile Gambin**. Les deux premières citées ayant partagé le plus de temps avec moi au laboratoire, je les remercie pour leur contribution scientifique grâce aux nombreuses discussions et parfois même aides directes sur tel ou tel aspect de mon projet. Merci aussi pour les conversations intéressantes et le soutien apporté. Merci à **Cecilia** pour m'avoir donné envie de découvrir l'Argentine (*vendré a visitarte en Argentina !*), pour sa célèbre *Friday mood*, ainsi que pour avoir été le jukebox ambulant du laboratoire pendant ces quelques années (**David Rémy**, on te passe le témoin, en espérant que tu n'oublieras pas Aya) !

Je ne peux par ailleurs passer outre l'aide précieuse que **Gaëlle Martin** m'a apportée pour la seconde partie de ma thèse. Elle s'est démultipliée pour réaliser maintes expériences à mes côtés et donner un coup d'accélérateur au projet, et ce malgré une certaine adversité à travers des cellules, des vecteurs ou du collagène, parfois récalcitrants. Je tiens à lui exprimer ma reconnaissance pour son implication, sa persévérance, et bien sûr pour ses nombreux gâteaux qui m'ont sauvé de nombreuses fois de l'hypoglycémie ! Je lui souhaite le meilleur et plein de réussite pour ses nouvelles fonctions.

Difficile d'écrire mes remerciements de thèse sans évoquer, et par la même occasion remercier du fond du cœur, mes deux collègues, que dis-je amies, préférées, **Emilie Lagoutte** et **Clémentine Villeneuve**. Je peux sans hésiter affirmer que ces 4 années de thèse n'auraient pas eu la même saveur sans elles, qui m'ont aidé, soutenu, supporté et ont été là dans tous les moments importants de ces dernières années. Aussi bien les moments joyeux, au laboratoire mais aussi (surtout ?) en dehors (anniversaires, sorties, soirées jeux où les jeux se sont parfois faits rares, et même mariage...), que les moments plus difficiles où j'ai vraiment pu compter sur elles pour m'aider et me remotiver ! Je ne risque pas de l'oublier. Je souhaite à chacune de dénicher et de tracer sa propre route pour qu'elle soit la meilleure possible et j'espère que, même si celle-ci s'éloigne géographiquement (parce que Türkü, pour la beauté du geste, c'est bien,

mais c'est quand même un peu loin !), nous parviendrons à garder contact le plus longtemps possible.

En dernier lieu, je tiens sincèrement à remercier tous ceux qui n'ont pas directement été impliqués dans mon travail de thèse, mais qui m'ont soutenu et qui ont été pour moi un appui précieux tout au long de ces années. Mes amis, dont la présence à mes côtés dans tous les moments importants de ma vie est pour moi une richesse inestimable et irremplaçable. Mes parents, ma sœur et ma famille proche, qui m'ont d'une part permis de me construire tel que je suis aujourd'hui, et d'autre part ont fait un effort considérable pour essayer de comprendre et s'intéresser à mes travaux de recherche malgré leur complexité.

Je réserve le mot de la fin à ma femme, Charlotte, qui m'a encouragé pendant ma thèse et bien plus encore et m'appuie aussi pendant cette période de transition. Ma reconnaissance pour cet indéfectible soutien se passe de mots et j'espère pouvoir le lui rendre pour sa propre thèse à venir !

Table of contents

Acknowledgements.....	3
Table of contents.....	7
Table of illustrations	10
Abbreviations.....	11
Introduction	13
 Chapter 1: Breast cancer development and progression.....	 13
1. Normal breast histology, development and function	13
1.1. <i>Breast anatomy and histology.....</i>	<i>13</i>
1.2. <i>Mammary epithelium organization</i>	<i>14</i>
1.3. <i>Breast development and function</i>	<i>16</i>
2. Breast cancer development and progression.....	18
2.1. <i>Breast cancer development and classification</i>	<i>18</i>
2.2. <i>From in situ to invasive carcinoma, breast cancer metastatic program.....</i>	<i>20</i>
 Chapter 2: Extracellular matrices and cell invasion.....	 23
1. Extracellular matrices associated with cancer cell invasion	23
1.1. <i>Basement membranes.....</i>	<i>23</i>
1.2. <i>Stromal extracellular matrix</i>	<i>25</i>
1.3. <i>Biomechanical properties of extracellular matrices.....</i>	<i>27</i>
2. Extracellular matrices modifications in breast cancer	28
2.1. <i>De novo matrix deposition and changes in composition.....</i>	<i>28</i>
2.2. <i>Modifications of matrix biophysical properties</i>	<i>29</i>
2.3. <i>Matrix remodeling.....</i>	<i>31</i>
3. <i>In vitro</i> reconstitution of extracellular matrices	32
3.1. <i>Reconstitution of basement membrane-like matrices.....</i>	<i>32</i>
3.2. <i>Reconstitution of interstitial matrices</i>	<i>34</i>
3.3. <i>Modulation of biophysical properties of reconstituted matrices</i>	<i>35</i>
 Chapter 3: Mechanisms of cell migration	 37
1. Cell-matrix interactions during cell migration.....	38
1.1. <i>Integrin-mediated adhesion to the extracellular matrix</i>	<i>38</i>

1.2.	<i>Additional matrix receptors involved in tumor cell invasion</i>	41
1.3.	<i>Mechanical interplay in cell-matrix interactions</i>	42
2.	Multi-pronged roles of cell cytoskeletal networks during cell migration	44
2.1.	<i>Function and regulation of actin polymerizing structures</i>	44
2.2.	<i>Contribution of contractility in cell movement</i>	47
2.3.	<i>Role of microtubules during cell migration</i>	48
3.	Nucleus function and biomechanics during 3D cell migration	50
3.1.	<i>Cytoskeleton to nucleus force transmission during migration</i>	50
3.2.	<i>Nuclear mechanical stresses during migration: from mechanosensing to DNA damage</i>	52
4.	Cancer cell invasion: different strategies of tumor cell migration	55
4.1.	<i>Collective versus individual invasion</i>	55
4.2.	<i>Different modes of individual cell invasion</i>	56
4.3.	<i>The epithelial to mesenchymal transition</i>	57
	Chapter 4: Invadopodia, cancer cells cutting weapons for matrix degradation	59
1.	Podosomes and invadopodia: two faces of the same coin?	59
1.1.	<i>Discovery of invadosomes and their nomenclature</i>	59
1.2.	<i>Cell type and substrate specificity of invadosomes</i>	60
1.3.	<i>Biological relevance in physiology and disease</i>	62
2.	Initiation and formation of invadopodia	63
2.1.	<i>Membrane receptors and initiation signals</i>	63
2.2.	<i>Polymerization of actin and recruitment of actin binding partners</i>	64
3.	Maturation and disassembly of invadopodia	67
3.1.	<i>Tks5: a key scaffolding protein in invadopodia</i>	67
3.2.	<i>Proteases: invadopodia cutting blades</i>	69
3.3.	<i>Mechanisms of invadopodia disassembly</i>	70
	Chapter 5: Matrix metalloproteinases, key enzymes in cell invasion	71
1.	Matrix metalloproteinases and their physio-pathological functions	71
1.1.	<i>Soluble matrix metalloproteinases</i>	71
1.2.	<i>Membrane-type matrix metalloproteinases</i>	73
2.	Regulation of matrix metalloproteinase function: example of MT1-MMP	75
2.1.	<i>Regulation of MT1-MMP expression</i>	75
2.2.	<i>Post-translational activation of matrix metalloproteinases</i>	76
2.3.	<i>Regulation of MT1-MMP cell surface exposure and turnover</i>	77
2.4.	<i>MT1-MMP trafficking and delivery to invadopodia</i>	78

Working hypotheses and objectives	83
Article 1	87
Article 2	115
Conclusions and discussion	167
1. Cancer cells engage MT1-MMP-based matrix proteolysis on-demand during confined migration	167
2. Mechanical nuclear stresses and their consequences in cancer cell invasion	168
2.1. <i>Mechanisms of nuclear deformation during migration.....</i>	<i>168</i>
2.2. <i>Nuclear mechanosensing during 3D migration</i>	<i>169</i>
2.3. <i>NE integrity during confined migration and role of MT1-MMP</i>	<i>170</i>
2.4. <i>Mechanical and functional interplay between invadopodia and the nucleus ..</i>	<i>171</i>
3. Invadopodia are self-assembling and force-producing proteolytic structures	172
3.1. <i>Collagen receptors in invadopodia formation</i>	<i>173</i>
3.2. <i>MT1-MMP in invadopodia: from cover to cover</i>	<i>174</i>
3.3. <i>Force production in invadosomes</i>	<i>175</i>
3.4. <i>Integration of invadopodia-based force production to cell invasion mechanisms</i>	<i>179</i>
4. Concluding remarks	181
References	183
Annexe	219

Table of illustrations

Figure 1: Schematic representation of a sagittal breast section.....	14
Figure 2: Mammary epithelium polarized organization.....	15
Figure 3: Overview of the mouse mammary gland development	18
Figure 4: The metastatic cascade: a multi-step process	21
Figure 5: Basement membrane composition and organization	24
Figure 6: Type I collagen structure and assembly.....	26
Figure 7: Stromal extracellular matrix remodeling during breast cancer progression	31
Figure 8: Comparison of cell invasion in Matrigel and type I collagen.....	33
Figure 9: Effects of collagen concentration and temperature of polymerisation on pore size. 35	
Figure 10: Cell migration: a multi-step process	38
Figure 11: Integrins bi-directional signalling mechanisms	40
Figure 12: Integrin-mediated molecular clutch and its role in mechanosensing.....	43
Figure 13: Specialized actin structures in motile cells	46
Figure 14: Overview of nucleus-cytoskeleton interactions and their mechanical interplay during confined migration	51
Figure 15: Effects of matrix proteolysis inhibition on nuclear deformations during confined migration	54
Figure 16: Different modes of cell invasion.....	55
Figure 17: Invadosomes diversity according to the substrate and the cell type	61
Figure 18: Schematic representation of invadopodia multi-step assembly.....	66
Figure 19: TKs adaptor proteins.....	68
Figure 20: Schematic representation of MMPs and their ECM substrates	72
Figure 21: Role of MT1-MMP in breast tumor xenografts <i>in situ</i> to invasive transition	75
Figure 22: Model for MT1-MMP delivery at invadopodia by endosomal tubules	80
Figure 23: Model of invadopodia-, MT1-MMP-based matrix digest-on-demand response triggered by nuclear confinement during cancer invasion	168
Figure 24: Schematic representation of force production in podosomes and collagenolytic invadopodia	177
Figure 25: Could collagen remodeling of single cells be integrated at a multicellular level? 180	

Abbreviations

ADAM: A disintegrin and a metalloproteinase
ADP: Adenosine diphosphate
ATP: Adenosine triphosphate
BM: Basement membrane
CAF: Cancer-associated fibroblast
Cdc42: Cell division control protein 42 homolog
CSC: Cancer stem cell
DCIS: Ductal carcinoma *in situ*
DDR: Discoidin domain receptor
ECM: Extracellular matrix
EGF: Epidermal growth factor
EMT: Epithelial to mesenchymal transition
ER: Endoplasmic reticulum
FA: Focal adhesion
GDP: Guanine diphosphate
GEF: Guanine nucleotide exchange factor
GF: Growth factor
GTP: Guanine triphosphate
HER2: Human epidermal growth factor receptor 2
IDC: Invasive ductal carcinoma
JIP3/4: c-Jun N-terminal kinase (JNK)- interacting proteins 3/4
KASH: Klarsicht, ANC-1 and SYNE/Nesprin-1 and-2 Homology
LE: Late endosomes
LINC: Linker of nucleocytoskeleton and cytoskeleton
LOX: Lysyl oxidase
MET: Mesenchymal to epithelial transition
MMP: Matrix metalloproteinase
MT: Microtubule
MT-MMP: Membrane-type matrix metalloproteinase
MTOC: Microtubule organizing center
NE: Nuclear envelope

NM II: Non-muscle myosin II

N-WASP: Neural-Wiskott-Aldrich syndrome protein

PI: Phosphoinositides

RTK: Receptor tyrosine kinase

ROCK: Rho-associated coiled-coil containing kinase

ROS: Reactive oxygen species

SH2/3: Src homology 2/3

SUN: Sad1 or UNC-84

TACS: Tumor-associated collagen signature

TGF- β : Transforming growth factor β

TNBC: Triple-negative breast cancer

Tks4/5: tyrosine kinase substrate with four/five Src homology 3 domains

WASH: Wiskott-Aldrich syndrome protein and Scar homolog

WASP: Wiskott-Aldrich syndrome protein

Introduction

Chapter 1: Breast cancer development and progression

One of the main characteristics of living animals is their ability to reproduce themselves and perpetuate their offspring. A large variety of modes of reproduction as well as organs dedicated to reproduction or parenting have emerged throughout evolution (Blackburn, 1992). Among vertebrates, mammals (from the latin word *mamma*, for breast) distinguish themselves by the presence of one or several exocrine mammary glands producing milk for offspring feeding. Mammary glands are termed breasts for the Primates order.

1. Normal breast histology, development and function

1.1. *Breast anatomy and histology*

Mature human breasts are epidermal appendices covering pectoral muscles of the chest and composed of several layers of different tissues. The fundamental and functional units of human mammary glands are called alveoli and serve for milk production and storage. They are clustered together in lobules that are drained by lactiferous ducts converging at the nipple tip where milk is expelled (Guinebretière et al., 2005). Alveoli, lobules and ducts are embedded in a connective tissue composed of several cell types and a stromal extracellular matrix (ECM) consisting mostly in type I collagen that supports mammary gland structure. Adipocytes, which represent the major cell type in connective tissue, surround the gland in a 0.5 to 2.5 cm thick subcutaneous layer and fill the intervals between lobules (**see Figure 1**). They serve as a reservoir of fat during milk production but are also thought to be important for communication between other cell types, epithelial growth and mammary gland angiogenesis (*i.e.* formation of new blood vessels from pre-existing vessels) through their endocrine function (Hovey and Aimo, 2010). The connective tissue is also infiltrated by vascular and lymphatic vessels as well as immune cells that play an important role in mammary gland morphogenesis and branching in addition of their well-known function in immunity (Reed and Schwertfeger, 2010). Finally fibroblasts, which contribute to mammary gland development as well, can also be found within the stromal environment (Polyak and Kalluri, 2010; Unsworth et al., 2014).

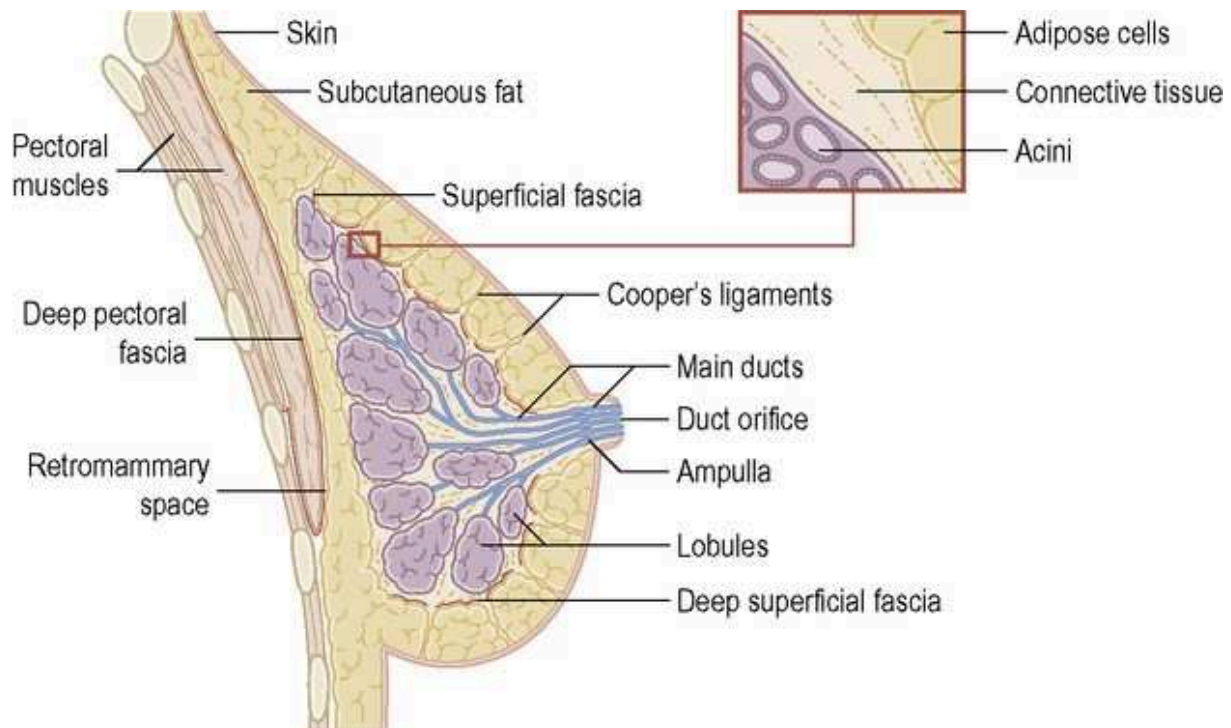


Figure 1: Schematic representation of a sagittal breast section

The human mammary gland is composed of several lobules, subdivided in multiple acini, and surrounded by a connective tissue consisting of extracellular matrix and various cell types, most notably adipocytes. Milk produced by epithelial cells in acini is drained out to the breast nipple by lactiferous ducts.

Image from the Radiology Key database (<https://radiologykey.com/breast-4/>)

1.2. Mammary epithelium organization

Mammary ducts are simple epithelia composed of a bilayer of luminal milk-secreting cells surrounded by contractile myoepithelial cells named basal cells (see **Figure 2A**). Myoepithelial cells serve for milk expulsion from ducts lumen to the nipple and sit on a specialized dense ECM called basement membrane (BM) mainly composed of laminins and type IV collagen (Sekiguchi and Yamada, 2018). Similar to most epithelia, the mammary epithelium forms a cohesive tissue due to the presence of different types of adherent junctions detailed below.

Luminal cells connect to their neighbors through tight junctions, adherens junctions, desmosomes and gap junctions. Tight junctions (also called *zonula occludens*) form a belt of protein complexes around the cell surface to prevent bi-directional leakage of soluble molecules in the lumen and the epithelium (Eckert and Fleming, 2008; Green et al., 2010). Located right under tight junctions, the adherens junctions (or *zonula adherens*) bridge plasma membranes of two neighboring cells due to the homodimerization in trans of E-cadherin transmembrane

proteins within the extracellular space. They play a role in organizing and anchoring the actin cytoskeleton at the cell plasma membrane (Engl et al., 2014). Desmosomes (or *macula adherens*) also connect cells together with proteins from the cadherin family (such as desmogelin or desmocollin) and facilitate plasma membrane anchorage of intermediate filaments contributing to mechanical stress resistance within the tissue (Garrod and Chidgey, 2008). Furthermore, gap junctions (or *macula communicans*) play a critical role in cell-cell communication by directly connecting the cytoplasm of two neighboring cells through the association of two transmembrane hemichannels formed by connexin proteins (McLachlan et al., 2007). Interactions between luminal and myoepithelial cells are mediated through desmosomes and gap junctions. Myoepithelial cells further bind underneath BM via specialized desmosomes called hemidesmosomes, that form through the attachment of integrin proteins to ECM ligands (Uematsu et al., 2005).

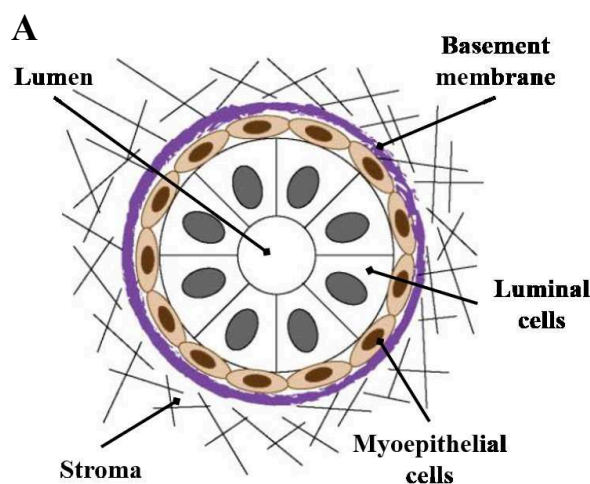
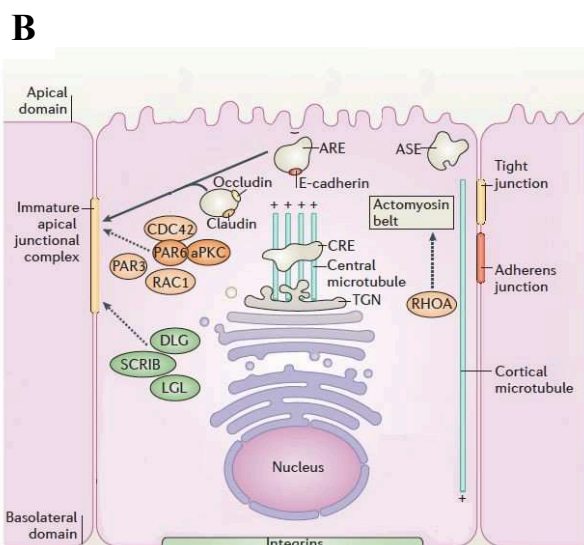


Figure 2: Mammary epithelium polarized organization

(A) Schematic cross-section of a bi-layered mammary duct. Milk-secreting luminal cells (in white) are located on the inner apical side while contractile myoepithelial cells (in orange) are present in the outer basal cell layer and contact the underlying basement membrane (violet). The mammary epithelium is embedded in a connective tissue called stroma mostly composed of type I collagen fibers (in gray).

Image adapted from Pedro Monteiro's thesis "Role of WASH and exocyst complexes in tumor cell invasion" (2014).



(B) Apico-basal polarity in epithelial cells. Three molecular complexes (Par, Crumbs and Scribble complexes) cooperate to define and maintain the epithelial apico-basal polarity. Tight junctions and adherens junctions are formed with neighboring cells and desmosomes bridge luminal with myoepithelial cells at the basal membrane surface.

Image adapted from Rodriguez-Boulant and Macara, "Organization and execution of the epithelial polarity programme" *Nat. Rev. Mol. Cell Biol.* (2014) 15(4), 225-242.

Cell polarity, defined as an asymmetric distribution of proteins, lipids and other macromolecules within the cell cytoplasm or the plasma membrane is another key feature of the mammary epithelium. In particular, luminal cells present functionally distinct poles respectively called the apical pole, facing the lumen, and the basolateral pole, contacting neighboring luminal cells and underneath myoepithelial cells. Differences between apical and basolateral plasma membrane composition result from a polarized trafficking and secretory machinery (endoplasmic reticulum or ER, Golgi apparatus and endosomal compartments) directed towards the apical pole (Rodriguez-Boulau and Macara, 2014). This polarity is established and maintained by three main multiprotein polarity complexes respectively named Crumbs, Par and Scribb (McCaffrey and Macara, 2012; Rodriguez-Boulau and Macara, 2014). The Crumbs complex, localized along the apical plasma membrane and at tight junctions, and the Par complex, only present at tight junctions, together determine the apical identity (Nance and Zallen, 2011; Pocha and Knust, 2013). By contrast, the Scribb complex counteracts this apical identity and is restrained to the basolateral membrane where it localizes to E-cadherin-based adhesions (Humbert et al., 2006). Polarized cells also display a specific organization of cytoskeleton networks with an actin belt assembling along adherens and tight junctions at the apical pole, and parallel arrays of microtubules (MTs) aligned along the apico-basal axis that serve as rails for intracellular transports and organelle positioning (Akhmanova and Hoogenraad, 2015; Nance and Zallen, 2011) (see **Figure 2B**).

On the other hand, myoepithelial cells differ from luminal cells in their morphology, identity and function. They form a continuous layer of elongated cells oriented parallel to the duct long axis. During lactation and upon oxytocin activation, they promote milk expulsion by contraction mediated by their high levels of cytoplasmic filamentous α -smooth muscle actin and myosin (Haaksma et al., 2011). They can be distinguished from luminal cells by their differential composition in cytokeratins (CK) intermediate filaments, CK5 and 14 stamping basal identity while CK8 and 18 serve as luminal proxies (Gudjonsson et al., 2005).

1.3. Breast development and function

Previously mentioned epithelial features arise during embryonic and postnatal development and are tightly regulated throughout the individual lifetime. Most of our understanding of mammary gland development is derived from studies performed in mice which provide insights into human breast development. The mammary gland developmental program is a unique process comporting different phases controlled by hormonal cues, that occur in part during embryogenesis, but mostly postnatally at puberty or during pregnancy

periods (Macias and Hinck, 2012). The mammary epithelium originates embryologically from the ectoderm where cells locally aggregate into several layers to form a placode that will then elongate and invade into the stroma. It is only in late stages of foetal development (starting at embryonic day 16 in mice) that a proper bi-layered ductal lumen emerges from intercellular spaces (Huebner and Ewald, 2014). At the beginning of puberty, hormones and growth factors produced by the pituitary and ovarian glands trigger the proliferation, expansion and subsequent invasion of ducts terminal ends into the surrounding connective tissue. Secondary side branching events from original ducts lead to an increased complexity of the network and completely filled the mammary stroma (**see Figure 3A**). Even though mammary glands are present in all mammals, their development during puberty is usually restricted to females due to differential hormonal stimulation and lack of some hormonal receptors in males (Howard and Gusterson, 2000).

In order to feed the new-born child and fulfil their milk-secreting primary function, mammary glands experience profound modifications during pregnancy including secondary and tertiary branching and subsequent development of alveolar structures. Initial alveolar buds emanate from the proliferation of epithelial cells in the interstitial adipose tissue where they progressively split and differentiate into distinct alveoli specialized in milk production and secretion (Watson and Khaled, 2008). Progesterone and prolactin, two hormones respectively produced by the ovarian and the pituitary glands are required for these fundamental transformations leading to a lactation-competent gland (Briskin et al., 1998). After birth, suckling by the new-born infant triggers oxytocin release from the pituitary gland which in turn activate contractility of myoepithelial cells to enable milk expulsion to the nipple. Later, concomitant with weaning, regression of alveoli and secondary ducts branches occur in a process called involution where the mammary gland return to its “resting” pre-pregnancy state (Macias and Hinck, 2012) (**see Figure 3B**).

The ability to sustain several cycles of expansion and involution and its strong regenerative capacities indicated the existence of stem cells in the mammary epithelium. Over the last decade, several studies have demonstrated the existence and identified based on specific markers mammary stem cells with the capacity of regenerating an entire functional mammary epithelium (Inman et al., 2015; Lloyd-Lewis et al., 2017). Tissue regeneration but also tissue maintenance by stem cells are tightly regulated processes. However, defects in epithelium homeostasis can occur through an individual lifetime with potential dramatic consequences such as uncontrolled cell proliferation that can lead to neoplasia and evolve into cancer.

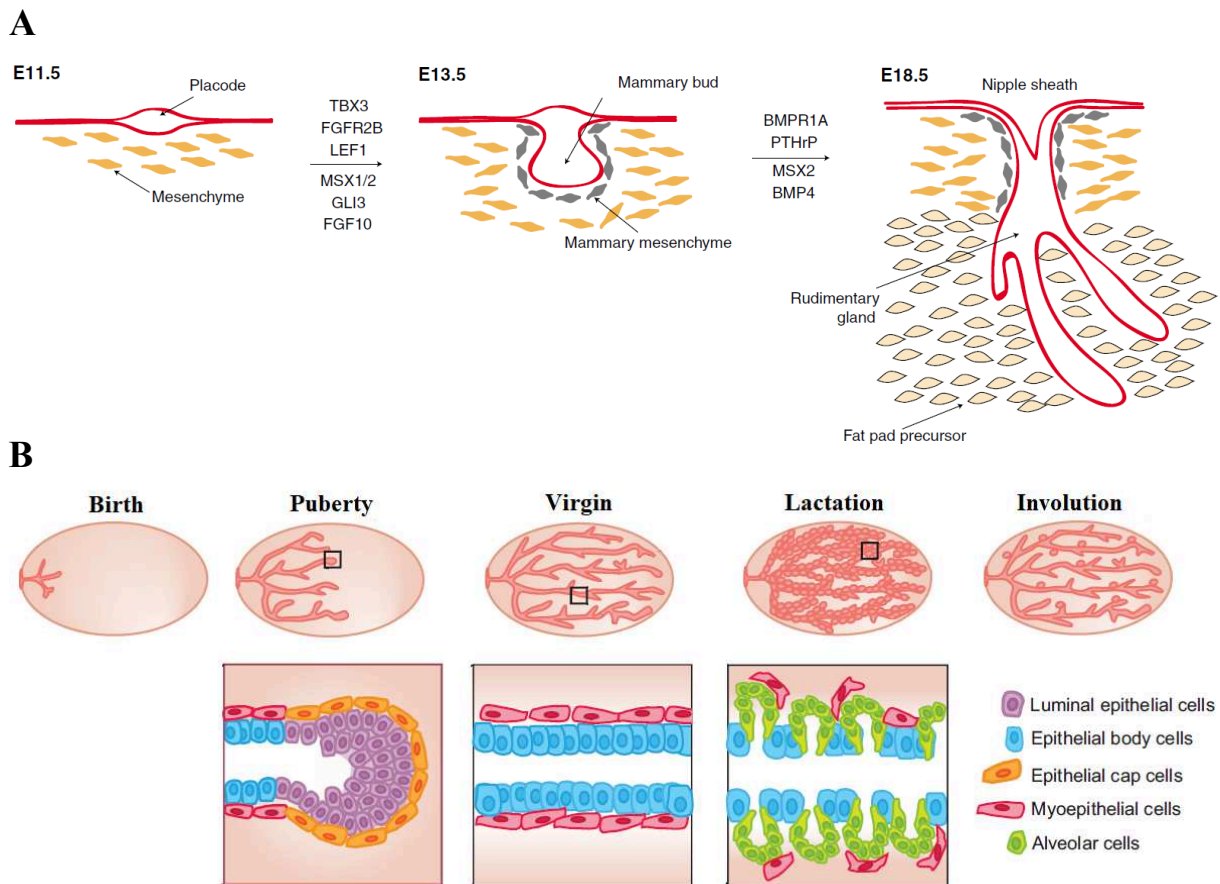


Figure 3: Overview of the mouse mammary gland development

(A) Embryonic development. Cluster of epithelial cells (or placode), sink into the underlying mesenchyme at E13.5 to become the mammary buds. These buds then elongate to form sprouts, which develop a lumen with an opening to the skin, marked by the formation of the nipple sheath. When term approaches, at E18.5, the sprouts become small arborized glands that invade the fat pad. Development is essentially arrested at this stage until puberty.

(B) Post-natal development. At puberty, sexual hormones induce epithelial ducts expansion into the mammary fat pad, due to highly proliferative multilayered terminal end buds (inset), to form the adult virgin mice mammary gland. Pregnancy is accompanied by hormonal changes that signal a large expansion of epithelial cells to form alveolar structures secreting milk during lactation. Alveoli (inset) expand and fill the majority of the fat pad. Upon weaning, cell death and ECM remodeling trigger involution and give rise to a state that resembles the resting adult mammary gland.

Images adapted from Watson and Khaled, "Mammary development in the embryo and adult: a journey of morphogenesis and commitment" Development. (2008) 135(6), 995-1003, and Inman et al., "Mammary gland development: cell fate specification, stem cells and the microenvironment" Development. (2015) 142(6), 1028-1042.

2. Breast cancer development and progression

2.1. *Breast cancer development and classification*

Breast cancer is the most common cancer among women and the second most common cancer overall worldwide. France follows the same trend with one of the highest incidence rate in the world (around 60 000 new cases diagnosed every year) and 12 000 lethal issues per year

representing the deadliest cancer among women (“Les cancers en France”, report from INCA or Institut National du Cancer, 2017). In less than 10% of the cases, breast cancers originate from hereditary mutations in the germ line, which mainly affect BRCA 1 and 2 genes (among others such as TP53, PTEN, CHEK2 or ATM) with a very high penetrance (Campeau et al., 2008). The other 90% of breast cancer cases with no hereditary predispositions, share a very complex and diverse mutational landscape characterized by scarce high-frequency mutations in contrast with a large number of low-frequency mutations and genomic defects in tumor cells (Teschendorff and Caldas, 2009).

This genetical diversity in breast cancer translates into high heterogeneity in clinic, and classification systems have been developed to organize and standardize it. Historically, breast cancer classification has been relying on the histopathological type, grade and stage of the tumor. From an histological point of view, breast cancers are divided into ductal or lobular *in situ* carcinoma (tumor cells are restricted to the mammary duct or lobule respectively) and invasive carcinoma, and subdivided into numerous subtypes based on architectural and morphological features of the tumor (Malhotra et al., 2010). The grade of the tumor is attributed after scoring different characteristics from the biopsy such as nuclear polymorphism or mitotic count while the stage is determined using the TNM system including clinical and pathological information such as tumor size (T), status of regional lymph nodes (N) and spread to distant metastatic sites (M). Additionally, pathological biomarkers have been implemented and expression of estrogen receptor (ER), progesterone receptor (PR) and amplification status of human epidermal growth factor receptor 2 (HER2) are now routinely used to stratify patients for prognostic predictions and treatments. Based on this, targeted therapies have emerged and have been successfully used in clinic in particular the trastuzumab, used in patients presenting HER2 amplification.

Over the last decades however, advances in large-scale analysis techniques have provided more and more insights in the biology of breast cancer and revealed five molecular “intrinsic” subtypes based on gene expression profiles (luminal A, luminal B, HER2-enriched, Claudin-low and Basal-like, sometimes called triple negative breast cancer TNBC) and a Normal-breast-like group (Perou et al., 2000). Luminal A and B are expressing genes usually present in normal breast luminal cells and are characterized by ER expression, no HER2 amplification and low or high expression of proliferation genes (such as MKI67) respectively. Together they represent 50 to 70% of breast cancers (Eroles et al., 2012). HER2-enriched cancers correspond to 15 to 20% of breast cancers and are characterized mostly by high expression levels of HER2 due to amplification or repetitions of the HER2 gene (Eroles et al., 2012). The basal-like phenotype

corresponds to 10% of breast carcinomas. They expressed common genes of normal breast myoepithelial cells and are negative for ER and PR expression as well as HER2 amplification. Basal-like tumors have worse prognosis than luminal ones and a high relapse rate (Dent et al., 2007). The claudin-low subtype, which represents around 10% of breast cancer and is characterized by low expression of genes involved in cellular junctions, has been identified more lately and is associated with poor prognosis (Herschkowitz et al., 2007). Although not used in clinic yet because of the cost involved, this stratification complements and amplifies the information given by classical approaches (Parker et al., 2009).

Along with the identification of breast cancer molecular subtypes, an active field of research in breast cancer biology is the study of cancer stem cells (CSCs) underlying the idea that, within a tumor, exists a limited subset of cells responsible for tumor initiation and progression (Stingl and Caldas, 2007). The two main hypotheses propose that CSCs either originate from normal cells within the mammary stem cell hierarchy explaining why breast cancer subtypes and breast normal cells shared part of their gene expression profiles; or arise from a common normal stem cell deriving into different subtypes with accumulating mutational events (Malhotra et al., 2010). Despite important advances in the field, more work needs to be done to establish a functional classification of breast cancers based on the ‘cell of origin’ and the proportion of CSCs with a potential to greatly improve prognosis prediction and clinical outcome.

2.2. *From in situ to invasive carcinoma, breast cancer metastatic program*

The current model of breast cancer progression is a sequential process starting from neoplasia (abnormal proliferation of cells) to ductal or lobular *in situ* carcinoma that can become an invasive carcinoma and eventually form secondary tumors also known as metastasis. Ductal *in situ* carcinoma (DCIS) is a premalignant non-invasive lesion characterized by tumor cell proliferation within the ductal-lobular system and leaving the myoepithelial cell layer and the BM untouched (Cowell et al., 2013). DCIS is considered as a precursor of invasive ductal carcinoma (IDC) because of their anatomical proximity as well as histological but also molecular continuity (Burkhardt et al., 2010; Wellings and Jensen, 1973). If DCIS is generally associated with a good clinical outcome, its progression to IDC in 20 to 50% of the cases correlates with a drop of patients’ survival (Sanders et al., 2005) and attempts to predict which DCIS lesions will turn into IDC have not been successful so far.

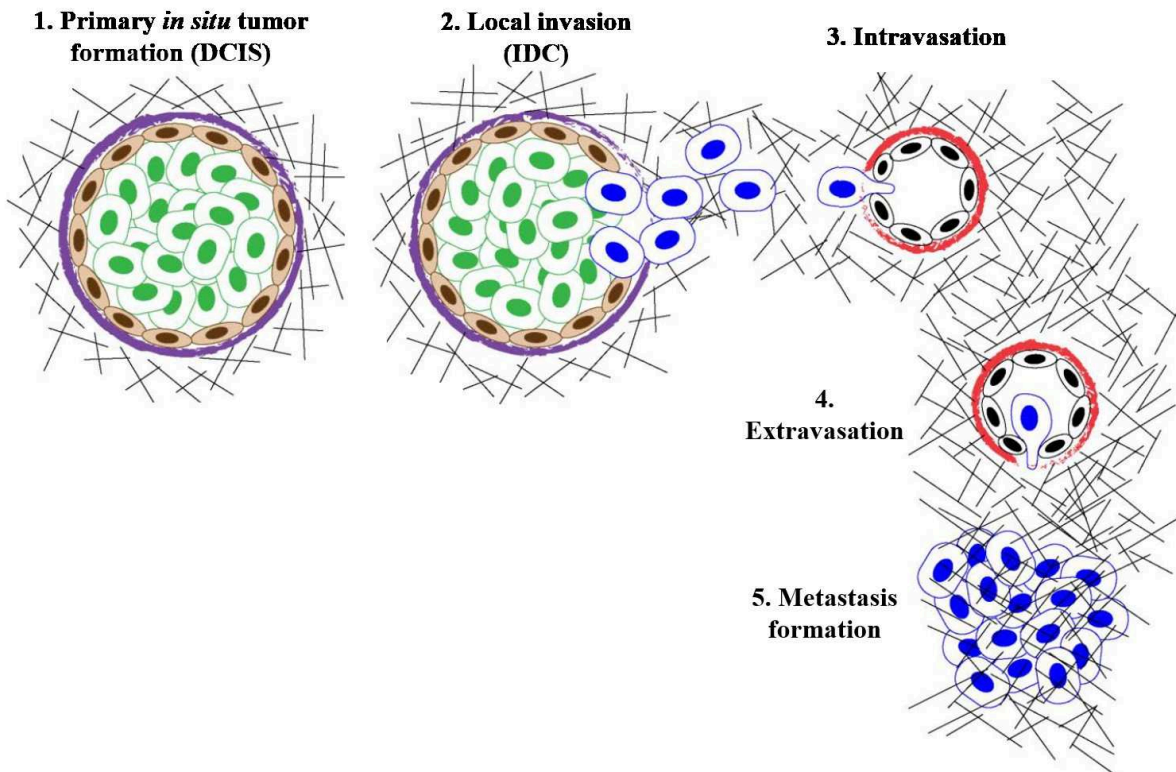


Figure 4: The metastatic cascade: a multi-step process

(1) Initially, transformed epithelial cells (green) undergo abnormal proliferation within the mammary duct: it's the ductal carcinoma *in situ* (DCIS) stage. (2) Some tumor cells (blue) can progressively acquire invasive capacities, disperse the myoepithelial cell layer (orange) and breach the BM (violet) to invade into adjacent tissues composed mostly of type I collagen fibers (gray). Cells are able to enter into blood vessels and reach the general circulation in a process called intravasation (3). In distant microvessels from different organs, tumor cells can attach to endothelial cells, which facilitates their extravasation (4). After settling in the metastatic target organ, tumor cells may colonize the destination tissue and establish secondary tumors called metastasis (5).

Image adapted from Pedro Monteiro's thesis "Role of WASH and exocyst complexes in tumor cell invasion" (2014).

The transition from *in situ* to invasive lesions requires tumor cells to gain invasive capacities enabling them to escape from the epithelium, cross the myoepithelial layer and perforate the BM to invade through the surrounding stroma. This process is accompanied by substantial modifications of both the microenvironment and cells intrinsic parameters that are developed in the following sections. Evading the primary tumor constitutes the first stage of a multi-step process called the metastatic cascade (see **Figure 4**). In this model, escaping tumor cells invade through the connective tissue mostly composed of a dense type I collagen network where they can encounter blood or lymph vessels and reach the general circulation in a process called intravasation. The opposite process, called extravasation, allows tumor cells to break out from vessels and invade into a tissue distant from the primary tumor. Both intravasation and

extravasation necessitate tumor cells to transmigrate through the BM and the endothelial epithelium (Chiang et al., 2016). Tumor cells can eventually seed into the destination tissue and form a secondary tumor called metastasis. This linear progression is based on the accumulation of genetic and epigenetic modifications in tumor cells leading to morphological changes allowing cells to progressively gain invasive capacities. It has been however recently challenged by several observations made in patients and in mice models where tumor cells disseminate at very early stages of breast cancer progression (Harper et al., 2016; Hosseini et al., 2016; Schmidt-Kittler et al., 2003). In this parallel progression model, which was first described in the 1950s, tumor cells escape the primary tumor at early stages to colonize distant sites (Collins et al., 1956). Early metastasis will then proliferate and progress independently from the primary tumor (Klein, 2009). If these models rely on different cancer progression hypothesis and call for differentiated decision-making for treatments in clinic, they both depend on the ability of tumor cells to escape primary tumor and migrate into the surrounding environment.

Chapter 2: Extracellular matrices and cell invasion

Extracellular matrices (ECMs) are defined as three-dimensional networks of secreted molecules immobilized outside of the cells and consist of fibrous proteins (collagens, elastin) and non-fibrous proteins (fibrillin, fibronectin, laminins, glycosaminoglycans or GAGs, proteoglycans or PGs etc ...) (Mecham, 2012). ECMs compose the connective tissue and ensure a physical support for cells but are also involved in physio-pathological processes among which cell proliferation, survival, differentiation, as well as tissue morphogenesis, homeostasis and compartmentalization (Chaudhuri et al., 2014; Dzamba and DeSimone, 2018; Lu et al., 2011).

1. Extracellular matrices associated with cancer cell invasion

1.1. *Basement membranes*

Basement membranes (BMs) are dense sheet-like structures first observed and identified by electron microscopy (Vracko and Strandness, 1967). They contact epithelial cells basally and separate the epithelial layer from the stroma in almost all tissues. In addition to their initially described role as a structural and adhesion support for tissues, BMs also serve in a wide range of functions including tissue compartmentalization, control of cell behavior (polarity, survival, proliferation etc ...), and organ-specific functions such as stabilization of sarcomeres in skeletal muscles or selectivity in glomerular filtration in kidneys (Glentis et al., 2014; Yurchenco, 2011). BMs are interconnected networks mainly composed of type IV collagen, laminin proteins as well as glycoproteins (nidogens, Heparan Sulfate Proteoglycans or HSPGs) (Kalluri, 2003).

Type IV collagen is a non-fibrillar collagen representing around 50% of adult BM that can self-assemble into networks. It consists of three α -chains assembling in heteromeric protomers that present a central triple-helical domain, a C-terminal globular domain called NC1 involved in trimerization and a N-terminal 7S domain important for network formation (see **Figure 5A**). Only three different protomers can emerge from the six genetically different α -chains ($\alpha 1$ - $\alpha 6$) and display tissue-specific expression patterns (Khoshnoodi et al., 2008). Each protomer assembles in dimers through interactions between NC1 domains, and dimers associate into tetramers through their 7S domains to form the basic unit of type IV collagen networks. These units can further assemble into suprastructures mediated by end-to-end or lateral interactions between collagen IV protomers, along with disulfides covalent crosslinks (Glentis et al., 2014; Rowe and Weiss, 2008). Type XV, XVIII or VI collagens can also be integrated in BM composition and participate to establish the tissue-specificity.

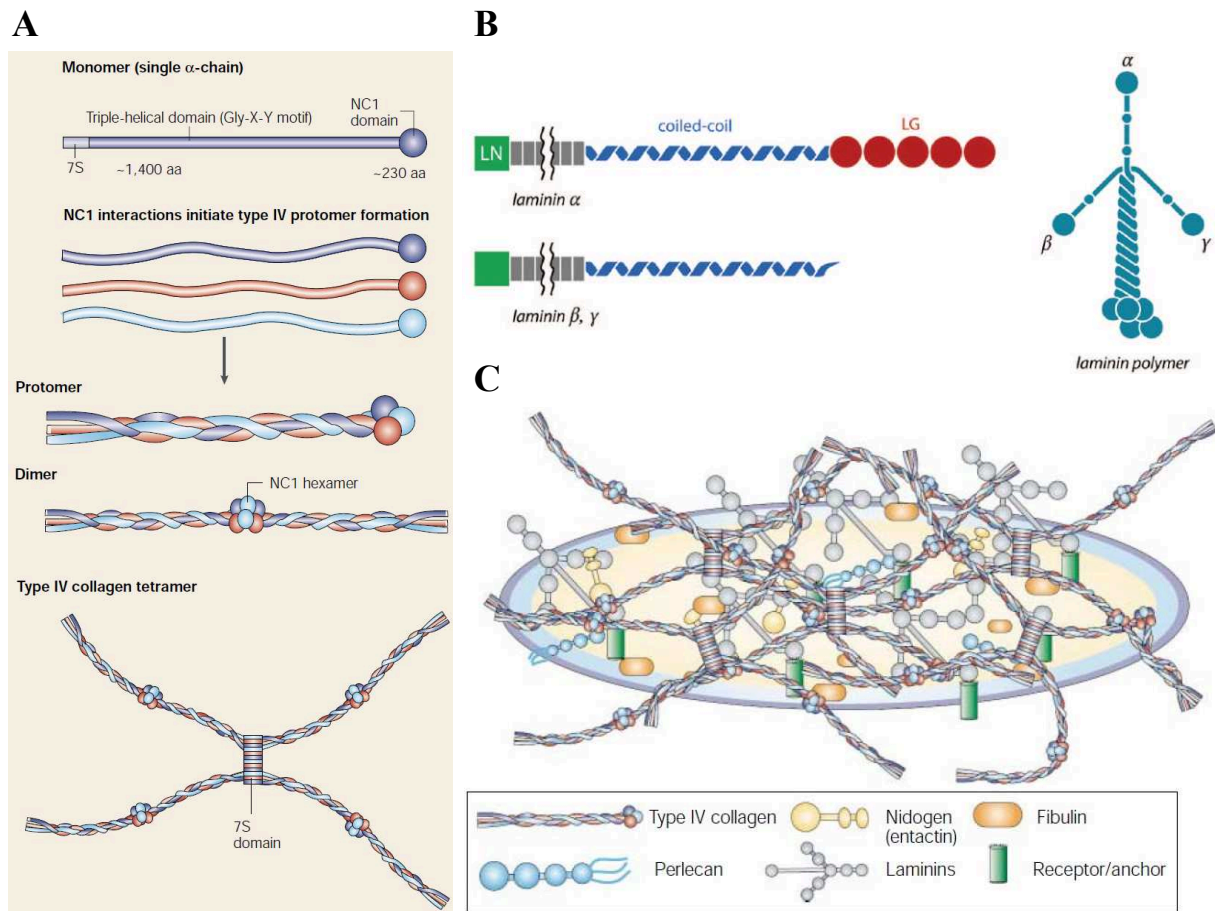


Figure 5: Basement membrane composition and organization

(A) Type IV Collagen assembly. Type IV collagen protomers consist of three domains: a N-terminal 7S domain, a C-terminal globular NC1 domain, and a long triple-helical domain. Each protomer can dimerize, and four dimers associate to form the nucleus for the type IV collagen scaffold.

(B) Schematic representation of laminins. Each laminin chain is composed of 3 chains containing several domains namely LN (N-terminal domain), coiled-coil domain important for heterotrimers formation and, in case of the α -chain, LG globular domain, involved in cell surface adhesion.

(C) Organization of the BM scaffold. Laminins deposition and polymerization lead to their association with type IV collagen through nidogen. Other components of the BM interact with the laminin polymer and the type IV collagen network to organize a functional BM.

Images adapted from Kalluri et al., "Basement membranes: structure, assembly and role in tumour angiogenesis" *Nat. Rev. Cancer* (2003) 3(6), 422-433, and Glentis et al., "Assembly, heterogeneity, and breaching of the basement membranes" *Cell Adh Migr* (2014) 8(3), 236-245.

After type IV collagen, laminins are the most abundant proteins in BMs. They are composed of a long α -chain and two small β - and γ -chains that associate by their central coiled-coil region to form heterotrimers. It exists 5 isoforms of α -chains, 4 isoforms of β -chains and 3 isoforms of γ -chains that can generate 16 different laminins in vertebrates (Yurchenco, 2011). Laminins N-termini, called LN domains, emerged as arms from each chain of the trimeric structure and are implicated in laminins polymerization. Supramolecular organization is also triggered via binding of the α -chain long arm, a C-terminal domain called LG composed of several globular motifs, to receptors exposed at the cell surface including integrins, sulfated

glycolipids or dystroglycans (McKee et al., 2007; Nishiuchi et al., 2006; Yurchenco, 2011) (see **Figure 5B**).

Self-assembling laminin and type IV collagen networks are subsequently stabilized and connected by interactions with other BM components including nidogens, bridging collagen IV and laminins, perlecan, connecting nidogen to laminins, as well as agrin or other types of collagen (Battaglia et al., 1992; Yurchenco, 2011) (see **Figure 5C**). BM constituent proteins are mostly secreted by epithelial cells and accumulated along their cell surface by plasma membrane receptors, but can be partly synthesized by mesenchymal cells from the stroma that do not bind BM (Kedinger et al., 1998). Following this complex assembly, mature BM form a dense and thin (0.1 to 1 μm) specialized ECM lattice allowing passive diffusion of small molecules through pores of 10 to 90 nm diameter but physically filtering out larger elements (Rowe and Weiss, 2009, 2008). To accommodate this limited space, cells have developed different strategies to transigrate through BMs and reach the underneath stroma.

1.2. Stromal extracellular matrix

Collagen is the most abundant protein in mammals and constitutes a major component of the stromal ECM (Bella, 2016). Collagen molecules consist of combinations of 3 out of more than 40 different α -chains forming in total 28 distinct homo- or hetero-trimers of collagen in humans (Mouw et al., 2014). α -chains assemble in a structurally conserved triple helix motif containing regions of repeated Gly-X-Y amino acids sequence (where X and Y are any amino acid) (Brodsky and Persikov, 2005). Fibrous type I collagen (formed by two $\alpha 1$ -chains and one $\alpha 2$ -chain) is the major structural element in the ECM and is generally synthesized and assembled by fibroblasts in a complex multi-step process. Following transcription and translation, α -chains are imported and modified in the rough endoplasmic reticulum (ER) so that they can form a triple-helical molecule called procollagen. Procollagen then undergo modifications in the Golgi apparatus and is packaged into secretory vesicles before being delivered in the extracellular space. There, C- and N-termini domains are cleaved out by different proteases to generate collagen molecules that can self-assemble into fibril aggregates at the cell surface through interaction with their newly exposed C- and N-termini telopeptides (Christiansen et al., 2000; Holmes et al., 2018; Mouw et al., 2014). Further modifications are made during collagen fibrils assembly including interactions with accessory molecules, and, in the final steps of biosynthesis, crosslinking bridges built by extracellular lysyl oxidases (LOX) to stabilize the supramolecular structure and enhance mechanical properties (Lucero and Kagan,

2006). Subsequent assembly into higher supramolecular organization such as collagen fibers or bundles can occur depending on tissue characteristics (see **Figure 6**).

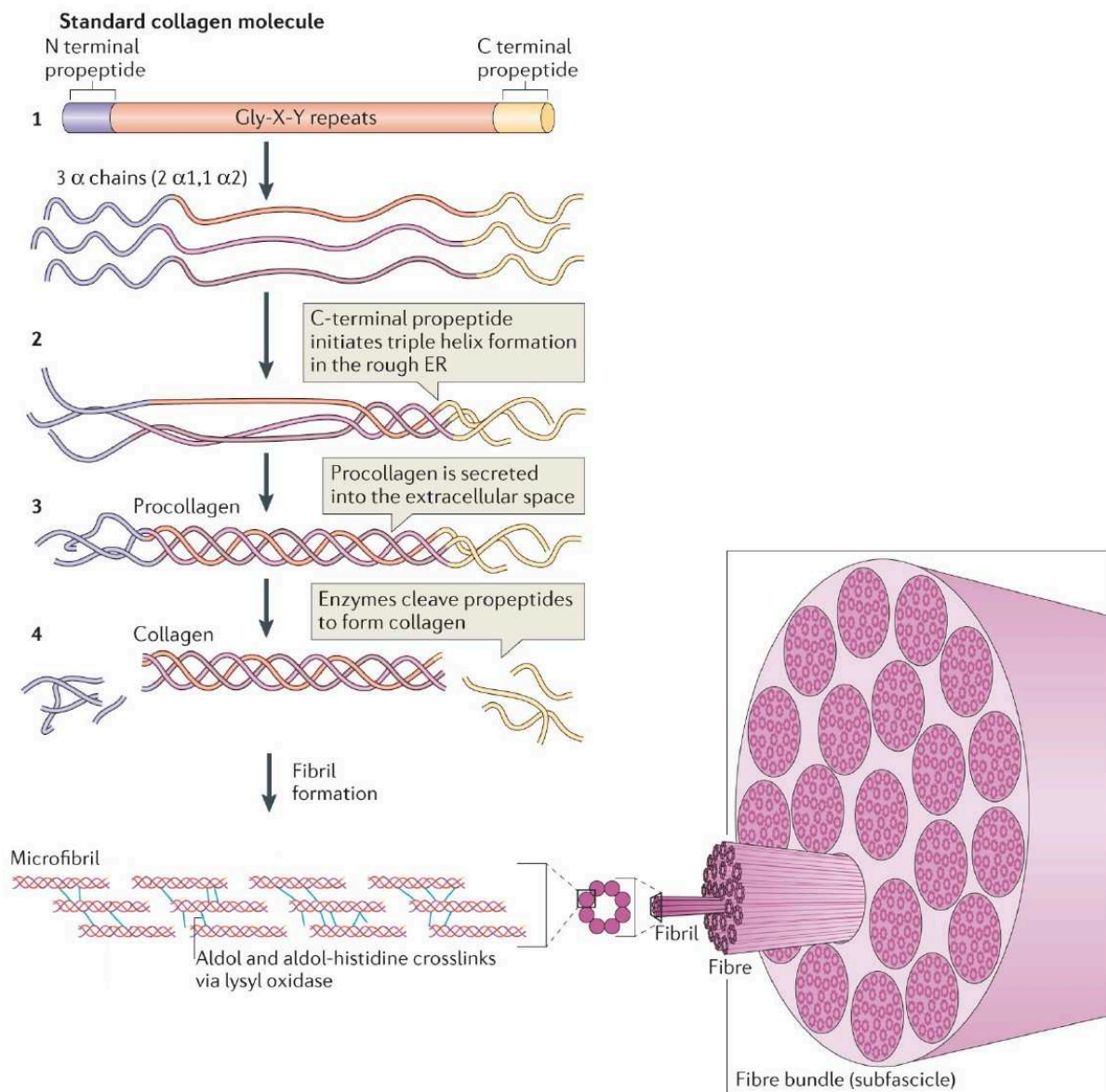


Figure 6: Type I collagen structure and assembly

Fibrillar collagen molecules are characterized by terminal propeptide sequences, which flank a series of Gly-X-Y repeats (where X and Y represent any amino acids but are frequently proline and hydroxyproline) forming the central triple helical structure (1). Three α -chains (two α 1 and one α 2 for type I collagen) are assembled into a trimer to form procollagen (2) which is secreted into the extracellular space (3) and converted into collagen by the removal of the N- and C-propeptides via metalloproteinase enzymes (4). Extracellularly, collagen is assembled into microfibrils after formation of intra- and inter-molecular covalent crosslinks by lysyl oxidase enzymes. Several additional steps of collagen molecules bundling can subsequently occur in the connective tissue.

Images adapted from Kalluri et al., "Extracellular matrix assembly: a multiscale deconstruction" Nat. Rev. Mol. Cell Biol. (2014) 15(12), 771-785.

In addition to collagen, non-fibrous proteoglycans and glycosaminoglycans constitute key ECM elements and are responsible for ECM hydration. They also regulate, together with elastin fibers that provide structural integrity and deformability, ECM viscosity and resistance to compressive forces (Dzamba and DeSimone, 2018). Ultimately, multiple other proteins including laminins or fibronectin, act as functional bridges between ECM macromolecules, cells or soluble molecules in the extracellular space thereby reinforcing the ECM network and resulting in ECM tissue-specificity as a consequence of its unique composition. Topology and biomechanical properties, depending on ECM relative composition, is critical for several biological processes including cell differentiation or migration and is able to evolve under pathological conditions such as cancer progression (Muncie and Weaver, 2018; Schedin and Keely, 2011).

1.3. Biomechanical properties of extracellular matrices

ECMs can bind to multiple molecules and function as reservoirs of soluble growth factors or cytokines among others, therefore providing surrounding cells with biochemical cues. Similarly, as described above, ECMs are complex and intricate networks of polymers and macromolecules forming a specific topological and geometrical scaffold defined by diverse physical parameters including density, porosity, stiffness, elasticity, ordering or alignment that are partly connected to each other. Elasticity represents the capacity of a matrix to come back to its initial state (shape and size) after a mechanical deformation, when the source of distortion is removed. Most materials are following linear elasticity for small deformations and can be described by the Hooke's law stating that there is a linear relationship between tensile force applied to a spring and its displacement. It can be generalized to the following relationship between stress σ (or force applied) and strain ε (or deformation): $\sigma = E \times \varepsilon$, with E the elastic modulus or Young's modulus measuring the resistance to force of an object. For larger deformations, a material can enter in a viscoelastic regime where applied forces generate permanent changes in shape or size. This is particularly true for polymers considering monomer molecules can be displaced within the supramolecular structure which hence undergoes durable transformation. Stiffness is a physical quantity, different yet related to elasticity, defined as the amount of force required to cause a unit of deformation. Practically, these two parameters are often interchanged and most studies measure ECM elastic modulus E and refer as to stiffness. Ultimately, the persistence length is another mechanical parameter used to describe the stiffness of polymers such as collagen fibers, that directly relates to the elastic modulus using the

following equation: $P = \frac{E \times \pi \times r^4}{4 \times \kappa_B \times T}$ with P the persistence length, E the elastic modulus, r the radius of the polymer chain section, κ_B the Boltzmann constant and T the temperature. Substrate relative stiffness can be sensed by cells through a mechanism called mechanotransduction whereby a mechanical stimulus is transformed in an integrable biochemical signal by the cell (Fedorchak et al., 2014; Trichet et al., 2012). ECM stiffness has emerged as a key regulator of cell biology functions including cell differentiation or migration and differ greatly in different tissues (Ehrbar et al., 2011; Engler et al., 2006; Swift et al., 2013).

Additionally, matrix density and low porosity can limit the available space for the migrating cell body and in particular its largest and stiffest organelle, the nucleus (Wolf et al., 2013). Nuclear stiffness and deformability largely depend on expression levels of nuclear lamins as described in more details in the following chapter. Migrating cells can therefore adopt different strategies to overcome these physical limitations and facilitate their progression by adjusting their own intrinsic properties or modifying the adjacent ECM. For instance, immune surveillance necessitates immune cells to patrol within tissues, cross the endothelial BM and migrate into connective tissue. They do so due to their low expression levels of lamins resulting in a highly deformable nucleus that can squeeze to adapt BM constricting pores during entry or exit of blood vessels (Rowe and Weiss, 2008; Willis et al., 2013). On the other hand, migrating cells can exert forces on the ECM by pulling and pushing schemes to enlarge constricting space as matrix elasticity permits (Kraning-Rush et al., 2013; Wolf and Friedl, 2011). When ECM physical limitations exceed cells abilities to deform, migration involves ECM proteolytic remodeling based on the expression of membrane-tethered or soluble proteases including matrix metalloproteinases (MMPs), ADAMs (for a disintegrin and a metalloproteinase) or cathepsins that generate proteolytic tracks matching migrating cell diameter (Wolf et al., 2013; Wolf and Friedl, 2011). Molecular machineries underlying these mechanisms are further developed in **Chapters 3 to 5**.

2. Extracellular matrices modifications in breast cancer

2.1. *De novo matrix deposition and changes in composition*

Epithelial cells are in intimate contact with the ECM which provides a mechanical support and a biochemical context that are essential to several cell functions and more generally tissue homeostasis. ECM composition and organization are therefore tightly controlled in physiological condition but can undergo profound modifications during cancer development.

In turn, these changes can actively contribute to cancer progression by promoting cell migration and metastasis, thereby creating a positive feedback loop (Insua-Rodríguez and Oskarsson, 2016; Walker et al., 2018).

Significant changes in ECM composition occur during breast cancer progression including differential production and deposition of fibrillar type I, II and III collagen, fibronectin, proteoglycans or laminins (Insua-Rodríguez and Oskarsson, 2016; Malik et al., 2015). Fibronectin for instance is excessively produced by both cancer cells and cancer-associated fibroblasts (CAFs), corresponding to stromal cells transformed by the tumor microenvironment, and has been shown to promote carcinogenesis and cancer progression (Attieh and Vignjevic, 2016; Orimo and Weinberg, 2006). At the same time, the balance between laminin isoforms is altered: anti-tumorigenic laminin 111 is downregulated whereas pro-invasive laminins such as laminins 511 or 332 are produced and secreted in the stromal environment (Benton et al., 2009; Carpenter et al., 2009; Kusuma et al., 2012). Similarly, changes in ECM composition in glycoproteins and glycosaminoglycans can be observed with higher levels of hyaluronic acid and versican but lower levels of decorin or lumican as compare to homeostatic tissue (Insua-Rodríguez and Oskarsson, 2016; McAtee et al., 2014).

Altogether, accumulation of ECM components, termed desmoplasia (or fibrosis when not associated with cancer), and changes in ECM composition can affect cancer cells in many different ways. Beyond the conventional role of scaffold that facilitates cell migration, additional matrix deposition can also activate distinct intracellular signalling pathways or further stimulate previously activated pathways. Consequences of this activation are increased proliferation, loss of cell polarity, induction or reinforcement of the epithelial to mesenchymal transition (or EMT, **see Chapter 3**) and invasive capacities among others (Egeblad et al., 2010; Tzanakakis et al., 2018). Notably, ECM alterations can be associated with the formation of a metastatic niche and promote “stem pathways” favoring tumor cell survival in hostile environments in disseminated breast cancer cells (Oskarsson et al., 2011; Pein and Oskarsson, 2015). In addition, increased matrix deposition and modified organization are associated with extensive changes in biomechanical properties of the ECM.

2.2. Modifications of matrix biophysical properties

Accumulation of ECM in the tumor microenvironment promotes cancer progression and invasion as shown in the previous section but increased density of ECM components around the primary tumor is also forming a capsule-like physical barrier that may prevent dissemination in some cases (Fang et al., 2014). Coming along with novel ECM deposition, modifications of

the ECM biophysical properties including stiffness or alignment could explain this apparent paradox (Cox and Erler, 2011).

In vivo visualization of collagen fibers by second-harmonic generation (SHG) in breast cancer mouse models, and further observed in patient biopsies, have revealed unique stromal phenotypes correlating with different stages of cancer progression called tumor-associated collagen signatures (TACS) that are numbered from 1 to 3 (Conklin et al., 2011; Provenzano et al., 2008, 2006). TACS1 represent a physiological curly and anisotropic distribution of collagen fibers but slightly denser than the normal situation, occurring at very early stages of tumor formation. TACS2 corresponds to an accumulation of straight collagen fibers parallel to the tumor boundaries as tumor increases in size while TACS3 coincides with a strong reorientation of straight collagen fibers perpendicularly to the tumor front which corresponds to sites of local invasion (Provenzano et al., 2006) (**Figure 7**). Interestingly, TACS3 was described as an independent prognostic indicator for poor clinical outcome (Conklin et al., 2011). Aligned bundles of collagen fibers promotes cell migration both *in vitro* and *in vivo* and could serve as preferential tracks allowing contact guidance of cancer cells for dissemination to blood vessels in breast cancer (Gritsenko et al., 2012; Han et al., 2016; Sander, 2014). If mechanisms of local collagen fibers alignment remain largely elusive, CAFs and macrophages, together with cancer cells, may play a role in matrix and collagen reorganization (Ingman et al., 2006; Yang et al., 2011).

De novo matrix deposition and increased tissue density is often accompanied by enhanced stromal ECM stiffness and has been used in breast cancer detection based on higher risk of cancer development for increased mammographic densities (Boyd et al., 1998). ECM stiffness is partly due to enzymatic collagen crosslinking in breast cancer where LOX and the LOX family enzymes are frequently over-expressed (Barker et al., 2012; Erler et al., 2006). Extracellular LOX has been shown to participate in ECM alignment and crosslinking, which trigger cell adhesion to the matrix as well as signalling events, hence stimulating cells invasive capacities (Levental et al., 2009). Both ECM stiffening and alignment are significantly reduced upon LOX inhibition *in vivo* indicating a predominant role of enzymatic collagen crosslinking over non-enzymatic processes including glycosylation or transglutamination (Levental et al., 2009). Overall, changes in ECM composition, density and crosslinking status trigger a global stiffness increase in mammary tissue ranging from few hundreds of Pa (Pascals) in normal tissue to several kPa in the stiffest tumors (Butcher et al., 2009).

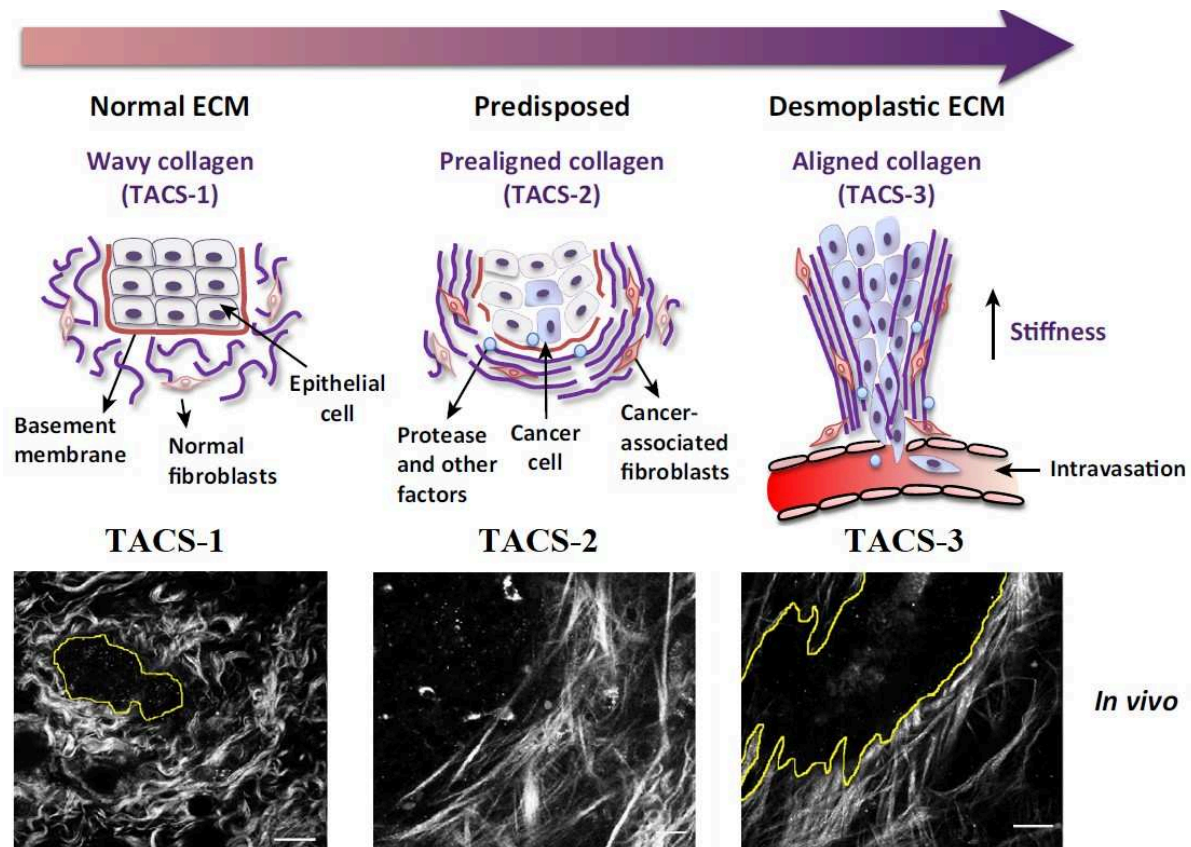


Figure 7: Stromal extracellular matrix remodeling during breast cancer progression

(**Top panel**) Schematic representations of ECM fibers remodeling at different stages of breast cancer progression, corresponding to *in vivo* observations partially recapitulated in bottom panel.

(**Bottom panel**) Second harmonic generation images of different tumor-associated collagen signature (TACS) in Wnt-1 mouse tumor model. TACS-1: region of curly but denser collagen around a non-palpable mass delineated in yellow. TACS-2: collagen fibers alignment parallel to tumor boundaries (on the left). TACS-3: alignment of collagen fibers perpendicular to tumor boundaries (depicted in yellow) at sites of cell invasion. Scale bar: 25 μ m.

Images adapted from Malik et al., "Biomechanical and biochemical remodeling of stromal extracellular matrix in cancer" *Trends Biotechnol.* (2015) 33(4), 230-236, and Provenzano et al., "Collagen reorganization at the tumor-stromal interface facilitates local invasion" *BMC Med* (2006) 4(1), 38.

2.3. Matrix remodeling

Multiple matrix-degrading enzymes support ECM proteolysis during critical developmental processes or wound healing but cancer cells can utilize and repurpose this machinery to favor cell invasion (Rowe and Weiss, 2008; Wolf and Friedl, 2011). Cancer development and progression are often associated with up-regulation of MMPs, ADAMs and other proteolytic enzymes (Kessenbrock et al., 2015; Rowe and Weiss, 2009). In breast cancer, overexpression of MMP14, also known as MT1-MMP (Membrane-Tethered-1 MMP), correlates with the progression from non-invasive DCIS to IDC lesions and is an essential

component of the BM transmigration program (Lodillinsky et al., 2015; Rowe and Weiss, 2008). However, it has been shown in colon cancer and in several developmental models that actin-based force production from transmigrating cells or assisting cells such as CAFs can replace to some extent MMP-based BM transmigration (Glentis et al., 2017; Kelley et al., 2014). Whether and how these processes can be transposed to breast cancer remain undetermined. In addition, during migration in the stromal environment, it is commonly believed that proteolysis is required against ECM components opposing cell movement when the cell body and its nucleus fail to accommodate matrix pore size (Wolf et al., 2013; Wolf and Friedl, 2011).

The role of matrix-degrading enzymes in promoting cancer progression and cell invasion is multi-faceted and not restricted to physical manipulation of the surrounding ECM by the well-described direct proteolytic activity (Kessenbrock et al., 2010). Indirect effects of proteases, not least of all MMPs, include the release of active growth or pro-angiogenic factors, chemokines and bioactive cleaved peptides that were embedded in the ECM scaffold and further contribute to tumor growth, inflammation or angiogenesis (Cowden Dahl et al., 2008; Sounni et al., 2010; Tatti et al., 2008). ECM components degradation can also indirectly reveal cryptic binding sites for cell receptors including integrins thus inducing pro-tumorigenic pathways (Hangai et al., 2002; Kessenbrock et al., 2015).

Overall, interactions of tumor cells with their surrounding microenvironment have emerged as crucial entry points for regulation and manipulation of several cancer hallmarks and an increasing number of studies attempted to take into account and recapitulate this interplay *in vitro* by reconstituting ECM constituents during the last decade.

3. *In vitro* reconstitution of extracellular matrices

3.1. *Reconstitution of basement membrane-like matrices*

Considering the importance of the BM to support and interact with almost every epithelium within the human body, many efforts have been produced to develop *in vitro* substrata mimicking native BMs. Naturally-derived or extracted materials have been first used to coat tissue culture dishes in order to study cell growth and migration, as well as interaction with and remodeling of the matrix. Among them, the widely used Matrigel (a trade name also known as Cultrex or EHS matrix) is a soluble extract of matrix proteins produced by tumor cells in the EHS (for Engelbreth-Holm-Swarm) sarcoma mouse model (Kleinman and Martin, 2005). A major interest of Matrigel resides in its reasonably similar composition, including

laminins, type IV collagen, nidogen and proteoglycans and structure when polymerized at 37°C, as compared to native BMs (Kleinman and Martin, 2005; Rowe and Weiss, 2008). In addition, polymerized Matrigel support cell adhesion, differentiation as well as proliferation and was therefore extensively used to specifically study cell-matrix interactions as well as matrix degradation by actin-rich pro-invasive structures named invadopodia (Hotary et al., 2006; Rowe and Weiss, 2008) (**Figure 8A**). Nevertheless, a higher proportion of laminins than of type IV collagen, as well as the absence of collagen crosslinking in comparison with native BMs have raised important limitations for the use of Matrigel in investigating cell invasion and transmigration (Rowe and Weiss, 2008; Willis et al., 2013). Furthermore, physical properties of BMs are not fully maintained as Matrigel exhibit reduced elasticity, potentially affecting interpretations of Matrigel-centered experiments on cell invasion (Candiello et al., 2007; Soofi et al., 2009).

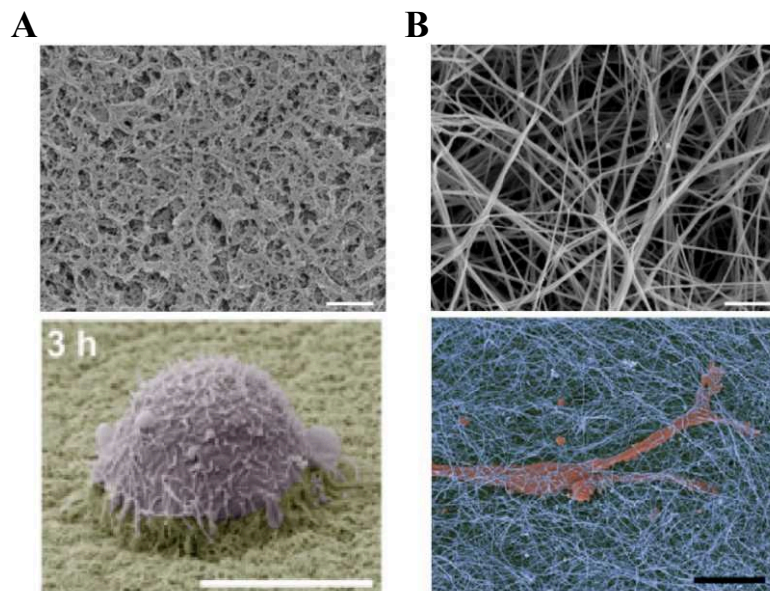


Figure 8: Comparison of cell invasion in Matrigel and type I collagen

(A) *Top panel:* Scanning electron microscopy image of polymerized Matrigel. Scale bar: 1 µm. *Bottom panel:* Scanning electron micrograph of MDA-MB-231 breast cancer cells invading through Matrigel at 3h. Scale Bar: 10 µm.

(B) *Top panel:* Scanning electron microscopy image of polymerized rat-tail acid-extracted type I collagen at 3 mg/mL. Scale bar: 1 µm. *Bottom panel:* Scanning electron micrograph of MDA-MB-231 cells invading through acid-extracted type I collagen at 6h. Scale bar: 10 µm.

Images adapted from Poincloux et al., “Matrix invasion by tumour cells: a focus on MT1-MMP trafficking to invadopodia” J Cell Sci. (2009) 122(17), 3015-3024, and Poincloux et al., “Contractility of the cell rear drives invasion of breast tumor cells in 3D Matrigel” Proc. Natl. Acad. Sci. U.S.A. (2011) 108(5), 1943-1948.

Another interesting approach has been the use of cell-free native peritoneal BM explants from mice or rats (Hotary et al., 2006; Rowe and Weiss, 2008; Schoumacher et al., 2013). This technique provides a self-assembling material that is known to allow cells trafficking *in vivo*, and is useable for *ex vivo* culture, yet do not permit high throughput experiments. Ultimately, a growing part of the recent literature has focused on developing synthetic hydrogels to mimic BMs in a more tuneable fashion. Hydrogels are covalently or non-covalently crosslinked polymer networks of polypeptides such as poly-(acrylic acid) (PAA), poly-(ethylene glycol) (PEG) or poly-(acrylamide) (PAAm) with highly adjustable mechanical properties including stiffness, crosslinking and density as well as controlled scaffold structure and chemical composition (Cruz-Acuña and García, 2017; Wisdom et al., 2018). Additionally, adhesive ligands or other growth factors can be bound to synthetic polymers hydrogels to further simulate native basement membrane characteristics (Cruz-Acuña and García, 2017; Zhu, 2010).

3.2. Reconstitution of interstitial matrices

Reconstitution of interstitial ECMs *in vitro* has been an equally challenging procedure given the extreme complexity to reconstitute the full biophysical and biochemical features of native ECMs. Considering that type I collagen is the principal component of ECMs, the most commonly used technique of ECM reconstitution has been the utilization of collagen extracts polymerized and coated on cell culture dishes (Sabeh et al., 2009, 2004; Willis et al., 2013). Type I collagen is extracted from rat tail tendon either by acid or enzyme, namely pepsin, extraction. Acid extraction allows the recovery of a relatively pure collagen that, when polymerized under specific pH, ionic and temperature conditions, exhibit more or less similar aspect and diameter of collagen fibers observed *in vivo* (Oldberg et al., 2007; Willis et al., 2013). Pepsin-extraction leave triple-helical domains intact but enzymatically remove collagen telopeptides required for collagen intramolecular crosslinking. Thus, upon polymerization, the collagen structure is slightly changed with larger collagen fibrils diameter and an increase pore size as compared to native collagen. These modifications affect cell invasive capacities with a faster and more importantly protease-independent cell migration in pepsin-extracted in comparison to acid-extracted collagen (Sabeh et al., 2009; Willis et al., 2013; Wolf et al., 2013). If enzyme-mediated extraction of collagen may be good to recapitulate loosely organized tissues *in vivo*, acid-extracted collagen remains the best way to study the engagement of matrix-degrading enzymes and structures during cell migration (**Figure 8B**).

Similar to BM reconstitution, synthetic hydrogels combined with different techniques of polymerization and deposition have recently been used to reconstruct stromal ECM with

tuneable characteristics (Ayres et al., 2010). Although non-degradable initially, bio-engineering have made these matrices progressively competent for proteases activity, most notably MMPs (Ehrbar et al., 2011; Frantz et al., 2010; Rosso et al., 2005). However, artificial matrices do not mimic the architecture of native collagen, particularly its pore size, and their physiological relevance to study cell migration remains debated. Alternatively, modifying the fabrication conditions of collagen extracted gels have been proposed to adjust biomechanical properties on purpose (Artym, 2016; Nuhn et al., 2018; Wolf et al., 2013).

3.3. Modulation of biophysical properties of reconstituted matrices

Accurately regulating biomechanical properties of reconstituted ECMs is crucial to study cell migration in conditions that recapitulate the extensive modifications experienced by ECMs during several processes including cancer. Simple variations in polymerizing conditions of type I collagen, including concentration of collagen or temperature of polymerization, have been shown to impact the resulting matrix pore size (Mickel et al., 2008; Wolf et al., 2013; Yang et al., 2010) (**Figure 9**).

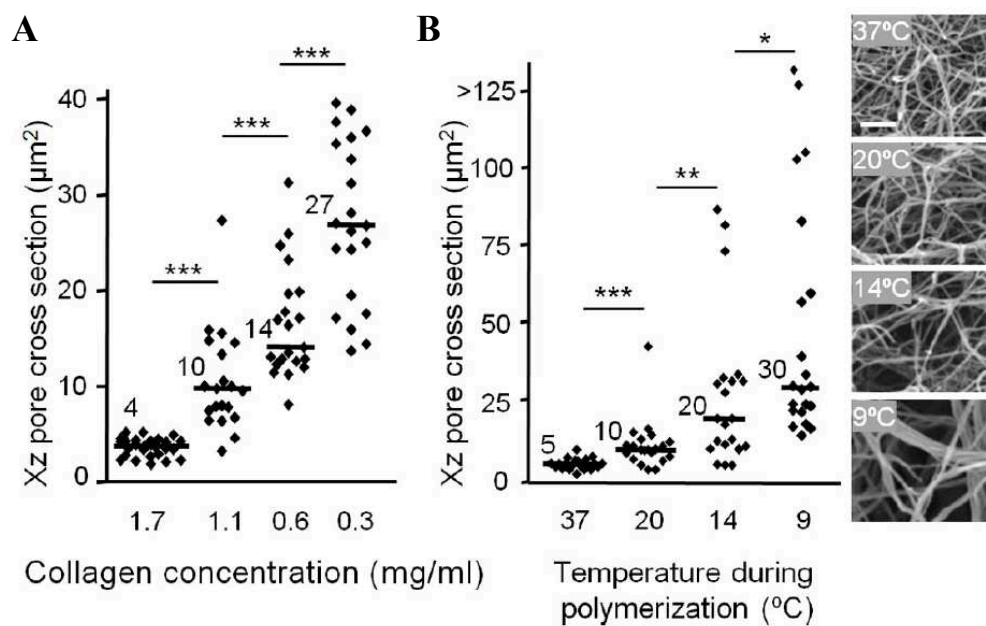


Figure 9: Effects of collagen concentration and temperature of polymerisation on pore size

(A) Quantification of pore cross-section in 3D rat-tail acid-extracted type I collagen gels of varying concentrations as indicated.

(B) Quantification of pore cross-section in 3D rat-tail acid-extracted type I collagen gels polymerized at varying temperatures, as indicated. Corresponding scanning electron microscopy images are shown on the right column. Scale bar: 1 µm.

Images adapted from Wolf et al., "Physical limits of cell migration: Control by ECM space and nuclear deformation and tuning by proteolysis and traction force" J Cell Biol. (2013) 201(7), 1069-1084.

In turn, migratory properties of invasive cells are affected in the sense that cells exhibit protease-independent (*i.e.* insensitive to MMPs inhibitors) migration in larger pore size matrices whereas MMPs activity is required in smaller pore size (Wolf et al., 2013). These results stressed out the fact that cancer cells can adapt their invasive properties to changing microenvironmental conditions and switch from one to another mode of migration, even though mechanisms underlying this transition remain largely elusive (Friedl and Wolf, 2010; Petrie et al., 2017; Wolf et al., 2003).

Modulation of collagen gel stiffness can also be achieved by tuning collagen concentration or crosslinking status. For the latter, incubation with recombinant or cell-derived LOX, but also induction of non-enzymatic glycation upon ribose or glucose treatment, lead to higher collagen crosslinking and ultimately stiffness increase (Levental et al., 2009; Mason et al., 2013). Additionally, manipulation of matrix fibers alignment has been implemented in several recent studies and correlated with cell directed migration (Fraley et al., 2015; Han et al., 2016; Nuhn et al., 2018). Altogether, experimental manipulations of ECM biophysical properties remarkably point out how invasive cells sense and respond to mechanical and chemical cues during cell migration (van Helvert et al., 2018).

Chapter 3: Mechanisms of cell migration

Much of our understanding of the fundamental mechanisms of cell migration comes from studies performed on single cells moving on stiff 2D substrata (typically glass or plastic). This simplistic experimental set-up provided a mechanistic paradigm for cell migration described hereafter. Cell migration is herein defined as the normal ability of cells to move in response to biochemical or biomechanical signals in contrast to cell invasion which is referring to an abnormal capacity to migrate within surrounding ECMs or tissues.

Cell migration is a sequential process whereby cells acquire a polarized morphology with distinct front and rear regions and translocate their body in a directed manner. At the leading edge, polymerization of actin filaments in structures including lamellipodia or filopodia constitute an active driving force to push forward the cell plasma membrane during the extension phase (Lauffenburger and Horwitz, 1996; Mattila and Lappalainen, 2008). Subsequently, engagement of adhesion receptors in cell-matrix contact sites formed in the newly extended protrusion mediates cell adhesion to the substrate (Parsons et al., 2010). Then, contraction of actomyosin cytoskeletal structures called stress fibers between front and rear adhesion regions triggers cell body translocation (Tojkander et al., 2012). Immediately following cell movement, release of adhesion contact sites at the back of the cell results in trail retraction and recycling of plasma membrane adhesion receptors to the leading edge (Ridley et al., 2003) (see **Figure 10**).

Progressive complexification of experimental models, together with the addition of a third dimension, led to the description of a vast diversity of cell invasion modes that differ from the initial paradigm to different degrees (Petrie and Yamada, 2016). The role as well as the regulation of intrinsic cellular components involved in cell migration and invasion, including adhesion receptors, the cytoskeleton, and the nucleus are described in the following sections.

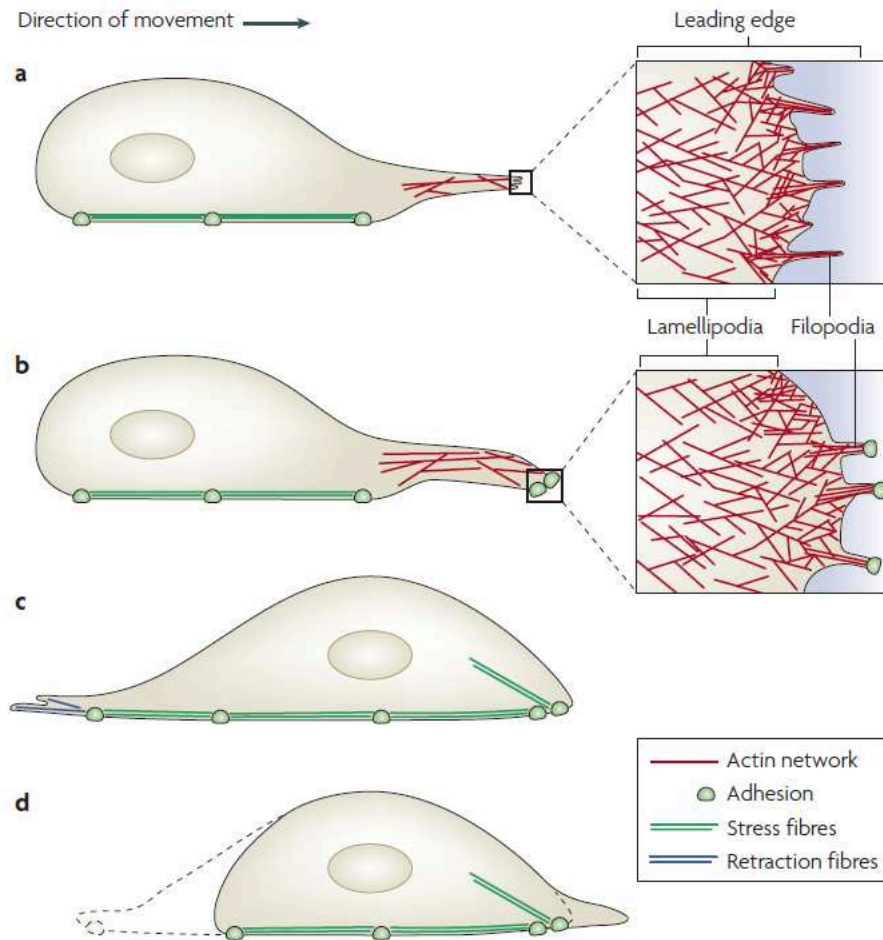


Figure 10: Cell migration: a multi-step process

Cell movement is initiated by actin polymerizing structures composed of lamellipodia and filopodia which extend a membrane protrusion at the cell leading-edge (**a**). New adhesions with the substratum are formed under the cellular protrusion (**b**). Upon actomyosin-based contraction between rear and front adhesions that are linked together with actin stress fibers, the nucleus and the cell body are propelled forward (**c**). Finally, disassembly of adhesion sites at the rear of the cell is followed by trailing edge retraction (**d**).

Images adapted from Mattila and Lappalainen, “Filopodia: molecular architecture and cellular functions” Nat. Rev. Mol. Cell Biol. (2008) 9(6), 446-454.

1. Cell-matrix interactions during cell migration

1.1. *Integrin-mediated adhesion to the extracellular matrix*

In every cellular process, the biological context given by the surrounding extracellular environment influences cell fate and behavior. Transmembrane receptors located at the cell surface detect and transmit various extracellular signals such as soluble molecules (for example growth factors or chemokines), but also ECM ligands, from the extracellular space to the cell cytoplasm and act as front-line regulators of processes including but not limited to cell differentiation, proliferation or migration. The vast majority of cell migration modes requires

adhesion to the ECM which is mediated by different ECM receptors most notably integrins, receptor tyrosine kinases (RTKs) or glycoprotein receptors.(Pandya et al., 2017).

Integrins are strict heterodimers composed of one α -chain and one β -chain from respectively 18 and 8 known isoforms in mammals. To date, 24 different types of integrins have been described with various tissue-specific expression and a large diversity of ECM ligands ranging from laminins, vitronectin and fibronectin to collagens (Humphries et al., 2006). Integrins are exposed at cell surface either in a close and inactive conformation or in an active form resulting from a conformational switch induced by the intracellular attachment of talin to integrin cytoplasmic tail that is mandatory for subsequent binding to ECM ligands. (Hamidi and Ivaska, 2018). Following integrin activation, engagement with ECM molecules drives the recruitment and the assembly of multiple protein complexes to form supramolecular structures of more than 150 proteins called focal adhesions (FAs). During migration, integrin-mediated adhesions serve both as physical anchors linking the cell cytoskeleton to the ECM and as regulating hubs for downstream signalling events in a process called “outside-in” signalling (Hamidi and Ivaska, 2018; Huttenlocher and Horwitz, 2011) (**Figure 11**).

In particular, talin, vinculin, zyxin and α -actinin proteins physically connect actin filaments with integrins engaged with the ECM. At the leading edge, this bridge allows small and highly dynamic nascent adhesions to function as molecular clutches by counteracting rearward actin flow induced by cell membrane resistance against actin polymerization, allowing cell membrane to protrude forward (Elosegui-Artola et al., 2016; Parsons et al., 2010; Swaminathan and Waterman, 2016). In addition, larger focal complexes and FAs forming with stabilization of integrin clusters connect both ends of large actin bundles or stress fibers at cell front and rear to allow the forward propulsion of the cell body upon actomyosin-mediated traction forces (Huttenlocher and Horwitz, 2011; Livne and Geiger, 2016; Parsons et al., 2010). Adhesion complexes are also important in 3D cell migration and share some similarities, particularly their general composition, with their 2D alter-egos (Cukierman et al., 2001; Doyle and Yamada, 2016). However, slight changes in integrins content, with $\alpha 5$ integrin predominantly found in 3D environment for instance, and in focal adhesion size as well as exact role in regulating cell speed have been observed (Doyle et al., 2015; Fraley et al., 2010). Alternatively, integrins have been involved in other adhesion structures during migration in 3D collagen gels based on tube-like arrangement of clathrin/adaptor protein 2 (AP-2) complexes (Elkhatib et al., 2017).

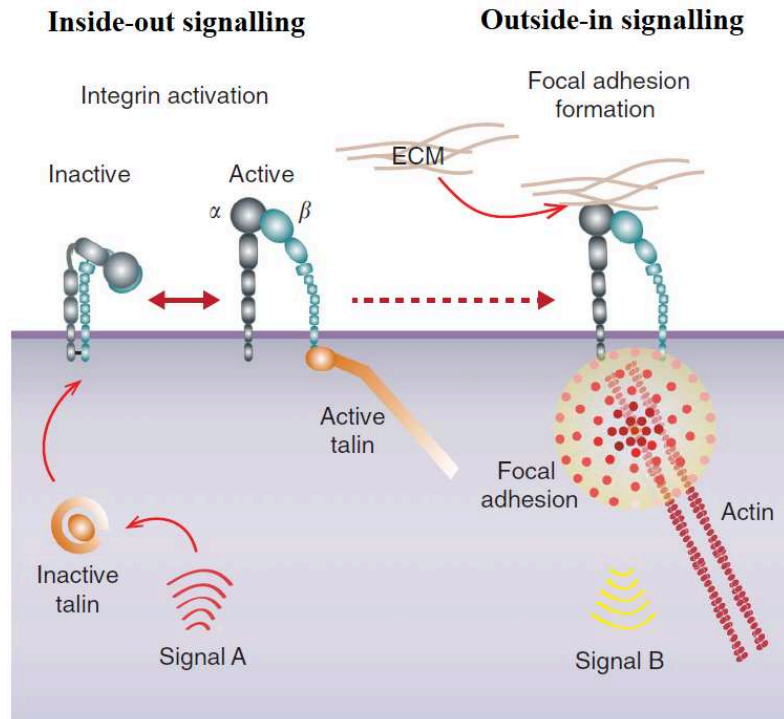


Figure 11: Integrins bi-directional signalling mechanisms

Binding of talin to integrin cytoplasmic tail (signal A) triggers integrin activation by promoting integrin open conformation in an *inside-out signalling*. This conformation favors integrin interaction with ECM ligands which induces focal adhesion formation, actin cytoskeletal reorganization and affects downstream cellular pathways (signal B) in an *outside-in signalling*.

Images adapted from Hamidi et al., "The complexity of integrins in cancer and new scopes for therapeutic targeting" Br. J. Cancer. (2016) 115(9), 1017-1023.

Dynamic formation and turnover of these integrin-based adhesions are essential for cell migration and intimately linked to cell speed. Polarized trafficking and recycling of integrin receptors to the cell leading edge is therefore tightly regulated (De Franceschi et al., 2015; Paul et al., 2015b). Hence, dysregulation of integrin activity or trafficking is associated with different pathological disorders including cancer where integrins have been implicated in every step of the metastatic cascade (De Franceschi et al., 2015; Muller et al., 2009). In cancer cells, negative regulatory loops are often perturbed, and integrins binding to ECM ligands can potentially induce critical signalling pathways promoting cell proliferation, survival or invasion. Similarly, cross-talks between growth factor receptors and integrins have been involved in carcinogenesis as well as in the transition from non-motile to invasive cancer cells (Bianconi et al., 2016; Hamidi and Ivaska, 2018). Considering the integrin family diversity, their role is frequently tumor-type specific, with $\beta 1$ integrins overexpression mostly participating in breast carcinogenesis for instance, and in some cases remains controversial (Cagnet et al., 2014; Pan et al., 2018; Parvani et al., 2013; Ramirez et al., 2011).

1.2. Additional matrix receptors involved in tumor cell invasion

Although substantial attention has been dedicated to integrins, studies have also highlighted the role of other ECM receptors in cell invasion, including discoidin domain receptors (DDRs) and glycoprotein receptors such as selectins, syndecans or CD44. DDR1 and DDR2 belong to the RTKs family, and contain a cytoplasmic catalytic tyrosine kinase domain able to undergo autophosphorylation, together with a juxtamembrane domain, and two extracellular domains, namely discoidin and discoidin-like domains, binding to ECM ligands (Rammal et al., 2016). Upon dimerization, DDR2 binds to native and mostly fibrillar collagen (in particular types I, II and III) while DDR1, which consists of five different isoforms, can bind to a broader collagen spectrum including fibrillar but also non-fibrillar type IV, V or VI collagens (Fu et al., 2013b; Leitinger, 2003; Vogel et al., 1997). Of note, DDR receptors do not bind to denatured collagen, *i.e.* gelatin (Leitinger, 2014, 2003). In both cases, attachment to collagen triggers receptor autophosphorylation, recruitment of diverse Src Homology domain 2 (SH2)- and phosphotyrosine binding (PTB) domain-containing proteins regulating different aspects of cell behavior including proliferation, ECM adhesion and remodeling, and migration (Henriet et al., 2018; Leitinger, 2014; Rammal et al., 2016). Importantly, DDRs expression is often dysregulated in diseases including cancer where somatic mutations in DDR genes have been associated with several types of cancer (Toy et al., 2015; Valiathan et al., 2012). More specifically, in cell invasion, DDRs have often been linked with MMPs as well as matrix degrading structures including invadopodia, illustrating potential cross-talks between DDRs and cells matrix-degrading machinery to promote cell invasion (Fu et al., 2013a; Juin et al., 2014; Majkowska et al., 2017). However, consequences of DDRs mutations or differential expression are extremely context- and tissue-dependent as both DDR1 and DDR2 have been implicated in pro- and anti-invasive effects in cancers (Castro-Sanchez et al., 2010; Hansen et al., 2006; Koh et al., 2015; Zhang et al., 2013).

Many other ECM receptors have been implicated in specific aspects of cancer cell invasion. Selectins, which are transmembrane glycoproteins binding to proteins containing carbohydrates groups, allow leukocytes to arrest and extravasate from blood vessels in inflammation and can be exploited by cancer cells to promote extravasation and metastasis (Barthel et al., 2007; Bendas and Borsig, 2012). Syndecans are transmembrane proteins binding to ECM components such as fibronectin or collagen through GAGs that are involved in cancer progression either directly by inducing various signalling networks, or indirectly after cleavage by MMPs and release of active soluble peptides in a process called shedding (Barbouri et al.,

2014; Vuoriluoto et al., 2011; Wiesner et al., 2010; Yang et al., 2011). Altogether, these observations point out the critical role of cell adhesion to the ECM in fundamental mechanisms of migration and invasion.

1.3. Mechanical interplay in cell-matrix interactions

In parallel with adhesion, direct interactions by cell surface receptors with ECM ligands provide migrating cells the ability to mechanically sense but also respond to physical cues from the surrounding environment. This bidirectional relationship between cells and the ECM, termed mechanoreciprocity, is composed of two distinct parts. A mechanosensing part whereby cells perceive different physical properties of the ECM such as stiffness, architecture (including alignment and topology) or crosslinking, and an active mechanical feedback under which cells develop pushing and pulling schemes to remodel surrounding matrix and achieve migration (van Helvert et al., 2018).

Mechanosensing of cell-matrix interactions substantially rely on integrins as receptors together with mechanosensitive proteins and the actin cytoskeleton while highly analogous systems with cadherins in place of integrins are involved in cell-cell interactions (Leckband and de Rooij, 2014; Sun et al., 2016). Multiple proteins of the FA complex can unfold and change conformation upon increased tension including actin binding proteins such as talin or vinculin, and signalling molecules such as focal adhesion kinase (FAK) and p130Cas. Stretching of talin upon force reveals additional binding sites to actin and vinculin, leading to vinculin recruitment and reinforcement of the integrin-actin bond (Jahed et al., 2014; Sun et al., 2016). Similarly, unfolding of FAK and p130Cas upon mechanical stress switches on various signalling cascades leading to direct response through cytoskeleton re-organization via modulation of Rho-GTPases (for guanine triphosphatases), or long-term feedback with signal transduction to the nucleus and modification of genes expression (Guilluy et al., 2011; Sun et al., 2016; Swaminathan et al., 2016). In addition, recent studies have shown that cells mechanosensitivity to matrix stiffness depends on the previously mentioned mechanism of integrin-mediated molecular clutch (Chan and Odde, 2008; Elosegui-Artola et al., 2016; Plotnikov et al., 2012). On stiff substrates, forces produced by actin polymerization and actomyosin trigger talin stretching leading to vinculin recruitment and concomitant reinforcement of actin-integrins bonds with increasing tension. In contrast, on soft substrates, internal forces fail to induce talin and subsequent vinculin unfolding but rather stretch the compliant substrate. With increasing tension, integrin-ECM linkages eventually reach their breaking strength and detach leading to less stable FAs (Case and Waterman, 2015; Chan and Odde, 2008) (**Figure 12**). Stiffness

sensing is of particular importance in migration where cells can sense variations of matrix stiffness and exhibit oriented migration toward stiffer substrates, a process called durotaxis (Plotnikov et al., 2012). Simultaneously, mechanisms of recognition and integration of ECM alignment and topology by migrating cells remain less clear and are only starting to be explored (Ray et al., 2017; Starke et al., 2014; Tabdanov et al., 2018).

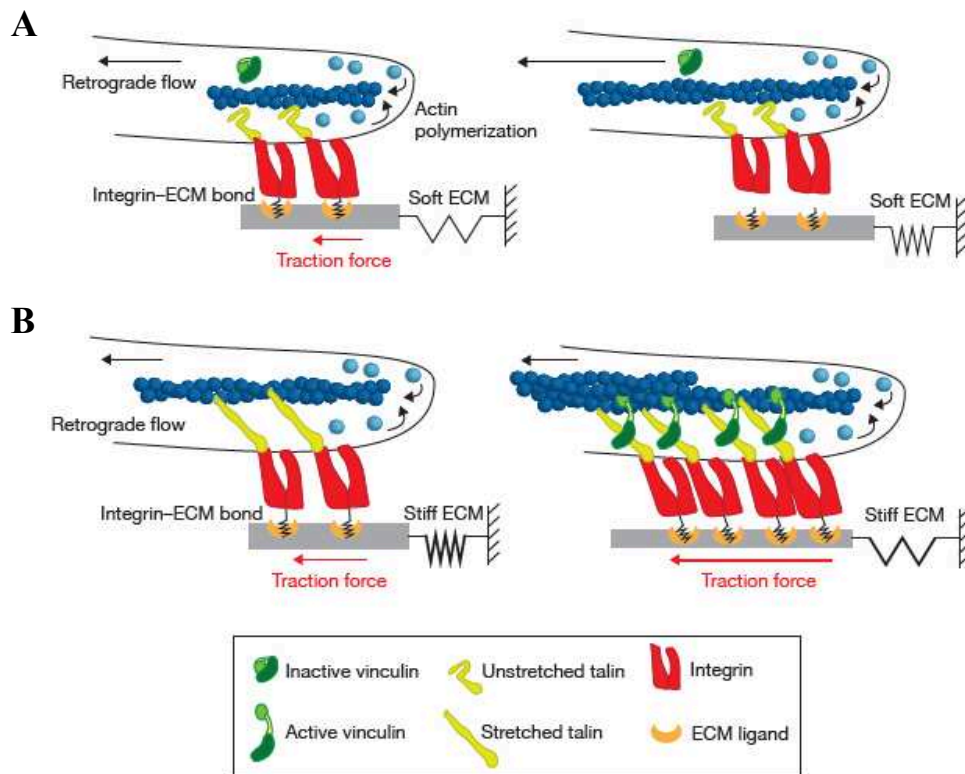


Figure 12: Integrin-mediated molecular clutch and its role in mechanosensing

(A) On soft substrates the integrin-ECM bond dissociates before talin unfolding and vinculin binding because of the slow load transmission due to substrate compliance.

(B) On stiff substrates, fast load transmission to the ECM by integrins results in talin unfolding and vinculin binding, therefore inducing the reinforcement of actin-mediated traction forces.

Images adapted from Swaminathan and Waterman, "The molecular clutch model for mechanotransduction evolves" Nat. Cell Biol. (2016) 18(5), 459-461.

Mechanical responses from cells are mediated through the actin cytoskeleton and similarly transmitted to the ECM through adhesion receptors in an outside-in force transmission. Pulling forces mediated by myosin contraction and pushing forces arising from actin polymerization can therefore physically rearrange the ECM scaffold during cell migration and are discussed in following sections. (Beningo et al., 2006; Blanchoin et al., 2014). Matrix remodeling can further involve matrix proteases cell surface exposition or secretion to degrade ECM components, thus increasing matrix deformability and compliance (Kirmse et al., 2011; van Helvert et al., 2018).

2. Multi-pronged roles of cell cytoskeletal networks during cell migration

2.1. *Function and regulation of actin polymerizing structures*

The actin cytoskeleton is involved in virtually all cellular processes ranging from cell division, control of cell morphology, intracellular trafficking or cell movement. Actin can organize into a wide variety of cellular structures providing cells a real toolbox to adapt to different situations. Specifically, migration and invasion require tightly organized and spatio-temporally regulated actin machineries across the cell body (Blanchoin et al., 2014).

Actin is a globular protein that can assemble in double-stranded helical filaments when it is bound to adenosine triphosphate (ATP). After polymerization, actin-bound ATP is hydrolysed into adenosine diphosphate (ADP) and phosphate (Pi) which can slowly dissociate from the filament (Pollard, 2016). Actin filaments have two asymmetric ends with respect to elongation rates, respectively the barbed end polymerizing around 10 times faster than the pointed end (Pollard, 2016). The initial nucleation stage is thermodynamically unfavorable and represents the rate-limiting step of actin polymerization. Once trimers are assembled, actin filaments elongate depending on the concentration of available actin monomers. However, actin filament assembly can be potentiated by nucleation factors including actin-related protein 2/3 (Arp2/3) complex and formins. In migrating cells, actin structures polymerized via the Arp2/3 complex are found in the lamellipodium, or in pro-migratory invadosome structures, while filopodia are formins-mediated actin structures (Blanchoin et al., 2014). Availability of soluble actin monomers is regulated by profilin, a small protein that binds to actin monomers with high affinity and both catalyses the exchange of ADP with ATP and favors polymerization induced by nucleation factors at actin filaments barbed ends (Pollard and Borisy, 2003).

Lamellipodia are arranged as sheets of complex actin networks formed by Arp2/3-driven actin polymerization beneath the plasma membrane of the cell leading edge (Svitkina and Borisy, 1999). Arp2/3 complex is composed of seven subunits including Arp2 and Arp3 and is responsible for the formation of branched actin networks. Briefly, Arp2/3 complex connects the side of a pre-existing so-called mother actin filament and initiate a daughter filament with an angle of approximatively 70°. The initiation step occurs via conformational changes in the Arp2 and Arp3 subunits leading to the formation of a dimer able to template actin filament assembly (Pollard, 2016; Rouiller et al., 2008). Arp2/3 complex activation requires nucleation-promoting factors belonging to the Wiskott-Aldrich syndrome protein (WASP) family which are themselves activated by different actin regulators including small Rho GTPases. In the lamellipodium, membrane-bound Rac GTPase together with phospholipids activate the WAVE

(WASP family verprolin homologous protein) complex which in turn interacts with and activates Arp2/3 at the cell leading edge (Campellone and Welch, 2010; Chen et al., 2010) (see **Figure 13A**). In 3D, elongated migrating cells do not exhibit a large and well organized lamellipodium *per se*, but rather present long and highly dynamic protrusions composed of branched actin, to extend and retract at the cell leading edge. Branched actin networks can also be found in invadosomes where Arp2/3 activation is mediated through the neural-WASP (N-WASP) complex activated by the membrane-attached Rho GTPase cell division control protein 42 homolog (Cdc42) and other proteins described in **chapter 5** (Oser et al., 2009). Accumulation and polymerization of Arp2/3-mediated side branches in close proximity with a surface result in force production, a mechanism underlying plasma membrane forward protrusion in the lamellipodia, invadosomes or migrating cell membrane protrusions (Blanchoin et al., 2014; Mogilner and Oster, 2003; Prass et al., 2006; Sibony-Benyamini and Gil-Henn, 2012; Svitkina, 2018).

On the other hand, filopodia are thin protrusions extending beyond cell front edge to probe and sense the extracellular environment during migration. They are composed of parallel actin bundles with growing ends facing towards the plasma membrane (Blanchoin et al., 2014; Mattila and Lappalainen, 2008). The molecular mechanisms of filopodia initiation are not fully understood but parallel actin filaments can emerge either from convergent elongation of Arp2/3-generated networks, or direct polymerization of actin filaments initiated by formins together with proteins from the enabled/vasodilator-stimulated phosphoprotein (Ena/VASP) family (Mattila and Lappalainen, 2008; Yang and Svitkina, 2011). Formins are composed of two formin homology domain (FH1 and FH2). FH1 recruits and stabilizes actin monomers bound to profilin while FH2 interacts and remains attached to actin filament barbed ends promoting processive actin filament assembly (Paul and Pollard, 2009). In parallel, Ena/VASP proteins prevent the attachment of capping proteins, further enhancing elongation of actin filaments (Edwards et al., 2014; Mattila and Lappalainen, 2008). An essential stage of filopodia generation and maintenance is the subsequent crosslinking of parallel actin filaments by fascin to form tight and rigid actin bundles. (Mattila and Lappalainen, 2008; Vignjevic et al., 2006) (see **Figure 13B**). Similar to Arp2/3-based actin networks, actin incorporation in parallel filaments composing filopodia is able to generate pushing forces against the membrane leading to protrusion (Cojoc et al., 2007; Kovar and Pollard, 2004). Considering that the molecular mechanisms initiating filopodia formation are still debated, there is no clear consensus on how these structures are regulated even though Rho GTPases, including Cdc42, are likely to be involved (Mattila and Lappalainen, 2008; Yang and Svitkina, 2011).

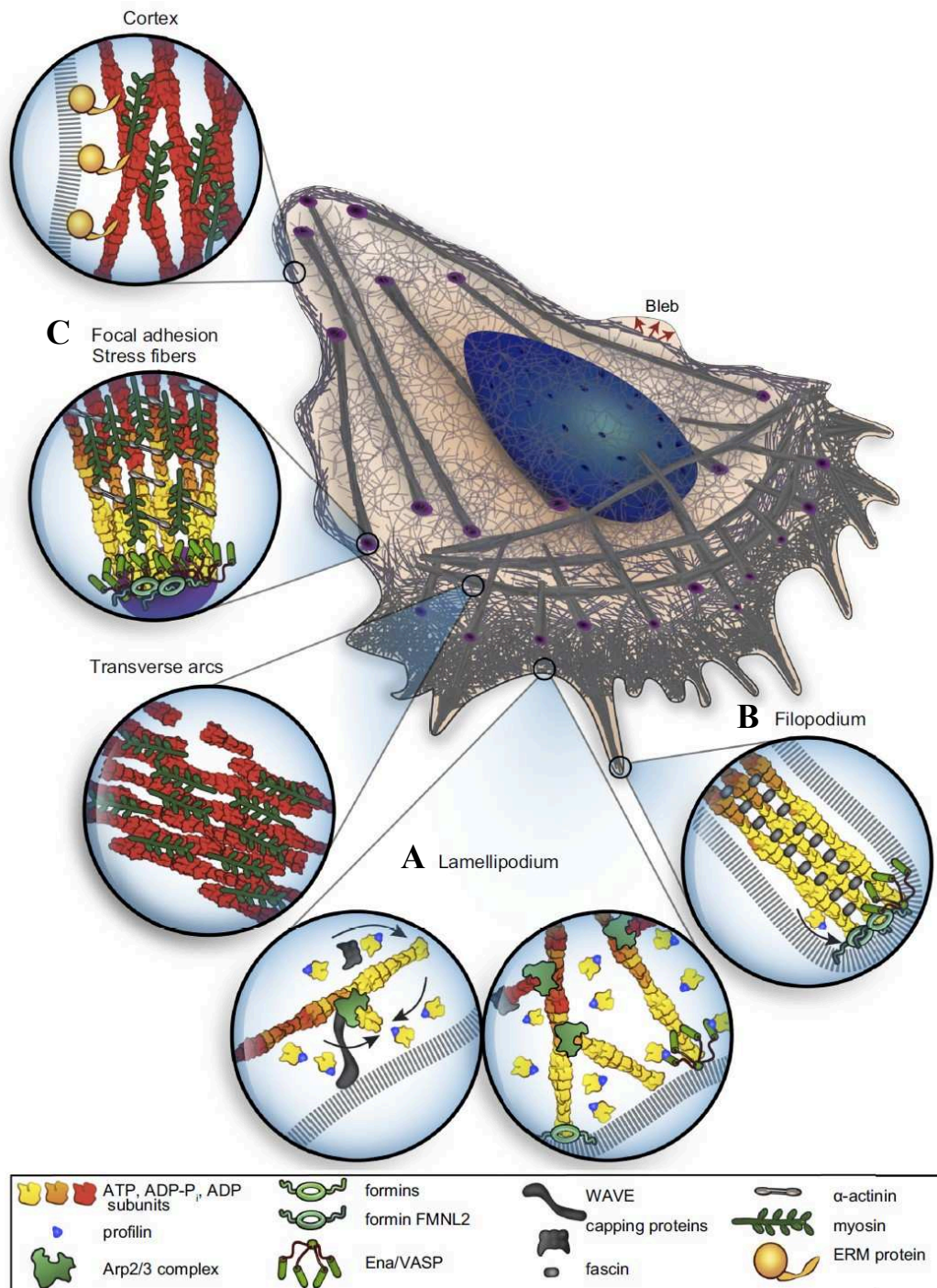


Figure 13: Specialized actin structures in motile cells

Different specialized and functional actin structures localize in various cell locations.

(A) The cell lamellipodium consist of Arp2/3 complex mediated branched actin networks pushing forward the plasma membrane to support migration.

(B) Formins together with multiple other proteins generate parallel networks of actin filaments that are the structural basis of filopodia structures specialized in sensing of the extracellular environment.

(C) Stress fibers are contractile bundles of actin filaments connecting focal adhesion complexes at cell edges. Myosin localizes along these filaments where it can contract to trigger rear retraction and cell body translocation.

*Images adapted from Blanchoin et al, "Actin dynamics, architecture, and mechanics in cell motility" *Physiol. Rev.* (2014) 94(1), 235-263.*

Overall, actin polymerizing structures are the driving forces of membrane protrusion in cells and therefore play a prominent role in migration. In addition, migrating cells display and require dynamic contraction and retraction activities to move forward but also to squeeze in case of confined migration. Specific actin structures, working in close association with contractile motors are underlying such processes.

2.2. Contribution of contractility in cell movement

Actin-based motors are grouped in the myosin superfamily and subdivided into several classes involved in a wide range of cellular processes including cargo trafficking, cytokinesis after cell division or contraction in muscles. Class II myosins are responsible for contraction forces in tissues (in muscles for instance), but also at the cellular level in every eukaryotic cell (Conti and Adelstein, 2008; Hartman and Spudich, 2012). In particular, non-muscle myosin II (NM II) has been extensively connected to the regulation of cell adhesion and migration (Pecci et al., 2018; Vicente-Manzanares et al., 2009). NM II is composed of three pairs of peptides, two heavy chains (or MHC) and four light chains (or MLC) consisting of two essential light chains (ELC) stabilizing myosin structure and two regulatory light chains (RLC) controlling NM II activity. MHC are comprised of N-terminal globular domains, followed by neck regions connecting with MLC, and a long helical coiled-coil rod used for dimerization of two heavy chains (Vicente-Manzanares et al., 2009). MHC globular heads bind to ATP and undergo reversible conformational changes upon ATP hydrolysis, therefore transforming chemical energy into mechanical work (Heissler and Sellers, 2016; Vicente-Manzanares et al., 2009). NM II C-terminal rod domains can associate together to form myosin bipolar filaments and produce opposing forces when attached to anti-parallel actin filaments therefore provoking contraction (Shutova and Svitkina, 2018). NM II is activated by phosphorylation of RLC by several kinases including myosin light chain kinase MLCK, Rho-associated coiled-coil containing kinase ROCK and citron kinase (Burgess et al., 2007). The Ca^{2+} -calmodulin axis controls MLCK activation while small GTPase Rho A activates both ROCK and citron kinase (Lawson and Ridley, 2018; Narumiya et al., 2009; Vicente-Manzanares et al., 2009).

In migrating cells, NM II is present in stress fibers, consisting of crosslinked bundles of actin fibers connecting peripheral FAs, and triggers forward propulsion of the cell body in parallel with retraction of the trailing edge (Vicente-Manzanares et al., 2007) (see **Figure 13C**). More recently, actomyosin activity has been associated with the formation of a different type of cell protrusion involved in cell migration, termed cellular blebs (Charras and Paluch, 2008).

Cell plasma membrane is usually maintained under tension by a thin layer of actin and actin-associated proteins termed cell cortex. Occasionally, actomyosin contractility in the cortex increases hydrostatic pressure and separates the plasma membrane from the cortex inducing a spherical protrusion called membrane bleb (Bergert et al., 2012; Goudarzi et al., 2012; Maugis et al., 2010). Bleb retraction occurs by the recruitment of proteins tethering cell plasma membrane and cortex thus decreasing intracellular pressure (Charras and Paluch, 2008). Cycles of bleb expansion and retraction enable cell movement by exerting forces on the substrate to push forward the cell membrane independently of actin polymerization (Charras and Paluch, 2008; Lorentzen et al., 2011; Paluch and Raz, 2013). This strategy of migration is particularly used in some confined or 3D migration modes whereby, together with low degree of cell-matrix adhesion, invading cells efficiently squeezed in free spaces (Bergert et al., 2015; Charras and Paluch, 2008). Similarly, NM II-based contractility in association with the nucleus, used as a piston, is able to significantly enhance cytoplasmic intracellular pressure to form a unique bleb triggering cell motility, a strategy called lobopodial migration (Petrie et al., 2017, 2014). Contractile forces are also required to directly compress the nucleus and promote translocation during confined migration, a process that can be harmful for its integrity as described in **section 3.2** (Hatch and Hetzer, 2016; Lammerding and Wolf, 2016)

Overall, actomyosin-driven contractility plays a crucial role in cell movement that is likely to be most prominent in 3D migration as studies performed in NM II-deficient cells have shown that, despite reduced traction forces, depleted cells are able to migrate on 2D substrata but not in 3D (Jorrich et al., 2013; Shih and Yamada, 2010; Vicente-Manzanares et al., 2009).

2.3. Role of microtubules during cell migration

If actin alone seems to be sufficient for migration of some cell types, including small leukocytes, another cytoskeletal network composed of microtubules (MTs) is further involved in epithelial cells or fibroblasts locomotion and particularly important for directed migration (Bouchet and Akhmanova, 2017; Etienne-Manneville, 2013; Keren et al., 2008). MTs consist of heterodimers of α - and β -tubulin assembling longitudinally into protofilaments that associate laterally to form hollow tubes. MTs are polarized structures with a slow growing (-)-end where α -tubulin is facing outward and a fast growing (+)-end where β -tubulin is exposed (Akhmanova and Steinmetz, 2015; Etienne-Manneville, 2010). MTs polymerization occurs when tubulin heterodimers are bound to GTP and alternates between disassembly phases called “catastrophes” or shrinkages subsequent to GTP hydrolysis into GDP leading to more instability and rescue phases resulting in MTs growth (Akhmanova and Steinmetz, 2015). In mammalian

cells, the MT network is spatially organized via one or several MT-organizing centers (MTOCs), generally the centrosome, which is localized close to the nucleus at the cell center (Etienne-Manneville, 2013; Vinogradova et al., 2009). MT-associated proteins (MAPs) and motors are implicated in most MTs functions in the cell, ranging from trafficking and organelle positioning to cell division and migration (Etienne-Manneville, 2010).

Theoretically, MT polymerization can generate a force able to deform and push forward the plasma membrane similar to actin (Etienne-Manneville, 2013; Mogilner and Oster, 2003; Ridley et al., 2003). Except in few cell types such as neurons or astrocytes where drug-induced MT depolymerization results in strong inhibition of cell protrusion, very few MTs are present in cells lamellipodia suggesting a limited role in generating membrane protrusion (Etienne-Manneville, 2013). Additionally, targeted delivery of proteins and extra-membrane by exocytosis is essential for polarized migration and strongly relies on MTs (Gierke and Wittmann, 2012; P. M. Miller et al., 2009). MTs (+)-ends are in close proximity with the cell leading edge, where (+)-ends tracking proteins (+TIPs) mediate a physical interaction with anterior structures including FAs, and play an essential role in their regulation and turnover (Etienne-Manneville, 2013; Paul et al., 2015b; Stehbens and Wittmann, 2012). MTs-associated motors are able to deliver Rho GTPases together with their activating guanine nucleotide exchange factor (GEF) protein including Rac and Cdc42 at the cell migrating front, therefore locally controlling actin assembly (Etienne-Manneville, 2013; Osmani et al., 2010; Petrie et al., 2012). Actomyosin contractility is also sensitive to MTs-dependent signalling through RhoA activation (Chang et al., 2008; Rhee et al., 2007).

Furthermore, in directed migration, the whole MT network is asymmetrically distributed with an accumulation of MTs directed toward the front edge as a consequence of the establishment of a nucleus-centrosome axis aligned with the direction of migration. Albeit the underlying molecular mechanisms are not fully understood, the centrosome is located in front of the nucleus in most migrating cells, including fibroblasts and epithelial cells, while it is situated at the rear in small immune cells (Luxton and Gundersen, 2011). In the former, it is thought that anchoring or transient attachment of MTs at the cell leading edge, possibly through FAs, combined with the activity of the MTs (-)-end directed motor dynein pull the centrosome anteriorly in the direction of migration (Dujardin et al., 2003; Etienne-Manneville, 2013; Etienne-Manneville and Hall, 2001; Luxton and Gundersen, 2011). In parallel, MT-attached dynein and its regulator Lis1 localize around the nucleus surface and may provide pulling forces able to drag the nucleus towards the centrosome in the direction of migration. Indeed, interfering with either dynein function or the physical connection between cell cytoskeleton and

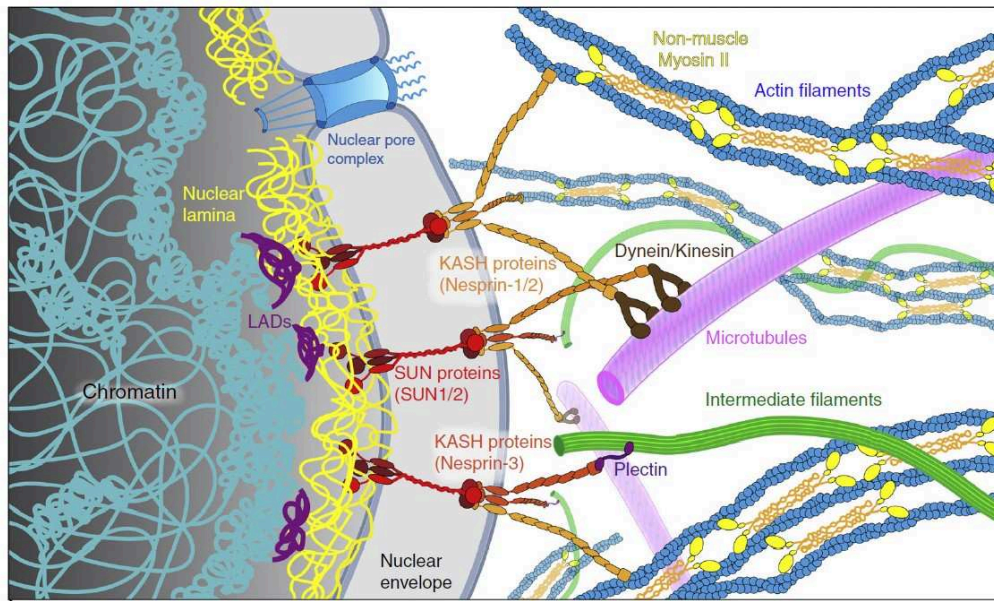
the nucleus, affect nucleus movement, in particular during 3D neuronal migration but also in 2D migration of fibroblasts (Dujardin et al., 2003; Luxton et al., 2010; Tsai et al., 2007; Zhang et al., 2009). Altogether, these observations highlight the various functions of MTs in promoting cell migration in concert with the actin cytoskeleton. It also points out the essential link between cell cytoskeleton and the nucleus, the biggest and stiffest cell organelle, in particular in confined cell migration.

3. Nucleus function and biomechanics during 3D cell migration

3.1. *Cytoskeleton to nucleus force transmission during migration*

Profound cytoskeletal reorganization, partially described in precedent sections, allows cells to move their entire body with minimal constraints on planar surfaces. However, migration in 3D results in increased physical limitations due to complex matrix organization and restricted free space for cell translocation. In this context, the limited deformability of the nucleus, which represents the biggest and stiffest organelle in the cell, can impede cell movement (Davidson et al., 2014; Friedl et al., 2011; Wolf et al., 2013). Nuclear rigidity and deformability depend on the nuclear lamina, composed of lamin proteins, that form a dense and protective proteinaceous meshwork underneath the inner nuclear membrane. Most cells express both A-type lamins, predominantly lamins A and C deriving from alternative splicing of the LMNA gene, and B-type lamins, principally B1 and B2 from LMNB1 and LMNB2 genes respectively (Davidson and Lammerding, 2014). Lamins assemble in homodimers through their coiled-coil rod domains, that further associate in filaments by head-to-tail and lateral interactions. The different types of lamin filaments form distinct, potentially interpenetrating, fibrous networks underlying the nuclear envelope (NE) (Davidson and Lammerding, 2014; Kolb et al., 2011) (**see Figure 14A**). Nucleus stiffness strongly scales with A-type lamins expression levels, and cells with reduced lamins A/C levels exhibit increased motility in confined 3D migration due to higher nuclear deformability (Harada et al., 2014; Lammerding et al., 2006; McGregor et al., 2016). Lamins levels are therefore critically regulated and vary greatly depending on cell types but also on the environmental conditions suggesting cells could dynamically adjust their nuclear stiffness during migration, even though the underlying molecular mechanisms remain to be determined (Buxboim et al., 2014; Ihalainen et al., 2015; Swift et al., 2013). Notably, large nuclear deformations associated with migrating cells with reduced lamins A/C levels also correlate with a drop in cell survival indicating that lamins protect nuclear content against physical alterations arising from confined migration (Harada et al., 2014).

A



B

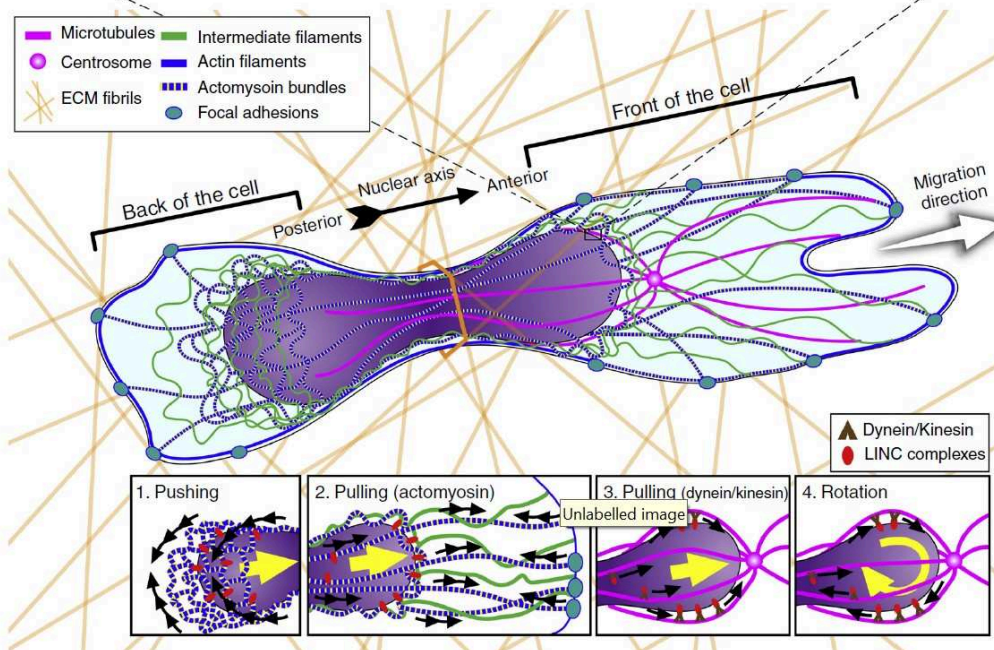


Figure 14: Overview of nucleus-cytoskeleton interactions and their mechanical interplay during confined migration

(A) Cell cytoskeleton interact with the nucleus through direct interactions with KASH proteins or through adaptors including plectin (IFs) or dynein and kinesin (MTs). KASH bind to SUN proteins in the internuclear space, which themselves connect the nuclear lamina, to form the LINC complex. Nuclear chromatin can interact with lamins through their lamin-associated domains (LADs).

(B) During confined migration, actomyosin contraction promotes nuclear deformation by pushing forces when exerted at cell rear (1), or pulling forces together with IFs in the front (2). MTs-associated motors located on the NE, most notably dynein, apply pulling tension on the nucleus (3) or rotations (4). These physical stimuli are transmitted to the nucleus via the LINC complex and may trigger different mechanotransduction events or compromise NE integrity.

Images adapted from McGregor et al, "Squish and squeeze-the nucleus as a physical barrier during migration in confined environments" Curr. Opin. Cell Biol. (2016) 40, 32-40.

Nuclear deformations likely result from the passive physical resistance of the ECM that translates into compressive forces on the cell body, as well as from active traction forces generated and transmitted by the cytoskeleton to the nucleus of migrating cells (Friedl et al., 2011; Lombardi and Lammerding, 2011). Nucleo-cytoskeletal coupling is mediated by proteins from the linker of nucleocytoskeleton and cytoskeleton (LINC) complex that spans inner and outer membranes of the NE and physically connect the nuclear lamina with cytoskeletal networks (Gundersen and Worman, 2013; Liu et al., 2016; Sosa et al., 2013). It comprises inner nuclear membrane (INM) Sad1 or UNC-84 (SUN) proteins and outer nuclear membrane (ONM) Klarsicht, ANC-1 and SYNE/Nesprin-1 and-2 Homology (KASH) proteins interacting together within the perinuclear space (Sosa et al., 2013; Starr and Fridolfsson, 2010) (see **Figure 14A**). Out of the five genes encoding SUN proteins in mammals, only SUN 1 and SUN 2 are widely expressed. They consist in a nucleoplasmic N-terminus domain binding to lamins (lamin A for SUN 1 and SUN 2), a single transmembrane domain and a conserved C-terminus known as the SUN domain, binding to KASH proteins in the perinuclear space (Gundersen and Worman, 2013; Starr and Fridolfsson, 2010). Meanwhile, six KASH proteins have been described in mammals, namely Nesprins 1 to 4 with several isoforms, KASH5 and LRMP (or lymphoid-restricted membrane protein) characterized by a conserved KASH domain at their C-terminus, including a segment of their single transmembrane domain and the peptide residing in the perinuclear space (Sosa et al., 2013). N-termini domains of KASH proteins greatly vary in size and bind to different cytoskeletal elements therefore determining LINC complex specificity. In particular, Nesprins 1 and 2, that are extremely large proteins exceeding 800 kDa, can bind both actin cytoskeleton via calponin homology domains, and MT motors such as kinesin-1 and dynein (Antoku et al., 2015; Chang et al., 2015; Yu et al., 2011; Zhang et al., 2009). Intermediate filaments can also connect to the nucleus through the crosslinking protein plectin that binds to Nesprin 3 while Nesprin 4 binds to kinesin-1 and MTs (Roux et al., 2009; Wilhelmsen et al., 2005). This physical link enables cytoskeleton-based force transmission to the nucleus, including pulling forces by frontward actomyosin contractility or MT-associated motors and pushing schemes through rearward actomyosin contractility (Petrie et al., 2014; Thiam et al., 2016; Thomas et al., 2015; Tsai et al., 2010; Wu et al., 2014) (see **Figure 14B**).

3.2. Nuclear mechanical stresses during migration: from mechanosensing to DNA damage

Mechanical stresses and deformations of the nucleus emanating from the cytoskeleton and the passive resistance from the matrix trigger various biological consequences. These

include regulation of signalling and gene expression as it has recently become apparent that the nucleus is a key mechanosensitive organelle able to respond to physical stimuli (Fedorchak et al., 2014; Wang et al., 2009). Mutations in lamins genes, in particular LMNA, cause a variety of diseases called laminopathies presenting, among others, defects in mechanosensing capacities (Chambliss et al., 2013; Cupesi et al., 2010; Osmanagic-Myers et al., 2015; Schreiber and Kennedy, 2013). Comparable mechanosensing defects were observed when interfering with the LINC complex, most notably silencing of Nesprins, indicating a critical role of the LINC complex in force transmission to the nucleus (Banerjee et al., 2014; Chancellor et al., 2010; Isermann and Lammerding, 2013). Recently, several studies have shown that mechanical stimuli can be transformed in biochemical signalling by the nucleus. For instance, physical tension transmitted through Nesprin 1 to isolated nuclei induces the phosphorylation of the INM protein emerin through Src kinase activation, resulting in reinforcement of laminA/C and SUN proteins interactions and a local increase in nuclear stiffness (Guilluy et al., 2014). Similarly, lamin A/C organization and phosphorylation status, potentially affecting accessibility for protein interactions, including transcription factors, and gene regulation, have been correlated to changes in cytoskeletal tension or in ECM stiffness (Buxboim et al., 2014; Ihalainen et al., 2015). Other mechanochemical conversion mechanisms involve changes in genes expression that can originate from stress-induced changes in chromatin organization and accessibility to transcription factors (Hernandez et al., 2016; Kim and Wirtz, 2015; Le et al., 2016; Wang et al., 2009). If these emerging molecular mechanisms governing nuclear responses to mechanical stimulation are likely to be of paramount importance in many cellular processes and tissue functions, their effective role during cell migration remains elusive so far (Aureille et al., 2017).

On the other hand, physical stresses applied on the nucleus may generate extensive nuclear deformations and compromise NE integrity, with potential dramatic consequences for genome stability (Bell and Lammerding, 2016). Two recent studies reported that cells migrating in constricting environment, including collagen gels and microfluidic devices with pore size diameter below few micrometers, experience local NE ruptures (Denais et al., 2016; Raab et al., 2016). NE breakdowns occasion uncontrolled cytoplasm-nucleoplasm trafficking, exposing nuclear DNA to cytoplasmic nucleases eventually leading to DNA damage. These damages are promptly repaired by DNA repair system and NE resealed using cells endosomal sorting complexes required for transport-III (ESCRT-III) complexes but inhibition of these machineries is often lethal or lead to important genomic alterations (Denais et al., 2016; Irianto et al., 2017a; Raab et al., 2016). Interestingly, NE breakages are frequently observed in mutated or low-lamin A/C expressing cells due to enhanced nuclear fragility and cell survival drops

following constricted migration, indicating that sensitivity to nuclear stresses could somehow scale with LMNA levels (De Vos et al., 2011; Harada et al., 2014; Irianto et al., 2017a; Vargas et al., 2012). Lamins but also DNA repair machineries are frequently dysregulated in tumor cells and migration may therefore further promote genomic and genetic instability, possibly contributing to cancer progression (Bell and Lammerding, 2016). In parallel, interfering with matrix proteolysis by inhibition of MMPs coincides with increased nuclear deformations as well as NE collapses, suggesting that MMP-based matrix degradation could prevent, or release, mechanical tension exerted on the nucleus during migration (Denais et al., 2016; Wolf et al., 2013, 2007) (see **Figure 15**).

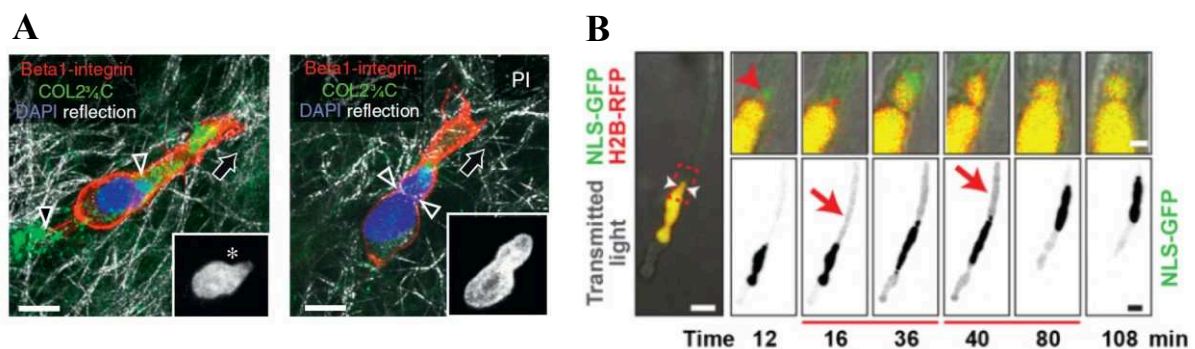


Figure 15: Effects of matrix proteolysis inhibition on nuclear deformations during confined migration

(A) HT-1080 fibrosarcoma cells overexpressing MT1-MMP exhibit increased nuclear deformation (blue, and insets) when migrating in 3D fibrillar collagen (gray) in the presence of a protease inhibitor cocktail (right) as compared to normal condition (left). $\beta 1$ integrin (red) indicates cell edges while COL2^{3/4}-C (green), which recognizes a cleaved collagen epitope, shows a strong proteolytic activity in front of the nucleus (left) or a residual activity at the site of deformation (right) (white arrowheads). Black arrows point out the direction of migration. Scale bar: 10 μ m.

(B) HT-1080 cells expressing NLS-GFP (Nuclear Localization Sequence, green) and H2B-RFP (Histones, red) display NE ruptures during migration in collagen gel with MMPs inhibitor. NE ruptures are visualized with green signal leaking from nuclear interior into cell cytoplasm (bottom panel, red arrows). Top panel insets show nuclear bleb formation (red arrowheads) prior NE rupture. White arrowheads indicate minimal nuclear diameter. Scale bars: 10 μ m, insets: 2 μ m.

Images adapted from Wolf et al., "Extracellular matrix determinants of proteolytic and non-proteolytic cell migration" Trends in Cell Biology. (2011) 21(12), 736-744, and Denais et al., "Nuclear envelope rupture and repair during cancer cell migration" Science (2016) 352(6283), 353-358.

A proper balance between nuclear deformability and ECM confinement, tuned by lamins levels, matrix proteolysis and cell cytoskeleton activity, is hence required for efficient cell migration in restricted 3D environments. Several modes of migration combining these different parameters have been employed and adapted depending on environmental conditions by invasive cancer cells and are further described below.

4. Cancer cell invasion: different strategies of tumor cell migration

4.1. *Collective versus individual invasion*

Active cell migration is fundamental to various physiological processes including morphogenesis, immune surveillance and response, but also tumor dissemination and metastasis where it is termed invasion (Friedl and Wolf, 2010). *In vivo* cell invasion mostly occurs in three-dimensional (3D) connective tissue and exhibits a large variety of migratory strategies going from single cell to multicellular collective invasion (Clark and Vignjevic, 2015; Friedl and Gilmour, 2009) (see **Figure 16**). Individual invasion requires cells to lose epithelial features such as cell-cell adhesion and gain invasive characteristics involving strong cytoskeleton reorganization, modification of cell to matrix adhesion and in certain cases expression and secretion of matrix proteases. These aspects are further developed in subsequent paragraphs.

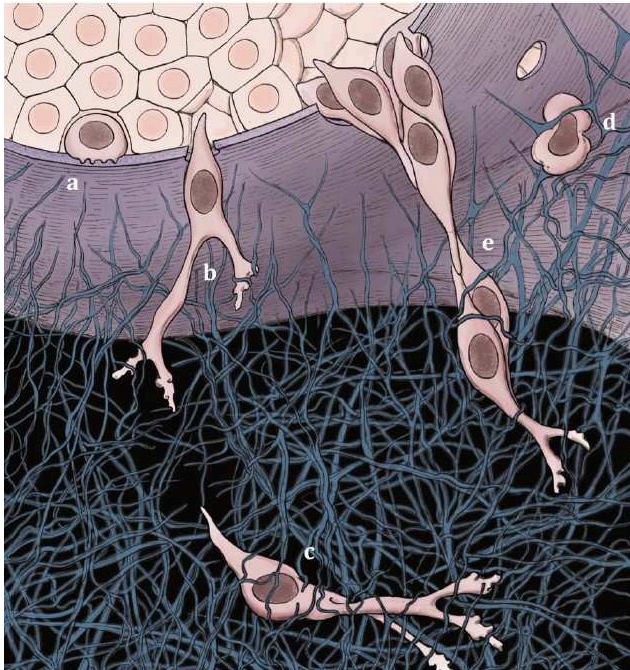


Figure 16: Different modes of cell invasion

To escape the primary tumor, cancer cells degrade and breach the basement membrane by matrix-degrading enzymes (a-b) before invading through the stroma. Cell invasion can be an individual (c-d) or a collective process (e). Single cells migrate using either an elongated-mesenchymal mode with strong cell-matrix adhesion contacts and ECM proteolysis (c) or a rounded-amoeboid type of migration with low cell-matrix adhesion but high cell contractility and deformability (d).

Image adapted from Poincloux et al, "Matrix invasion by tumour cells: a focus on MT1-MMP trafficking to invadopodia" J Cell Sci. (2009) 122(17), 3015-3024.

Collective modes of invasion imply coordinated and directed movement of groups from two to several hundred of cells. It can refer to multicellular streaming when cells are attracted by chemokines or follow a specific ECM architecture and move one after each other using the same track within the tissue. In this case, migrating cells are not maintaining cohesive contact with neighboring cells and can display any individual invasive mode (Friedl and Alexander, 2011; Kedrin et al., 2008). In contrast, tumor budding involves clusters of 5 to 10 adherent cells moving in close vicinity of the tumor front mass (Bronsert et al., 2014; Grigore et al., 2016). Additionally, collective cell invasion entails large groups of cells maintaining long-term cell-

cell adhesions that can even form lumen if epithelial polarity is preserved among migrating cells (Nabeshima et al., 1999; Wolf et al., 2007). It is also characterized by a cellular hierarchization with leader cells composing the front edge of the multicellular group and presenting mesenchymal migratory features and follower cells presenting strong cell-cell adhesions that are passively dragged along the migration track by leader cells. Collective invasion modes, except for multicellular streaming, are typically slower than individual invasion modes but it has been proposed that the large cell mass could secrete pro-migratory factors as well as matrix proteases in high amounts, protect inner cells from immune clearing or migratory-based stresses and support invasion of cells with low motility, thereby promoting overall tumor invasion (Pandya et al., 2017; Wolf et al., 2003). Noticeably, cancer cells display remarkable capacities to adapt to different extracellular environments and switch from one invasion mode to another depending on the microenvironment structure together with cell intrinsic properties such as matrix adhesion or actomyosin contractility (Friedl and Wolf, 2010; Petrie and Yamada, 2016).

4.2. Different modes of individual cell invasion

Cancer cells invading individually in the extracellular microenvironment can also exhibit different strategies of invasion. The two most widely used modes of single cell invasion are the elongated mesenchymal mode and the rounded amoeboid mode (Pandya et al., 2017). They can be easily distinguished by, and were first defined based on, profound morphological differences in invading cells. Cells using amoeboid invasion have a spherical-shape and squeeze into pre-existing spaces between matrix components as a result of high actomyosin contractility mediated by the activation of Rho and its downstream effector ROCK (Sahai and Marshall, 2003; Sanz-Moreno et al., 2008). Together with low degree of cell-matrix adhesion and low cell membrane attachment to cortex, cell contractility enables cell movement by membrane blebbing that push forward the cell body (Bergert et al., 2015; Charras and Paluch, 2008). Importantly, it has been shown that this mode of invasion is very rarely associated with matrix proteolysis but instead requires a highly deformable cell body and nucleus to constrict and translocate within matrix-free spaces (Wolf et al., 2003). However, the fact that these experiments used permissive pepsin-extracted collagen (**see chapter 2**) as a substrate somehow restrict the biological relevance of these findings. Amoeboid movement is extensively used by migrating immune cells but have also been observed by intravital imaging in melanoma and breast cancer xenograft models (Giampieri et al., 2009; Madsen and Sahai, 2010; Pinner and Sahai, 2008). Other uncommon individual modes of migration have been recently described

such as the lobopodial mode of migration in fibroblasts and fibrosarcoma cells, which relies on an intracellular pressure-based protrusion generated actomyosin contractility in front of the nucleus as described above (Petrie et al., 2017, 2014). Besides, a filopodia spike-based invasion mode have also been described in carcinoma cells based on the formin FHOD3 and independent of Arp2/3 complex activity (Paul et al., 2015a).

On the other hand, invasive cells can adopt an elongated morphology involving actin-rich protrusions and strong cell-matrix adhesion structures at the front leading edge which characterized a mesenchymal mode of invasion (Polette et al., 1998; Wolf et al., 2003). Expression of cell surface or secretion of matrix proteases for focalized matrix degradation in the invasive front generating small tracks or tunnels within the ECM is typically associated with mesenchymal invasion (Friedl and Wolf, 2009). Furthermore, strong focal adhesions (FAs) limit mesenchymal cells velocity resulting in slower speed as compare to amoeboid migration (Sanz-Moreno et al., 2008). Normal fibroblasts, as well as most tumor cells originating from connective tissues display a mesenchymal mode of migration, but epithelial carcinoma cells can also do so when they undergo epithelial to mesenchymal transition (EMT) (Friedl and Wolf, 2009).

4.3. The epithelial to mesenchymal transition

EMT is a biological process whereby epithelial cells are losing part of their epithelial features to gain mesenchymal characteristics including increased migratory capacities and resistance to cell death or apoptosis. Cells can undergo EMT during developmental events such as gastrulation or neural crest formation, in wound healing or injury, but also in cancer progression where EMT is often associated with the first stages of cancer cells invasiveness and metastasis (Hanahan and Weinberg, 2011; Kalluri and Weinberg, 2009; Thiery et al., 2009). Phenotypically, EMT is characterized by the loss of adherent junctions and cell polarization, a deep reorganization of the cell cytoskeleton and the acquisition of a spindle-shaped morphology, as well as the expression of matrix proteolytic enzymes, which altogether lead to an increased motility (Kalluri and Weinberg, 2009; Peinado et al., 2004). At the molecular level, EMT main feature is considered to be the partial or total loss of E-cadherin expression, while levels of N-cadherin increase (Peinado et al., 2004). In addition, cytoskeletal organization is profoundly changed with cytokeratin proteins downregulation replaced by mesenchymal intermediate filaments vimentin as well as activation of proteins involved in invadopodia structures (Eckert et al., 2011; Hugo et al., 2007). Higher expression of matrix-degrading

enzymes, particularly MMP-2 and MMP-9 is also observed and enable ECM remodeling to promote cell invasion (Lee et al., 2008; Lin et al., 2011; Radisky et al., 2005).

EMT can be induced by multiple extracellular factors including transforming growth factor β (TGF- β), fibroblast growth factor (FGF), hepatic growth factor (HGF), epidermal growth factor (EGF), platelet-derived growth factor (PDGF) as well as the activation of Wnt and Notch signalling proteins (Devarajan et al., 2012; Nakamura et al., 2011; Strutz et al., 2002; Xu et al., 2009). Among these, TGF- β which is thought to be the major regulator of EMT, is secreted by fibroblasts, immune cells and macrophages as well as cancer cells themselves that can increase their production of active TGF- β during cancer progression (Hanahan and Weinberg, 2011; Xu et al., 2009; Zarzynska, 2014). TGF- β binding to its receptor induces a phosphorylation cascade leading to the formation of the SMAD complex consisting of SMAD 2, 3 and 4 proteins. The complex then translocates into the nucleus where it can bind multiple transcription factors and regulate expression levels of other transcription factors including Snail 1/2/3 proteins, Zeb and Twist (Lv et al., 2013; Papageorgis et al., 2010; Valcourt et al., 2005). These transcription factors govern the EMT differential transcriptional program by modulating the expression of different sets of genes, including E-cadherin or MMPs as mentioned above, that can overlap to some extent (Moreno-Bueno et al., 2006; Saunders and McClay, 2014).

EMT is a reversible process and cells can undergo the opposite transformation, called mesenchymal to epithelial transition (MET), to reacquire epithelial features (Thiery et al., 2009). This mechanism is proposed to support metastasis implantation in distant organs, where mesenchymal-like cancer cells go through MET to seed into secondary tissues after invasion and dissemination (Gunasinghe et al., 2012; Yang and Weinberg, 2008).

Chapter 4: Invadopodia, cancer cells cutting weapons for matrix degradation

Matrix proteolysis is required in numerous physiological processes, particularly in wound healing or in mammary and bone development and involves specialized actin-rich structures generically named invadosomes. Similarly, several modes of cancer cell invasion described above critically rely on cells ability to degrade the ECM resulting in tumor cells hijacking of normal proteolytic machinery.

1. Podosomes and invadopodia: two faces of the same coin?

1.1. Discovery of invadosomes and their nomenclature

The first description of invadosomes came from a study on transformed fibroblasts published in 1980. In this work, the authors inoculated Rous-sarcoma viruses (RSV) in normal fibroblasts and observed by immunofluorescence a relocalization of several proteins associated with peripheral FAs, including vinculin and α -actinin, to clusters of round patches mostly found on the ventral surface of the cells, which they termed rosettes (David-Pfeuty and Singer, 1980). Further observations defined rosettes as discrete membrane protrusions enriched in actin filaments resulting in profound plasma membrane and actin cytoskeleton reorganization upon RSV-mediated transformation (Tarone et al., 1985). Finally, another important piece of work showed that these structures were ECM contact sites and display significant degradative capacities when cells are cultured on top of fibronectin-coated dishes (Chen, 1989; Chen et al., 1984). These additional features served as foundations to establish a definition of invadosomes as actin-enriched dynamic protrusions forming at cell-ECM contacts that support proteolytic activity (Gimona et al., 2008; Linder et al., 2011; Murphy and Courtneidge, 2011).

At that time, these structures were successively termed podosomes, for their analogy with cellular feet, and invadopodia for their specific degradative and invasive characteristics (Chen, 1989; Murphy and Courtneidge, 2011; Tarone et al., 1985). Furthermore, if initial findings were made in transformed cells, other groups also identified comparable structures in normal cells including osteoclasts, macrophages and dendritic cells (Linder, 2007; Marchisio et al., 1987; Zamboni-Zallone et al., 1988). A recent consensus clarifying the nomenclature emerged and specified the use of podosomes for normal cells, invadopodia for cancer cells and invadosomes as a generic term referring to both collectively (Murphy and Courtneidge, 2011; Paterson and Courtneidge, 2017).

1.2. Cell type and substrate specificity of invadosomes

Despite their high similarity, podosomes and invadopodia differ in few features including morphology, dynamics as well as biological function. Their molecular composition, further described in next sections, is also not completely identical even though most components are shared (Buccione et al., 2009; Linder, 2007). Podosomes form in normal cells and display various morphologies and sizes depending on the cell type. Macrophages and smooth muscle cells, produce numerous (around a hundred or more) dot-like podosome structures with an actin core surrounded by adhesion proteins, generally localized at the periphery of the cell, that can cluster and organize together in suprastructures (Burgstaller and Gimona, 2005; Linder et al., 2011, 1999; Meddens et al., 2016). In osteoclasts, highly motile clusters or rings of podosomes eventually stabilize at cell edges in a belt-like structure (Destaing et al., 2003; Saltel et al., 2008). Finally, endothelial cells exhibit typical circular rosette structures composed of interconnected podosomes that remain stable overtime and display a fixed diameter of around 10 μm (Moreau et al., 2003; Osiak et al., 2005) (**see Figure 17A**). Podosomes generally present a protrusive actin-core surrounded by an adhesion ring consisting of integrins, FA-related proteins and myosin (Bhuwania et al., 2012; Joosten et al., 2018; Linder and Wiesner, 2016; van den Dries et al., 2013). As a result of their high number and important turnover (few minutes lifetime), podosome structures usually present a broad yet superficial proteolysis of the underlying matrix (Linder et al., 2011). In contrast, cancer cells tend to form fewer and smaller discrete actin dots usually situated in the cell center that are able to regroup and merge overtime (**see Figure 17B**). These so-called invadopodia are less dynamic than podosomes and can remain stable for more than an hour. Additionally, invadopodia display important focal degradative capacities resulting in local but deep ECM degradation (Linder et al., 2011; Schoumacher et al., 2010). Transformed fibroblasts exhibit an in-between phenotype with structures reminiscent of small rosettes yet associated with strong proteolysis (Abram et al., 2003). Differences in matrix degradation between invadosomes may result from their distinct dynamics, with more stable structures being more degradative as a consequence of the time required for matrix dissolution by proteases.

Another important parameter that determines and regulates invadosome formation and morphology is the extracellular matrix. Most studies on invadosomes have been relying on observations of cells cultured on Matrigel or denatured collagen (*i.e.* gelatin). These assays constitute powerful tools to define invadosome molecular constituents as well as analyzing BM remodeling and indeed reproduce with good accuracy what was observed on native BM later

on (Schoumacher et al., 2013, 2010). However, they are limited in reconstituting physiological stromal matrix because of their two-dimensionality, as well as composition and stiffness. To overcome some of these limitations, recent studies have used type I fibrillar collagen as a substratum to show that *bona fide* invadosomes form as linear non-protrusive structures along collagen fibers and therefore called this new class linear invadosomes (Juin et al., 2014, 2012; Monteiro et al., 2013) (see **Figure 17C**). Few studies have addressed the question of the third dimension by embedding cells in type I collagen or Matrigel and observed finger-like membrane protrusions enriched in actin filaments able to degrade the surrounding matrix in both normal and cancer cells (Furmaniak-Kazmierczak et al., 2007; Lizárraga et al., 2009; Van Goethem et al., 2011, 2010).

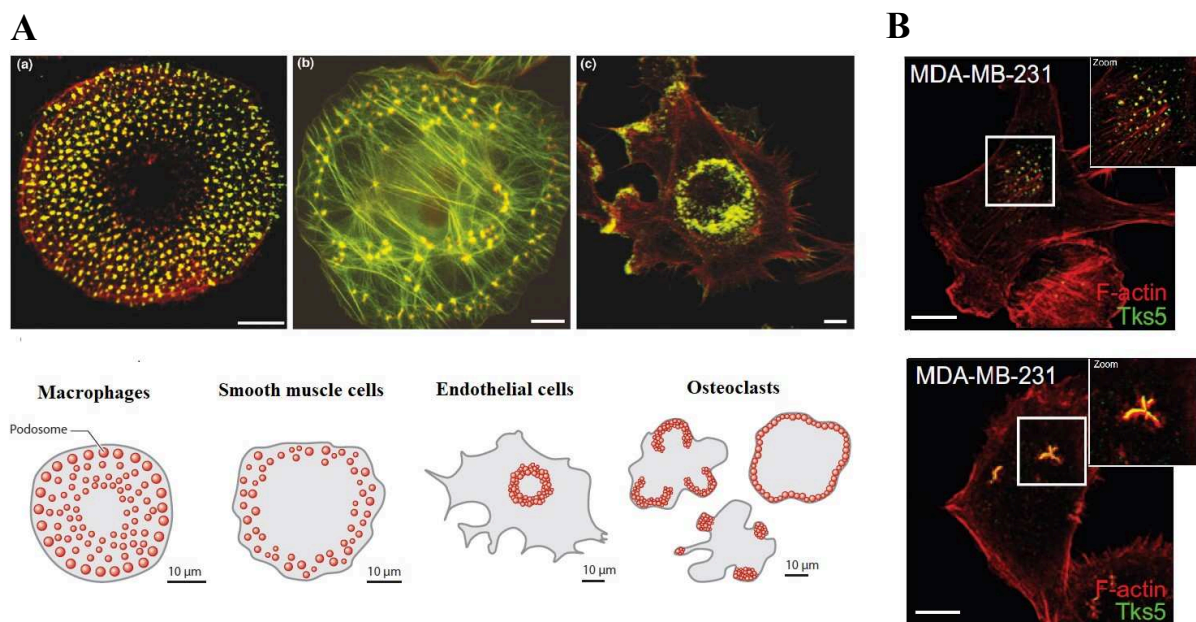


Figure 17: Invadosomes diversity according to the substrate and the cell type

(A) Podosomes number, morphology and organization differ depending on cell types as shown by fluorescence (upper panel) and schematic images (lower panel). Macrophages display dot-like podosomes excluded from the cell center (a). More peripheral podosomes with a similar morphology are observed in vascular smooth muscle cells (b). Endothelial cells form ring-like “rosettes” structures with clusters of podosomes (c). In osteoclasts, motile clusters of podosomes with different organizations can be found. Red: F-actin. Green: WASP (a), α -actinin (b-c). Scale bars: 10 μ m.

(B) MDA-MB-231 breast cancer cells form focal protrusion located close to the cell center when plated on gelatin (top) or elongated linear structures along fibrillar type I collagen (bottom). Insets are zoomed-in images boxed regions. Staining: F-actin (red) and Tks5 (green). Scale bars: 5 μ m.

Images adapted from Linder et al., “The matrix corroded: podosomes and invadopodia in extracellular matrix degradation” *Trends Cell Biol.* (2007) 17(3), 107-117, and Di Martino et al., “The microenvironment controls invadosome plasticity” *J. Cell. Sci.* (2016) 129(9), 1759-1768.

These results suggest that invadosome formation and morphology are regulated at least in part by matrix topology and composition. Matrix rigidity has also been identified as a strong

modulator of invadosome formation and proteolytic activity, indicating a potential function for invadopodia as mechanosensors similar to FAs (Alexander et al., 2008; Artym et al., 2015; Collin et al., 2008; Linder and Wiesner, 2016; Mrkonjic et al., 2017; Parekh et al., 2011; Pourfarhangi et al., 2018).

Whether podosomes and invadopodia are distinct entities or identical structures adapting to the environmental context is still under debate, but according to their strict definition in normal or transformed cells respectively, they present major differences in biological relevance and functions.

1.3. Biological relevance in physiology and disease

Matrix degradation is supposedly important in a considerable amount of biological processes, yet very few direct evidences of invadosomes contribution in these have been characterized so far. This stems from the fact that most studies have been describing invadosome composition, assembly and dynamics in *in vitro* assays, while *in vivo* observations remain scarce (Génot and Gligorijevic, 2014). However, dysregulation of core invadosome components has been associated with several human diseases affecting immunity, development and various cancers (Iqbal et al., 2010; Linder et al., 1999; Paterson and Courtneidge, 2017). Wiskott-Aldrich syndrome patients present mutations in the podosomal protein WASP resulting in altered podosome function and subsequent defects in macrophage chemotactic migration and bone resorption (Calle et al., 2004; Linder et al., 1999; Wiesner et al., 2014). Most of these defects can be corrected by re-expression of exogenous WASP, demonstrating the key role of WASP in immune and bone functions (Charrier et al., 2005). Furthermore, endothelial cells bordering blood vessels use podosomes to degrade the surrounding BM and facilitate formation of new branches and vessels during sprouting and angiogenesis, respectively (Curado et al., 2014; Rottiers et al., 2009; Seano et al., 2014; Spuul et al., 2016). Finally, depletion of invadosome core proteins Tks4 and 5 (for tyrosine kinase substrate with 4/5 Src homology 3 domains), previously called Fish, induces strong developmental defects including craniofacial malformations and decreased pigmentation, that have been shown to derive from defective neural crest cell migration due to their inability to form actin-rich structures resembling podosomes in zebrafish (Iqbal et al., 2010; Murphy et al., 2011).

On the other hand, invadopodia are almost exclusively associated with cell invasion in tissues and participate to every step of the metastatic cascade (Paterson and Courtneidge, 2017). Several core invadopodia components including cortactin, Tks5 but also proteases such as MT1-MMP, are overexpressed in various cancers and contribute to disease progression (Blouw

et al., 2015; Kirkbride et al., 2011; Lodillinsky et al., 2015; Paz et al., 2014). Recent functional studies have highlighted the role of invadopodia in tumor metastasis formation. Depletion of either cortactin or Tks5 robustly reduces extravasation of circulating cancer cells and subsequent metastasis formation in bladder and lung metastatic models (Leong et al., 2014; Tokui et al., 2014). In addition, diminution of invadopodia formation in rat and mouse mammary tumors directly correlates with reduced cell invasion and dissemination as well as lung metastasis colonization (Eckert et al., 2011; Gligorić et al., 2014, 2012). Ultimately, invadopodia activity has also been shown to support tumor growth in multiple cancer models including melanoma, fibrosarcoma and breast carcinoma (Blouw et al., 2015; Clark and Weaver, 2008; Hotary et al., 2003; Iizuka et al., 2016). Altogether, these results suggest that invadosomes play a pivotal role in diverse biological and pathological processes including but not restricted to development, tissue functions, along with cell invasion and metastasis. Nevertheless, since key invadosome components are not only present in invadopodia or podosomes but also involved in other cellular structures, further work will be needed to assess their specific contribution in physiology and disease.

2. Initiation and formation of invadopodia

2.1. *Membrane receptors and initiation signals*

Initial events triggering invadopodia formation occur at the cell-ECM interface and mostly depend on ECM receptors. Among them, integrins have been associated with both invadopodia and podosome formation (Buccione et al., 2009; Hoshino et al., 2013; Murphy and Courtneidge, 2011). In particular, active $\beta 1$ subunit, in association with either $\alpha 2$, $\alpha 3$ or $\alpha 5$, was found to be localized at invadopodia, but whether it is uniquely required for mature invadopodia function or also for their initiation remain a matter of debate (Artym et al., 2015; Beaty et al., 2013; Destaing et al., 2010; Mueller et al., 1999). Some reports also showed that engagement of integrin $\alpha v \beta 3$ was necessary for both formation and function of podosome structures in osteoclasts, as well as invadopodia in lung carcinoma cells (Deryugina et al., 2001; Nakamura et al., 1999; Peláez et al., 2017) (see **Figure 18A**). However, in Src-transformed fibroblasts expressing both $\beta 1$ and $\beta 3$ integrins, inhibition of invadopodia formation is only mediated by $\beta 1$ but not $\beta 3$ depletion (Destaing et al., 2010). Additionally, $\beta 3$ is present in podosome clusters in osteoclasts but excluded from the core where the non-integrin CD44 adhesion receptor plays a critical role (Chabadel et al., 2007). In comparison, formation of linear invadopodia in breast cancer cells plated on top of a fibrillar network of type I collagen does not seem to depend on

integrin receptors but rather involve the DDR1 receptor (Juin et al., 2014). Altogether, these observations suggest that adhesion receptors involved in invadosome formation are cell-type dependent and may be controlled by ECM composition and organization.

In parallel to adhesion cues, other extracellular signals such as growth factors (GF) including EGF can trigger and/or enhance invadopodia formation (Beaty and Condeelis, 2014; Hoshino et al., 2013; Mader et al., 2011; Yamaguchi et al., 2005). Similarly, stimulation of cancer but also normal cells with TGF- β or HGF increases invadosome number indicating an essential contribution in invadopodia formation in addition to their well-described role as inducers of EMT (Daubon et al., 2011; Mandal et al., 2008; Pignatelli et al., 2012; Rajadurai et al., 2012) (see **Figure 18A**). Over the last decade, other GF or chemokines have been implicated in invadopodia formation and function including vascular endothelial growth factor (VEGF), heparin-binding-EGF (HB-EGF) or stromal cell derived factor 1 α (SDF1 α) (Díaz et al., 2013a; Lucas et al., 2010; Smith-Pearson et al., 2010). Furthermore, GF receptors can crosstalk with other proteins including integrins, suggesting that invadopodia formation could be affected by a functional interplay between different extracellular stimuli (Beaty et al., 2013; Hoshino et al., 2013; Levental et al., 2009).

2.2. Polymerization of actin and recruitment of actin binding partners

Downstream intracellular pathways induced by ECM ligands or GF binding to membrane receptors converge into signalling nodes including kinases such as tyrosine kinase Src or phosphoinositide-3-kinases (PI3Ks) as well as the Rho GTPase Cdc42 (Beaty and Condeelis, 2014; Castro-Castro et al., 2016; Murphy and Courtneidge, 2011). Depletion of Cdc42 or expression of a dominant-negative form abolishes the formation of invadopodia, while expression of a constitutively active form of Cdc42 is sufficient to induce the formation of *de novo* structures (Desmarais et al., 2009; Di Martino et al., 2014; Razidlo et al., 2014). The Cdc42 downstream effector N-WASP activates Arp2/3 complex which promotes actin polymerization and the formation of a branched actin network in invadopodia structures. Similarly, silencing of N-WASP or its partner WASP interacting protein (WIP) reduce invadopodia number *in vitro* and further affect metastasis *in vivo* (García et al., 2014; Gligorijevic et al., 2012; Monteiro et al., 2013) (see **Figure 18B**). Cdc42 activation is mediated by GEF proteins and multiple Cdc42 GEFs have been associated with invadopodia formation including Fanciogenital dysplasia protein Fgd1, Vav1, β -pix or Tuba depending on the cell type and the matrix (Ayala et al., 2009; Genot et al., 2012; Juin et al., 2014; Md Hashim et al., 2013; Razidlo et al., 2014). Other actin nucleators of the diaphanous-related formin (DRF) family are

highly enriched in invadopodia and their inhibition correlates with lower invadopodia-based degradation (Kim et al., 2016; Lizárraga et al., 2009). This indicates that polymerization of parallel actin filaments contributes to invadopodia function, possibly mediating invadopodia extension within the matrix (Castro-Castro et al., 2016; Schoumacher et al., 2010). In podosomes, local actin polymerization in the actin-rich protrusive core is accompanied and tuned by actomyosin contraction in the peripheral adhesion ring (Gawden-Bone et al., 2010; Meddens et al., 2016; van den Dries et al., 2013). Podosomes require these two systems to generate pushing forces on synthetic substrates (Bouissou et al., 2017; Labernadie et al., 2014; van den Dries et al., 2014). Whether and how invadopodia participate to cancer cells mechanical responses on physiological ECM by generating forces remain to be explored.

In parallel to actin nucleators, actin-binding proteins including cortactin, cofilin, fascin or α -actinin also regulate actin filaments organization, dynamics and crosslinking in invadopodia structures (Beaty and Condeelis, 2014; Castro-Castro et al., 2016). Cortactin is highly enriched at invadopodia and therefore represents a widely used marker of these structures (Artym et al., 2006; Ayala et al., 2008; Clark et al., 2007). Cortactin is an actin-binding protein stabilizing Arp2/3 complex nucleation sites on actin filament branches and is involved in early steps of invadopodia assembly (Artym et al., 2006; Sharma et al., 2013). Combined activation of GF receptors and integrins leads to Src and non-receptor tyrosine kinase Abelson-related gene (Arg) activation that eventually triggers cortactin phosphorylation on tyrosine 421 (Y⁴²¹) and 466 (Y⁴⁶⁶) (Beaty et al., 2013; Bradley and Koleske, 2009; Mader et al., 2011). Cortactin phosphorylated form subsequently recruits Nck1 adaptor protein, N-WASP and Arp2/3 to induce branched actin polymerization (Oser et al., 2010, 2009) (see **Figure 18**). It also releases the actin severing protein Cofilin, which stimulates actin filament turnover and generates free barbed-ends allowing polymerization of new branched filaments by the Arp2/3 complex (Magalhaes et al., 2011; Oser and Condeelis, 2009; Yamaguchi et al., 2005). According to its pro-invasive role, cortactin is frequently overexpressed or dysregulated in cancer and has been implicated in cancer progression and metastasis (Castro-Castro et al., 2016; Kirkbride et al., 2011; Weaver, 2008). Actin bundling proteins including fascin and α -actinin, as well as actin branch destabilizing protein such as Coronin 1C, have been involved in invadopodia function, further highlighting the importance of a tight regulation of actin dynamics in these structures (Beghein et al., 2018; Castagnino et al., 2018; Li et al., 2010; Van Audenhove et al., 2016).

Polymerization of actin filaments initiates invadopodia formation but is not sufficient to generate a mature degradative structure and subsequent stages of maturation therefore entail additional proteins recruitment and proteases accumulation. In this process, another

cytoskeletal network, the MTs system, have been shown to be critical for invadopodia function, possibly through the delivery of invadopodial components (Linder et al., 2011; Schoumacher et al., 2010). In line with this, regulation of MTs stability through α -tubulin acetylation has been implicated in MT1-MMP transport to invadopodia as well as directed cell migration invasion (Castro-Castro et al., 2012; Montagnac et al., 2013).

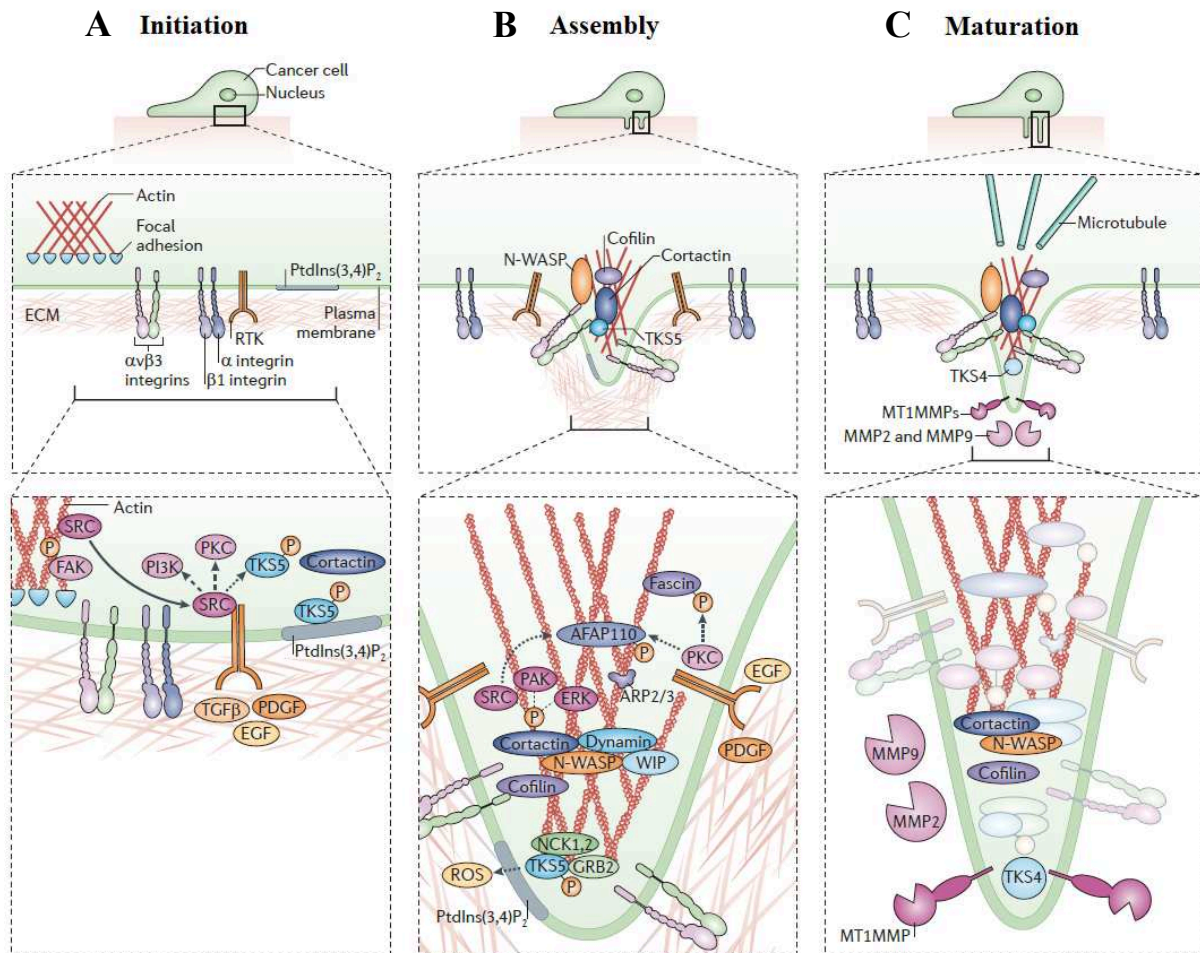


Figure 18: Schematic representation of invadopodia multi-step assembly

(A) Binding of various membrane receptors including integrins and RTKs to ECM ligands or soluble GFs trigger the initial step of invadopodia formation. Subsequent activation of kinases such as Src induces the recruitment and/or activation of core invadopodia proteins involved in signalling as well as actin polymerization and dynamics (Cdc42, cortactin, Tks adaptor proteins).

(B) These proteins initiate the formation of a branched actin network protruding into the underlying matrix through the activation of N-WASP and the Arp2/3 complex.

(C) Maturation of invadopodia structures consist in the recruitment and exocytosis of matrix-degrading enzymes including MMPs and ADAMs. Mature invadopodia are able to locally degrade the surrounding ECM, thus promoting cell invasion.

Image adapted from Murphy et al, "The 'ins' and 'outs' of podosomes and invadopodia: characteristics, formation and function" Nat. Rev. Mol. Cell Biol. (2011) 12(7), 413-426.

3. Maturation and disassembly of invadopodia

3.1. *Tks5: a key scaffolding protein in invadopodia*

Recruitment at invadopodia of the adaptor protein Tks5, coincides with the stabilization of labile precursors into more stable structures and immediately precedes proteases trafficking to invadopodia and ECM degradation (Murphy and Courtneidge, 2011; Sharma et al., 2013). Tks5 is a scaffold protein encoded by the SH3PXD2A gene consisting in a N-terminal Phox homology (PX) domain, five Src homology 3 (SH3) domains, several Src putative phosphorylation sites and multiple proline-rich regions (PRR) (Courtneidge, 2012; Saini and Courtneidge, 2018). It exists three Tks5 splice variants, namely α (or Tks5long), which is the only isoform containing the PX domain, β and Tks5short as well as a related Tks4 protein comprising four SH3 domains and encoded by the SH3PXD2B gene (Cejudo-Martin et al., 2014; Li et al., 2013, p. 5; Saini and Courtneidge, 2018). Tks5 and Tks4 only share 36% of overall structural similarities but exhibit higher similarities (from 60 to 80%) amidst their respective SH3 domains (Buschman et al., 2009; Courtneidge, 2012) (**see Figure 19**). Surprisingly, albeit a vast interactome, Tks5 almost exclusively localizes at invadopodia and is therefore used as a very specific marker of these structures (Castro-Castro et al., 2016; Saini and Courtneidge, 2018). Tks5 knockdown triggers a strong reduction of invadopodia structures as well as ECM degradation depending on the cell type, while silencing of Tks4 has an intermediate phenotype, suggesting important but not completely overlapping roles for Tks adaptor proteins in invadopodia formation (Buschman et al., 2009; Iizuka et al., 2016; Seals et al., 2005; Stylli et al., 2009).

The PX domain allows Tks5 binding to membrane phosphoinositide-3,4-biphosphate (PI(3,4)P₂) present at invadosome surface (Oikawa et al., 2008; Saini and Courtneidge, 2018; Sharma et al., 2013) (**see Figure 18B**). Formation of PI(3,4)P₂ at invadopodia is a multi-step process depending on PI3K activation (potentially by GF receptors or integrins) followed by phosphoinositide-4,5-biphosphate (PI(4,5)P₂) transformation into phosphoinositide-3,4,5-triphosphate (PI(3,4,5)P₃) and subsequent dephosphorylation into PI(3,4)P₂ by 5-phosphatases including SH2-domain containing phosphoinositide-3,4,5-trisphosphate 5-phosphatase (SHIP) or synaptojanin 2 (Hawkins and Stephens, 2016; Li et al., 2013; Sharma et al., 2013; Yamaguchi et al., 2011).

remains unclear (Bedard and Krause, 2007; Courtneidge, 2012). Additionally, Tks5 recruits and interacts with proteases involved in invadopodia-based ECM degradation including ADAM proteins as well as MMPs, as described in the following chapter (Abram et al., 2003; Eckert et al., 2017; Saini and Courtneidge, 2018). Overall, these results identify Tks adaptor proteins as essential recruitment and signalling platforms for invadopodia formation and maturation.

3.2. *Proteases: invadopodia cutting blades*

Functional invadopodia exhibit robust degradative capacities of the surrounding ECM and thereby concentrate catalytically active proteases (see **Figure 18C**). Three main classes of matrix-degrading enzymes, potentially reflecting the diversity of substrates encountered by cancer cells during invasion, have been associated to invadopodia so far: zinc-regulated metalloproteinases, cathepsin proteases and serine proteases (Linder, 2007). The former is subdivided into two subclasses namely ADAMs and MMPs. Considering their substantial role in invadopodia-related matrix degradation and more generally in cancer progression, particularly membrane-anchored MT1-MMP, the following chapter is devoted to a detailed description of MMPs. On the other hand, ADAM proteins function as transmembrane sheddases, which can cleave membrane proteins in the extracellular space and release possibly active soluble peptides (Huovila et al., 2005; Seals and Courtneidge, 2003). Among the 34 ADAM proteins described up to now, half of them present a functional catalytic domain, including ADAM12 which is often dysregulated in cancers and has been implicated in invadosome function (Abram et al., 2003; Stautz et al., 2012; van Hinsbergh et al., 2006). ADAM12 interacts with several proteins localized at invadopodia such as Tks5 but also integrin $\beta 1$, where it promotes invadopodia formation and activity by triggering shedding and release of EGFR ligands ectodomains as well as regulating Src activity (Albrechtsen et al., 2011; Díaz et al., 2013b; Eckert et al., 2017; Stautz et al., 2010).

The cathepsin protease family comprises 15 members designated as cathepsin A or G for serine proteases, D or E for aspartyl proteases and B, C, F, H, K, L, O, S, V, W or Z for cysteine proteases, which have been connected with physiological and pathological processes including carcinogenesis (Khaket et al., 2019; Patel et al., 2018). Cathepsins are processed and activated in endo-lysosomal compartments where they have been primarily known to function as acid pH-dependent endopeptidases (*i.e.* cleaving proteins in nonterminal amino-acid bridges) (Patel et al., 2018). Over the last decade however, cathepsins have been involved in extracellular matrix degradation, specifically in invadosomes (Han et al., 2009; Jevnikar et al., 2012; Tu et al., 2008; Vizovišek et al., 2019). Indeed, pericellular acidification of the invadopodia space

controls cathepsin B and S activity, which in turn promotes cancer cells invasiveness in Matrigel, (Brisson et al., 2011; Gillet et al., 2009; Greco et al., 2014). Ultimately, seprase, also called fibroblast activation protein α (FAP α), and Dipeptidyl-peptidase-4 (DPP-4) are transmembrane serine proteases present in invadopodia where they facilitate local matrix degradation and participate to cell invasion (Gherzi et al., 2006; Knopf et al., 2015; Mueller et al., 1999; O'Brien and O'Connor, 2008).

3.3. *Mechanisms of invadopodia disassembly*

Invadopodia structures assemble within minutes and can persist over time with a lifetime ranging from about ten minutes for dynamic structures to few hours for the more stable ones (Beaty and Condeelis, 2014; Jeannot and Besson, 2017). While the mechanism underlying invadopodia formation has been extensively studied (see above), very little is known regarding the molecular mechanisms controlling invadopodia disassembly and turnover. Degradation of ECM ligands or shedding of transmembrane proteins by proteases accumulating in invadopodia may switch off initiation signals and consequently cause invadopodia disassembly (Calle et al., 2006; Murphy and Courtneidge, 2011). Moreover, destabilization and disassembly of the branched actin network are presumably critical stages of invadopodia disassembly, but whether other proteins turnover, including transmembrane proteins, are invariably coupled to actin dynamics remains to be determined (Murphy and Courtneidge, 2011). Several studies pointed out the role of the phosphorylation of actin-binding proteins such as cortactin and AFAP-110, but also paxillin in invadosomes turnover (Badowski et al., 2008; Dorfleutner et al., 2008; Petropoulos et al., 2016). The question of invadopodia dissolution has recently been addressed by a study assessing the activity of the Rho GTPase Rac1 in invadopodia (Moshfegh et al., 2014). This work proposes an signalling axis based on Rac1 activation by its GEF Trio to induce phosphorylation of cortactin by serine/threonine kinase PAK1 and subsequent destabilization and disassembly of the branched actin network (Jeannot and Besson, 2017; Moshfegh et al., 2014).

Phosphoinositide phosphorylation by kinases is of crucial importance in invadopodia formation, hence lipid phosphatases are likely to play a role in invadopodia dismantlement. Tumor suppressor phosphatase and tensin homolog (PTEN) has therefore been implicated in invadopodia destabilization in Src-transformed fibroblasts, but further work will be needed to determine other phosphatases contribution in this process (Mukhopadhyay et al., 2010). Alternatively, decrease of matrix stiffness following ECM degradation may switch off invadopodia promoting signals and therefore trigger their disassembly.

Chapter 5: Matrix metalloproteinases, key enzymes in cell invasion

The ECM plays an essential role in multiple physiological processes including development or tissue functions. ECM homeostasis is therefore tightly regulated to maintain an optimal equilibrium between matrix production and degradation as discussed in previous chapters (Bonnans et al., 2014). Matrix remodeling is mediated by specific matrix-degrading enzymes among which MMPs are the most prominent representative, and is associated with various diseases including cancers when dysregulated (Bonnans et al., 2014; Itoh, 2015; Kessenbrock et al., 2015).

1. Matrix metalloproteinases and their physio-pathological functions

1.1. Soluble matrix metalloproteinases

MMPs are zinc-containing proteases belonging to the metzincin enzyme superfamily. More than 20 different MMPs are expressed in human and subdivided into two subgroups namely soluble and membrane-type proteins (Bonnans et al., 2014). All MMPs contain three shared domains: a signal peptide domain composed of few amino acids at the N-terminal end and required for translocation through the ER membrane, a propeptide domain with a cysteine-containing motif that is able to bind and inhibit the catalytic domain, which contains a zinc-binding motif and carries the proteolytic activity (Bonnans et al., 2014; Kessenbrock et al., 2010). Except for soluble MMP 7 and MMP26, all MMPs also comprise an hemopexin-like domain connected to the three aforementioned domains at the C-terminus by a flexible hinge or linker region (**see Figure 20**). The hemopexin-like region is composed of four repeats resembling the glycoprotein hemopexin and a disulphide bond between the two extreme repeat domains. It is involved in substrate specificity as well as non-catalytic functions of MMPs such as interactions with proteins, including other MMPs (Kessenbrock et al., 2010). Most MMPs are soluble and therefore secreted in the extracellular space where they can bind ECM ligands and execute their primary function of proteolysis (Lu et al., 2011). MMPs display a vast repertoire of substrates ranging from BM components such as laminins or type IV collagen to fibronectin and all types of fibrillar collagens (Bonnans et al., 2014; Lu et al., 2011). In addition, MMPs can cleave membrane receptors such as GF receptors, integrins, CD44 or even other MMPs (Lu et al., 2011; Page-McCaw et al., 2007; Shiomi et al., 2010) (**see Figure 20**).

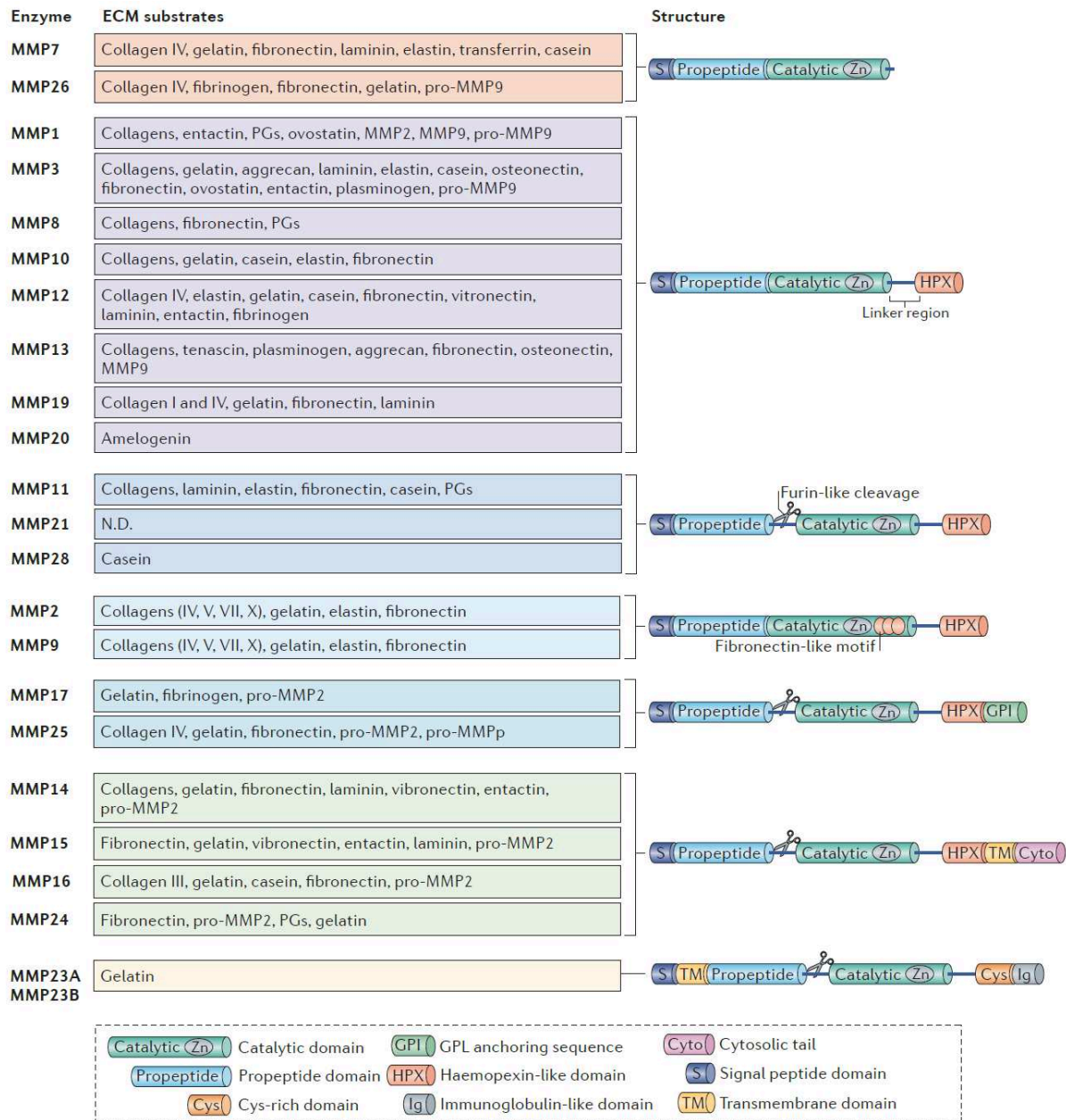


Figure 20: Schematic representation of MMPs and their ECM substrates

MMPs are multidomain proteolytic enzymes sharing three main domains: a signal peptide domain, a pro-peptide domain and a catalytic domain. A C-terminal hemopexin-like region is also present in the majority of MMPs and mostly determines their substrate specificity. Depending on the presence of a transmembrane domain or a GPI anchor sequence, MMPs can be membrane-bound or soluble. MMPs cleave a large variety of ECM ligands with their catalytic domain containing a zinc-ion binding motif. MMPs are synthesized as inactive zymogen, and required further activation by protein convertases such as furin that cleave out the pro-peptide self-inhibitory domain.

Image adapted from Bonnans et al, "Remodeling the extracellular matrix in development and disease" Nat. Rev. Mol. Cell Biol. (2014) 15(12), 786-801.

MMPs are constitutively expressed in normal tissues where they are involved in several developmental processes including bone resorption or mammary gland branching, but also angiogenesis and wound healing (Bonnans et al., 2014; Lu et al., 2011; Rohani and Parks,

2015). By contrast, a large majority of MMPs are frequently overexpressed in cancers and have been particularly implicated in tumor cell invasion and metastasis formation (Kessenbrock et al., 2015; Lu et al., 2011). More specifically, several soluble MMPs including MMP-1, -2 and -9 are overexpressed in human breast cancer and are thought to participate to tumor dissemination by facilitating cancer cells transmigration through BMs (Pellikainen et al., 2004; Poola et al., 2005; Ren et al., 2015; Rowe and Weiss, 2008). However, additional studies on the specific role of MMP-2 and MMP-9 gelatinases during BM transmigration did not conclude on a leading role of these proteases taken individually, but rather in association with other MMPs, most predominantly MT1-MMP (Hotary et al., 2006; Rowe and Weiss, 2009). More recently, new functions independent of MMPs catalytic activity have emerged, including protein interactions or signalling and have been associated with cancer progression (Shay et al., 2015; Turunen et al., 2017). Notably, several studies have shown that an intact hemopexin domain is needed for cell migration and invasion in different models via non-proteolytic functions of MMPs (Cao et al., 2004; Dufour et al., 2008; Glasheen et al., 2009; Rupp et al., 2008).

1.2. Membrane-type matrix metalloproteinases

In parallel to soluble MMPs, six membrane-anchored MMPs, referred as MT-MMPs (for membrane-type MMPs), are expressed in humans. MMP-14, MMP-15, MMP-16, MMP24 respectively called MT1, MT2, MT3 and MT5-MMPs, contain a transmembrane domain preceding a linker and a short C-terminal tail. Alternatively, MMP17 and MMP25, also known as MT4 and MT6-MMPs exhibit a C-terminal glycosylphosphatidylinositol (GPI) sequence directly following the hemopexin domain and enabling anchoring into membranes (Bonnans et al., 2014; Itoh, 2015; Kessenbrock et al., 2010) (see **Figure 20**). MT1 and MT6-MMPs can homodimerize at the cell surface, a process mediated by the interaction of the hemopexin and transmembrane domains, or through the “stem regions” localized between the hemopexin and GPI domains respectively (Itoh et al., 2011; Tochowicz et al., 2011; Zhao et al., 2008). Dimerization is essential for MT1-MMP-catalyzed collagen degradation as well as MMP-2 activation as described in more details in the following sections (Itoh et al., 2008, 2006). Similar to their soluble counterparts, MT-MMPs degrade diverse ECM substrates that can overlap between proteases (Bonnans et al., 2014; Itoh, 2015). In particular, MT1-MMP has the widest substrate range and can degrade several types of collagen including type I, II, III and possibly IV. For the later, results diverge between experiments performed either on native BM, where MT1-MMP seems to be essential for degradation, or on purely *in vitro* reconstituted BM-like substrates, in which a direct degradation of collagen IV by MT1-MMP is refuted (Gioia et al.,

2007; Hotary et al., 2006; Itoh, 2015). MT2-MMP also degrades type I fibrillar collagen but to a much lesser extent as compared to MT1-MMP, while MT3-MMP only proteolyzes type III collagen (Morrison and Overall, 2006; Shimada et al., 1999). Other MT-MMPs do not cleave fibrillar collagens and MT1-MMP is consequently considered as the principal protease degrading collagen (Itoh, 2015; Sabeh et al., 2004).

Just like soluble MMPs, MT-MMPs are involved in numerous physiological processes including angiogenesis, mammary gland morphogenesis, skeletal development, wound healing or inflammation (Feinberg et al., 2018; Inman et al., 2015; Itoh, 2015; Page-McCaw et al., 2007). MT1-MMP has attracted a lot of attention due to its significant pro-invasive role in cancer (Hotary et al., 2006, 2000; Sato et al., 1994). In addition, MT1-MMP-deficient mice present substantial developmental defects among which craniofacial dysmorphism, arthritis, osteopenia, as well as fibrosis, whereas mice lacking other individual MT-MMPs show only subtle defects affecting specific organs (Holmbeck et al., 1999; Komori et al., 2004; Rikimaru et al., 2007; Shi et al., 2008). Implication of MT1-MMP in pathological contexts is also well-described particularly in atherosclerosis, obesity or arthritis and naturally cancers (Hotary et al., 2006, 2003; M.-C. Miller et al., 2009; Sabeh et al., 2010). Upregulated in various cancers, MT1-MMP expression levels are more specifically increased in invasive as compared to *in situ* carcinoma in human breast samples (Lodillinsky et al., 2015; Marchesin et al., 2015). Furthermore, MT1-MMP expression is required for the transition from a non-invasive to an invasive tumor in a mouse xenograft model, suggesting that MT1-MMP is particularly associated with breast cancer progression (Lodillinsky et al., 2015) (**see Figure 21**). MT1-MMP plays a major part in tumor cell invasion by degrading surrounding ECM including BMs as shown in an *ex vivo* model of native BM and type I collagen fibrillar networks (Hotary et al., 2006; Monteiro et al., 2013; Wolf et al., 2013, 2007). In support of a substantial role in cancer cell invasion, MT1-MMP favors tumor growth in 3D and is involved in tumor cells infiltration and extravasation from blood vessels therefore promoting metastasis formation (Hotary et al., 2003; Lodillinsky et al., 2015; Perentes et al., 2011; Szabova et al., 2008). MT1-MMP-based matrix degradation is mediated by MT1-MMP delivery and concentration in invadopodia structures at the cell surface, a tightly regulated process further described in subsequent sections (Castro-Castro et al., 2016; Poincloux et al., 2009; Sakurai-Yageta et al., 2008; Steffen et al., 2008). In addition to matrix degradation, MT1-MMP-mediated shedding of other membrane receptors including ADAMs, integrins, DDR1, CD44 or syndecans also influences tumor progression and cell invasion (Albrechtsen et al., 2011; Deryugina et al., 2002; Endo et al., 2003; Fu et al., 2013a; Suenaga et al., 2005; Wiesner et al., 2010). Altogether, these

observations demonstrate that MT-MMPs are multi-faceted proteins that can be dysregulated in multiple ways in cancers (Turunen et al., 2017).

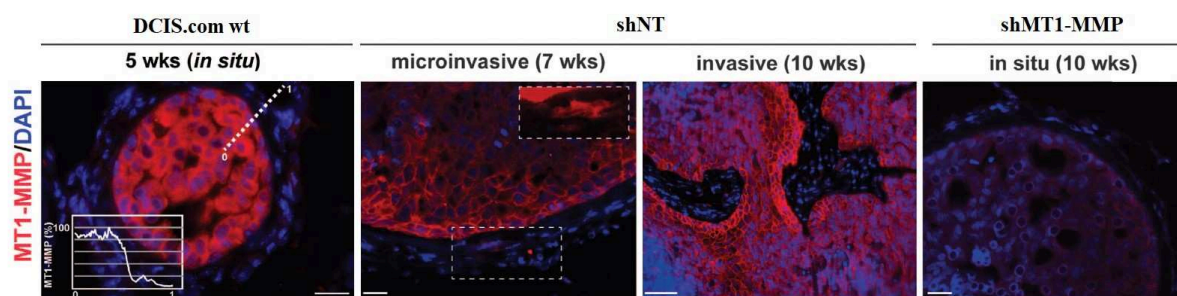


Figure 21: Role of MT1-MMP in breast tumor xenografts *in situ* to invasive transition

Intraductal injections of DCIS.com cells in mice induce formation of tumors. Xenograft tumors were analyzed for MT1-MMP expression (in red) at indicated times in control (wt and shNT) cells or in cells silenced for MT1-MMP (shMT1-MMP). MT1-MMP is expressed homogeneously in xenograft *in situ* (5 weeks) but is upregulated at tumor edges and invasive front in micro-invasive (7 weeks) and invasive (10 weeks) stages respectively, where it correlates with BM breaching. Depletion of MT1-MMP mostly generates *in situ* tumors unable to invade into surrounding stroma even at 10 weeks. Insets: fluorescence intensity profile of MT1-MMP along the dotted line, or zoom-in of the boxed region. Blue: DAPI. Scale bar: 20 μ m except for invasive condition, 50 μ m.

Image adapted from Lodillinsky et al, "p63/MT1-MMP axis is required for in situ to invasive transition in basal-like breast cancer" Oncogene. (2016) 35(3), 344-357.

2. Regulation of matrix metalloproteinase function: example of MT1-MMP

MT1-MMP is thought to be the main executor of tumor cell transmigration program into tissues (Hotary et al., 2006; Lodillinsky et al., 2015; Rowe and Weiss, 2008; Willis et al., 2013). Cancer cells adjust their MT1-MMP cell surface levels and activity at different stages ranging from synthesis, trafficking or turnover at the membrane (Castro-Castro et al., 2016).

2.1. Regulation of MT1-MMP expression

MT1-MMP gene expression is controlled by different transcription factors responding to specific tumor microenvironmental cues, even if the detailed mechanisms of gene activation are not clearly understood (Itoh, 2015; Turunen et al., 2017). Various transcription factors, such as specificity protein 1 (SP-1), early growth response protein 1 (EGR-1), or E2F bind or indirectly interact with MMP-14 gene regulatory sequences (Haas et al., 1999; Hong et al., 2014; Johnson et al., 2012). In general, the inactivation of tumor suppressor pathways accompanies the up-regulation of MMP-14 gene by these transcription factors in cancer cells: inactivation of the Retinoblastoma protein (Rb) in lung cancer promotes MT1-MMP increased expression by E2F for instance (Johnson et al., 2012). Similarly, hypoxia inducible transcription

factor 2α (HIF- 2α) positively regulates MT1-MMP gene expression levels in renal carcinoma cells deficient for the tumor suppressor von Hippel-Lindau protein (VHL) (Petrella et al., 2005). In addition, several transcription factors known as master regulators of the EMT including the Snail family have been associated with up-regulation of MT1-MMP expression (Lamouille et al., 2014; Ota et al., 2009; Rowe et al., 2009; Zhang et al., 2013).

Extracellular signals converging to these transcription factors originate from soluble ligands including GF such as TGF- β or FGF, cytokines including interleukines and tumor necrosis factor α (TNF- α) and glycoproteins from the Wnt family (Blavier et al., 2006; Cathcart et al., 2016; Sugiyama et al., 2010; Turunen et al., 2017). Several studies have also shown that structural ECM components such as type I collagen trigger cell surface MT1-MMP up-regulation as well (Gilles et al., 1997; Sakai et al., 2011; Shields et al., 2012). Alternatively, an increasing number of miRNAs have been implicated in the post-transcriptional regulation of MT1-MMP and may represent important candidates to explain the molecular mechanisms underlying cancer-associated up-regulation of MT1-MMP expression as they are also typically dysregulated in cancers (Li et al., 2015; Turunen et al., 2017; Zuo et al., 2015).

2.2. Post-translational activation of matrix metalloproteinases

MMPs are synthesized in a catalytically inactive form called proenzyme or zymogen, as a consequence of the self-inhibitory activity of the pro-domain which binds to the catalytic domain through the zinc ion. Zymogen activation is hence needed to obtain functionally active proteases, and is often mediated by protein convertases acting either intracellularly or in the extracellular space (Kessenbrock et al., 2015; Sternlicht and Werb, 2001). Intracellular activation generally occurs into the Golgi apparatus where serine proteases such as furin or furin-like protein release MMP auto-inhibition by proteolytic cleavage of the pro-domain (Sternlicht and Werb, 2001). More specifically, MT1-MMP is activated by furin and furin-like endopeptidases and exocytosed as an active enzyme at the cell surface (Ra and Parks, 2007; Sternlicht and Werb, 2001; Yana and Weiss, 2000). Alternatively, soluble MMPs can be activated in the extracellular space by serine proteases such as plasmin, but also by other MMPs (Itoh, 2015; Sternlicht and Werb, 2001).

In parallel, endogenous MMP inhibitors including the four members of the tissue inhibitor of metalloproteinase (TIMP) family, $\alpha 2$ -macroglobuline, $\alpha 1$ -proteinase inhibitor, $\alpha 1$ -chymotrypsin and thrombospondin-2 prevent excessive matrix degradation by binding to and inactivating MMPs (Bonnans et al., 2014; Kessenbrock et al., 2010; Nagase et al., 2006). Regulation of MMP activity involves complex positive and negative feedback loops wherein

MMPs degrade and inactivate both convertase proteins and their relative inhibitors (Kessenbrock et al., 2010). A well-studied example is the activation of MMP-2 by MT1-MMP. In the current model, TIMP-2 N-terminal domain binds to and inactivates the catalytic domain of one molecule of the MT1-MMP homodimer present at the cell surface (Strongin et al., 1995). Pro-MMP2 can subsequently interact by its hemopexin domain with the free C-terminal domain of TIMP-2 and forms a triad composed of MT1-MMP dimer, TIMP-2 and pro-MMP-2 (Itoh and Seiki, 2006). The functional TIMP-2-free MT1-MMP molecule in the dimer recognizes and cleaves pro-MMP-2 to release the self-inhibition mediated by its pro-domain, thereby liberating catalytically active MMP-2 into the extracellular space (Itoh, 2015; Will et al., 1996). TIMP-3 is also a potent inhibitor of MT1-MMP activity and observations of stronger MMP-2 activation by MT1-MMP in cells deficient for TIMP-3 rather than TIMP-2 suggest a more important role in regulating MT1-MMP activity (English et al., 2006; Itoh, 2015). Furthermore, MMPs trafficking, secretion, as well as cell surface localization in the case of MT1-MMP, constitute alternative ways of controlling MMP activity in cells, and are detailed in the following sections (Castro-Castro et al., 2016; Itoh, 2015; Poincloux et al., 2009).

2.3. Regulation of MT1-MMP cell surface exposure and turnover

Newly synthesized MT1-MMP protein is transported along the typical biosynthetic pathway through the ER and the Golgi apparatus and delivered to the plasma membrane where it is thought to be rapidly internalized by different endocytic pathways (Castro-Castro et al., 2016; Poincloux et al., 2009). Following internalization, MT1-MMP accumulates into endolysosomal compartments, from which it can be further recycled and addressed to invadopodia structures through polarized trafficking in a complex process detailed in the next section (Castro-Castro et al., 2016; Marchesin et al., 2015; Monteiro et al., 2013). MT1-MMP fast turnover at the plasma membrane is presumably important to locally concentrate and ensure a constant delivery of active proteases at invadopodia structures. MT1-MMP endocytosis is mediated through both clathrin- and caveolin-dependent pathways (Poincloux et al., 2009). Interaction of the clathrin adaptor complex AP-2 with a di-leucine (L⁵⁷¹L⁵⁷²) motif located in the cytoplasmic tail of MT1-MMP triggers the incorporation of MT1-MMP into nascent clathrin-coated pits (CCPs) and it is required for internalization (Jiang et al., 2001; Remacle et al., 2003; Uekita et al., 2001). Together with the Dynamin-2 GTPase, Endophilin A2 is essential for endocytic vesicles fission from the plasma membrane and for MT1-MMP uptake (Jiang et al., 2001; Wu et al., 2005). Several studies have shown that downregulation or inhibition of these proteins impair matrix degradation and MT1-MMP internalization while others reported

increased matrix-degrading activity when endocytosis was inhibited or MT1-MMP cytoplasmic tail was truncated (Baldassarre et al., 2003, 2015; Destaing et al., 2013; Jiang et al., 2001; Li et al., 2008; Wu et al., 2005). These results suggest that efficient MT1-MMP internalization and recycling from the cell surface may play a differential role in the regulation of MT1-MMP matrix-degrading activity depending on the context and presumably the cell type.

Another internalization route based on caveolae-mediated uptake has been proposed for MT1-MMP, relying on the fact that MT1-MMP and the caveolar marker caveolin-1, are found together in detergent-resistant membrane fractions (Annabi et al., 2004, 2001; Gálvez et al., 2004; Remacle et al., 2003). The role of caveolae in MT1-MMP uptake and function remains however under debate as caveolin-1 depletion has been shown to interfere with MT1-MMP-mediated matrix degradation in breast cancer cells while loss of caveolin in a breast cancer mouse model correlates with cancer progression and increased metastasis formation (Williams et al., 2004; Yamaguchi et al., 2009). Alternatively, other caveolae cellular functions including lipid signalling or membrane resistance to stress could contribute to tumor cell invasion in MT1-MMP-dependent or independent ways (Goetz et al., 2011; Parton and del Pozo, 2013; Yang et al., 2016). Nonetheless, the rapid clearance of MT1-MMP from the cell surface raises the question of how the protease achieves effective matrix degradation, which requires persistent contact with ECM ligands at the plasma membrane. A possible mechanism came from the fact that MT1-MMP anchoring to invadopodia, through a direct interaction between its LLY cytoplasmic motif (also involved in AP-2 interaction) with F-actin, drastically reduced MT1-MMP turnover at cell surface (Hoshino et al., 2012; Yu et al., 2012). Additionally, MT1-MMP-binding with type I collagen fibers via its hemopexin domain strongly reduces MT1-MMP endocytosis and cell surface turnover suggesting a role of the ECM in controlling MT1-MMP surface levels (Lafleur et al., 2006). Concurrently, MT1-MMP recycling and trafficking to invadopodia constitute a major regulation step for MT1-MMP cell surface exposure and consequently, activity (Castro-Castro et al., 2016).

2.4. MT1-MMP trafficking and delivery to invadopodia

Primary observations in breast cancer cells, later on confirmed in several carcinoma cell lines, led to the identification of late endo-lysosomal compartments, characterized by the presence of vesicle associated membrane protein 7 (VAMP-7) as well as Rab-7 GTPase, as recycling routes for MT1-MMP delivery to invadopodia (Chevalier et al., 2016; Macpherson et al., 2014; Monteiro et al., 2013; Rossé et al., 2014; Steffen et al., 2008). If this recycling pathway has been recently validated in invasive breast cancer models, other vesicular

compartments identified by different Rab GTPases have drawn attention on their potential regulation of MT1-MMP returning to plasma membrane (Chevalier et al., 2016; Linder and Scita, 2015; Macpherson et al., 2014). Hence, a Rab-8-dependent exocytic pathway is associated with MT1-MMP recycling to invadopodial plasma membrane and Rab-8 dysregulation induces late endosomes (LEs)/lysosomes mispositioning as well as actin cytoskeleton reorganization and polarity defects (Bravo-Cordero et al., 2016, 2007; Chou et al., 2016; Sato et al., 2007; Vidal-Quadras et al., 2017). Furthermore, post-endocytic trafficking of MT1-MMP based on Rab-2A, but also fast endocytic/exocytic cycles of MT1-MMP controlled by Rab-5A and Rab-4, have been identified and associated with tumor progression and metastasis formation in breast cancer models (Frittoli et al., 2014; Kajiho et al., 2016). Altogether, these results underline the complex framework of recycling circuitries utilized by cancer cells to expose MT1-MMP at the cell surface for invasion (Linder and Scita, 2015).

Polarized recycling of endo-lysosomes to the invadopodial plasma membrane requires concerted action of actin, MTs and cytoskeleton-related proteins. Accordingly, MT1-MMP-positive LEs/lysosomes are characterized by the presence of discrete actin patches at the endo-lysosomal membrane surface that correspond to small branched actin networks generated by Arp2/3 complex through activation by Wiskott-Aldrich syndrome protein and Scar homolog (WASH) complex and cortactin (Monteiro et al., 2013; Rossé et al., 2014). Perturbations of these actin structures by WASH1 subunit downregulation, or inhibition of MT1-MMP-cortactin interaction mediated by LIM domain kinases (LIMK) coincide with decreased MT1-MMP surface delivery, matrix degradation and invasion in breast cancer cells (Lagoutte et al., 2016; Monteiro et al., 2013). WASH recruitment on MT1-MMP-positive LEs/lysosomes is potentially mediated by a Rab7/retromer multiprotein complex axis and involved in endosomal vesicles sorting and trafficking (Harbour et al., 2012, 2010). In addition, recruitment of key proteins for MT1-MMP-positive endo-lysosomes tethering and exocytosis such as the exocyst complex and c-Jun N-terminal kinase (JNK)- interacting proteins 3 and 4 (JIP3 and JIP4) by WASH is essential for MT1-MMP-dependent cell invasion (Liu et al., 2009; Marchesin et al., 2015; Monteiro et al., 2013; Sakurai-Yageta et al., 2008).

Late endosomes and lysosomes are transported along MTs by molecular motors controlling their direction and speed (Granger et al., 2014). In particular, aforementioned proteins JIP3 and JIP4 present at MT1-MMP-positive endo-lysosomal surface bind to both kinesin-1 MT-plus-end directed motor and dynein/dynactin complex regulating MT-based minus-end trafficking (Cockburn et al., 2018; Liu, 2017; Marchesin et al., 2015). In line with the observation that invadopodia contain MTs, interfering with any of these motors, but also

with kinesin-2 which has been similarly associated with MT1-MMP polarized trafficking toward invadopodia, strongly compromises invadopodia but also podosome function (Marchesin et al., 2015; Schoumacher et al., 2010; Wiesner et al., 2010). The current model is that MT1-MMP delivery to invadopodia involves the formation of tubules emanating from MT1-MMP-positive LEs/lysosomes directed to the plasma membrane (Castro-Castro et al., 2016; Marchesin et al., 2015; Monteiro et al., 2013; Steffen et al., 2008). Endosomal tubule formation supposedly results from a tug-of-war mechanism between opposing dynein/dynactin minus-end- and kinesin-1 plus-end-directed motors. In this model, both motors are anchored to the endo-lysosomal and invadopodial plasma membrane surfaces and activated through JIP3 and JIP4 by the small GTP binding protein ADP-ribosylation factor 6 (ARF6) (Castro-Castro et al., 2016; Marchesin et al., 2015; Montagnac et al., 2009) (see **Figure 22**).

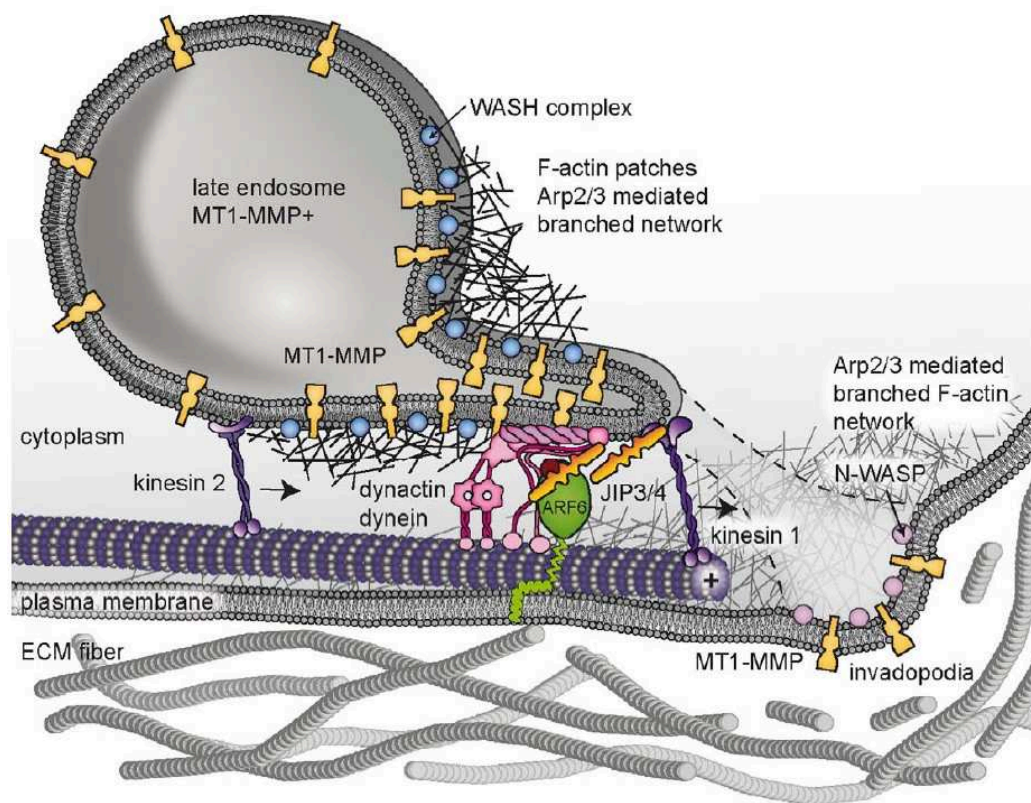


Figure 22: Model for MT1-MMP delivery at invadopodia by endosomal tubules

MT1-MMP-positive LEs/lysosomes move along MTs through the action of MT-associated motors. Among these, kinesin-1 and dynein/dynactin recruitment at the endo-lysosomal surface is mediated by JIP3 and JIP4 proteins. Close to the invadopodial surface, membrane-bound ARF6-GTP interacts with endo-lysosomal JIP3/JIP4 to bridge the two membranes together. This may prevent dynein/dynactin (-)-end movement, while kinesin-1 keep on pulling toward the MT (+)-end, therefore inducing a tug-of-war mechanism between stalled dynein/dynactin and active kinesin-1 which initiates tubule formation and elongation.

Image adapted from Marchesin et al., "ARF6-JIP3/4 regulate endosomal tubules for MT1-MMP exocytosis in cancer invasion" J. Cell Biol. (2015) 211(2), 339-358.

Finally, several protein complexes initiate endo-lysosomal membrane fusion with the cell plasma membrane for MT1-MMP transfer to the surface. The exocyst complex bridges endo-lysosomal membrane, through its interaction with WASH, to invadopodial membrane via binding to the small GTPases Cdc42 and/or RhoA (Monteiro et al., 2013; Sakurai-Yageta et al., 2008). Hence, WASH contributes to endosomal tubulation and connection to the plasma membrane but whether the different endo-lysosomal and invadopodial actin networks connect, fuse or undergo dissolution during this process remains to be determined. Following this tethering step, a complex formed by Soluble N-ethylmaleimide-sensitive-factor attachment protein (SNAP) receptors (SNAREs) proteins together with a SNAP protein, mediates the fusion between the endo-lysosomal membrane and the plasma membrane. VAMP7 is the MT1-MMP-positive LE/lysosomal SNARE protein interacting with its plasma membrane alter-ego syntaxin4 in a SNAP23-dependent way to promote MT1-MMP exocytosis at invadopodia (Steffen et al., 2008; Williams et al., 2014; Williams and Coppolino, 2011). Altogether, these observations illustrate the complex regulation of MT1-MMP cell surface levels and highlight the exquisite coordination between LEs/lysosomes recycling, tubular formation mediated by the actin and MT cytoskeletons and exocytosis at the invadopodial plasma membrane.

Working hypotheses and objectives

Cancer dissemination requires tumor cells to cross the basement membrane and invade through the stroma composed of a dense fibrillar collagen network (Rowe and Weiss, 2008). While the leading protrusion of cancer cells can squeeze through submicrometric gaps in the stroma, the nucleus which represents the largest and stiffest cell organelle may be a limitation to confined cell movement as nuclear stiffness prevents deformation and transmigration through matrix pores (Friedl et al., 2011). Engagement of matrix-degrading proteases such as Matrix Metalloproteinases (MMPs) including trans-membrane membrane type 1 (MT1)-MMP then becomes essential for pore enlargement and for cell invasion (Wolf et al., 2013). A large body of work indicates that carcinoma cells adjust their level of surface-exposed MT1-MMP through trafficking from late endosome/lysosome storage compartments to actin-rich structures, named invadopodia (Monteiro et al., 2013; Poincloux et al., 2009; Steffen et al., 2008). Whether and how cell confinement mediated by the microenvironment influence MT1-MMP surface localization and exocytosis to invadopodia remains unexplored.

In addition, the ability of cancer cells to form invadopodia strongly correlates with invasiveness, and invadopodia components, including actin-binding protein cortactin, or scaffold protein Tks5, are up-regulated in various cancers (Paterson and Courtneidge, 2017; Paz et al., 2014). Invadopodia have been mostly studied in cells plated on top of gelatin (*i.e.* denatured collagen), in which they form protrusive extensions of the membrane that degrade gelatin. When tumor cells are plated on more physiological substrata such as fibrillar type I collagen, actin-rich membrane subdomains called linear invadopodia form along collagen fibers (Juin et al., 2012). Linear invadopodia share core components with their protrusive counterparts including cortactin, Tks5 and MT1-MMP (Di Martino et al., 2014; Monteiro et al., 2013). Although invadopodia are critical for cancer cell invasive capacities, molecular mechanisms underlying their formation, dynamics and role in 3D cell invasion remain poorly understood. To address some of these outstanding questions, my PhD work was subdivided into two parts, which are detailed hereafter.

Prior work from the host lab showed that breast cancer cell invasion in a 3D collagen gel with small pore size induced nuclear deformations that were strongly enhanced upon inhibition of MT1-MMP activity, while reducing the level of confinement by increasing the pore size, diminished nuclear deformation without affecting migration. This indicated that confining extracellular matrix (ECM) fibers impose a physical stress against cell nuclei which can be

reduced by MT1-MMP-mediated collagenolysis. Based on these findings, we hypothesized that MT1-MMP proteolytic machinery is engaged by a mechanotransduction mechanism to relax physical constraints imposed by ECM fibers opposing cell movement. I focused my project along two main objectives:

- I addressed whether cells can adapt the MT1-MMP-based proteolytic machinery to the degree of confinement.
- I described the molecular mechanisms underlying force transmission to the nucleus and their contribution to tumor cells adaptive response.

Working in close collaboration with two post-doctoral fellows of the host lab, I used confocal fluorescence microscopy to image breast (MDA-MB-231) and fibrosarcoma-derived (HT-1080) cancer cells invading into fibrillar collagen of varying confinement levels. We found that migration in nucleus-confining conditions triggered an adaptive response, which includes invadopodia formation along nucleus-constricting fibers, polarization and exocytosis of MT1-MMP-positive vesicles and proteolysis of collagen fibers in front of the nucleus to support nucleus movement. By contrast, this adaptive response was switched off in low-confinement conditions by increasing collagen gel mesh size using different temperatures of polymerization, or modulating nuclear stiffness tuned by lamin levels. Additionally, we evaluated the contribution of molecular components of the LINC complex to tumor cells adaptive response as force transmission to the nucleus critically relies on LINC complex making a bridge between the nuclear lamina and cytoplasmic cytoskeleton components (McGregor et al., 2016). The discovery of an adaptive response involving the invadopodia/MT1-MMP axis during tumor cell invasion was reported in an article, which I shared first co-authorship and that is presented in the next section (**see Article 1**).

In the second part of my project, I set out to further investigate the formation and dynamics of invadopodia in breast cancer cells invading in thick 2D (2.5D) and 3D fibrillar collagen environments. My initial observations using live-imaging of MDA-MB-231 cells expressing Tks5-GFP, a highly specific invadopodia marker, suggested that invadopodia form as ring-like structures along constricting fibers ahead of the nucleus. I observed that these structures generated forces to expand and push fibers aside, thus widening ECM pores to promote nuclear transmigration through narrow spaces. Consequently, I aimed to decipher the fundamental mechanisms of invadopodia-mediated force production and how it coordinates with MT1-MMP-based collagenolysis. I used a pharmacological approach to inhibit actin polymerization, actomyosin activity as well as MT1-MMP activity to assess their respective

contribution in force generation and transmission to the matrix at invadopodia. Finally, I described the particular actin cytoskeletal organization in invadopodia at high resolution using metal replica electron microscopy in collaboration with Dr. S. Vassilopoulos (Myology Institute, Paris). In addition, I collaborated with a theoretician, Dr. R. Voituriez (LPTMC, Paris), to propose a physical model describing the force balance in the invadopodia/collagen-fiber ensemble.

In addition, my work revealed that invadopodia form exclusively in association with a small proportion of collagen fibers, implying the activation of specific adhesion receptors. Several collagen receptors, including integrins and discoidin domain receptors (DDRs) have been implicated in invadopodia formation, although with conflicting results (Artym et al., 2015; Destaing et al., 2010; Juin et al., 2014). In order to identify ECM receptors mediating invadopodia formation, I used immunostaining to determine the cellular distribution of collagenic receptors and measured invadopodia assembly in cells silenced for the different collagenic receptors. All together, these results are reported in a second manuscript, which is currently submitted for publication (see **Article 2, Ferrari *et al.***).

Article 1

LINC complex-Lis1 interplay controls MT1-MMP matrix digest-on-demand response for confined tumor cell migration

Elvira Infante ^{1,*,+}, Alessia Castagnino ^{1,*}, Robin Ferrari ^{1,*}, Pedro Monteiro ^{1,*}, Sonia Agüera-González ¹, Perrine Paul-Guilloteaux ^{1,2}, Melanie J. Domingues ¹, Paolo Maiuri ³, Matthew Raab ¹, Catherine M. Shanahan ⁴, Alexandre Baffet ¹, Matthieu Piel ¹, Edgar R. Gomes ⁵, and Philippe Chavrier ^{1,+}

¹ Institut Curie, PSL Research University, CNRS, UMR 144, 26 rue d'Ulm, F-75005, Paris, France

² Institut Curie, Cell and Tissue Imaging Facility (PICT-IBiSA), 26 rue d'Ulm, F-75005, Paris, France

³ IFOM, the FIRC Institute of Molecular Oncology, Via Adamello 16, 20139 Milan, Italy

⁴ BHF Centre of Research Excellence, Cardiovascular Division, King's College, 125 Coldharbour Lane, SE5 9NU London, UK

⁵ Instituto de Medicina Molecular, Faculdade de Medicina, Universidade de Lisboa, Avenida Professor Egas Moniz, 1649-028 Lisboa, Portugal

* These authors contributed equally.

+ Corresponding authors, e-mail: elvira.infante@kcl.ac.uk; philippe.chavrier@curie.fr






Published in Nature Communications: 22nd June 2018.

ARTICLE

DOI: 10.1038/s41467-018-04865-7

OPEN

LINC complex-Lis1 interplay controls MT1-MMP matrix digest-on-demand response for confined tumor cell migration

Elvira Infante¹, Alessia Castagnino¹, Robin Ferrari¹, Pedro Monteiro¹, Sonia Agüera-González¹, Perrine Paul-Gilloteaux ^{1,2}, Mélanie J. Domingues¹, Paolo Maiuri ³, Matthew Raab¹, Catherine M. Shanahan⁴, Alexandre Baffet¹, Matthieu Piel ¹, Edgar R. Gomes ⁵ & Philippe Chavrier ¹

Cancer cells' ability to migrate through constricting pores in the tissue matrix is limited by nuclear stiffness. MT1-MMP contributes to metastasis by widening matrix pores, facilitating confined migration. Here, we show that modulation of matrix pore size or of lamin A expression known to modulate nuclear stiffness directly impinges on levels of MT1-MMP-mediated pericellular collagenolysis by cancer cells. A component of this adaptive response is the centrosome-centered distribution of MT1-MMP intracellular storage compartments ahead of the nucleus. We further show that this response, including invadopodia formation in association with confining matrix fibrils, requires an intact connection between the nucleus and the centrosome via the linker of nucleoskeleton and cytoskeleton (LINC) complex protein nesprin-2 and dynein adaptor Lis1. Our results uncover a digest-on-demand strategy for nuclear translocation through constricted spaces whereby confined migration triggers polarization of MT1-MMP storage compartments and matrix proteolysis in front of the nucleus depending on nucleus-microtubule linkage.

¹Institut Curie, PSL Research University, CNRS, UMR 144, 26 rue d'Ulm, F-75005 Paris, France. ²Institut Curie, Cell and Tissue Imaging Facility (PICT-IBiSA), 26 rue d'Ulm, F-75005 Paris, France. ³IFOM, the FIRI Institute of Molecular Oncology, Via Adamello 16, 20139 Milan, Italy. ⁴BHF Centre of Research Excellence, Cardiovascular Division, King's College, 125 Coldharbour Lane, SE5 9NU London, UK. ⁵Instituto de Medicina Molecular, Faculdade de Medicina, Universidade de Lisboa, Avenida Professor Egas Moniz, 1649-028 Lisboa, Portugal. These authors contributed equally: Elvira Infante, Alessia Castagnino, Robin Ferrari, Pedro Monteiro. Correspondence and requests for materials should be addressed to E.I. (email: elvira.infante@kcl.ac.uk) or to P.C. (email: philippe.chavrier@curie.fr)

Recent studies revealed that limited deformability of the nucleus prevents constricted cell movement and that nuclear stiffness is a critical element for the ability of normal and cancer cells to migrate through confined extracellular matrix (ECM) environments^{1–4}. Nuclear rigidity depends on lamin A (LMNA) levels, component of the nuclear lamina acting as a rigid and protective shell underneath the inner nuclear membrane^{5,6}. Down-modulation of LMNA in cancer cells correlates with increased nuclear deformability and enhanced cell migration in confined environments by facilitating nucleus squeezing through ECM pores^{1–4,7–9}.

Also critical for metastasis is the capacity of cancer cells to remodel ECM barriers¹⁰. Invasion by carcinoma cells is potentiated by pericellular matrix proteolysis, executed by transmembrane membrane-type 1 matrix metalloproteinase (MT1-MMP)^{11,12}. MT1-MMP is up-regulated during tumor progression and its up-regulation predicts the invasive potential of cancerous breast lesions^{13,14}. In 3D type I collagen network, pericellular ECM proteolysis is associated with the invasive cell protrusion ahead of the nucleus, and is reduced at the cell leading edge, involved in cell-matrix adhesion to support 3D migration^{15,16}. With decreasing matrix pore size, cancer cell invasion critically depends on MT1-MMP surface expression to enlarge matrix pores^{2,11}. Inhibition of MT1-MMP function impairs confined cell movement and correlates with increased nuclear deformation, nuclear envelope (NE) rupture and DNA damage^{2,15,17}.

Cancer cells adjust their levels of surface-exposed MT1-MMP through trafficking from late endosomal/lysosomal storage compartments¹⁸. Whether and how matrix porosity and cell confinement influence MT1-MMP surface localization remain unexplored. To address these outstanding questions, we used live cell imaging of breast carcinoma and fibrosarcoma cells invading through 3D collagen gels of controlled porosity. We report that invasion through small pore size collagen meshwork triggers an adaptive response with polarized centrosome-centered distribution of MT1-MMP-positive storage endosomes ahead of the nucleus and enhanced MT1-MMP-based pericellular proteolysis of confining collagen fibrils. In contrast, endosome polarization is lost and collagenolysis decreases in cells invading through a permissive large pore size collagen environment. Importantly, modulating LMNA levels with known consequences on nuclear stiffness impinges on MT1-MMP-positive endosome polarity and collagenolysis. We provide evidence that endosome polarization and MT1-MMP-dependent collagenolysis require integrity of the linker of nucleoskeleton and cytoskeleton (LINC) complex that connects the nuclear lamina to cytoskeletal elements in the cytoplasm and the dynein regulator Lis1 involved in nucleus-microtubule cytoskeleton linkage¹⁹. Our data support a model whereby focal MT1-MMP-mediated ECM proteolysis response is engaged by mechanical signals during confined migration to facilitate nuclear movement and promote tumor cell invasion.

Results

Confinement and nuclear stiffness regulate collagenolysis. The morphology and collagenolysis activity of invasive MDA-MB-231 cells embedded in the 3D fibrillar type I collagen network were analyzed by staining for microtubules and a cleaved collagen neoepitope. After a short 2.5 hrs incubation, different cell morphologies were observed (Fig. 1a): (i) pre-invasive rounded cells with collagen degradation surrounding the cell edge, (ii) cells that initiated invasion as exemplified by limited collagen degradation track behind the cell and at the basis of the nascent protrusion ahead of the nucleus, (iii) fully invasive cells showing typical elongated mesenchymal organization with collagen

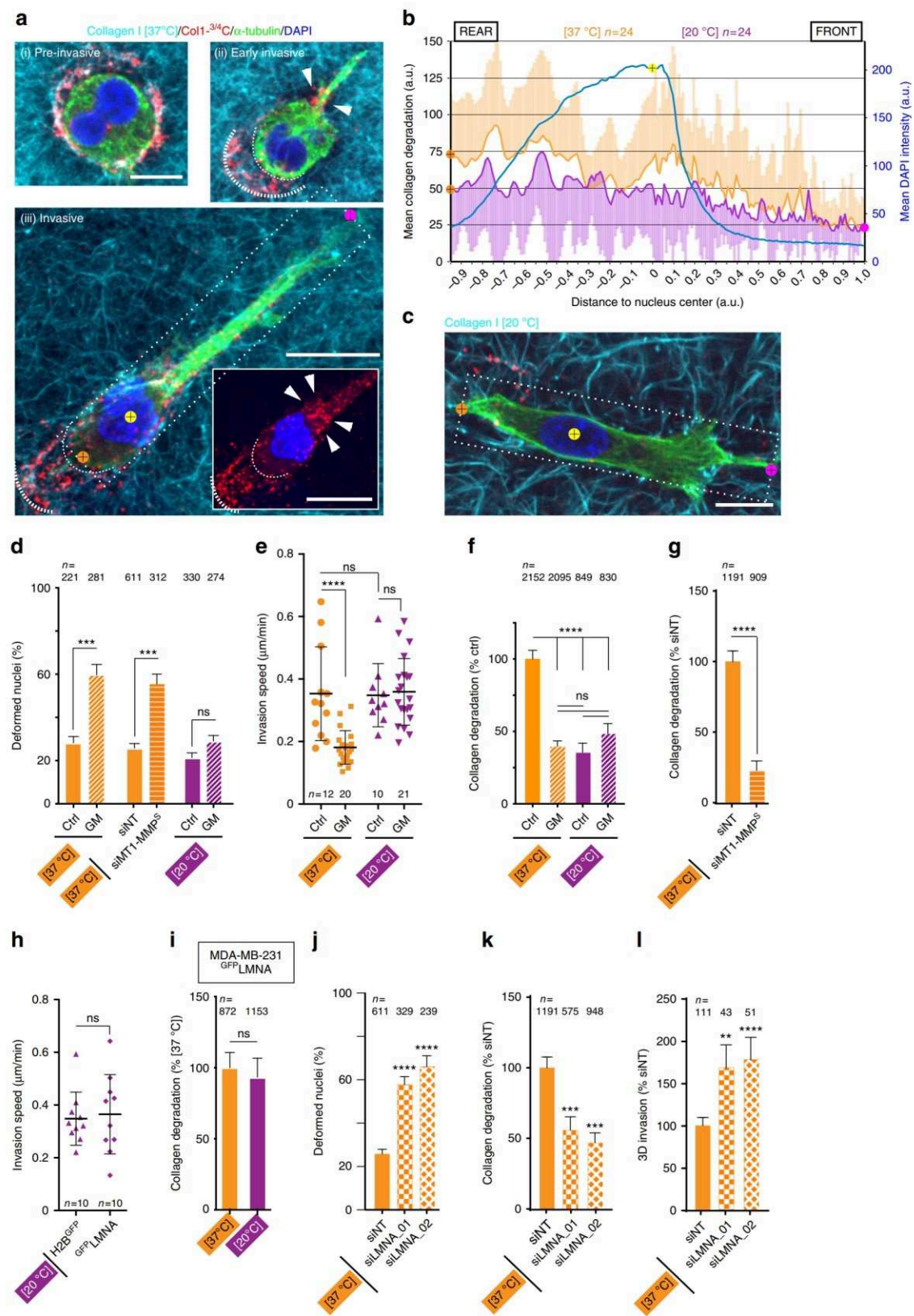
degradation in front of the nucleus and cleared collagen from the cell path probably through the action of collagenases, consistent with previous observations²⁰. Importantly, when fluorescence intensity of cleaved collagen was measured along the long cell axis of several invasive cells and averaged, a robust pericellular collagenolysis in association with the bulky part of the cell anterior to the nucleus was observed, while collagen degradation was minimal at the cell front (Fig. 1b). In agreement with previous findings^{2,3,17}, we observed that $28 \pm 2.9\%$ of invasive cells in the 3D collagen gel presented various degrees of nuclear deformation as the nucleus moved through constricting spaces (Fig. 1d and Supplementary Fig. 1a). Moreover, inhibition of MMP activity upon GM6001 (GM) treatment, which reduced invasion speed in 3D collagen by ~2-fold and interfered with pericellular collagenolysis (Fig. 1e, f and Supplementary Fig. 1b), correlated with a strong enhancement of nuclear deformation (~55–60% deformed nuclei, see Fig. 1d and Supplementary Fig. 1c). Similarly, MT1-MMP silencing using small interfering (si)RNA led to a robust inhibition of pericellular collagenolysis and increased nuclear deformation (Fig. 1d, g and Supplementary Fig. 1b). Altogether, these findings indicated that surface-exposed MT1-MMP enabled efficient cell movement in confinement by mediating proteolysis anterior of the nucleus.

Physical features of the matrix and cellular parameters can affect cancer cell motility such as matrix porosity and nuclear stiffness, respectively^{1–4}. We explored potential relations between these parameters and MT1-MMP-dependent pericellular collagenolysis. Matrix pore size was increased by reducing collagen polymerization temperature to 20 °C instead of 37 °C, the condition used so far, while keeping collagen concentration constant (2.0 mg/ml); this led to a ~2-fold increase in the distance between fibrils (Supplementary Fig. 1d, e)^{2,21}. GM treatment did not result in a significant increase of nuclear deformation in cells invading through the gel of higher porosity (Fig. 1d). In addition, invasion speed in the large pore size gel was not affected by GM treatment contrasting with inhibition observed in the smaller pore size gel (Fig. 1e). These data indicated that in a permissive large pore size collagen environment causing reduced nuclear constriction, MT1-MMP was dispensable for invasion, in agreement with previous observation². Strikingly, we found that invasion through the higher porosity gel correlated with a ~60% reduction of pericellular collagenolysis as compared to the small pore size collagen network and a lack of proteolysis anterior of the nucleus (Fig. 1b, c, f and Supplementary Fig. 1b). Similarly, pore size enlargement correlated with a significant decrease of collagenolysis by HT-1080 fibrosarcoma cells, while invasion speed was similar in large and small pore size gels (Supplementary Fig. 1f–h). These data indicated that modulation of cell confinement correlated with changes in MT1-MMP-dependent pericellular proteolysis of constricting collagen fibrils.

Next, the influence of lamin A expression levels, with well described relationship with nuclear stiffness and deformability was tested on MT1-MMP-dependent response. Nuclei from GFP^{LMNA}-overexpressing cells slowed down or even stalled within the 2.5 µm-diameter constrictions of microfabricated channels as compared to GFP^{H2B}-expressing cell nuclei that crossed the constriction in 1–2 h (Supplementary Fig. 2a–d). These findings are in agreement with increased nuclear stiffness induced by elevated LMNA levels^{1,5}. GFP^{LMNA} overexpression did not affect MT1-MMP level nor association of LINC complex components Nesprin-1 and SUN1 to the NE (Supplementary Fig. 2a and e, f). Invasion speed of MDA-MB-231 cells in 20 °C polymerized collagen gel (large pore size) was not affected by overexpression of GFP^{LMNA} as compared to GFP^{H2B} (Fig. 1h). However, contrasting with the reduction of collagenolysis by MDA-MB-231 cells in the permissive large pore size collagen gel

(Fig. 1f), collagenolysis levels of ^{GFP}LMNA-overexpressing cells remained elevated in large, as compared to small, pore size collagen environment (Fig. 1i and Supplementary Fig. 2g). These observations revealed a relationship between LMNA overexpression, known to increase nuclear stiffness and elevated

levels of MT1-MMP-mediated ECM proteolysis during 3D invasion. Reciprocally, reduction of LMNA levels has been shown to increase nuclear deformability^{4,22,23}. LMNA was silenced to ≤5% of endogenous levels using two independent siRNAs with no



change in MT1-MMP expression nor visible alteration in cytoskeletal organization (Supplementary Fig. 3a, b). Reduced LMNA levels correlated with increased nuclear deformation in 3D collagen gel polymerized at 37 °C (55–65% deformed nuclei including 25% polymorphic lobulated nuclei, Fig. 1j) and in cells plated on a thick fibrous collagen layer (Supplementary Fig. 3b). In addition, LMNA KD correlated with increased migration speed of ^{GFP}H2B-expressing cells in microchannels (Supplementary Fig. 2c, d). Collectively these data indicated that LMNA-depleted cells had more deformable nuclei and retained full migratory capacity. Remarkably, MT1-MMP-dependent collagenolytic activity in the small pore size collagen gel decreased by ~2-fold upon LMNA KD (Fig. 1k and Supplementary Fig. 3c). Despite reduced collagenolysis, silencing of LMNA correlated with a 1.5–1.7-fold increase of invasion (Fig. 1l and Supplementary Fig. 3d). Thus, reduced LMNA expression enhanced the invasive potential of breast tumor cells by increasing nucleus deformability and its capacity to squeeze through constricted spaces, while MT1-MMP response was lowered down. All together, these findings indicated that MT1-MMP-mediated pericellular collagenolysis is an adaptive response that is switched on during confined migration in the dense ECM environment, suggesting a relationship between environment, nuclear biomechanics and modulation of active MT1-MMP at the cell surface.

Polarization of MT1-MMP endosomes during confined migration. In order to identify the mechanism underlying increased collagenolysis during constricted migration, we looked at the dynamic distribution of MT1-MMP-positive storage endosomes in MDA-MB-231 cells invading in 3D collagen by automated endosome tracking over time. In cells invading through the small pore size collagen gel, MT1-MMP-containing endosomes clustered in a region anterior to the nucleus relative to the direction of movement (Fig. 2a and Supplementary Movie 1);

~50% of MT1-MMP-positive endosomes polarized in a 90° quadrant in front of the nucleus relative to movement with a non-uniform distribution as demonstrated by Rao's Spacing test ($P < 0.001$, Fig. 2b). In contrast, we observed a striking uniform endosome distribution in MDA-MB-231 cells invading in the large pore size collagen gel polymerized at 20 °C ($P > 0.1$, Fig. 2d, e and Supplementary Movie 2). Relationship between MT1-MMP endosome polarity and collagen gel porosity was similarly observed in HT-1080 cells (Fig. 2c, f). Then, we examined the consequences of modulating LMNA levels, nuclear deformability and gel porosity on endosome polarization in MDA-MB-231 cells. In the permissive gel polymerized at 20 °C, decreased nuclear deformability upon LMNA^{GFP} overexpression correlated with a remarkable polarization of MT1-MMP endosomes in front of the nucleus (Fig. 2g, h, compare to Fig. 2d, e, and see Supplementary Movie 3). Conversely, silencing of LMNA correlated with a loss of endosome polarization in front of the nucleus in cells invading through the confining gel polymerized at 37 °C and instead a bimodal endosome distribution was observed (Fig. 2i, j, compare to 2a, b, and see Supplementary Movie 4). Collectively, these findings suggested that endosome polarization in front of the nucleus is part of the response to adjust pericellular collagenolysis and widen constricting pores in the matrix.

The centrosome is positioned ahead of the nucleus. We observed that the centrosome was located in front of the nucleus in cells invading through the 3D small pore size collagen gel and noticed that the centrosome was often located in the vicinity of maximal nuclear constriction when invasion was impaired upon MMP inhibition (Fig. 3a, b). MT1-MMP endosome positioning and clustering around the centrosome are controlled by interactions with the microtubule network and dynein and kinesin motor activity²⁴. Thus, nucleus-centrosome linkage and

Fig. 1 MT1-MMP-dependent pericellular collagenolysis is an adaptive response to matrix porosity. **a** MDA-MB-231 cells were embedded in 2.0 mg/ml fluorescent type I collagen (cyan) and polymerization was induced at neutral pH at 37 °C. Cells were fixed after 2.5 hrs and stained for cleaved collagen neopeptide (Col1-^{3/4}C antibody, red), α -tubulin (green) and DAPI (blue). Dashed box indicates the region used for line-scan analysis in panel b with yellow, orange and pink dots indicating nucleus center, posterior and anterior limits of regions used for line-scan analysis. Dashed lines indicate initial cell position (thick) and cell rear (thin), respectively. Inset shows nucleus and cleaved collagen signal and arrowheads point to nucleio-anterior collagenolysis. **b** Averaged maximal fluorescence intensity profiles of cleaved collagen in 37 °C (orange curve) or 20 °C (purple curve) polymerized collagen \pm SD (left Y-axis) and DAPI (right Y-axis) along cell axis. n , number of cells used to calculate averaged intensity profiles from three independent experiments; "0" on X-axis corresponds to nucleus center. **c** MDA-MB-231 cells embedded in 20 °C polymerized gel analyzed as in **a**. **d** Morphological analysis of DAPI-stained nuclei (see Supplementary Fig. 1a for nucleus shape scoring criteria) in MDA-MB-231 cells in 3D collagen matrix under indicated experimental conditions. Data are mean \pm SEM from three independent experiments (except Ctrl at [37 °C], $N = 2$ and siNT, $N = 6$); (n), number of cells analyzed. P -values of Kruskal-Wallis test as compared to control condition in each dataset. **e** MDA-MB-231 cells expressing H2B^{GFP} were embedded in 3D 37 °C or 20 °C polymerized gels. Cells were treated with ethanol (Ctrl) or GM as indicated. Nuclei were automatically tracked from time-lapse sequences obtained from three independent experiments and plot shows the distribution of nuclei speed. n , number of cells analyzed from three independent experiments. Data were transformed using the log transformation $y = \log(y)$ to make data conform to normality and analyzed using one-way ANOVA test. **f, g** Pericellular collagenolysis by MDA-MB-231 cells treated with GM (**f**) or silenced for MT1-MMP (**g**) in 37 °C or 20 °C polymerized gels measured as mean intensity of Col1-^{3/4}C signal per cell (see Supplementary Fig. 1b for representative images). Values for vehicle-treated (panel f) or siNT-treated cells in 37 °C polymerized gel (**g**) were set to 100%. n , number of cells analyzed from three to five independent experiments (except experiments in 20 °C polymerized gel, $N = 2$); Kruskal-Wallis (**f**) and Mann-Whitney (**g**) tests. **h** MDA-MB-231 cells expressing H2B^{GFP} or ^{GFP}LMNA were embedded in 3D collagen gel polymerized at 20 °C and invasion speed was analyzed as in **e**. n number of cells analyzed from three independent experiments. Unpaired t -test. **i** Pericellular collagenolysis by MDA-MB-231 cells expressing ^{GFP}LMNA in 37 °C (set to 100%) or 20 °C polymerized gels (see Supplementary Fig. 2g for representative images). n , number of cells analyzed from three independent experiments; Mann-Whitney test. **j** Analysis of nuclear deformation in MDA-MB-231 cells knocked down for LMNA in 37 °C polymerized gel as in **d**. Data are mean \pm SEM from three independent experiments (except siNT, $N = 6$); (n), number of cells analyzed. P -values of One-way ANOVA test as compared to control condition. **k** Pericellular collagenolysis by MDA-MB-231 cells knocked down for LMNA in 37 °C polymerized gel normalized to mean intensity of siNT-treated cells \pm SEM (see Supplementary Fig. 3c for representative images); n number of cells analyzed from three independent experiments; Kruskal-Wallis test. **l** Relative invasion of cells penetrating 3D collagen to depths $\geq 30 \mu\text{m}$ (see Supplementary Fig. 3d for representative images). Data represent mean \pm SEM normalized to invasion of control cells from three independent experiments. n number of cells analyzed from three independent experiments; Kruskal-Wallis test. ** $P < 0.01$; *** $P < 0.001$; **** $P < 0.0001$; ns, not significant. Scale bar = $10 \mu\text{m}$

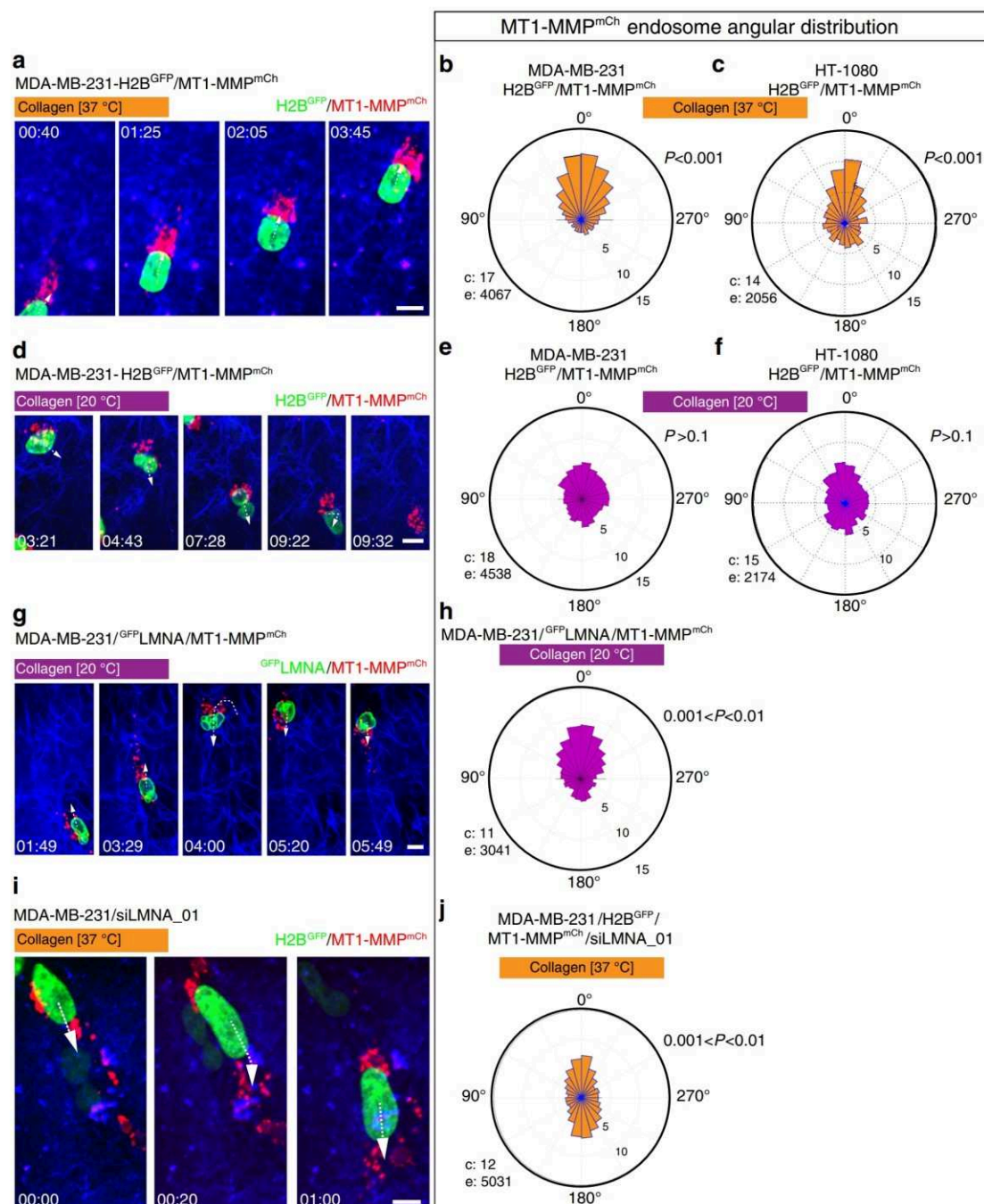


Fig. 2 Polarization of MT1-MMP endosomes is part of the adaptive MT1-MMP-dependent collagenolysis response during confined invasion. **a** MDA-MB-231 cells expressing MT1-MMP^{mCh} (red) and H2B^{GFP} (green) were embedded in the 3D small pore size collagen gel and analyzed by time-lapse confocal spinning-disk microscopy (see Supplementary Movie 1). The gallery shows representative non-consecutive frames from a representative movie obtained from three independent experiments (time in h:min). Arrows show the direction of migration. **b, c** Rose plots showing the percentage of MT1-MMP endosomes in 15° segments relative to the direction of nucleus movement (0°) scored from time-lapse sequences of MDA-MB-231 (**b**) or HT-1080 (**c**) cells. c number of cells, e number of endosomes analyzed from three independent experiments. *P*-values for circular uniformity Rao's Spacing test are provided. **d** Representative frames from a time-lapse sequence of MDA-MB-231 cells invading in the large pore size collagen gel (see Supplementary Movie 2). **e, f** Angular distribution of MT1-MMP endosomes relative to the direction of nuclear movement as in **b, c**. **g** Gallery from a representative time-lapse sequence of MDA-MB-231 cells expressing MT1-MMP^{mCh} (red) and GFP^{LMNA} (green) embedded in the large pore size gel (see Supplementary Movie 3). **h** Rose plot of MT1-MMP endosome angular distribution from three independent experiments. **i** Representative frames of a movie of MDA-MB-231 cells treated with siRNA against LMNA invading through 37 °C polymerized gel (see time-lapse in Supplementary Movie 4). **j** Rose plot of MT1-MMP endosome angular distribution from three independent experiments. Scale bars=10 μm

centrosome positioning in front of the nucleus could underlie polarization of MT1-MMP endosomes during constricted migration. Anchoring of the nucleus to the centrosome involves LINC complex components SUN and nesprins, which interact

with cytoskeletal elements including microtubules^{25–28}. We used overexpression of the dominant negative KASH domain of nesprin-2 (GFP^{DN-KASH}) known to antagonize SUN-nesprin interactions, which displaced nesprin-1 and -2 from the NE of

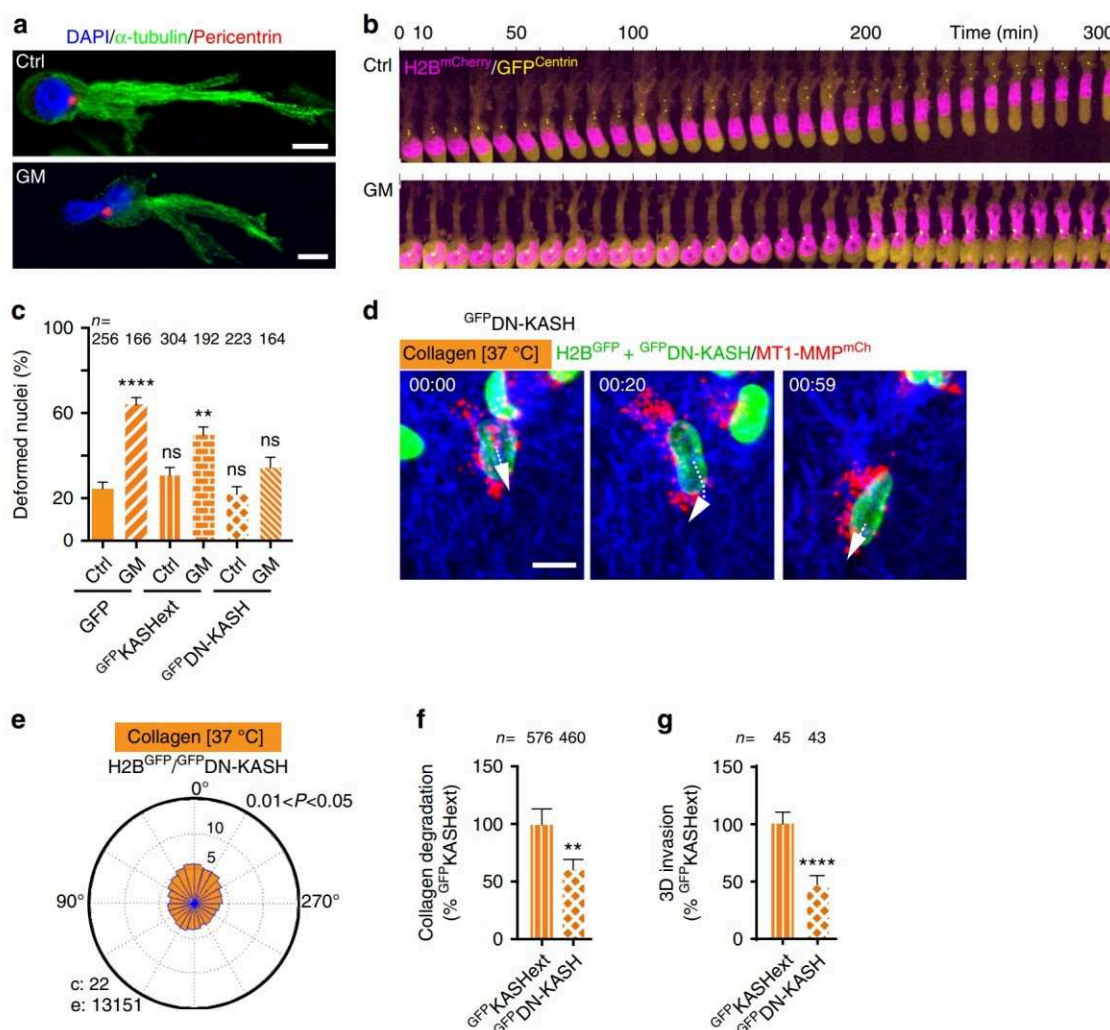


Fig. 3 Nucleus-centrosome linkage through LINC complex is involved in MT1-MMP endosome polarization and collagenolysis-based invasion. **a** MDA-MB-231 cells in 3D collagen I polymerized at 37 °C treated or not with GM MMP inhibitor and stained for α -tubulin (green), centrosomal pericentrin (red) and nucleus (blue). **b** Galleries from representative time-lapse sequences of MDA-MB-231 cells expressing H2B^{mCherry} (magenta) and GFP^{Centrin-1} (yellow) invading through type I collagen gel as in **a**. **c** Morphological analysis of DAPI-stained nuclei as in Fig. 1d. Data are mean \pm SEM from three independent experiments. (n), number of cells analyzed. P-values of Kruskal-Wallis test as compared to non-treated GFP-expressing cells. **d** Representative frames of a movie of MDA-MB-231 cells expressing MT1-MMP^{mCh} (red) and H2B^{GFP} together with GFP^{DN-KASH} (green) invading through the small pore size collagen gel polymerized at 37 °C (see time-lapse sequence in Supplementary Movie 5). **e** Rose plots of endosome angular distribution from three independent experiments as in Fig. 2b. P-value for circular uniformity Rao's Spacing test is provided. **f** Pericellular collagenolysis by MDA-MB-231 cells expressing GFP^{DN-KASH} in 37 °C polymerized gel normalized to mean intensity of GFP^{KASHext}-expressing cells \pm SEM (see Supplementary Fig. 4e for representative images); n, number of cells analyzed from three independent experiments; Mann-Whitney test. **g** 3D invasion of GFP^{DN-KASH}-expressing cells in the small pore size gel normalized to invasion of GFP^{KASHext}-expressing cells \pm SEM from three independent experiments as in Fig. 1l. n number of cells analyzed from three independent experiments (see Supplementary Fig. 4f for representative images); Mann-Whitney test. **P < 0.01; ****P < 0.0001; ns non significant. Scale bars=10 μ m

MDA-MB-231 cells (Supplementary Fig. 4a–c), and correlated with a ~10-fold increase in centrosome-nucleus distance (Supplementary Fig. 4d)^{29,30}. In contrast, GFP^{KASHext} with a C-terminal extension preventing binding to SUN did not affect nesprin association to the NE nor nucleus-centrosome linkage (Supplementary Fig. 4a–d). Increase in nuclear deformation during 3D invasion in the 37 °C polymerized gel upon MT1-MMP inhibition was suppressed when nucleus-centrosome linkage was loosened by GFP^{DN-KASH} expression but not by GFP^{KASHext} (Fig. 3c). Moreover, front polarization of MT1-MMP-positive endosomes was lost upon GFP^{DN-KASH} overexpression in MDA-MB-231 cells in the small pore size collagen gel (Fig. 3d, e and Supplementary Movie 5). These effects were accompanied by a ~50% reduction of pericellular collagenolysis

and invasive potential upon GFP^{DN-KASH} overexpression as compared to GFP^{KASHext} (Fig. 3f, g and Supplementary Fig. 4e, f). To rule out some global cytoskeletal defects due to perturbation of nucleus-cytoskeletal linkage induced upon DN-KASH expression, we compared cytoskeletal changes induced by constitutively active Rac1 in cells expressing GFP^{DN-KASH} or not. Expression of activated Myc^{Rac1L61} in MDA-MB-231 cells induced the archetypical cortactin-positive lamellipodial extension and cell spreading phenotype (Supplementary Fig. 4g, h). DN-KASH, like the inactive KASHext construct, did not interfere with Rac1L61-induced effects (Supplementary Fig. 4g, h). Thus we concluded that interfering with LINC complex function did not prevent actin filament assembly induced by Rac1 activation at the cell cortex. All together, these findings suggested that

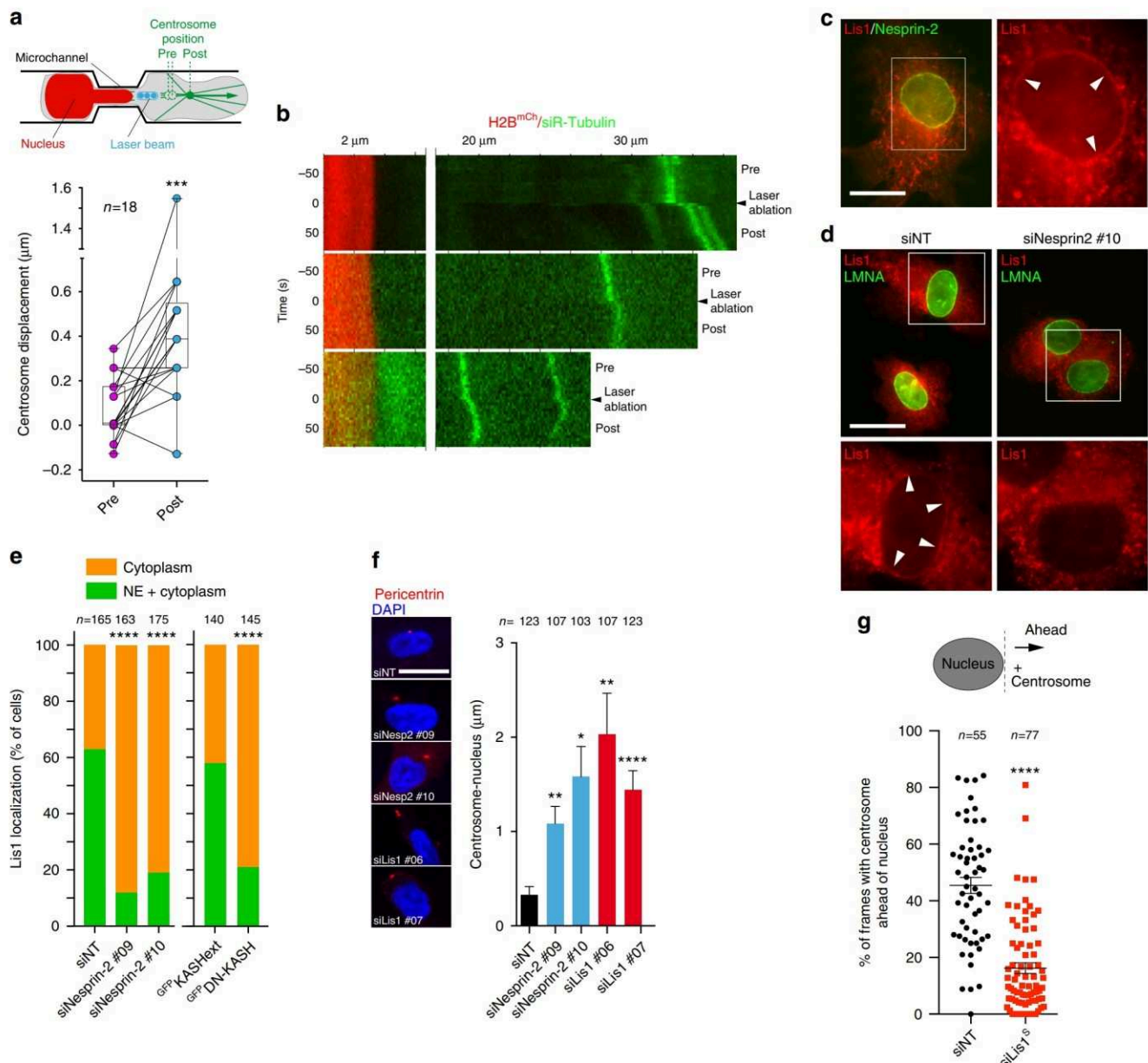


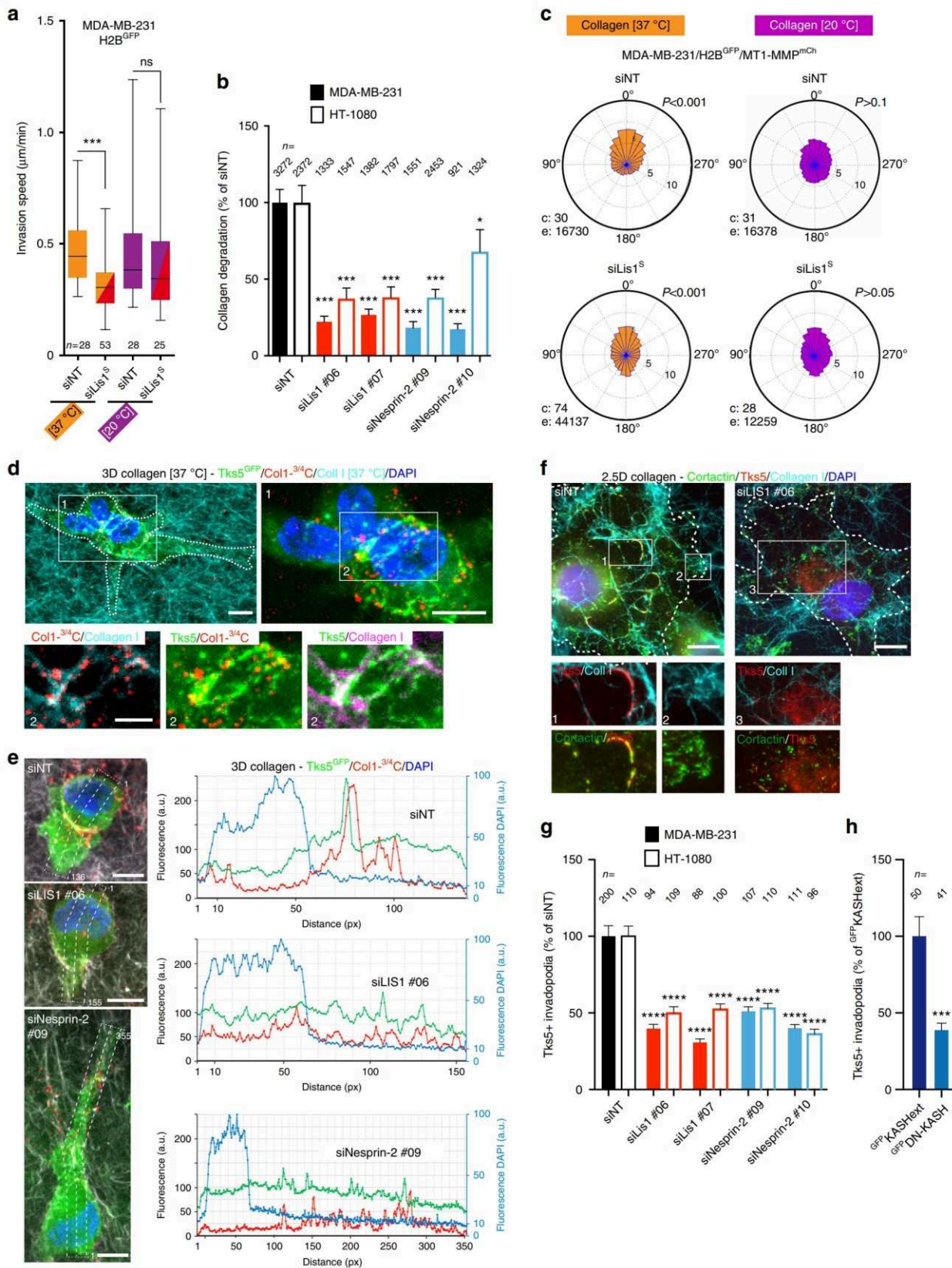
Fig. 4 Lis1 contributes to nucleus-centrosome linkage in MDA-MB-231 cells. **a** Schematic representation of MDA-MB-231 cell expressing H2B^{mCherry} and with SiR-tubulin-labeled microtubules migrating through the microfabricated channel. Centrosome displacement was measured before (pre) and after (post) irradiation with the laser beam (blue dots) focused between the nucleus and the centrosome. Dashed green circles, positions of the centrosome before laser irradiation; green dot, centrosome position after irradiation. For each cell analyzed ($n=18$), the graph shows paired mean centrosome displacements (in μm) before (pre) and after (post) irradiation; Wilcoxon signed rank test. **b** Kymographs showing elastic recoil of the centrosome after laser irradiation (time 0). H2B^{mCherry}-labeled nucleus is shown in red, SiR-tubulin-labeled microtubules and the centrosome are in green. **c** Lis1 and Nesprin-2 immunostaining in MDA-MB-231 cells treated with nocodazole. **d** MDA-MB-231 cells treated or not with nesprin-2 siRNA were treated with nocodazole and immunostained for Lis1 and LMNA. Insets in c and d represent Lis1 signal of the boxed regions. Arrowheads point at regions of Lis1 association with the NE. **e** Percentage of cells with Lis1 association with the NE was scored in cells treated with indicated siRNA. n , number of cells analyzed from three independent experiments; Fisher exact test. **f** Pericentrin and DAPI immunostaining. Scale bars=5 μm . Mean centrosome-nucleus distance (μm) in MDA-MB-231 cells in 3D collagen under indicated conditions \pm SEM; n , number of cells analyzed from three (siLis1 and siNesprin-2) or two (siLMNA) independent experiments; Kruskal-Wallis test. **g** Centrosome position related to the nucleus was scored as schematized from time-lapse sequences of MDA-MB-231 cells expressing GFP-centrin-1 and H2B^{mCherry} and treated with Lis1 siRNA or with control siNT during invasion through the small pore size collagen gel. The graph represents the percentage of frames with the centrosome ahead of the front edge of the nucleus for each cell analyzed and the corresponding Box-and-whisker plot. n , number of cells analyzed from three independent experiments; Mann-Whitney test. * $P < 0.05$; ** $P < 0.01$; *** $P < 0.001$; **** $P < 0.0001$. Scale bars=10 μm .

perturbation of LINC complex function and nucleus-centrosome linkage interfered with front polarization of MT1-MMP storage compartments and with pericellular collagenolysis during confined migration in 3D.

Nesprin-2 and Lis1 mediate nucleo-centrosome attachment. Current models in neuronal cells suggest that nucleus-centrosome linkage involves interaction of cytoplasmic dynein anchored at the NE with centrosome-anchored microtubules, while

counterbalancing forces are exerted on the centrosome through cortically anchored microtubules^{31–33}. We used laser ablation to probe forces in the nucleus-centrosome axis during confined migration of MDA-MB-231 cells in microfabricated channels (Fig. 4a). Centrosome movement was recorded by time-lapse

imaging, revealing low-amplitude oscillatory movement (Fig. 4a, b, pre). Microtubules located between the nucleus and the centrosome were then ablated by UV laser irradiation; the centrosome underwent elastic recoil towards the cell leading edge probably due to unbalanced pulling forces exerted from cortical sites in the



advancing cell protrusion (Fig. 4a, b, post). All together, these data supported the existence of tension forces in the nucleus-centrosome axis during confined migration of MDA-MB-231 cells.

Dynein motor and its regulator Lis1, which is essential for high-load dynein functions, have been implicated in nucleus-centrosome linkage during neuronal migration^{34–37}. The prevailing model is that SUN-nesprin1/2 complexes mediate nucleo-centrosome attachment by providing anchors to cytoplasmic dynein/Lis1 complexes to pull the nucleus toward the centrosome³⁸. Strong enrichment of Lis1 at the NE has been reported in different cell types upon nocodazole treatment^{39–41}. Using similar conditions, we observed partial co-localization of Lis1 and Nesprin-2 at the NE in MDA-MB-231 cells (Fig. 4c). Lis1 was also associated with cytoplasmic vesicles (Fig. 4c, d). Interestingly, Nesprin-2 KD or ^{GFP}DN-KASH expression correlated with a significant reduction of Lis1 association with the NE (Fig. 4d, e). Collectively, these data suggested a contribution of nesprin-2 and LINC complex to Lis1 association with the NE. These observations also highlighted a possible function for Lis1 at the NE. Silencing of Lis1 in MDA-MB-231 cells (85–90% depletion by two independent siRNAs, Supplementary Fig. 5a, b) resulted in a significant 3–4-fold increase of centrosome-nucleus distance (Fig. 4f), similar to findings in Lis1-deficient neurons^{19,34,35}. Silencing of Nesprin-2 (Supplementary Fig. 5c) also increased centrosome-nucleus distance (Fig. 4f), although to a lesser extent as compared to DN-KASH overexpression (Supplementary Fig. 4d). In addition, when centrosome position was scored relative to the nucleus based on movies of MDA-MB-231 cells invading through the small pore size collagen gel polymerized at 37 °C, we found that the centrosome was at ~50% of the time positioned ahead of the nucleus in control cells in agreement with data described above (Fig. 4g). Conversely, the centrosome was only at ~15% of the time positioned in front of the nucleus in cells knocked down for Lis1 (Fig. 4g). Based on these observations we concluded that interfering with Lis1 function affected centrosome positioning in front of the nucleus during confined migration in the collagen matrix, suggesting a role for Lis1 in nucleus-centrosome linkage in MDA-MB-231 cells.

Nesprin-2 and Lis1 regulate nucleo-anterior collagenolysis. The consequences of Lis1 silencing on MT1-MMP-based invasion were analyzed. Lis1 KD significantly reduced the invasion speed of MDA-MB-231 cells in the small pore size gel, while it did not affect invasion in the permissive 20 °C polymerized collagen environment (Fig. 5a). Correlating with the reduction of invasive potential in the small pore size collagen gel, depletion of Lis1 resulted in a strong reduction of pericellular collagenolysis by

MDA-MB-231 and HT-1080 cells in the confining collagen environment similar to silencing of LINC complex component Nesprin-2 (Fig. 5b). In addition, we found that Lis1 depletion interfered with MT1-MMP endosome polarization ahead of the nucleus during confined migration in the small pore size collagen gel (Fig. 5c and Supplementary Movie 6). Endosome polarization was lost in the large pore size gel irrespective of Lis1 expression (Fig. 5c). Of note, silencing of Lis1 in MDA-MB-231 cells did not alter the overall distribution of MT1-MMP endosomes (Supplementary Fig. 5d). In contrast, overexpression of the p50^{Glued}/dynamitin subunit known to disrupt dynein complex function led to a dramatic redistribution of MT1-MMP endosomes to the cell periphery (Supplementary Fig. 5d)^{24,42}. Therefore, we concluded that Lis1 was unlikely to play a significant role in microtubule-based traffic of MT1-MMP-containing endosomes and that it mainly contributed to MT1-MMP-dependent invasion through the regulation of nucleus/centrosome linkage and centrosome positioning.

Collagen degradation is mediated by F-actin, Tks5-positive invadopodia forming at the cell cortex in association with collagen fibrils, where MT1-MMP accumulates^{43–47}. MDA-MB-231 cells embedded in a small pore size 3D collagen network formed typical Tks5-positive structures in association with nucleus-constricting fibrils and with collagenolysis (Fig. 5d, e, siNT). In contrast, cells knocked down for nesprin-2 or Lis1 showed reduced accumulation of Tks5 and collagen degradation in front of the nucleus (Fig. 5e), in agreement with global decrease in collagenolysis (Fig. 5b). Cortactin- and Tks5-positive structures were also visible at the ventral surface of MDA-MB-231 cells in contact with a ~5–10 µm thick (2.5D) layer of fibrous collagen polymerized at 37 °C allowing quantification of invadopodia formation (Fig. 5f)^{46,47}. Silencing of Lis1 in MDA-MB-231 or HT-1080 cells resulted in a strong inhibition of the formation of Tks5-positive structures (Fig. 5f, g). Total level of Tks5 or MT1-MMP proteins were not affected by Lis1 silencing (Supplementary Fig. 5e). Endogenous Lis1 protein was silenced and Lis1 levels were restored by transfection with a cDNA encoding a siRNA-resistant variant of Lis1^{GFP} (Lis1^{R#06/GFP}, Supplementary Fig. 5f, g). Lis1^{R#06/GFP} rescued assembly of Tks5-positive structures in knocked down cells similar to control levels arguing for a specific effect of Lis1 depletion (Supplementary Fig. 5h). Silencing of Nesprin-2 similarly interfered with formation of Tks5 structures (Fig. 5g), as did disruption of LINC complex function by DN-KASH (Fig. 5h). Altogether, our findings indicated that interfering with LINC complex and Lis1 function in nucleus-centrosome attachment affects pericellular collagenolysis in association with cortical cell-matrix contact sites (see model in Fig. 6).

Fig. 5 Lis1 and LINC complex function is required for invadopodia assembly and activity. **a** Effect of Lis1 KD on invasion speed of MDA-MB-231 cells expressing H2B^{GFP} in 3D collagen gels polymerized at 37 °C or 20 °C (as in Fig. 1e). *n*, number of cells analyzed from three independent experiments. Data were transformed using the log transformation $y = \log(y)$ to make data conform to normality and analyzed using one-way ANOVA test. **b** Pericellular collagenolysis (mean Col1-^{3/4}C signal per cell normalized to mean intensity of siNT-treated cells ± SEM) by MDA-MB-231 and HT-1080 cells silenced for Lis1 or Nesprin-2 in collagen polymerized at 37 °C (as in Fig. 1k). *n*, number of cells analyzed from three independent experiments. Kruskal-Wallis test as compared to siNT. **c** Angular distribution of MT1-MMP^{mCh} endosomes in Lis1-depleted cells in 37 °C or 20 °C polymerized collagen gel (as in Fig. 2b). See Supplementary Movie 6. **d** Maximal projection of a series of sixteen confocal sections (7.5 µm width) of MDA-MB-231 cells expressing Tks5^{GFP} (green) in 3D collagen gel polymerized at 37 °C (Cyan) stained for cleaved collagen (red) and nucleus (blue). Scale bars, 10 µm. Bottom row, two-by-two channel combinations corresponding to boxed region #2. Scale bar=5 µm. **e** MDA-MB-231 cells silenced for Lis1 or nesprin-2 embedded in 3D collagen as in **d**, stained for Tks5^{GFP} (green) and cleaved collagen (red). Right row shows intensity profiles of Tks5^{GFP}, Col1-^{3/4}C and DAPI maximum intensities along the long-cell axis (dotted line-enclosed regions). **f** MDA-MB-231 cells silenced for Lis1 were incubated on a thick fibrous type I collagen layer (cyan). Invadopodia in association with collagen fibrils are labeled for cortactin (green) and Tks5 (red). Insets, two-by-two channel combinations of boxed regions. Tks5 is excluded from cortactin-positive lamellipodia (inset #2). Scale bars=10 µm. **g** Quantification of Tks5 signal in MDA-MB-231 and HT-1080 cells treated with indicated siRNAs plated on a thick layer of type I collagen. Y-axis indicates ratio of Tks5 area to total cell area normalized to mean value in siNT-treated cells (as percentage) ± SEM. *n*, number of cells analyzed from three independent experiments. Kruskal-Wallis test. **h** Quantification of Tks5 signal in MDA-MB-231 expressing ^{GFP}KASHext or ^{GFP}DN-KASH as in panel g from two independent experiments; Mann-Whitney test. **P* < 0.05; ****P* < 0.001; *****P* < 0.0001

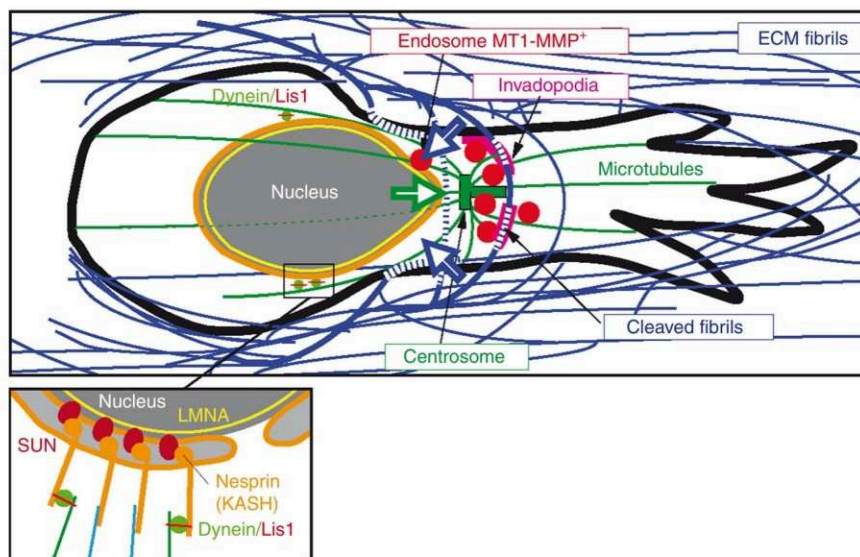


Fig. 6 Model of LINC complex-, Lis1-dependent nucleus-centrosome linkage control of MT1-MMP matrix digest-on-demand response. Confined migration of tumor cells through dense 3D collagen network results in nucleus confinement by constricting collagen fibrils. Nucleus-microtubule cytoskeleton linkage through LINC complex and dynein heavy load factor Lis1 and cortical anchoring of microtubules is required for centrosome and MT1-MMP endosome positioning and for targeted delivery of MT1-MMP to invadopodia. Nucleus movement is facilitated by localized invadopodia-based pericellular proteolysis of confining fibrils ahead of the nucleus. Open arrows represent nuclear pulling force and counteracting forces from the matrix. Inset, scheme of nucleus-cytoskeletal linkage through LINC complex components nesprin and SUN in association with lamins. Lis1, probably in complex with dynein associates to the NE depending on Nesprin-2 and is involved in nucleus-microtubule linkage

Discussion

Several converging studies revealed that nuclear stiffness and nuclear deformability are critical factors that limit confined cell migration through adjacent tissue and basement membrane transmigration by carcinoma cells^{1–4,7}. In addition, recent reports have shown that confinement can generate mechanical stress on the nucleus as exemplified by nuclear deformations and loss of NE integrity and DNA damage^{3,17,48,49}. Increased nucleus deformability as a consequence of LMNA down-modulation can facilitate the migration of cancer cells through small constrictions in reconstituted 3D matrix environments^{2–4,8,9}. Nucleus migration through constricted spaces is also central to several developmental processes⁵⁰.

Our findings reveal a novel mechanism in which tumor cells adapt to the 3D matrix environment based on a digest-on-demand response to support confined migration in the tissue matrix. This mechanism depends on LINC complex-mediated linkage of the nucleus to the microtubule-centrosome network and to high-load dynein adaptor Lis1 (see Fig. 6). It is known that mechanical coupling of the nucleus to the cell cortex through cytoskeletal elements enables force transmission to the nucleus in a LINC complex-dependent manner^{30,51}. Our data suggest a model whereby anchoring of dynein and its regulator Lis1 to the NE mediated by the LINC complex is involved in generation of forward nucleus pulling force on the microtubule-centrosome system^{19,26,35,52–54}. We hypothesize that nucleus forward-pulling forces generate nuclear deformation due to the resistance opposed by constricting matrix fibrils during confined cell migration and that nucleo-cortex linkage may contribute to the assembly of invadopodial structures at plasma membrane-matrix contact sites resulting in focal degradation of confining fibrils (Fig. 6). It may seem paradoxical that interfering with LINC complex or Lis1 function affects invadopodia formation in cells cultured on top of a 2D collagen layer (see Fig. 5f–h). However, under these conditions we observed some pulling and pushing activities of cells on the surrounding collagen fibrils, and cells also squeezed through fibrils, all situations that may lead to some level of

physical constraints and confinement. Noticeably, a previous study reported no effect of SUN1 or nesprin-2 KD on invadopodia formation and function in a melanoma cell line⁵⁵. This discrepancy with our data may be related to difference in matrix environment, i.e., 2D non-fibrillar denatured collagen (gelatin) vs. fibrous native type I collagen in our study with distinct collagenic receptors contributing to invadopodia formation^{55–59}.

Additional mechanisms of tumor cells have been described that lead to nuclear deformation through formation of perinuclear actin- and actomyosin-based structures in association with LINC complex components including nesprin-family proteins. These mechanisms enable nucleus squeezing through narrow spaces and correlate with increased invasiveness and metastatic potential^{60–63}. In addition, a nuclear piston mechanism based on actomyosin contractility has been described, which generates high pressure within the anterior cytoplasmic compartment and enables migration through the 3D confining matrix⁶⁴. This mechanism was recently reported to represent a strategy for nuclear forward movement through confining 3D environments that could compensate for low MMP activity⁶⁵. The adaptive MT1-MMP-based collagenolysis response to confinement that we described here and the nuclear piston mechanism may represent different molecular systems consequential to nuclear stiffness and nuclear forward movement during confined migration. An intriguing possibility is whether the nuclear piston mechanism may contribute to nucleo-anterior polarization of MT1-MMP compartments. More work will be needed to determine the contribution and integration of these mechanisms to the metastatic program to tumor cell plasticity. Future studies should also unravel how these mechanisms are integrated with and possibly control invadopodia formation and targeted delivery of MT1-MMP to the cell surface for dissolution of confining ECM fibrils.

Methods

Plasmid constructs. Construct expressing Tks5^{GFP} was a kind gift of Dr S. Courtneidge (OHSU, Portland, OR). Retroviral vector encoding H2B^{GFP} and GFP^{LMNA} were provided by F. A. Dick (UWO, London, ON, Canada) and T.

Misteli (Addgene #17662), respectively. Lentiviral vector encoding H2B^{mCh} was from M. Mercola (Addgene #21217). The GFP^{Centrin-1} plasmid was obtained from M. Bornens (Institut Curie, Paris, France). pRK5^{myc}Rac1L61 was a kind gift of Dr S. Etienne-Manneville (Institut Pasteur, Paris, France). GFP^{DN-KASH} and GFP^{KASHext} were generated by inserting the C-terminal domain of Nesprin-2 (corresponding to the last 331 amino acids) into the XhoI–BamHI site of pECFP-C1 (Takara Bio Inc.). KASHext was derived from the DN-KASH construct by adding a C-terminal VDGAGPGSTGSR amino acid extension²⁹. For Lis1 rescue experiment, LIS1^{GFP} construct was mutagenized to make it resistant to siLIS1#06 siRNA using the QuikChange Primer Design kit (Agilent) using: forward primer: 5'-CTCTGCTTCcGAGGATGCTACTATcAAAGTtTGGGAcTACGAGAC TGGAGATTTTGA-3'; reverse primer: 5'-AAAATCTCCAGTCTCGTAgTCCC AAcCtTtATAGTAGCATCCTCGgAAGCAGAG-3'.

Cell culture, stable and transient transfection and siRNA treatment. MDA-MB-231 cells (ATCC HTB-26) were grown in L15 medium supplemented with 15% foetal calf serum and 2 mM glutamine at 37 °C in 1% CO₂. HT-1080 fibro-sarcoma cells (ATCC CCL-121) were grown in DMEM GlutaMAX supplemented with 10% foetal calf serum. Cell lines were obtained from ATCC and were routinely tested for mycoplasma contamination. MDA-MB-231 cells stably expressing H2B^{GFP/mCh}, MT1-MMP^{mCh} or GFP^{LMNA} and MT1-MMP^{mCh} or HT-1080 cells stably expressing MT1-MMP^{mCh} were generated by lentiviral transduction. For transient expression, MDA-MB-231 cells or HT-1080 cells were transfected with plasmid constructs using AMAXA nucleofection (Lonza). Cells were analyzed by live cell imaging 24–48 h after transfection. For knockdown, MDA-MB-231 cells were treated with the indicated siRNA (50 nM, Dharmacon) using Lullaby (OZ Biosciences, France) and analyzed after 72 h of transfection. The following siRNAs were used: siNT (Non Targeting), siLMNA-01: 5'-GGUGGUGACGAUC UGGGCU-3'; siLMNA-02: 5'-CUGGGCAGGUGGUGACGAU-3'; siMT1-MMP^S (Smartpool): 5'-GGAUGGACACGGAGAAUUU-3'; 5'-GGAACAAGUACUAC CGUU-3'; 5'-GGUCUCAAUUGGCAACAAU-3'; 5'-GAUCAAGGCCAAUGUU CGA-3'; siLis1^S (Smartpool): 5'-CAAUUAAAGGUGUGGAAUA-3' (siLis1#06); 5'-UGAACUAAUUCGAGCUAAU-3' (siLis1#07); 5'-GGAGUGCCGUUGAUUG UGU-3'; 5'-UGACAAGACCCUACGCGUA-3'; siNesprin-2^S (Smartpool): 5'-AGG AAUUCUGCAACCGA-3' (siNesprin-2#09); 5'-GGUAGAAGCUAACCUCA A-3' (siNesprin-2#10); 5'-CCUAGAGUGUCGGAGGGA-3'; 5'-CACAGGAGCU UCACAAUA-3'.

Antibodies and reagents. The source and working dilution of commercial antibodies used for this study are listed in Supplementary Table 1. Monoclonal antibody against Nesprin-2A has been previously described^{66,67}. Nocodazole (Sigma) was diluted in DMSO and used at a concentration of 10 μM. GM6001 (Millipore) diluted in ethanol was used at a concentration of 40 μM. Hepatocyte growth factor (HGF) was purchased from PeproTech Inc. and used at 20 ng/ml.

Western blot analysis. Cells were lysed in SDS sample buffer, separated by SDS-PAGE, and detected by immunoblotting analysis with the indicated antibodies. Antibodies were visualized using the ECL detection system (GE Healthcare).

Indirect immunofluorescence microscopy. Samples were fixed with 4% para-formaldehyde, permeabilized with 0.1% Triton X-100, and then incubated with indicated antibodies. For alpha-tubulin staining samples were fixed with 4% para-formaldehyde at 37 °C for 30 min. For better visualization of Lis1 association with the NE, cells were incubated for 1 h in nocodazole (10 μM) prior to fixation^{35,39–41,68}. The analysis of MT1-MMPmCh endosome position relative to the cell center/cell periphery axis was performed, as described in ref. ²⁴.

Invadopodia formation assay. Coverslips were layered with 200 μl of ice-cold 2.0 mg/ml acidic extracted collagen I solution (Corning) in 1 × MEM mixed with Alexa Fluor 647-conjugated type I collagen (5% final). The collagen solution was adjusted to pH 7.5 using 0.34 N NaOH and Hepes was added to 25 μM final concentration. After 3 min of polymerization at 37 °C, the collagen layer was washed gently in PBS and 1 ml of the cell suspension in L15 medium with 15% FCS (10⁵ cells/ml) was added. Cells were incubated for 90 min at 37 °C in 1% CO₂ before fixation. Cells were pre-extracted with 0.5% Triton X-100 in 4% paraformaldehyde in PBS during 90 s and then fixed in 4% paraformaldehyde in PBS for 20 min and stained for immunofluorescence microscopy with Tks5 and Cortactin antibodies. Images were acquired with a wide-field microscope (Eclipse 90i Upright; Nikon) using a 100 × Plan Apo VC 1.4 oil objective and a highly sensitive cooled interlined charge-coupled device (CCD) camera (CoolSnap HQ2; Roper Scientific). A z-dimension series of images was taken every 0.2 μm by means of a piezoelectric motor (Physik Instrumente). For quantification of Tks5 associated with curvilinear invadopodia in cells plated on collagen fibers, five consecutive z-planes corresponding to the plasma membrane in contact with collagen fibers were projected and surface covered by Tks5 signal was determined using the thresholding command of ImageJ excluding regions <8 pixels to avoid non-invadopodial structures. Surface covered by Tks5 was normalized to the total cell surface and values normalized to control cells.

Quantification of pericellular collagenolysis. Cells treated with indicated siRNAs and expressing indicated GFP-tagged constructs were trypsinized and resuspended (2.5 × 10⁵ cells/ml) in 0.2 ml of ice-cold 2.0 mg/ml acidic extracted collagen I solution in 1 × MEM, pH 7.5 buffer. The pH of the collagen solution was raised to 7.5 using 0.34 N NaOH and Hepes was added to 25 μM final concentration. 40 μl of the cell suspension in collagen was added on a 18 mm-diameter glass coverslip and collagen polymerization was induced by incubation for 90 min at 20 °C or 30 min at 37 °C. After polymerization, complete medium was added and collagen-embedded cells were incubated for 16 h at 37 °C. After fixation in 4% paraformaldehyde in PBS at 37 °C for 30 min, samples were incubated with anti-Col1-^{3/4}C antibodies (2.5 μg/ml) for 2 h at 4 °C, washed extensively with PBS and counterstained with Cy3-conjugated anti-rabbit IgG antibodies and with Phalloidin-Alexa488 to visualize cell shape and with DAPI. Image acquisition was performed with an A1r Nikon confocal microscope with a 40 × NA 1.3 oil objective using high-sensitivity GaAsP PMT detector and a 595 ± 50 nm band-pass filter. Quantification of degradation spots was performed as previously described⁴⁷. Briefly, maximal projection of 10 optical sections with 2 μm interval from confocal microscope z-stacks (20 μm depth) were preprocessed by a laplacian of Gaussian filter using a homemade ImageJ macro (available as supplementary information in⁴⁷). Detected spots were then counted and saved for visual verification. No manual correction was done. Degradation index was the number of degradation spots divided by the number of cells present in the field, normalized to the degradation index of control cells set to 100. Nuclear deformation was visually and qualitatively assessed from maximal projection of 10 optical sections of DAPI signal from confocal microscope z-stacks (20 μm depth) by scoring nuclei as “normal” or “deformed” using criteria as described in Supplementary Fig. 1a.

3D type I collagen invasion assay. 200 μl of 2.0 mg/ml Collagen I was allowed to polymerize in transwell inserts (Corning) for 2 h at 37 °C as above. Cells were seeded on top of the collagen gel in complete medium and 20 ng/ml HGF was added to the medium in the bottom chamber of the transwell as chemoattractant. After 48 h of seeding, cells were fixed and stained with DAPI and visualized by confocal microscopy with serial optical sections captured at 10-μm intervals with a ×10 objective on a Zeiss LSM510 confocal microscope. Invasion was measured by dividing the sum of DAPI signal intensity of all slides beyond 30 μm (invading cells) by the sum of the intensity of all slides (total cells).

Live-cell imaging in 3D type I collagen. For Inter-fibril distance estimation, a 50 μl drop of 2.0 mg/ml fluorescently-labeled Collagen I was allowed to polymerize for 2 h at 37 °C or 20 °C as described above. Distances between collagen fibrils were measured from stacks of 30 optical sections acquired at 0.5 μm-interval with a SP8 Leica laser confocal microscope in the xy, xz, and yz planes (15 μm depth) using a 63 × 1.4NA oil objective, 4 detection channels (2 PMTs and 2 hybrid Detectors) and 405, 488, 561 and 633 nm laser lines. The system was steered by Leica Application Suite (LAS-X) software. For live cell imaging, glass bottom dishes (MatTek Corporation) were layered with 10 μl of a solution of 5 mg/ml unlabeled type I collagen mixed with 1/20–40 volume of Alexa Fluor 647-labeled collagen. Polymerization was induced at 37 °C or 20 °C for 3 min as described above, and the bottom collagen layer was washed gently in PBS and 1 ml of cell suspension (1.5–2.5 × 10⁵ cells/ml) in complete medium was added. Cultures were incubated for 30 min at 37 °C, then medium was gently removed and two drops of a mix of Alexa Fluor 647-labeled type I collagen/unlabeled type I collagen at 2.0 mg/ml final concentration were added on top of the cells (top layer). After polymerization at 37 °C or 20 °C for 90 min as described above, 1 ml of medium containing 20 ng/ml HGF was added to the cultures. z-stacks of images were acquired every 5 min (150 ms exposure time) during 16 h by confocal spinning disk microscopy (Roper Scientific) using a CSU22 Yokogawa head mounted on the lateral port of an inverted TE-2000U Nikon microscope equipped with a 40 × 1.4NA Plan-Apo objective lens and a dual-output laser launch, which included 491 nm and 561 nm 50 mW DPSS lasers (Roper Scientific). Images were acquired with a CoolSNAP HQ² CCD camera (Roper Scientific). The system was steered by Metamorph 7 software.

Automated tracking of endosome angular distribution. A homemade Matlab program (available on demand) was developed to track nuclei based on nuclear staining and create a velocity-dependent coordinate system to analyze MT1-MMP endosomes relative to the direction of displacement of the nucleus. Nuclei were automatically segmented from maximal z-stack projection of sequential time frames (see previous section) based on smoothing and thresholding and then were tracked based on the distance from their previous position. From the trajectory of each nucleus, speed (μm/min) and directionality (persistence) were computed for each consecutive pair of frames. A new polar coordinate system was defined such that the gravity center of the nucleus becomes the position (0,0) for all time points and that the velocity direction had an angle of 0°. This coordinate system was then changing for each time point and was different for each nucleus. Endosomes around each nucleus were automatically segmented by laplacian of gaussian spot enhancement and marker-control watershed segmentation based on regional maxima. The coordinates of the positions of the center of gravity of all endosomes

were then converted to this nucleus velocity-dependent coordinate system. Endosomes exactly in front of the nucleus in the direction of movement are then at 0° and endosomes exactly at the rear of the displacement vector are at 180°. All data created for endosomes for all processed nuclei and all movies for one condition were then pooled to create a polar histogram (radar plot), showing the distribution of endosomes relative to the direction of nuclear movement.

Averaged Col1-3/4C intensity profiles. Col1-3/4C neopeptide (collagen degradation) and DAPI (nucleus) intensity profiles were obtained using the line-scan function (maximal intensity) of Metamorph analyzing the back-to-front cell region including the nucleus for both signals (see Fig. 1a, c). Then, we used a homemade Matlab program (available on demand) to normalize line-scans to correct for line-scan length difference. Briefly, three reference points were manually defined based on the DAPI signal profile; the nucleus center and the back and front of the cell, respectively. These reference points were used to define a linear transformation such that they became 0, -1, and 1 coordinates, respectively on the normalized curves, allowing direct comparison of different profiles.

Centrosome-nucleus distance measurement. Cells were embedded in 2.0 mg/ml type I collagen polymerized at 37 °C as above. After 16 h, cultures were fixed with 4% paraformaldehyde and stained using polyclonal rabbit anti-pericentrin antibodies. Detection was performed with fluorescently-labeled anti-rabbit antibody. DNA was stained with DAPI. Centrosome-to-nucleus distance was determined by overlaying pericentrin and DAPI images and extending a line from the centrosome (center of pericentrin staining) to the nearest point of the nucleus rim; length of this line was measured using ImageJ software tools.

Microfabrication of microchannels. Micro-channels were prepared as previously described⁶⁹. Briefly, polydimethylsiloxane (PDMS) (GE Silicones, 10/1 w/w PDMS A/crosslinker B) was used to prepare 7 µm-wide micro-channels with 2.5 µm constrictions from a self-made mold. Channels with constrictions were washed with PBS at least three times and incubated with complete medium for at least 5 h before adding the cells.

Laser ablation. MDA-MB-231 cells expressing H2B^{mCh} migrating in PDMS channels were labeled with 50 mM SiR-tubulin-Cy5 (Spirochrome) in medium containing 20 ng/ml HGF during 3 hrs at 37 °C. Cells with the nucleus passing through the constrictions were selected. Z stacks (4 images, 0.5 µm z-step) images were acquired at 5 s interval during 75 s (pre-ablation). For photoablation, the 355 nm laser beam was focused to a region of interest selected between the nucleus and SiR-tubulin-labeled centrosome during a 40–80 ms pulse at 50–80% laser power. The conditions of ablation were monitored by the absence of recovery of SiR-tubulin signal. Z stacks were acquired as above for 25 s (post-ablation). The centrosome displacement was measured before and after laser ablation over 25 s periods of time and scored as positive in the direction of cell movement or negative otherwise. Pre- and post-ablation displacements are measured in the same cell and paired in the statistical analysis.

Statistics and reproducibility. All results are presented as the mean ± SEM of three independent experiments except for collagen degradation in 20 °C polymerized gel Fig. 1f (N = 2), centrosome-nucleus distance analysis in siLMNA-treated cells in Fig. 3e (N = 2) and Tks5 recruitment analysis in Fig. 5h (N = 2). GraphPad Prism (GraphPad Software) was used for statistical analysis. Statistical significance was defined as *P < 0.05; **P < 0.01; ***P < 0.001; ****P < 0.0001; ns, not significant. Data were tested for normal distribution using the D'Agostino-Pearson normality test and nonparametric tests were applied otherwise. One-way ANOVA, Kruskal-Wallis, Mann-Whitney or Wilcoxon signed rank tests were applied as indicated in the figure legends. Radial distributions of endosome localization with respect to instantaneous direction of nuclear movement were plotted and analyzed using the “circular” R package^{70,71}. Circular uniformity Rao's Spacing test was employed to test if angle distributions were significantly different from a uniform distribution (significant difference between data and a uniform distribution when P < 0.05).

Data availability. All data are available within the Article and Supplementary Files, or available from the authors upon request.

Received: 16 March 2017 Accepted: 9 May 2018

Published online: 22 June 2018

References

- Rowat, A. C. et al. Nuclear envelope composition determines the ability of neutrophil-type cells to passage through micron-scale constrictions. *J. Biol. Chem.* **288**, 8610–8618 (2013).

- Wolf, K. et al. Physical limits of cell migration: control by ECM space and nuclear deformation and tuning by proteolysis and traction force. *J. Cell. Biol.* **201**, 1069–1084 (2013).
- Harada, T. et al. Nuclear lamin stiffness is a barrier to 3D migration, but softness can limit survival. *J. Cell. Biol.* **204**, 669–682 (2014).
- Davidson, P. M., Denais, C., Bakshi, M. C. & Lammerding, J. Nuclear deformability constitutes a rate-limiting step during cell migration in 3-D environments. *Cell Mol. Bioeng.* **7**, 293–306 (2014).
- Lammerding, J. et al. Lamins A and C but not lamin B1 regulate nuclear mechanics. *J. Biol. Chem.* **281**, 25768–25780 (2006).
- Swift, J. et al. Nuclear lamin-A scales with tissue stiffness and enhances matrix-directed differentiation. *Science* **341**, 1240104 (2013).
- Fu, Y., Chin, L. K., Bourouina, T., Liu, A. Q. & VanDongen, A. M. Nuclear deformation during breast cancer cell transmigration. *Lab Chip* **12**, 3774–3778 (2012).
- Bell, E. S. & Lammerding, J. Causes and consequences of nuclear envelope alterations in tumour progression. *Eur. J. Cell Biol.* **95**, 449–464 (2016).
- Irianto, J., Pfeifer, C. R., Ivanovska, I. L., Swift, J. & Discher, D. E. Nuclear lamins in cancer. *Cell Mol. Bioeng.* **9**, 258–267 (2016).
- Rowe, R. G. & Weiss, S. J. Breaching the basement membrane: who, when and how? *Trends Cell Biol.* **18**, 560–574 (2008).
- Sabeh, F., Shimizu-Hirota, R. & Weiss, S. J. Protease-dependent versus -independent cancer cell invasion programs: three-dimensional amoeboid movement revisited. *J. Cell. Biol.* **185**, 11–19 (2009).
- Kessenbrock, K., Plaks, V. & Werb, Z. Matrix metalloproteinases: regulators of the tumor microenvironment. *Cell* **141**, 52–67 (2010).
- Perentes, J. Y. et al. Cancer cell-associated MT1-MMP promotes blood vessel invasion and distant metastasis in triple-negative mammary tumors. *Cancer Res.* **71**, 4527–4538 (2011).
- Lodillinsky, C. et al. p63/MT1-MMP axis is required for in situ to invasive transition in basal-like breast cancer. *Oncogene* **35**, 344–357 (2016).
- Wolf, K. et al. Multi-step pericellular proteolysis controls the transition from individual to collective cancer cell invasion. *Nat. Cell Biol.* **9**, 893–904 (2007).
- Doyle, A. D. & Yamada, K. M. Mechanosensing via cell-matrix adhesions in 3D microenvironments. *Exp. Cell Res.* **343**, 60–66 (2016).
- Denais, C. M. et al. Nuclear envelope rupture and repair during cancer cell migration. *Science* **352**, 353–358 (2016).
- Castro-Castro, A. et al. Cellular and molecular mechanisms of MT1-MMP-dependent cancer cell invasion. *Annu. Rev. Cell. Dev. Biol.* **32**, 555–576 (2016).
- Tsai, J. W., Bremner, K. H. & Vallee, R. B. Dual subcellular roles for LIS1 and dynein in radial neuronal migration in live brain tissue. *Nat. Neurosci.* **10**, 970–979 (2007).
- Wolf, K. & Friedl, P. Mapping proteolytic cancer cell-extracellular matrix interfaces. *Clin. Exp. Metastas.* **26**, 289–298 (2009).
- Raub, C. B. et al. Noninvasive assessment of collagen gel microstructure and mechanics using multiphoton microscopy. *Biophys. J.* **92**, 2212–2222 (2007).
- Lammerding, J. et al. Lamin A/C deficiency causes defective nuclear mechanics and mechanotransduction. *J. Clin. Invest.* **113**, 370–378 (2004).
- Pajeroski, J. D., Dahl, K. N., Zhong, F. L., Sammak, P. J. & Discher, D. E. Physical plasticity of the nucleus in stem cell differentiation. *Proc. Natl Acad. Sci. USA* **104**, 15619–15624 (2007).
- Marchesin, V. et al. ARF6-JIP3/4 regulate endosomal tubules for MT1-MMP exocytosis in cancer invasion. *J. Cell. Biol.* **211**, 339–358 (2015).
- Crisp, M. et al. Coupling of the nucleus and cytoplasm: role of the LINC complex. *J. Cell. Biol.* **172**, 41–53 (2006).
- Lee, J. S. et al. Nuclear lamin A/C deficiency induces defects in cell mechanics, polarization, and migration. *Biophys. J.* **93**, 2542–2552 (2007).
- Luxton, G. W., Gomes, E. R., Folker, E. S., Vintinner, E. & Gundersen, G. G. Linear arrays of nuclear envelope proteins harness retrograde actin flow for nuclear movement. *Science* **329**, 956–959 (2010).
- Ketema, M. & Sonnenberg, A. Nesprin-3: a versatile connector between the nucleus and the cytoskeleton. *Biochem. Soc. Trans.* **39**, 1719–1724 (2011).
- Stewart-Hutchinson, P. J., Hale, C. M., Wirtz, D. & Hodzic, D. Structural requirements for the assembly of LINC complexes and their function in cellular mechanical stiffness. *Exp. Cell Res.* **314**, 1892–1905 (2008).
- Lombardi, M. L. et al. The interaction between nesprins and sun proteins at the nuclear envelope is critical for force transmission between the nucleus and cytoskeleton. *J. Biol. Chem.* **286**, 26743–26753 (2011).
- Tsai, L. H. & Gleeson, J. G. Nucleokinesis in neuronal migration. *Neuron* **46**, 383–388 (2005).
- McKenney, R. J., Weil, S. J., Scherer, J. & Vallee, R. B. Mutually exclusive cytoplasmic dynein regulation by NudE-Lis1 and dynactin. *J. Biol. Chem.* **286**, 39615–39622 (2011).
- Gundersen, G. G. & Worman, H. J. Nuclear positioning. *Cell* **152**, 1376–1389 (2013).
- Shu, T. et al. Ndel1 operates in a common pathway with LIS1 and cytoplasmic dynein to regulate cortical neuronal positioning. *Neuron* **44**, 263–277 (2004).

35. Tanaka, T. et al. Lis1 and doublecortin function with dynein to mediate coupling of the nucleus to the centrosome in neuronal migration. *J. Cell. Biol.* **165**, 709–721 (2004).
36. Kardon, J. R. & Vale, R. D. Regulators of the cytoplasmic dynein motor. *Nat. Rev. Mol. Cell Biol.* **10**, 854–865 (2009).
37. McKenney, R. J., Vershinin, M., Kunwar, A., Vallee, R. B. & Gross, S. P. LIS1 and NudE induce a persistent dynein force-producing state. *Cell* **141**, 304–314 (2010).
38. Zhang, X. et al. SUN1/2 and Syne/Nesprin-1/2 complexes connect centrosome to the nucleus during neurogenesis and neuronal migration in mice. *Neuron* **64**, 173–187 (2009).
39. Smith, D. S. et al. Regulation of cytoplasmic dynein behaviour and microtubule organization by mammalian Lis1. *Nat. Cell Biol.* **2**, 767–775 (2000).
40. Coquelle, F. M. et al. LIS1, CLIP-170's key to the dynein/dynactin pathway. *Mol. Cell. Biol.* **22**, 3089–3102 (2002).
41. Baffet, A. D., Hu, D. J. & Vallee, R. B. Cdk1 activates pre-mitotic nuclear envelope dynein recruitment and apical nuclear migration in neural stem cells. *Dev. Cell* **33**, 703–716 (2015).
42. Burkhardt, J. K., Echeverri, C. J., Nilsson, T. & Vallee, R. B. Overexpression of the dynamin (p50) subunit of the dynactin complex disrupts dynein-dependent maintenance of membrane organelle distribution. *J. Cell. Biol.* **139**, 469–484 (1997).
43. Seals, D. F. et al. The adaptor protein Tks5/Fish is required for podosome formation and function, and for the protease-driven invasion of cancer cells. *Cancer Cell* **7**, 155–165 (2005).
44. Linder, S., Wiesner, C. & Himmel, M. Degrading devices: invadosomes in proteolytic cell invasion. *Annu. Rev. Cell. Dev. Biol.* **27**, 185–211 (2011).
45. Murphy, D. A. & Courtneidge, S. A. The 'ins' and 'outs' of podosomes and invadopodia: characteristics, formation and function. *Nat. Rev. Mol. Cell Biol.* **12**, 413–426 (2011).
46. Juin, A. et al. Physiological type I collagen organization induces the formation of a novel class of linear invadosomes. *Mol. Biol. Cell* **23**, 297–309 (2012).
47. Monteiro, P. et al. Endosomal WASH and exocyst complexes control exocytosis of MT1-MMP at invadopodia. *J. Cell. Biol.* **203**, 1063–1079 (2013).
48. Raab, M. et al. ESCRT III repairs nuclear envelope ruptures during cell migration to limit DNA damage and cell death. *Science* **352**, 359–362 (2016).
49. Irianto, J. et al. Nuclear constriction segregates mobile nuclear proteins away from chromatin. *Mol. Biol. Cell* **27**, 4011–4020 (2016).
50. Bone, C. R. & Starr, D. A. Nuclear migration events throughout development. *J. Cell. Sci.* **129**, 1951–1961 (2016).
51. Maniotis, A. J., Chen, C. S. & Ingber, D. E. Demonstration of mechanical connections between integrins, cytoskeletal filaments, and nucleoplasm that stabilize nuclear structure. *Proc. Natl Acad. Sci. USA* **94**, 849–854 (1997).
52. Fridolfsson, H. N. & Starr, D. A. Kinesin-1 and dynein at the nuclear envelope mediate the bidirectional migrations of nuclei. *J. Cell. Biol.* **191**, 115–128 (2010).
53. Starr, D. A. & Fridolfsson, H. N. Interactions between nuclei and the cytoskeleton are mediated by SUN-KASH nuclear-envelope bridges. *Annu. Rev. Cell. Dev. Biol.* **26**, 421–444 (2010).
54. Bone, C. R., Chang, Y. T., Cain, N. E., Murphy, S. P. & Starr, D. A. Nuclei migrate through constricted spaces using microtubule motors and actin networks in *C. elegans* hypodermal cells. *Development* **143**, 4193–4202 (2016).
55. Revach, O. Y. et al. Mechanical interplay between invadopodia and the nucleus in cultured cancer cells. *Sci. Rep.* **5**, 9466 (2015).
56. Mueller, S. C. et al. A novel protease-docking function of integrin at invadopodia. *J. Biol. Chem.* **274**, 24947–24952 (1999).
57. Destaing, O. et al. beta1A integrin is a master regulator of invadosome organization and function. *Mol. Biol. Cell* **21**, 4108–4119 (2010).
58. Juin, A. et al. Discoidin domain receptor 1 controls linear invadosome formation via a Cdc42-Tuba pathway. *J. Cell. Biol.* **207**, 517–533 (2014).
59. Artym, V. V. et al. Dense fibrillar collagen is a potent inducer of invadopodia via a specific signaling network. *J. Cell. Biol.* **208**, 331–350 (2015).
60. Khatau, S. B. et al. The distinct roles of the nucleus and nucleus-cytoskeleton connections in three-dimensional cell migration. *Sci. Rep.* **2**, 488 (2012).
61. Thomas, D. G. et al. Non-muscle myosin IIB is critical for nuclear translocation during 3D invasion. *J. Cell. Biol.* **210**, 583–594 (2015).
62. Thiam, H. R. et al. Perinuclear Arp2/3-driven actin polymerization enables nuclear deformation to facilitate cell migration through complex environments. *Nat. Commun.* **7**, 10997 (2016).
63. Jayo, A. et al. Fascin regulates nuclear movement and deformation in migrating cells. *Dev. Cell* **38**, 371–383 (2016).
64. Petrie, R. J., Koo, H. & Yamada, K. M. Generation of compartmentalized pressure by a nuclear piston governs cell motility in a 3D matrix. *Science* **345**, 1062–1065 (2014).
65. Petrie, R. J., Harlin, H. M., Korsak, L. I. & Yamada, K. M. Activating the nuclear piston mechanism of 3D migration in tumor cells. *J. Cell. Biol.* **216**, 93–100 (2017).
66. Randles, K. N. et al. Nesprins, but not sun proteins, switch isoforms at the nuclear envelope during muscle development. *Dev. Dyn.* **239**, 998–1009 (2010).
67. Duong, N. T. et al. Nesprins: tissue-specific expression of epsilon and other short isoforms. *PLoS ONE* **9**, e94380 (2014).
68. Hebbar, S. et al. Lis1 and Ndel1 influence the timing of nuclear envelope breakdown in neural stem cells. *J. Cell. Biol.* **182**, 1063–1071 (2008).
69. Heuze, M. L., Collin, O., Terriac, E., Lennon-Dumenil, A. M. & Piel, M. Cell migration in confinement: a micro-channel-based assay. *Methods Mol. Biol.* **769**, 415–434 (2011).
70. R Core Team. R: A Language and Environment for Statistical Computing <http://www.r-project.org/> (2014).
71. C. Agostinelli and U. Lund R package 'circular': Circular Statistics (version 0.4-7). <https://r-forge.r-project.org/projects/circular/> (2013).

Acknowledgements

We thank the Nikon Imaging Centre @ Institut Curie-CNRS and Cell and Tissue Imaging Facility of Institut Curie, member of the France Bio Imaging national research infrastructure (ANR-10-INBS-04) for help with image acquisition, Drs M. Bornens, S. Courtneidge, S. Etienne-Manneville, A-M Lennon-Duménil, F. Perez, M. Mercola, T. Mistelli, Q. Zhang and R. Vallee for providing reagents for this study and Dr I. Brito for help with statistical analysis. E.I. was supported by a postdoctoral fellowship from Ligue Nationale contre le Cancer, P.M. by a fellowship from Fondation ARC pour la Recherche contre le Cancer, R.F. by a fellowship from Ministère de l'Éducation Nationale, de l'Enseignement supérieur et de la Recherche, A.C. by a grant from Worldwide Cancer Research (Grant 16-1235 to P.C.) and S.A.G. by a grant provided by the program «Investissements d'Avenir» launched by the French Government and implemented by Agence Nationale pour la Recherche (ANR) with the reference ANR-10-LBX-0038 (Labex CelTisPhyBio) part of the IDEX PSL (ANR-10-IDEX-0001-02 PSL). Funding for this work was provided by the program «Investissements d'Avenir» launched by the French Government and implemented by Agence Nationale pour la Recherche (ANR) with the reference ANR-10-LBX-0038 (Labex CelTisPhyBio) part of the IDEX PSL (ANR-10-IDEX-0001-02 PSL) and by grants from Ligue Nationale contre le Cancer (Equipe labellisée 2015) and from Worldwide Cancer Research (Grant 16-1235) to P.C. and by core funding from Institut Curie and Centre National pour la Recherche Scientifique (CNRS).

Author contributions

E.I., A.C., R.F., and P.M. were equally involved in experimental design, experiments and data analysis; S.A.G. designed and performed microfabricated channel experiments with help from M.R. and M.P.; M.J.D. performed experiments and analyzed data; P.P.G. generated software for automated tracking analysis and contributed to data analysis; Pa.M. performed circular statistical tests; E.R.G. and A.B. suggested and contributed to designing experiments based on nucleus-cytoskeleton coupling; C.M.S. provided critical reagents and P.C. and E.I. conceived the study and wrote the manuscript.

Additional information

Supplementary Information accompanies this paper at <https://doi.org/10.1038/s41467-018-04865-7>.

Competing interests: The authors declare no competing interests.

Reprints and permission information is available online at <http://npg.nature.com/reprintsandpermissions/>

Publisher's note: Springer Nature remains neutral with regard to jurisdictional claims in published maps and institutional affiliations.



Open Access This article is licensed under a Creative Commons Attribution 4.0 International License, which permits use, sharing, adaptation, distribution and reproduction in any medium or format, as long as you give appropriate credit to the original author(s) and the source, provide a link to the Creative Commons license, and indicate if changes were made. The images or other third party material in this article are included in the article's Creative Commons license, unless indicated otherwise in a credit line to the material. If material is not included in the article's Creative Commons license and your intended use is not permitted by statutory regulation or exceeds the permitted use, you will need to obtain permission directly from the copyright holder. To view a copy of this license, visit <http://creativecommons.org/licenses/by/4.0/>.

© The Author(s) 2018

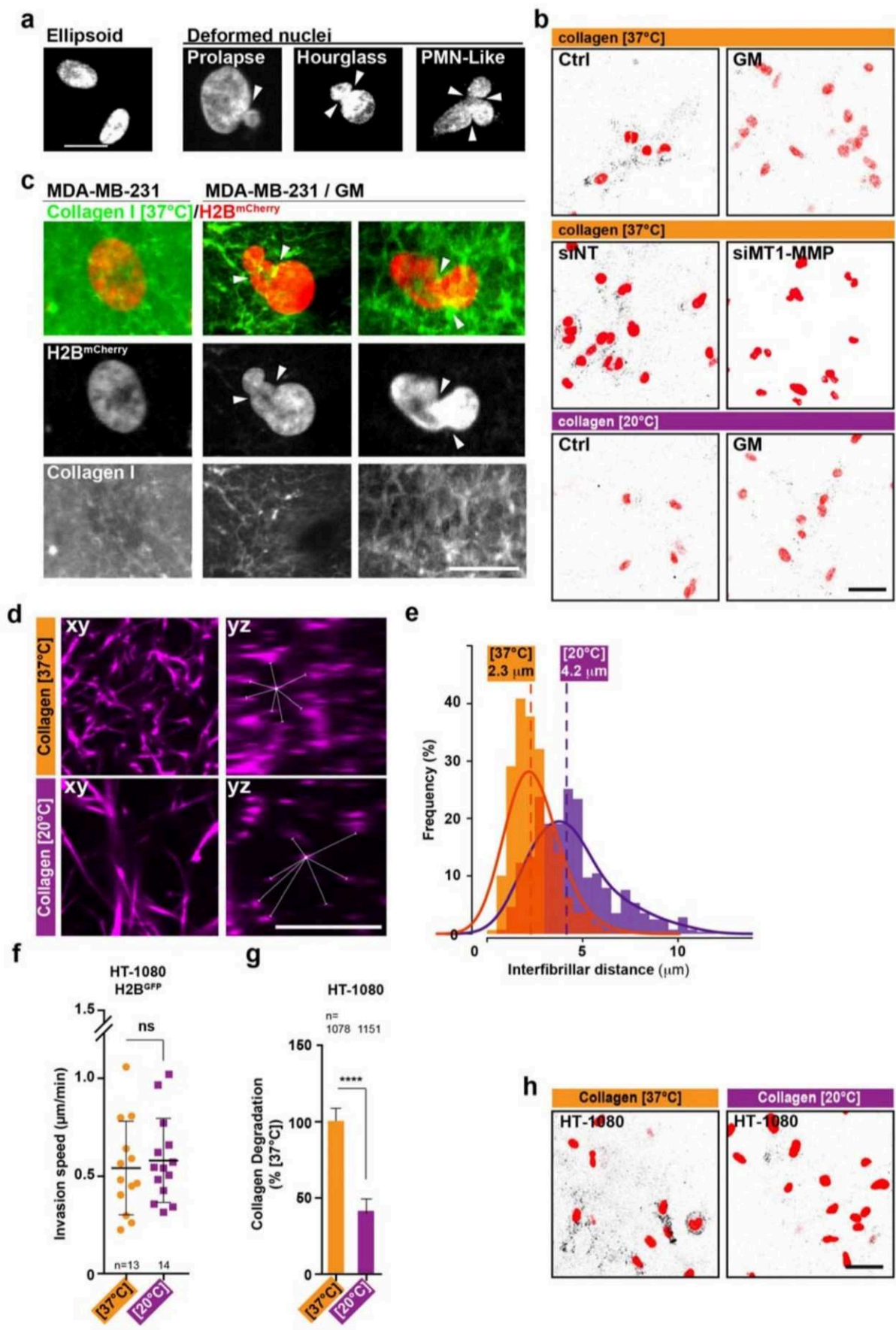
SUPPLEMENTARY MATERIAL

LINC complex-Lis1 interplay controls MT1-MMP matrix digest-on-demand response for confined tumor cell migration

Elvira Infante, Alessia Castagnino, Robin Ferrari, Pedro Monteiro, Sonia Agüera-González, Perrine Paul-Gilloteaux, Mélanie J. Domingues, Paolo Maiuri, Matthew Raab, Catherine M. Shanahan, Alexandre Baffet, Matthieu Piel, Edgar R Gomes and Philippe Chavrier

The Supplementary Material includes 5 Supplementary Figures, 1 Supplementary Table and 6 Supplementary Movies

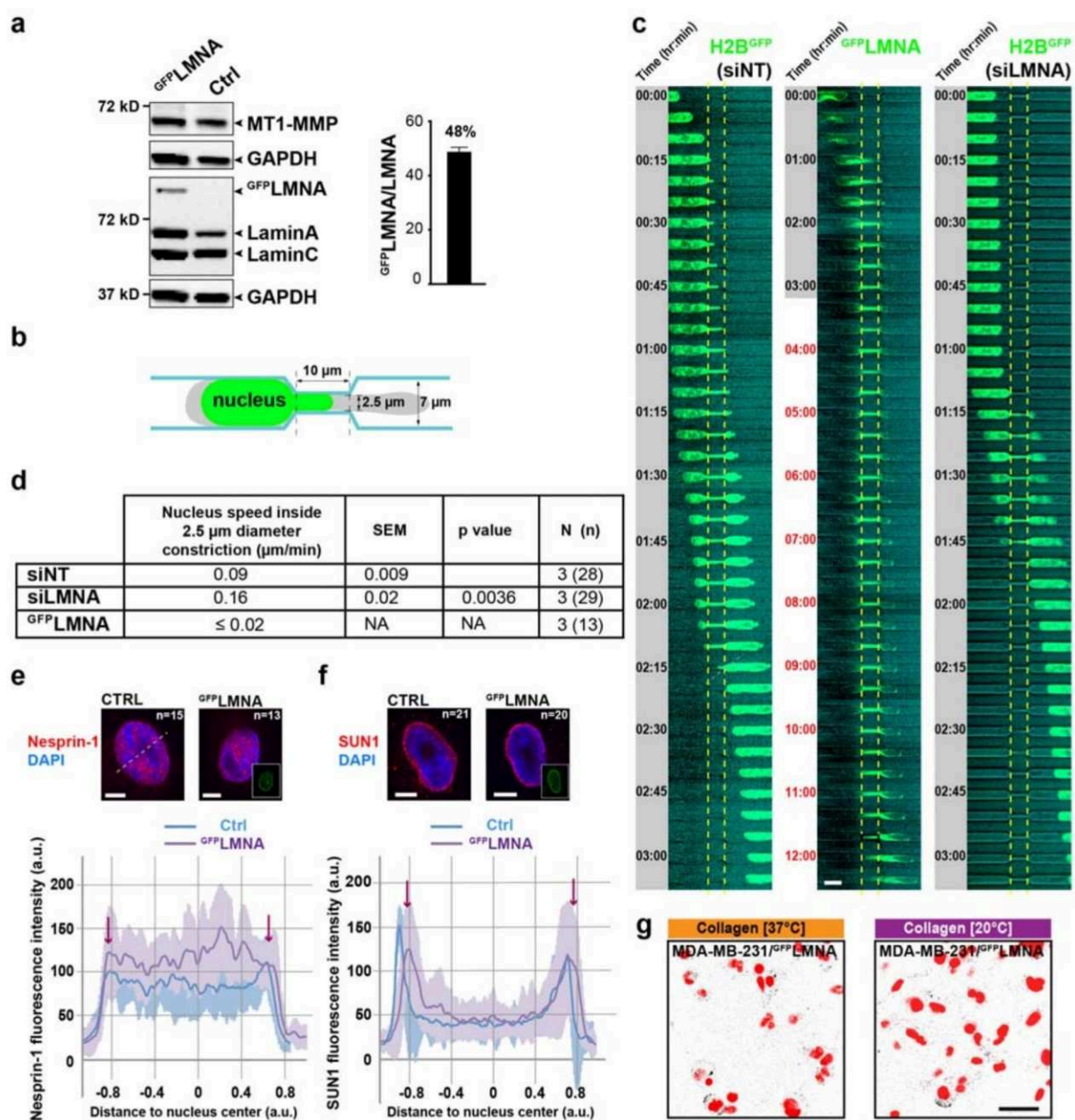
Supplementary Figure 1 accompanying Figure 1



Infante et al. Supplementary Figure 1

(a) Representative examples of DAPI-stained nuclei during confined migration of MDA-MB-231 cells in 3D 37°C-polymerized collagen gel showing scored nuclear deformations (see Fig. 1d, j and Fig. 3c). Scale bar, 10 μm . **(b)** Representative images of pericellular collagenolysis detected with Col1-^{3/4}C antibody (black signal in the inverted images). Nuclei were stained with DAPI (red). Scale bars, 50 μm . **(c)** MDA-MB-231 cells expressing H2B^{mCherry} were embedded in 3D fluorescently-labeled 37°C polymerized gel and treated with GM6001 (GM) or not and analyzed by confocal spinning disk microscopy. Arrows indicate confining collagen fibrils. Scale bar, 10 μm . **(d)** Confocal xy and yz (through dashed line in xy planes) sections of fluorescently-labeled 2.0 mg/ml type I collagen gels polymerized at 37°C or 20°C. Scale bar, 10 μm . **(e)** Inter-fibril distance distribution estimated from xy, xz and yz optical planes in 3D large and small pore size collagen gels. **(f)** Invasion speed of HT-1080 cells expressing H2B^{GFP} as in Fig. 1e. Unpaired t-test. **(g, h)** Pericellular collagenolysis by HT-1080 cells as in Fig. 1f and representative images (panel h, scale bar, 50 μm). *n*, number of cells analyzed from three independent experiments; Mann-Whitney test.

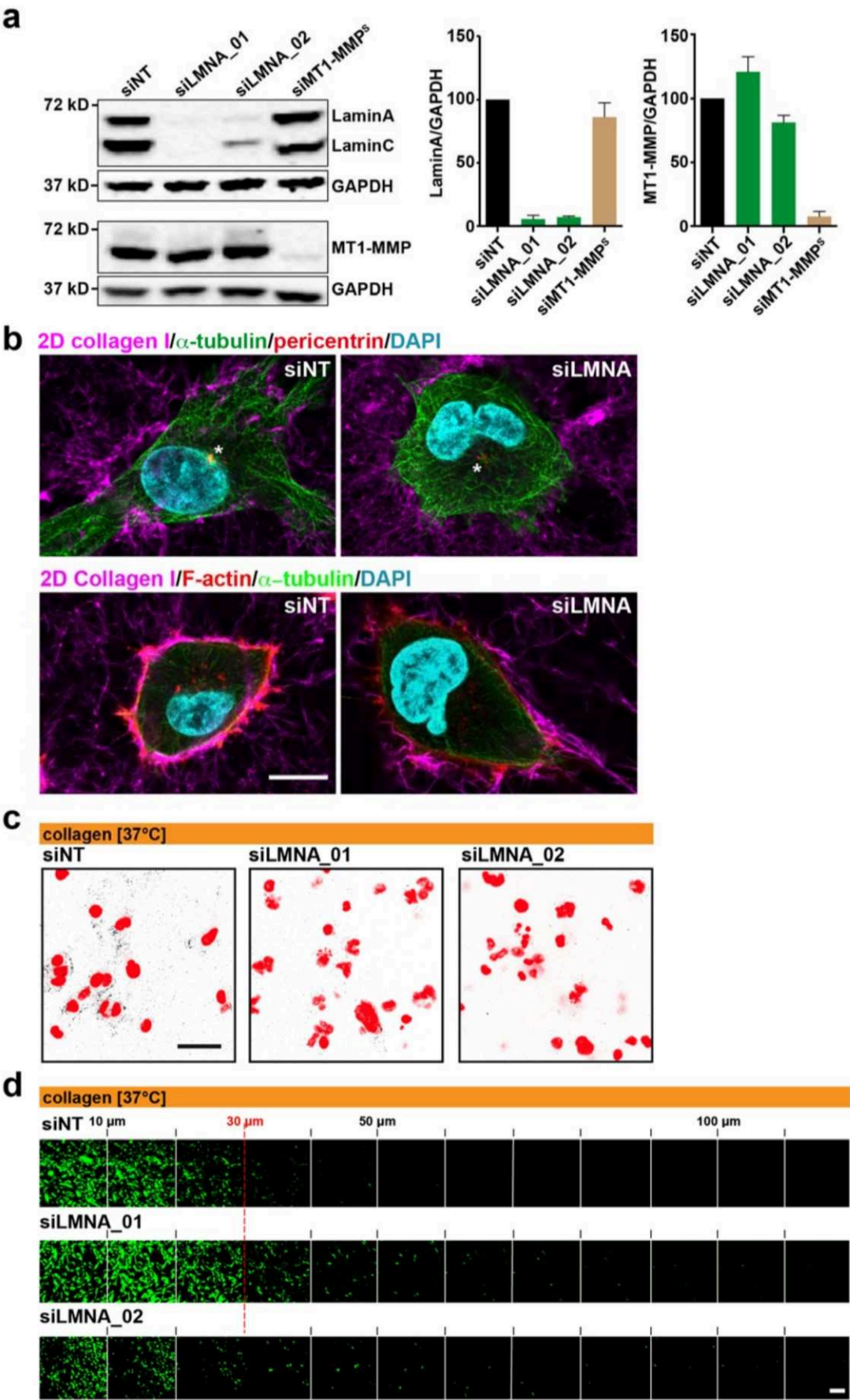
Supplementary Figure 2. Effect of ^{GFP}LMNA overexpression in MDA-MB-231 cells



(a) Representative immunoblots for MT1-MMP and laminA, laminC and ^{GFP}LMNA expression level with GAPDH as loading control. Cell lysates were prepared from control or ^{GFP}LMNA-overexpressing MDA-MB-231 cells. The graph is the quantification of ^{GFP}LMNA expression in comparison to endogenous LMNA level from three independent experiments. **(b)** Schematic overview of the microfabricated PDMS channels with 2.5 μm-diameter constriction. **(c)** Image galleries from

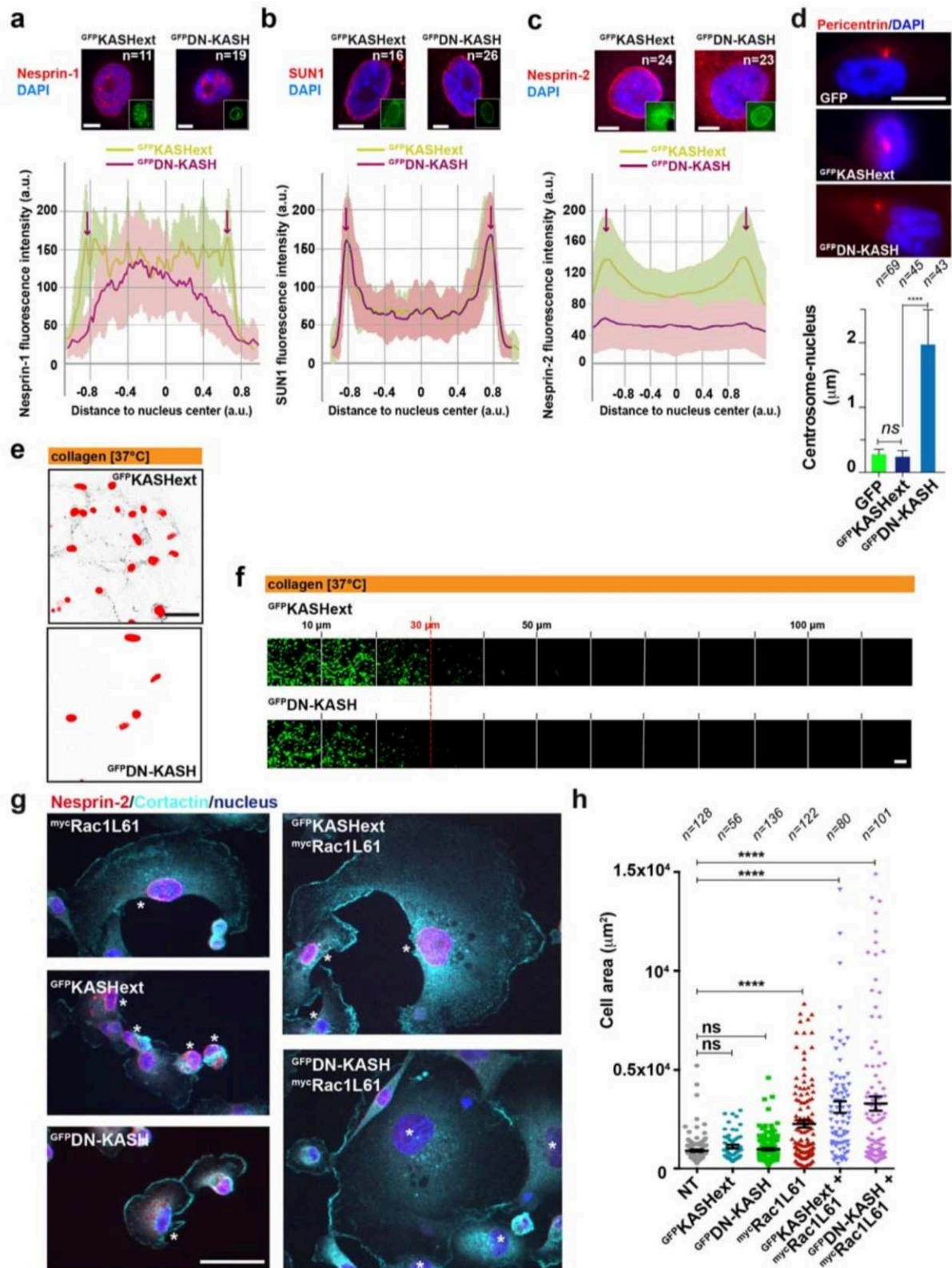
representative time-lapse sequence of ^{GFP}H2B-overexpressing MDA-MB-231 cells treated with control (siNT) or LMNA siRNA (siLMNA) or overexpressing ^{GFP}LMNA migrating inside a 7- μ m diameter microchannel including 2.5- μ m diameter constrictions (delimited by yellow dashed lines). Time is in hr:min (note different time scale for ^{GFP}LMNA-positive cell). Scale bar, 10 μ m. **(d)** Mean nucleus speed within 2.5 μ m-diameter constriction \pm SEM (μ m/min); N, number of independent experiments; *n*, number of tracked nuclei. Mann-Whitney test. NA, not applicable (out of thirteen ^{GFP}LMNA-positive nuclei analyzed, two crossed through the 2.5 μ m-diameter constriction with a speed of 0.02 μ m/min and eleven nuclei stalled during the 12-h movie). **(e, f)** Averaged nesprin-1 (red signal in representative images in panel e) or SUN1 intensity profiles (red signal in representative images in panel f) \pm SD from MDA-MB-231 cells expressing ^{GFP}LMNA or not along a line-scan across the nucleus (white dashed line). Arrows in the intensity profiles point to nuclear rim. Insets in the images show GFP signals. *n*, number of cells analyzed from two independent experiments. Scale bars, 5 μ m. **(g)** Representative images of pericellular collagenolysis by ^{GFP}LMNA-expressing MDA-MB-231 cells in small and large pore size collagen gels detected with Col1-^{3/4}C antibody (black signal in the inverted images). Nuclei were stained with DAPI (red). Scale bars, 50 μ m.

Supplementary Figure 3 accompanying Figure 2



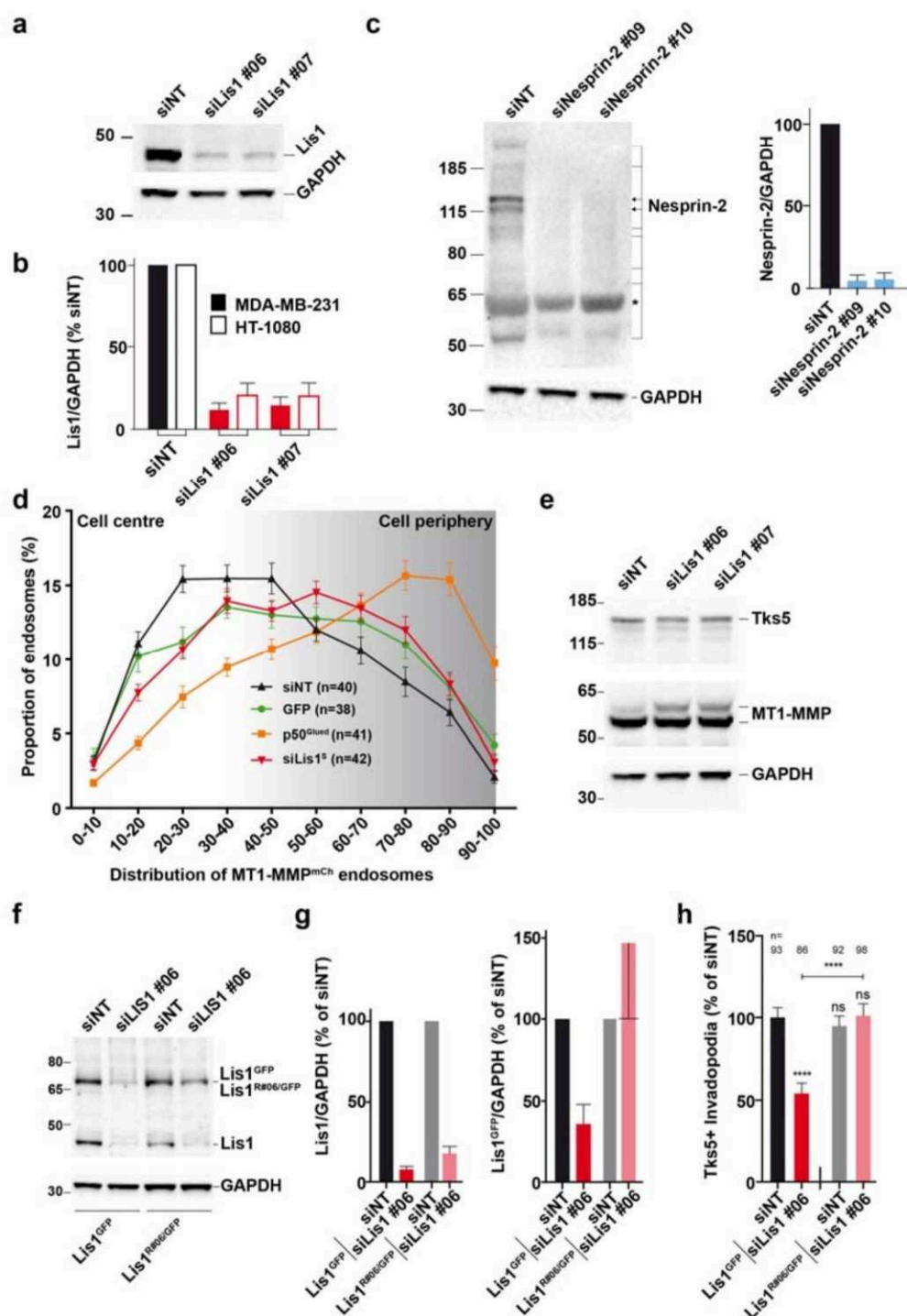
(a) Representative immunoblots for LaminA/LaminC (upper row) and MT1-MMP (lower row) with GAPDH as loading control. Cell lysates were prepared from MDA-MB-231 cells silenced for LMNA or MT1-MMP by siRNA treatment as indicated. Graphs represent LaminA and MT1-MMP expression relative to GAPDH in siRNA-treated cells from three independent experiments. **(b)** MDA-MB-231 cells treated with control (siNT) or LMNA siRNA were plated on top of a thick layer of fluorescently-labeled type I collagen fibrils (magenta), fixed after 90 min and stained for α -tubulin (green) and centrosomal pericentrin (red, asterisks) and nucleus (cyan, upper row), or for F-actin (red) and nucleus (cyan, lower row). Scale bar, 10 μ m. **(c)** Pericellular collagenolysis detected using anti-Col1-^{3/4}C antibodies in control (siNT) or siLMNA-treated cells in small pore size collagen gels. Scale bars, 50 μ m. **(d)** Representative images from invasion assays obtained from three independent experiments. Scale bar, 100 μ m

Supplementary Figure 4. Phenotypic consequences of dominant inhibitory DN-KASH expression



(a, c) Averaged Nesprin-1 (red signal in representative images in panel a), SUN1 (red signal in representative images in panel b) or Nesprin-2 (red signal in representative images in panel c) intensity profiles \pm SD from MDA-MB-231 cells expressing ^{GFP}DN-KASH or ^{GFP}KASHext constructs along a line-scan across the nucleus. Arrows in the intensity profiles point to nuclear rim. Insets in the images show GFP signals. *n*, number of cells analyzed from two independent experiments. Scale bars, 5 μ m. **(d)** Pericentrin and DAPI immunostaining (GFP signal is omitted). Scale bars, 5 μ m. Mean centrosome-nucleus distance (μ m) \pm SEM in MDA-MB-231 cells expressing ^{GFP}DN-KASH or ^{GFP}KASHext in 3D small pore size collagen gel; *n*, number of cells analyzed from two independent experiments; Kruskal-Wallis test. **(e)** Pericellular collagenolysis (black signal in the inverted images) of ^{GFP}KASH-positive cells in small pore size collagen gel. Nuclei were stained with DAPI (red). Scale bar, 50 μ m. **(f)** Representative images from invasion assays obtained from three independent experiments. Scale bar, 100 μ m. **(g)** MDA-MD-231 cells expressing the indicated constructs were plated on glass substratum for 16 hrs, fixed and stained for GFP (not shown), cortactin (cyan), nesprin-2 (red) and DAPI (blue). GFP-positive cells are indicated by asterisks. Scale bars, 25 μ m. **(h)** Cell area of GFP- or Myc-positive cells in μ m². *n*, number of cells analyzed from three independent experiments. Kruskal-Wallis test.

Supplementary Figure 5 accompanying Figure 5



(a) Silencing of Lis1 in MDA-MB-231 cells by two independent siRNAs. **(b)** Expression of Lis1 relative to GAPDH in lysates of MDA-MB-231 and HT-1080 cells, after normalization to siNT levels from three independent experiments. **(c)** Silencing of nesprin-2 in MDA-MB-231 cells by two independent siRNAs. The graph shows

nesprin-2 expression relative to GAPDH after normalization to levels in siNT cells from three independent experiments. *, non-specific band. **(d)** Distribution of MT1-MMP^{mCh} endosomes in MDA-MB-231 cells plated on a 2D substrate. Mean percentage of MT1-MMP^{mCh}-positive endosomes according to their cell center-to-cell periphery position \pm SEM; *n*, number of cells analyzed from three independent experiments. **(e)** Immunoblotting analysis showing that MT1-MMP and Tks5 expression is not affected by treatment with Lis1 siRNAs. **(f, g)** Expression of Lis1^{GFP/R#06} variant resistant to Lis1 siRNA #06. Graphs in panel g show the quantification of endogenous Lis1 (left) or overexpressed Lis1^{GFP} expression (right) relative to GAPDH normalized to levels in siNT cells from three independent experiments. **(h)** Formation of Tks5-positive invadopodia in Lis1-depleted cells is rescued by siRNA-resistant variant Lis1^{GFP/R#06}. The y-axis indicates the ratio of Tks5 area to the total cell area normalized to mean value in control cells (as percentage) \pm SEM. *n*, number of cells analyzed from three independent experiments. Kruskal-Wallis test.

Supplementary Table 1. Commercial antibodies used for this study

Antigen	Cie	Reference	Assay	Dilution
SUN1	Sigma	HPA008461	IF	1/600
Nesprin 2	Sigma	HPA008435	IF	1/100
MT1-MMP	Millipore	3328	WB	1/1000
Lamin A/C (636)	SantaCruz Biotechnology	sc-7292	WB	1/500
			IF	1/200
LIS-1 (H300)	SantaCruz Biotechnology	sc-15139	WB	1/200
			IF	1/100
GAPDH	SantaCruz Biotechnology	sc-25778	WB	1/10000
Coll-3/4C	ImmunoGlobe GmbH	0217-050	IF	1/100
Nesprin 1	Abcam	ab24742	IF	1/500
Pericentrin	Abcam	ab4448	IF	1/200
Alpha-tubulin	Sigma	T-9026	IF	1/600
			WB	1/10000
Tks5	Novus Biological	NBP1-90454	IF	1/200
			WB	1/500
Cortactin	Millipore	05-180	IF	1/200
			WB	1/2000
IgG-mouse-Cy5	Invitrogen	A31571	IF	1/500
IgG-mouse-Cy3	Jackson ImmunoResearch	715-165-151	IF	1/500
IgG-mouse-A488	Molecular Probes	A21202	IF	1/500
IgG-mouse-Hrp	Jackson ImmunoResearch	115-035-062	WB	1/20000
IgG-rabbit-A488	Molecular Probes	A11034	IF	1/200
IgG-rabbit-Cy3	Jackson ImmunoResearch	711-165-152	IF	1/800
IgG-rabbit-Hrp	Jackson ImmunoResearch	111-035-045	WB	1/10000
Alexa Fluor 488	Molecular Probes	A12379	IF	1/400

phalloidin				
Alexa Fluor 546 phalloidin	Molecular Probes	A22283	IF	1/200
GFP-Booster_ATTO 488	ChromoTek	gba488	IF	1/100

IF, Immunofluorescence; WB, Western blot.

Description of Additional Supplementary Files

Supplementary Movie 1. Polarization of MT1-MMP endosomes in front of the nucleus during 3D invasion. MDA-MB-231 cells expressing H2BGFP (green) and MT1-MMPmCh (red) were embedded in 37°C polymerized 3D fibrillar collagen-I (blue) and analyzed by confocal spinning disk fluorescence microscopy. Images were taken every 5 min. The indicated time is in h:min. Scale bar, 10 μ m. Representative movie out of seven from three independent experiments.

Supplementary Movie 2. Loss of MT1-MMP endosome polarity during invasion in permissive large pore size collagen. MDA-MB-231 cells expressing H2BGFP (green) and MT1-MMPmCh (red) were embedded in fibrillar 3D large pore size collagen gel (blue) polymerized at 20°C and analyzed by confocal spinning disk fluorescence microscopy. Images were taken every 5 min. The indicated time is in h:min. Scale bar, 10 μ m. Representative movie out of ten from three independent experiments.

Supplementary Movie 3. Increased nuclear stiffness upon LMNA overexpression induces MT1-MMP endosome polarization in permissive 3D collagen. MDA-MB-231 cells expressing GFPLMNA (green) and MT1-MMPmCh (red) were embedded in 3D collagen-I (blue) polymerized at 20°C and analyzed by confocal spinning disk fluorescence microscopy. Images were taken every 5 min. The indicated time is in h:min. Scale bar, 10 μ m. Representative movie out of nine from three independent experiments.

Supplementary Movie 4. Invasive migration of LMNA-depleted cells in the absence of MT1-MMP endosome polarization. MDA-MB-231 cells expressing H2BGFP (green) and MT1-MMPmCh (red) were treated with siRNA specific for LMNA. Cells were embedded in 37°C polymerized 3D fibrillar collagen-I (blue) and analyzed by confocal spinning disk fluorescence microscopy. Images were taken every 5 min. The indicated time is in h:min. Scale bar, 10 μ m. Representative movie out of eleven from three independent experiments.

Supplementary Movie 5. Polarity of MT1-MMP endosomes is impaired upon disruption of nesprin/SUN interaction. MDA-MB-231 cells expressing H2BGFP and GFPDN-KASH (nucleus + NE, green) and MT1-MMPmCh (red) were embedded in 37°C polymerized 3D small pore size collagen gel (blue) and analyzed by confocal spinning disk fluorescence microscopy. Images were taken every 5 min. The indicated time is in h:min. Scale bar, 10 μ m. Representative movie out of seven from three independent experiments.

Supplementary Movie 6. Impaired polarity of MT1-MMP endosomes upon Lis1 silencing. MDA-MB-231 cells expressing H2BGFP (green) and MT1-MMPmCh (red) were treated with siRNA specific for Lis1. Cells were embedded in 37°C polymerized 3D small pore size collagen gel (blue) and analyzed by confocal spinning disk fluorescence microscopy. Images were taken every 5 min. The indicated time is in h:min.

Article 2

Tumor cell invasion in fibrillar collagen I is mediated by MT1-MMP-based force-producing proteolytic contacts

Robin Ferrari ^{1,*}, Gaëlle Martin ², Oya Tagit ³, Alessandra Cambi ⁴, Raphaël Voituriez ⁵, Stéphane Vassilopoulos ⁶, and Philippe Chavrier ^{2,*}

¹ Sorbonne Université, Institut Curie, PSL Research University, CNRS, UMR 144, 26 rue d'Ulm, F-75005, Paris, France

² Institut Curie, PSL Research University, CNRS, UMR 144, 26 rue d'Ulm, F-75005, Paris, France

³ Department of Tumor Immunology, Radboud Institute for Molecular Life Sciences, Radboud University Medical Center, Nijmegen and Oncode Institute, The Netherlands

⁴ Department of Cell Biology, Radboud Institute for Molecular Life Sciences, Radboud University Medical Center, Nijmegen, The Netherlands

⁵ Sorbonne Université, CNRS, UMR 8237, Jean Perrin Laboratory, Paris, France

⁶ Sorbonne Université, INSERM UMRS 974, Institute of Myology, Paris, France

* Corresponding authors, e-mail: robin.ferrari@curie.fr; philippe.chavrier@curie.fr

Submitted in Nature Communications: 15th April 2019.

Abstract

Unraveling the mechanisms that govern invadopodia formation and function is an essential step towards the prevention of cancer spread. However, the current model of invadopodia, combining protrusive and matrix proteolytic activities, is based from observations of cancer cells on a quasi-2D substratum comprised of denatured collagen (*i.e.* gelatin). We looked at breast cancer cell invasion in fibrillar collagen and found that formation of collagenolytic invadopodia is triggered by surface-exposed MT1-MMP contacting surrounding collagen fibers. Electron microscopy analysis revealed focal assembly of an Arp2/3 branched actin network associated with the concave side of curved invadopodia. Actin polymerization was shown to produce forces, which were transmitted to underlying collagen fibers, along with cleavage of the fibers by MT1-MMP, to locally increase matrix compliance. Overall, these findings define a new paradigm for invadopodia as MT1-MMP-driven self-assembling proteolytic contacts that combine actin-driven force production and matrix-cleavage activity to widen matrix pores and facilitate invasion.

Introduction

The migration of cells through tissues is essential during embryonic development, tissue repair, and immune surveillance ¹. Deregulated invasive migration is also key to diseases, including cancer dissemination ². It is believed that invasive cancer cells negotiate tissue barriers by forming specialized F-actin based protrusions called invadopodia, which focally degrade the extracellular matrix (ECM), enabling cell penetration ³. MT1-MMP, a trans-membrane matrix metalloproteinase, is concentrated in invadopodia and is essential for invasion across the basement membrane and dense collagen tissues ⁴⁻⁷. Although all invadopodia types degrade the matrix based on MT1-MMP catalytic activity, their structure and activity can differ depending on the composition and mechanical properties of the matrix environment ⁸⁻¹⁰. In the classical model of cancer cells plated on a thin - quasi 2D - substratum of denatured collagen (*i.e.* gelatin), invadopodia resemble podosomes of normal hematopoietic cells, which consist of an actin-rich puncta supporting membrane protrusion ¹¹. Similarly, on a highly packed fibrillary collagen matrix obtained by centrifugation of the collagen gel, multiple punctate invadopodia form at the adherent plasma membrane ⁹. Differently, when exposed to sparser type I collagen fibers representative of the tumor environment consisting of ECM fibers interspaced with pores ^{5,12}, cancer cells form elongated actin-rich invadopodia in association with the matrix fibers ^{10,13,14}. We and others reported that mesenchymal cancer cells, which invade through the collagen gel with a ‘nucleus at the back’ configuration, preferentially form invadopodia ahead of the nucleus to support invasive path-generation by pericellular proteolysis ^{5,12,15}. Whether these linear collagenolytic invadopodia are endowed with membrane protrusive or deforming activity is presently unknown. Along with multiple invadopodia organizations, several ECM receptors including integrins and discoidin domain receptors (DDR) have been implicated in invadopodia formation, although with some conflicting results ¹⁶⁻¹⁸. Additionally, the mechanisms by which invasive cells coordinate topological and mechanical cues from the 3D ECM environment with invadopodia organization and function for matrix degradation and invasion are still largely unknown. Here, we set out to investigate the ultrastructural organization and dynamics of invadopodia in breast cancer cells invading through the 3D (patho)physiological fibrillary collagen environment. Using platinum replica electron microscopy, we unraveled the ultrastructural organization of invadopodia as Arp2/3 complex branched actin assemblies that form on the concave side of curved invadopodia/collagen-fiber ensemble. We found that collagenolytic invadopodia have a dual activity by repelling and degrading the collagen fibers to locally increase matrix compliance and demonstrated that actin

polymerization underlies the mechanism of force production by invadopodia. A theoretical model that describes the force balance in the invadopodia/collagen-fiber ensemble was developed. Altogether, our data unveiled a new invadopodia paradigm as self-assembling, force-producing proteolytic cell-matrix contacts that enable matrix pore enlargement to facilitate tumor-cell invasion.

Results

Ultrastructural organization of collagenolytic invadopodia. Invasive tumor cells seeded on a layer of fibrillar type I collagen formed bow-shaped actin-enriched structures in association with the underlying fibers (Figure 1ab)^{10,15}. These structures were positive for the invadopodia proteins Tks5, cortactin, and N-WASP, consistent with the implication of Arp2/3 complex in invadopodial actin assembly (Figure 1a and Supplementary Figure 1a)^{13,19,20}. Conspicuous bending and proteolytic cleavage of collagen molecules suggest a strong remodeling capacity of collagenolytic invadopodia, based on MMP activity, leading to the clearance of collagen fibers underneath the ventral surface and their bundling at the cell edge (Figure 1b and Supplementary Figure 1bc). We used platinum replica electron microscopy (PREM) to reveal the cytoskeletal architecture of collagenolytic invadopodia. Curvilinear matrix fibers could be tracked underneath the ventral plasma membrane because of their electron density (they appear white in inverted PREM images, Figure 1c). At higher magnification, a network of branched actin filaments (~100-300 nm-wide), closely apposed to the cytosolic face of the plasma membrane, was visible on the concave edge of the curved invadopodia/fiber ensemble (Figure 1d). The Arp2/3 complex component ArpC5 was detected by immunogold labeling at the plasma membrane overlaying the collagen fibers, representing an actin nucleation interface (Figure 1e and Supplementary Figure 1d). Tks5 was enriched in some electron-dense proteinaceous material present on the inner invadopodia rim (Figure 1f). Tks5 knockdown abolished F-actin-positive invadopodia formation, collagenolysis and fiber bending and remodeling, consistent with Tks5's strong pro-invasive and pro-metastatic potential (Figure 1g and Supplementary Figure 1e-h). Overall, these data highlight, with unprecedented resolution, the exquisite organization of collagenolytic invadopodia at contact sites with collagen fibers, with the assembly of a branched actin network on the concave side of the curved invadopodia/collagen-fiber ensemble as a main feature.

MT1-MMP mediates invadopodia formation along collagen fibers. These observations revealed that invadopodia form very selectively at plasma membrane/matrix contact sites, implying the activation of specific collagen receptor(s). Integrins and DDRs have been implicated in invadopodia formation, depending on matrix composition and organization, although with conflicting results^{9,16,17}. Silencing of $\beta 1$ integrin or DDR1 collagen receptors in MDA-MB-231 cells had no effect on the formation of Tks5-positive invadopodia (Supplementary Figure 2a-d). Levels of DDR1 transcripts were barely detectable in basal-like breast cancer MDA-MB-231 cells as previously reported^{21,22}, thus we silenced DDR1 in

mammary epithelial MCF10DCIS.com cells expressing ~60-fold higher level than mesenchymal MDA-MB-231 cells (not shown); DDR1 knockdown resulted in a strong increase in Tks5 invadopodia formation (Supplementary Figure 2e-g). Therefore, while beta 1 integrin was not required for the formation of collagenolytic invadopodia, DDR1 collagen receptor repressed invadopodia formation in epithelial breast cancer cells.

MT1-MMP is known to interact with type I collagen through its catalytic and hemopexin C ectodomains²³ and it accumulated in Tks5-positive invadopodia (Supplementary Figure 3ab). Thus, we assessed whether MT1-MMP was also required for invadopodia formation as judged by the recruitment and accumulation of Tks5 in association with the collagen fibers. As already reported, MT1-MMP knockdown abolished collagenolysis similar to Tks5 knockdown (Supplementary Figure 1g). Strikingly, silencing of MT1-MMP also resulted in a substantial reduction of invadopodia formation and collagen remodeling, which could be restored by the re-expression of wild-type MT1-MMP or by a catalytically inactive form with a mutation in the active site (MT1-MMP^{E240A})²⁴ (Fig. 1h-j, Supplementary Figure 3a and f and Table S1). Similarly, treatment with the general MMP inhibitor GM6001 did not affect invadopodia formation based on Tks5 recruitment although it compromised collagenolysis (Supplementary Figure 1bc and Supplementary Figure 3c-e). Invadopodia rescue and collagen remodeling required the cytoplasmic tail of MT1-MMP, especially the integrity of the LLY F-actin binding motif^{25,26} (Figure 1j, Supplementary Figure 3a and fg and Table S1). Deletion of the cytosolic tail or mutation in the LLY motif have been shown to interfere with MT1-MMP trafficking and hence could affect its localization (²⁷ and references herein). However, some level of the constructs was observed at the cell surface in association with collagen fibers (Supplementary Figure 3g). Collectively, these data identified MT1-MMP as the long-sought cell surface receptor required for invadopodia formation based on cortactin/F-actin (not shown) and Tks5 recruitment in association with the collagen fibers and for collagenolysis, while beta1 integrin and DDR1 do not contribute to the formation of collagenolytic invadopodia. Additionally, these findings demonstrate that MT1-MMP-mediated invadopodia formation does not require the collagenolytic activity.

Matrix pore opening is driven by ring-like invadopodia expansion. Invadopodia dynamics during confined migration in a 3D fibrous matrix environment is largely unknown. We observed that as MDA-MB-231 cells invaded the 3D collagen network, GFP-tagged Tks5 formed dynamic structures ahead of, or surrounding, the bulky nuclear region in association with constricting fibers (Figure 2a, Movie 1). Some structures strapped the cell body, like barrel

hoops, whereas some were smaller in size. We have previously reported that these Tks5-positive structures are *bona fide* collagenolytic invadopodia in 3D¹⁵. Tks5 invadopodia expanded in size over time, with an average diameter growth rate of $0.09 \pm 0.008 \mu\text{m}/\text{min}$ (see Table S1), suggesting that invadopodia expansion contributed to widening the matrix pores, facilitating nuclear and cell movement.

We switched to a simpler experimental set-up, consisting of cells grown on top of a 5-10- μm thick fibrous collagen layer (2.5D). Live-cell imaging showed that Tks5-positive invadopodia on the ventral cell surface elongated along the underlying collagen fiber at a rate of $0.15 \pm 0.02 \mu\text{m}/\text{min}$ (Table S1), producing typical bow- or ring-shaped structures (Figure 2b-d and Supplementary Figure 4a). Time sequences also showed that invadopodia/collagen-fiber ensembles undergo homothetic expansion over time, with an average radial velocity of $0.16 \pm 0.02 \mu\text{m}/\text{min}$ (Movie 2, Figure 2c and e, and Table S1). These observations show that force was produced at invadopodia, which was sufficient to push collagen fibers away. Moreover, invadopodia were dynamic, with an average lifetime of $\sim 41 \pm 1.7 \text{ min}$ (Table S1).

We frequently observed proteolytic rupture and recoil movement of the invadopodia/collagen-fiber ensemble (Figure 2fg, red arrowhead and Movie 3). The measurement of fiber relaxation over time revealed a typical viscoelastic behavior of the invadopodia/fiber ensemble with an initial velocity $V_0 = 3.1 \pm 0.22 \mu\text{m}/\text{min}$ (Figure 2gh and Table S1), which characterizes the tension-to-drag ratio of the fiber²⁸. Overall, these observations show that the invadopodia-associated fibers sustained mechanical tension and bending moment, which relaxed upon proteolytic rupture, confirming that cells produced and transmitted force to the fibers at the level of invadopodia, enabling matrix pore widening.

MT1-MMP proteolytic activity is required for invadopodia expansion and collagen remodeling. The frequency of rupture events decreased upon pharmacological inhibition of MT1-MMP catalytic activity by GM6001, showing that rupture required collagen cleavage (Figure 2f). Strikingly, longitudinal invadopodia growth and radial expansion of the invadopodia/matrix ensemble significantly slowed upon inhibition of MMP activity by GM6001 (Figure 2de and ij, Figure 3g and Movie 4). We performed laser ablation of invadopodia/collagen-fiber ensembles in cells, treated or not with GM6001, to probe fiber tension. Displacement curves were similar under both conditions, with no significant difference in initial recoil velocity related to the tension-to-drag ratio (Figure 2k, Supplementary Figure 4b-d, and Movie 5). Therefore, although there was no direct contribution of MT1-MMP

catalytic activity to force production, proteolysis of type I collagen molecules was essential for increasing fiber compliance and possibly facilitating inter-fiber sliding and pore expansion.

Actin polymerization-based force production at invadopodia. Invadopodia are composed of actin filaments (Figure 1). Actin-based mechanisms of force production can be mediated by myosin molecular motors or through the polymerization of actin filaments, which push the plasma membrane forward^{29,30}. We analyzed the mechanism of invadopodial force production by treating MDA-MB-231 cells with cytochalasin D (CytoD), an inhibitor of actin polymerization. Such treatment strongly impaired longitudinal and radial invadopodial growth and triggered their rapid disassembly (Figure 3a-c and h and Movie 6). We observed similar effects upon inhibition of the Arp2/3 actin nucleating complex by CK-666 (Figure 3d and h, Supplementary Figure 5ab, and Movie 7)³¹. In contrast, blebbistatin, an inhibitor of non-muscle myosin II, did not affect invadopodia elongation nor radial expansion. Similarly, inhibition of myosin regulatory light chain phosphorylation by the p160ROCK inhibitor Y-27632 did not affect invadopodia dynamics (Figure 3ef and h, Supplementary Figure 5cd, and Movies 8 and 9). Consistent with this result, non-muscle myosin II heavy chain (NMHC)-IIA did not associate with Tks5 invadopodia (Supplementary Figure 5e). Overall, these findings show a prominent role of actin polymerization in invadopodia force generation. This role was confirmed by laser ablation in cells treated with low-dose CytoD (100 nM) to reduce actin polymerization without triggering the rapid disassembly of pre-existing invadopodia. The initial recoil velocity was unperturbed after laser-induced rupture (Figure 3i and Supplementary Figure 5f); however, 100 nM CytoD significantly reduced the amplitude of invadopodia/collagen-fiber displacement, as shown by lower plateau values (Figure 3i). We concluded that stronger forces were applied by invadopodia in the control situation than in CytoD-treated cells, further establishing that actin polymerization powers invadopodia-produced forces.

Physical modeling of invadopodial actin-based force production. We developed a theoretical model that describes the force balance in the invadopodia/collagen-fiber ensemble based on our experimental observations. The model considers the shear stress in the assembling actin meshwork due to curvature of the invadopodia/collagen-fiber ensemble, which generates an outward pointing force, inducing further deformation and displacement of the fiber (see Supplementary information Equation 1 and Figure 4c, lower panel). Matrix fiber elasticity opposes to this force and represents the energetic cost to further bend and displace the ECM fiber (see Supplementary information Equation 2 and Figure 4c, lower panel). Given orders of

magnitude inferred from the literature and our observations (typically, the diameter and persistence length of the ECM fiber, actin gel viscosity, and the length of the contact), this model shows that for any sufficient initial curvature of the collagen fiber, actin polymerization-based forces can trigger further deformation and radial expansion (Figure 4abc and Supplementary Information Equations 3 & 4). The model predicts that the force required to remodel less compliant ECM fibers should scale up. We assessed the effect of increasing collagen I gel stiffness on invadopodia expansion as a measure of force. Chemical crosslinking (4% paraformaldehyde ⁹) drastically increased fiber resistance to deformation (the elastic modulus of the crosslinked collagen I matrix increased ~40-fold (Supplementary Figure 5g). Invadopodia still formed in association with crosslinked collagen fibers and collagenolysis occurred (Figure 3j and Supplementary Figure 5h). However, matrix clearance underneath the ventral cell surface was impaired, as well as invadopodia elongation and radial expansion rates, which substantially decreased (Figure 3kl and Movie 10). These data show that increased matrix rigidity and possibly reduced fiber slippage, due to matrix crosslinking, resisted invadopodia-based forces.

Discussion

Invadopodia are hallmarks of invasive cells, which localize MT1-MMP activity to cell-matrix contacts, allowing tissue barrier penetration. The classical model of invadopodia that combines an actin-based protrusive capacity with MMP activity is based mostly on the observation of cancer cells plated on gelatin (*i.e.* denatured collagen) as a substrate. Cells of the immune system such as macrophages also migrate through tissues thanks to F-actin-rich cone-shaped submicrometric invadopodia-like podosomes¹¹. Using human macrophages plated on a deformable substratum (*i.e.* nanometer-thick formvar elastic membrane) and atomic force microscopy, recent work visualized nanoscale deformations of the formvar membrane representing the protrusive force of podosomes. This elegant experimental set-up allowed the authors to propose a model whereby protrusive force at podosomes derives from actin assembly within the podosome actin core and on the contractility of actomyosin filaments connecting the actin core to a surrounding adhesive ring anchored to the substratum through integrins^{32,33}. An alternative, non-antagonistic, model has been discussed in which the invadopodial actin meshwork could push against the nucleus³⁴.

Although the gelatin model has been powerful to identify several invadopodia components and define their function, it suffers from several limitations, including extreme rigidity and two-dimensionality of the glass-coated gelatin substratum. Different from the classical model, we propose a new invadopodia paradigm, which stems from observations of cancer cells invading a fibrous type I collagen network, as self-assembling, force-producing, proteolytic cell-matrix contacts (Figure 4ab). Our data suggest a mechanism, in which MT1-MMP, independently of its collagenolytic activity, binds to and accumulates in association with the collagen fiber and initiates a signaling cascade leading to Tks5 recruitment and actin polymerization at plasma membrane/fiber contact sites. Interestingly, Sixt and colleagues observed that the geometry and density of the lamellipodial actin branched network could adapt and tune its protrusive force in response to the mechanical load³⁵. Along a similar line, our model proposes that, due to the curvature of the invadopodia/fiber ensemble, the shear stress in the actin meshwork allows efficient transformation of the energy of polymerization into an outward pointing force that is used to move the confining fiber, rather than being dissipated backward in the absence of curvature (see Figure 4c, lower panel). Our data also support the conclusion that the pushing force acts synergistically with proteolytic cleavage and increases matrix compliance by MT1-MMP to generate the invasive path. Dynamic patterns of actin assembly, similar to the mechanism of collagenolytic invadopodia expansion that we uncovered, have been observed in

several cellular contexts, including neutrophils, neuronal axons, and *Dictyostelium*³⁶⁻³⁹. These structures, which correspond to spatial-temporal chemical instabilities, have often been described by ‘predator-prey’ models inspired by Turing’s reaction-diffusion equations⁴⁰. We prefer the ‘donkey and carrot’ metaphor to epitomize invadopodia growth (Figure 4c, upper panel)^{25,26}.

This mechanism, in which MT1-MMP acts both as an initiator and executor component, contributes to making invadopodia self-assembling and -propagating machines for fiber recognition, weakening, and repulsion for collagen tunnel clearance during tumor cell invasion. The matrix-repelling proteolytic contact model may also be relevant in the context of tumor cells traversing the BM by enlargement of the BM transmigration pore after initial proteolytic breach at the in situ-to-invasive carcinoma switch or during intra- and extravasation of blood vessels or lymphatics^{4,6,7,41,42}. Recent findings also suggest that the relevance of force producing contacts may be generalized to non-invasive developmental BM remodeling programs, such as early vulval development in *C. elegans*^{43,44}.

References

- 1 Madsen, C. D. & Sahai, E. Cancer dissemination--lessons from leukocytes. *Dev Cell* **19**, 13-26, doi:10.1016/j.devcel.2010.06.013 (2010).
- 2 Friedl, P. & Alexander, S. Cancer invasion and the microenvironment: plasticity and reciprocity. *Cell* **147**, 992-1009, doi:10.1016/j.cell.2011.11.016 (2011).
- 3 Eddy, R. J., Weidmann, M. D., Sharma, V. P. & Condeelis, J. S. Tumor Cell Invadopodia: Invasive Protrusions that Orchestrate Metastasis. *Trends Cell Biol* **27**, 595-607, doi:10.1016/j.tcb.2017.03.003 (2017).
- 4 Hotary, K., Li, X. Y., Allen, E., Stevens, S. L. & Weiss, S. J. A cancer cell metalloprotease triad regulates the basement membrane transmigration program. *Genes Dev* **20**, 2673-2686 (2006).
- 5 Wolf, K. *et al.* Multi-step pericellular proteolysis controls the transition from individual to collective cancer cell invasion. *Nat Cell Biol* **9**, 893-904 (2007).
- 6 Lodillinsky, C. *et al.* p63/MT1-MMP axis is required for in situ to invasive transition in basal-like breast cancer. *Oncogene* **35**, 344-357, doi:10.1038/onc.2015.87 (2016).
- 7 Perentes, J. Y. *et al.* Cancer cell-associated MT1-MMP promotes blood vessel invasion and distant metastasis in triple-negative mammary tumors. *Cancer Res* **71**, 4527-4538 (2011).
- 8 Parekh, A. *et al.* Sensing and modulation of invadopodia across a wide range of rigidities. *Biophys J* **100**, 573-582, doi:10.1016/j.bpj.2010.12.3733 (2011).
- 9 Artym, V. V. *et al.* Dense fibrillar collagen is a potent inducer of invadopodia via a specific signaling network. *J Cell Biol* **208**, 331-350, doi:10.1083/jcb.201405099 (2015).
- 10 Juin, A. *et al.* Physiological type I collagen organization induces the formation of a novel class of linear invadosomes. *Molecular biology of the cell* **23**, 297-309 (2012).
- 11 Linder, S., Wiesner, C. & Himmel, M. Degrading devices: invadosomes in proteolytic cell invasion. *Annu Rev Cell Dev Biol* **27**, 185-211 (2011).
- 12 Wolf, K. *et al.* Physical limits of cell migration: control by ECM space and nuclear deformation and tuning by proteolysis and traction force. *J Cell Biol* **201**, 1069-1084, doi:10.1083/jcb.201210152 (2013).
- 13 Monteiro, P. *et al.* Endosomal WASH and exocyst complexes control exocytosis of MT1-MMP at invadopodia. *J Cell Biol* **203**, 1063-1079, doi:10.1083/jcb.201306162 (2013).
- 14 Castagnino, A. *et al.* Coronin 1C promotes triple-negative breast cancer invasiveness through regulation of MT1-MMP traffic and invadopodia function. *Oncogene*, doi:10.1038/s41388-018-0422-x (2018).
- 15 Infante, E. *et al.* LINC complex-Lis1 interplay controls MT1-MMP matrix digest-on-demand response for confined tumor cell migration. *Nat Commun* **9**, 2443, doi:10.1038/s41467-018-04865-7 (2018).
- 16 Destaing, O. *et al.* beta1A integrin is a master regulator of invadosome organization and function. *Molecular biology of the cell* **21**, 4108-4119 (2010).
- 17 Juin, A. *et al.* Discoidin domain receptor 1 controls linear invadosome formation via a Cdc42-Tuba pathway. *J Cell Biol* **207**, 517-533, doi:10.1083/jcb.201404079 (2014).
- 18 Artym, V. V., Zhang, Y., Seillier-Moisewitsch, F., Yamada, K. M. & Mueller, S. C. Dynamic interactions of cortactin and membrane type 1 matrix metalloproteinase at invadopodia: defining the stages of invadopodia formation and function. *Cancer Res* **66**, 3034-3043 (2006).
- 19 Yamaguchi, H. *et al.* Molecular mechanisms of invadopodium formation: the role of the N-WASP-Arp2/3 complex pathway and cofilin. *J Cell Biol* **168**, 441-452 (2005).
- 20 Seals, D. F. *et al.* The adaptor protein Tks5/Fish is required for podosome formation and function, and for the protease-driven invasion of cancer cells. *Cancer Cell* **7**, 155-165 (2005).
- 21 Takai, K. *et al.* Discoidin domain receptor 1 (DDR1) ablation promotes tissue fibrosis and hypoxia to induce aggressive basal-like breast cancers. *Genes Dev* **32**, 244-257, doi:10.1101/gad.301366.117 (2018).
- 22 Rhys, A. D. *et al.* Loss of E-cadherin provides tolerance to centrosome amplification in epithelial cancer cells. *J Cell Biol* **217**, 195-209, doi:10.1083/jcb.201704102 (2018).
- 23 Tam, E. M., Wu, Y. I., Butler, G. S., Stack, M. S. & Overall, C. M. Collagen Binding Properties of the Membrane Type-1 Matrix Metalloproteinase (MT1-MMP) Hemopexin C Domain. *J. Biol. Chem.* **277**, 39005-39014 (2002).

- 24 Rozanov, D. V. *et al.* Mutation analysis of membrane type-1 matrix metalloproteinase (MT1-MMP). The role of the cytoplasmic tail Cys(574), the active site Glu(240), and furin cleavage motifs in oligomerization, processing, and self-proteolysis of MT1-MMP expressed in breast carcinoma cells. *J Biol Chem* **276**, 25705-25714, doi:10.1074/jbc.M007921200 (2001).
- 25 Yu, X. *et al.* N-WASP coordinates the delivery and F-actin-mediated capture of MT1-MMP at invasive pseudopods. *J Cell Biol* **199**, 527-544 (2012).
- 26 MacDonald, E. *et al.* HRS-WASH axis governs actin-mediated endosomal recycling and cell invasion. *J Cell Biol* **217**, 2549-2564, doi:10.1083/jcb.201710051 (2018).
- 27 Poincloux, R., Lizarraga, F. & Chavrier, P. Matrix invasion by tumour cells: a focus on MT1-MMP trafficking to invadopodia. *J Cell Sci* **122**, 3015-3024, doi:10.1242/jcs.034561 (2009).
- 28 Liang, X., Michael, M. & Gomez, G. A. Measurement of Mechanical Tension at Cell-cell Junctions Using Two-photon Laser Ablation. *Bio Protoc* **6**, doi:10.21769/BioProtoc.2068 (2016).
- 29 Dmitrieff, S. & Nedelec, F. Amplification of actin polymerization forces. *J Cell Biol* **212**, 763-766, doi:10.1083/jcb.201512019 (2016).
- 30 Svitkina, T. The Actin Cytoskeleton and Actin-Based Motility. *Cold Spring Harbor perspectives in biology* **10**, doi:10.1101/cshperspect.a018267 (2018).
- 31 Nolen, B. J. *et al.* Characterization of two classes of small molecule inhibitors of Arp2/3 complex. *Nature* **460**, 1031-1034, doi:10.1038/nature08231 (2009).
- 32 Labernadie, A. *et al.* Protrusion force microscopy reveals oscillatory force generation and mechanosensing activity of human macrophage podosomes. *Nat Commun* **5**, 5343, doi:10.1038/ncomms6343 (2014).
- 33 Bouissou, A. *et al.* Podosome Force Generation Machinery: A Local Balance between Protrusion at the Core and Traction at the Ring. *ACS nano* **11**, 4028-4040, doi:10.1021/acsnano.7b00622 (2017).
- 34 Revach, O. Y. *et al.* Mechanical interplay between invadopodia and the nucleus in cultured cancer cells. *Scientific reports* **5**, 9466, doi:10.1038/srep09466 (2015).
- 35 Mueller, J. *et al.* Load Adaptation of Lamellipodial Actin Networks. *Cell* **171**, 188-200 e116, doi:10.1016/j.cell.2017.07.051 (2017).
- 36 Weiner, O. D., Marganski, W. A., Wu, L. F., Altschuler, S. J. & Kirschner, M. W. An actin-based wave generator organizes cell motility. *PLoS Biol* **5**, e221, doi:10.1371/journal.pbio.0050221 (2007).
- 37 Katsuno, H. *et al.* Actin Migration Driven by Directional Assembly and Disassembly of Membrane-Anchored Actin Filaments. *Cell Rep* **12**, 648-660, doi:10.1016/j.celrep.2015.06.048 (2015).
- 38 Allard, J. & Mogilner, A. Traveling waves in actin dynamics and cell motility. *Curr Opin Cell Biol* **25**, 107-115, doi:10.1016/j.ceb.2012.08.012 (2013).
- 39 Gerisch, G. *et al.* Mobile actin clusters and traveling waves in cells recovering from actin depolymerization. *Biophys J* **87**, 3493-3503, doi:10.1529/biophysj.104.047589 (2004).
- 40 Yang, Y. & Wu, M. Rhythmicity and waves in the cortex of single cells. *Philos Trans R Soc Lond B Biol Sci* **373**, doi:10.1098/rstb.2017.0116 (2018).
- 41 Leong, H. S. *et al.* Invadopodia are required for cancer cell extravasation and are a therapeutic target for metastasis. *Cell Rep* **8**, 1558-1570, doi:10.1016/j.celrep.2014.07.050 (2014).
- 42 Gligorijevic, B., Bergman, A. & Condeelis, J. Multiparametric classification links tumor microenvironments with tumor cell phenotype. *PLoS Biol* **12**, e1001995, doi:10.1371/journal.pbio.1001995 (2014).
- 43 Kelley, L. C., Lohmer, L. L., Hagedorn, E. J. & Sherwood, D. R. Traversing the basement membrane in vivo: a diversity of strategies. *J Cell Biol* **204**, 291-302, doi:10.1083/jcb.201311112 (2014).
- 44 Caceres, R. *et al.* Forces drive basement membrane invasion in *Caenorhabditis elegans*. *Proc Natl Acad Sci U S A* **115**, 11537-11542, doi:10.1073/pnas.1808760115 (2018).
- 45 Lizarraga, F. *et al.* Diaphanous-related formins are required for invadopodia formation and invasion of breast tumor cells. *Cancer Res* **69**, 2792-2800, doi:10.1158/0008-5472.CAN-08-3709 (2009).

- 46 Heuser, J. The production of 'cell cortices' for light and electron microscopy. *Traffic* **1**, 545-552
(2000).
- 47 te Riet, J. *et al.* Interlaboratory round robin on cantilever calibration for AFM force
spectroscopy. *Ultramicroscopy* **111**, 1659-1669, doi:10.1016/j.ultramic.2011.09.012 (2011).
- 48 van Helvert, S. & Friedl, P. Strain Stiffening of Fibrillar Collagen during Individual and
Collective Cell Migration Identified by AFM Nanoindentation. *ACS applied materials &
interfaces* **8**, 21946-21955, doi:10.1021/acsami.6b01755 (2016).

Methods

Plasmid constructs. Construct expressing Tks5^{GFP} was a kind gift of Dr S. Courtneidge (OHSU, Portland, OR). Plasmid expressing GFP-ArpC5B was a kind gift of Dr. A. Gautreau (Ecole Polytechnique, Paris, FR). MT1-MMP with internal pHluorin has been previously described ⁴⁵. E240A, ΔCter and LLY/A mutations were generated by PCR mutagenesis (see Supplementary Figure 2a).

Cell culture, stable and transient transfection and siRNA treatment. MDA-MB-231 cells obtained from ATCC (ATCC HTB-26) were grown in L15 medium supplemented with 15% fetal calf serum and 2 mM glutamine at 37°C in 1% CO₂ and MCF10DCIS.com cell line was purchased from Asterand and maintained in DMEM- F12 medium supplemented with 2 mM glutamine and with 5% horse serum. Cell lines were routinely tested for mycoplasma contamination. MDA-MB-231 cells stably expressing Tks5^{GFP} were generated by lentiviral transduction. For transient expression, MDA-MB-231 cells were transfected with plasmid constructs using Lipofectamine 3000 according to the manufacturer instructions (ThermoFisher). Cells were analyzed by live cell imaging 24-48 hr after transfection. For knockdown, MDA-MB-231 or MCF10DCIS.com cells were treated with the indicated siRNA (50 nM) using Lullaby (OZ Biosciences, France) and analyzed after 72 hrs of treatment. siRNAs used for this study are listed in Supplementary Table S2.

Antibodies and reagents. The source and working dilution of commercial antibodies and chemical reagents used for this study are listed in Supplementary Tables S3 and S4, respectively. Hepatocyte growth factor (HGF) was purchased from PeproTech Inc. and used at 20 ng/ml.

Western blot analysis. Cells were lysed in SDS sample buffer, separated by SDS-PAGE, and detected by immunoblotting analysis with the indicated antibodies. Antibodies were visualized using the ECL detection system (GE Healthcare).

RNA extraction, cDNA synthesis and qPCR analysis. Cells were pelleted by centrifugation and washed in PBS prior lysis and RNA extraction using RNeasy Mini Kit from Qiagen. cDNAs were produced from 1 μg of extracted RNA using High capacity DNA reverse transcription kit from Applied Biosystem and used for quantitative PCR using LightCycler 480 SYBR Green I Master from Roche Life Science. Each condition was realized in triplicate with the following controls: a sample of RNA without reverse transcriptase, a sample without RNA but with reverse transcriptase, a sample without both, as well as an internal control with a GAPDH qPCR

primer. The following qPCR primers were used: for MT1-MMP 5'-GGATACCCAATGCCCATTTGGCCA-3' and 5'-CCATTGGGCATCCAGAAGAGAGC-3' at 600 nM, for DDR1 5'-CAACCACAGCTTCTCCAGTGGCTA-3' and 5'-GCATGTTGTTACAGTGGACCTGCATA-3' at 500 nM, and for GAPDH 5'-AGCCACATCGCTCAGACAC-3' and 5'-GCCCAATACGACCAAATCC-3' at 500 nM. qPCR reaction was performed using LightCycler® 480 thermocycling machine. Briefly, samples were pre-incubated for 5 min at 95°C before undergoing 45 cycles of amplification composed of 20 s at 95°C, 15 s at 60°C and 15 s at 72°C. A final cycle of 5 s at 95°C and 1 min at 70°C was performed before extracting melting curves for analysis. For each sample average of Cycle Thresholds (CTs) were calculated and extreme values filtered out if standard deviations were above 1. Differences between mean CT values of each sample and mean CT values of GAPDH sample were calculated to obtain Δ CT. Differences between mean CT values of each sample and Δ CT were calculated for each sample and squared to obtain the relative mRNA level expression of each sample as compared to GAPDH control. Values were then normalized on siNT-treated control set to 100 percent.

Indirect immunofluorescence analysis of cells plated on collagen. Coverslips were layered with 200 μ l of ice-cold 2.0 mg/ml acidic extracted collagen I solution (Corning) in 1x MEM mixed with 4% Alexa Fluor 647-conjugated type I collagen. The collagen solution was adjusted to pH7.5 using 0.34 N NaOH and Hepes was added to 25 μ M final concentration. After 3 min of polymerization at 37°C, the collagen layer was washed gently in PBS and cells in suspension were added for 60 to 90 min at 37°C in 1% CO₂ before fixation. Cells were pre-extracted with 0.1% Triton X-100 in 4% paraformaldehyde in PBS during 90 s and then fixed in 4% paraformaldehyde in PBS for 20 min and stained for immunofluorescence microscopy with indicated antibodies.

Line-scan analysis of averaged fluorescence intensity profiles. Fluorescence intensity profiles of type I collagen and of indicated antibodies or dyes were obtained using the line-scan function (average intensity) of Metamorph software analyzing a region crossing one or several collagen fibers associated with invadopodia markers (depicted by a white line). Except stated otherwise, intensity profiles were normalized on each maximum to visualize the presence or absence of peaks of fluorescence intensity along with collagen fibers.

Electron Microscopy of unroofed cells. Adherent plasma membrane from MDA-MB-231 cells plated for 30 to 45 min on glass coverslips coated with a thin layer of collagen were disrupted by sonication as described previously ⁴⁶. Paraformaldehyde/glutaraldehyde-fixed

cells were further sequentially treated with OsO₄, tannic acid and uranyl acetate prior to dehydration and Hexamethyldisilazane drying (HMDS, Sigma-Aldrich). For immunogold labeling, 4% paraformaldehyde fixed plasma membranes were washed and quenched before incubation with primary and 15 nm gold-coupled secondary antibodies and further fixed with 2% glutaraldehyde. Dried samples were then rotary-shadowed with platinum and carbon with a high vacuum sputter coater (Leica). Platinum replicas were floated off the glass by angled immersion into hydrofluoric acid, washed several times by floatation on distilled water, and picked up on 200 mesh formvar/carboncoated EM grids. The grids were mounted in a eucentric side-entry goniometer stage of a transmission electron microscope operated at 80 kV (Philips, model CM120) and images were recorded with a Morada digital camera (Olympus). Images were processed in Adobe Photoshop to adjust brightness and contrast and presented in inverted contrast. For analyzes of Tks5-depleted cells, cells were transfected with indicated siRNAs (50 nM, Dharmacon) using Lullaby (OZ Biosciences, France) 72 hours prior to sample preparation.

Quantification of pericellular collagenolysis. Cells treated with indicated siRNAs were trypsinized and resuspended (2.5×10^5 cells/ml) in 200 μ l of ice cold 2.0 mg/ml collagen I solution prepared as previously described. 40 μ l of the cell suspension in collagen was added on glass coverslip and collagen polymerization was induced for 30 min by incubation at 37°C. L-15 complete medium was then added and cells embedded in collagen were incubated for 16h at 37°C in 1% CO₂. After fixation for 30 min at 37°C in 4% paraformaldehyde in PBS, samples were incubated with anti-Col1-^{3/4}C antibodies for 2h at 4°C. After extensive washes, samples were counterstained with Cy3-conjugated anti-rabbit IgG antibodies, Phalloidin-Alexa488 to visualize cell shape and mounted in DAPI. Image acquisition was performed with an A1R Nikon confocal microscope with a 40X NA 1.3 oil objective using high 455 sensitivity GaASP PMT detector and a 595 ± 50 nm band-pass filter. Quantification of degradation spots was performed as previously described¹³. Briefly, maximal projection of 10 optical sections with 2 μ m interval from confocal microscope z-stacks (20 μ m depth) were preprocessed by a laplacian of Gaussian filter using a homemade ImageJ macro (available as supplementary information¹³). Detected spots were then counted and saved for visual verification. No manual correction was done. Degradation index was the number of degradation spots divided by the number of cells present in the field, normalized to the degradation index of control cells set to 100.

Invadopodia assay. 5×10^4 cells were plated on collagen-coated coverslips, fixed after 60 min and stained with Tks5 and Cortactin antibodies. Images were acquired with a wide-field microscope (Eclipse 90i Upright; Nikon) using a 100 \times Plan Apo VC 1.4 oil objective and a

highly sensitive cooled interlined charge-coupled device (CCD) camera (CoolSnap HQ2; Roper Scientific). A z-dimension series of images was taken every 0.2 μm by means of a piezoelectric motor (Physik Instrumente). For quantification of Tks5 associated with invadopodia, three consecutive z-planes corresponding to the plasma membrane in contact with collagen fibers were projected using maximal intensity projection in Fiji and Tks5 signal was determined using the thresholding command excluding regions < 8 px to avoid non-invadopodial structures. Surface covered by Tks5 signal was normalized to the total cell surface and values normalized to that of control cells.

Live-cell imaging on type I collagen layer. For live imaging of cells on a fibrous collagen layer, glass bottom dishes (MatTek Corporation) were layered with 15 μl of a collagen solution as described above to produce a 5-10 μm thick layer of collagen. To crosslink collagen, polymerized collagen was incubated 20 min in PBS with 4% PFA and 5% Sucrose, and washed extensively in PBS before adding cell suspension in normal L-15 medium. 1 ml of cell suspension (7.5×10^4 cells/ml) in complete medium was added and incubated for 30 min at 37°C, 1% CO₂. Z-stacks (11 images, 0.5 μm z-step) images were acquired every min during 1h to 1h30 by confocal spinning disk microscopy. For drugs treatment, cells were cultured in 1 mL of complete medium with vehicle (DMSO) and imaged every min for 15 min. Then, 1 mL of drug-containing medium (2x concentration) was added and cells were further imaged for 60 min. Image sequences were acquired on a spinning-disk (Roper Scientific) using a CSU22 Yokogawa head mounted on the lateral port of an inverted TE-2000U Nikon microscope equipped with a 40x 1.4NA Plan-Apo objective lens and a dual-output laser launch, which included 491 nm and 561 nm, 50 mW DPSS lasers (Roper Scientific). Images were collected with a CoolSNAP HQ² CCD camera (Roper Scientific). The system was steered by Metamorph 7 software. Kymographs were obtained with Fiji software along a line spanning the invadopodia diameter.

Live-cell imaging in 3D type I collagen. Glass bottom dishes (MatTek Corporation) were layered with 10 μl of a solution of 5 mg/ml unlabeled type I collagen mixed with 1/25 volume of Alexa-Fluor 647-labeled collagen. Polymerization was induced at 37°C for 3 min as described above and the bottom collagen layer was washed gently in PBS; 1 ml of cell suspension (1×10^5 cells/ml) in complete medium was added and incubated for 30 min at 37°C. Medium was gently removed and two drops of a mix of Alexa Fluor 647-labeled type I collagen/unlabeled type I collagen at 2.0 mg/ml final concentration were added on top of the cells (top layer). After polymerization at 37°C for 90 min as described above, 2 ml of medium

containing 20 ng/ml HGF was added to the culture. Z-stacks of images were acquired every 10 min during 16 hrs by confocal spinning disk microscopy as described above.

Invadopodia elongation rate measurement. The length of Tks5-positive invadopodia, defined as curvilinear GFP-positive structures in association with collagen fibers, was analyzed overtime in cells plated on Alexa-Fluor 647-labeled collagen. Structures smaller than 10 px (~2 μ m) were not taken into account in the analysis. Invadopodia elongation rate was calculated by dividing the increment length between initial and final time-points by the time interval (in μ m/min). Positive growth rate corresponds to an increase of invadopodia length overtime (*i.e.* elongation), while negative growth rate represents a decrease of invadopodia length overtime (*i.e.* disassembly). In case of drug treatment, elongation rate was measured after drug addition.

Time projections, kymographs and invadopodia radial expansion rate measurement. For visualization and quantification of invadopodia radial expansion rate, time projections and kymographs of expanding circular invadopodia were performed. We used the temporal color-code function in Fiji to assign a different color for each of the five frames with a 10-min interval from a time-lapse sequence recorded every min. In addition, for each circular invadopodia, a line spanning the invadopodia was drawn and a kymograph was extracted using Multi-kymograph function in Fiji. Radial growth rate of expanding invadopodia was calculated as followed: $(\text{Diameter } t_n - \text{Diameter } t_0)/(t_n - t_0)$ (see Figure 3b-g).

Laser ablation and initial recoil velocity calculation. The laser ablation system was composed of a pulsed 355-nm ultraviolet laser (Roper Scientific) interfaced with an iLas system running in parallel with Metamorph 7 Software. This system was mounted on a confocal spinning disk (Yokagawa CSU-X1 spinning head on a Nikon Eclipse Ti inverted microscope) equipped with an EM-CCD camera (Evolve, Photometrics) and a 100x oil immersion objective (Nikon S Fluor 100x 0.5-1.3 NA). MDA-MB-231 cells expressing Tks5^{GFP} were plated on glass coverslips coated with a thin layer of Cy5-labelled collagen for 30 min at 37°C. To allow acute ablation of a single invadopodia/collagen fiber ensemble, curvilinear invadopodia of a total length greater than 4.5 μ m were selected. The ablation region was drawn as a line of 10-20 px long and 1 px thick crossing the middle of the invadopodia arc perpendicularly. Z-stacks (4 images, 0.5 μ m z-step) of images were acquired at 15 s interval during 2 min before ablation. For photo-ablation, the laser beam was focused on the region of interest during a 10-20 ms pulse at 65-85% laser power. Laser ablation settings were validated by the absence of recovery of GFP and Cy5 signal recovery overtime (in contrast to FRAP). Z stacks were acquired as above for 15 s interval during 3 min and then prolonged to 30 s interval for another 3 min to

ensure full capture of the movement. Displacement of the invadopodia/collagen fiber ensemble from its position at t_0 (rupture time), was calculated and the speed of fiber retraction at t_0 , *i.e.* ‘initial recoil velocity’ (V_0) was obtained after fitting the displacement curve with plateau followed by one-phase association exponential using GraphPad Prism (GraphPad Software) ²⁸.

AFM measurements and collagen stiffness quantification. The local stiffness of collagen gels was measured with a Catalyst BioScope (Bruker, Germany) atomic force microscope coupled to a confocal microscope (TCS SP5II, Leica) using the “point and shoot” feature of the Nanoscope software (Bruker). Silicon nitride cantilevers with nominal spring constants of 0.7 N/m (Scanasyst-Fluid, Bruker) were used without any tip modification. The system was calibrated first in air and then in PBS prior to each experiment by measuring the deflection sensitivity on a glass surface, which enabled determination of the cantilever spring constant using the thermal noise method ⁴⁷. AFM height images captured in peak-force tapping mode allowed for the selection of ‘point of interest’ to obtain the force curves. The forward (approach) and reverse (retraction) velocities were kept constant at 1 $\mu\text{m/s}$, ramping the cantilever by 0.5 μm with a 0.2 V (3.2 nN) threshold in a closed z loop. After baseline correction, approach curves were analyzed for determination of Young’s modulus of elasticity using Sneddon’s conical indenter model, for which Poisson’s ratio was set as 0.5 and the half angle of the indenter as 18° . Contact point-independent linear Sneddon equation was used for fitting the approach curves ⁴⁸. The region on the approach curve, through which the model was fit was determined via setting the lower and upper boundaries that corresponded to approximately 10 % and 70 % of the difference between the maximum and minimum forces exerted, respectively.

Statistics and reproducibility. All results were presented as mean \pm SEM of three independent experiments. GraphPad Prism (GraphPad Software) was used for statistical analysis. Statistical significance was defined as *, $P < 0.05$; **, $P < 0.01$; ***, $P < 0.001$; ****, $P < 0.0001$; ns, not significant. Data were tested for normal distribution using the D’Agostino-Pearson normality test and nonparametric tests were applied otherwise. One-way ANOVA, Kruskal-Wallis, Mann-whitney or two-way ANOVA with Sidak’s test for multiple comparisons tests were applied as indicated in the figure legends.

Data Availability. All relevant data are available from the authors.

Acknowledgments. The authors thank the Nikon Imaging Centre @ Institut Curie-CNRS and Cell and Tissue Imaging Facility of *Institut Curie*, member of the France Bio Imaging national

research infrastructure (ANR-10-INBS-04) for help with image acquisition, Dr V. Fraisier for help with laser ablation experiments, the Microscopical Imaging Center @ Radboud University Medical Center, Nijmegen (The Netherlands) for the use of the Atomic Force Microscope, Dr E. Infante for collagenolysis analysis in Tks5-depleted cells, Drs S. Courtneidge and A. Gautreau for providing reagents for this study and Agnieszka Kawska (<http://www.IlluScientia.com>) for artwork. R.F. was supported by fellowships from *Ministère de l'Education Nationale, de l'Enseignement supérieur et de la Recherche* and *Fondation ARC pour la Recherche sur le Cancer*. Funding for this work was provided by *Fondation ARC pour la Recherche sur le Cancer* (Programme labellisé 2017) to P.C. and core funding from *Institut Curie* and *Centre National pour la Recherche Scientifique* (CNRS).

a Fluorescence image of a cell showing F-actin (green) and nuclei (blue). An inset shows a line scan of intensity (0 to 100) versus pixel distance (0 to 30 px).

b Fluorescence image of a cell showing F-actin (red) and nuclei (blue). Scale bar is 10 μm.

c Fluorescence image of a cell showing F-actin (green) and nuclei (blue). Scale bar is 10 μm.

d Fluorescence image of a cell showing F-actin (green) and nuclei (blue). Scale bar is 10 μm.

e Fluorescence image of a cell showing F-actin (green) and nuclei (blue). Scale bar is 10 μm.

f Fluorescence image of a cell showing F-actin (green) and nuclei (blue). Scale bar is 10 μm.

g Fluorescence image of a cell showing F-actin (green) and nuclei (blue). Scale bar is 10 μm.

h Fluorescence image of a cell showing F-actin (green) and nuclei (blue). Scale bar is 10 μm.

i Fluorescence image of a cell showing F-actin (green) and nuclei (blue). Scale bar is 10 μm.

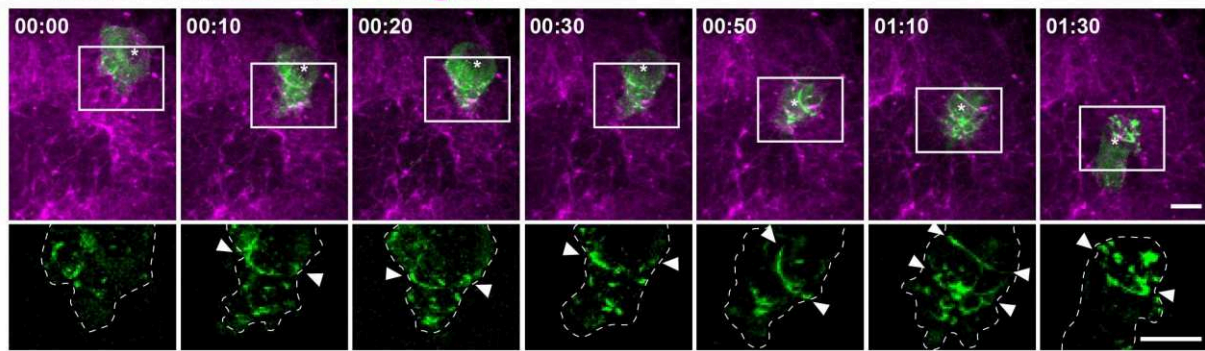
j Bar graph showing the percentage of TKS5+ invadopodia for different MT1-MMP constructs. The y-axis is 'TKS5+ Invadopodia (% of siNT)' ranging from 0 to 100. The x-axis shows five constructs: MT1-MMP, MT1-MMP^{E240A}, MT1-MMP^{ΔC}, and MT1-MMP^{ΔAY}. For each construct, two bars are shown: siNT (red) and siMT1^{UTR} (light red). Statistical significance is indicated by asterisks: **** p < 0.0001, ns = not significant.

Construct	siNT (%)	siMT1 ^{UTR} (%)	n
MT1-MMP	100	~30	250 (3)
MT1-MMP ^{E240A}	100	~80	117 (4)
MT1-MMP ^{ΔC}	100	~45	109 (4)
MT1-MMP ^{ΔAY}	100	~55	107 (3)

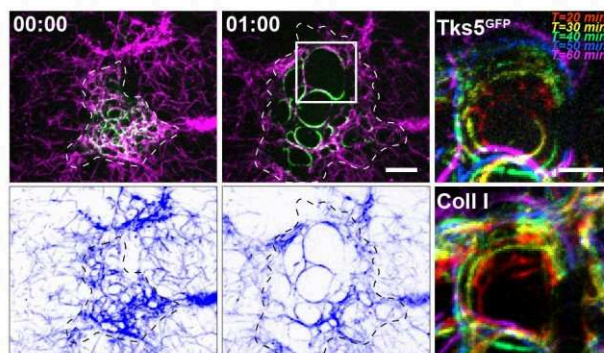
136

Figure 1. Organization of collagenolytic invadopodia. (a) Tks5 (red) and F-actin (green) staining of MDA-MB-231 cells cultured on type I collagen (gray) for 60 min. the nucleus is stained with DAPI (blue). Normalized fluorescence intensity profiles along the white line are shown in the inset. (b) Same image using inverted lookup tables (collagen fibers in blue, Tks5-positive invadopodia in red). Empty arrowheads point to curved invadopodia/fiber ensembles. Full arrowheads depict bundles of collagen fibers at the cell periphery. The cell contour is shown. Scale bar, 10 μ m. (c) PREM survey view of the cytoplasmic surface of the adherent plasma membrane in unroofed MDA-MB-231 cells plated for 60 min on a thin layer of collagen I (image is inverted). Arrowheads indicate bow- and ring-like shaped proteinaceous densities in association with bent collagen fibers underneath the cell body. Scale bar, 10 μ m. (d) Enlarged PREM image of bow-shape collagen fiber (arrowheads) and associated branched actin network along the concave side of the fiber (pseudo-colored in red). Clathrin-coated pits (CCP) and intermediate filaments (IF) are visible. (e, f) Anti-GFP immunogold PREM of MDA-MB-231 cells expressing Arp2/3 complex subunit ArpC5B^{GFP} (e) or Tks5^{GFP} (f). Immunogold particles are pseudo-colored in green and actin filaments in red. V, vesicle. (g) PREM image of the cytoplasmic face of the plasma membrane of MDA-MB-231 cells silenced for Tks5. Underlying collagen fibers are straight, with no associated proteinaceous density, nor actin filaments. Scale bar, 200 nm. (h, i) MDA-MB-231 cells silenced for MT1-MMP (h) or rescued by siRNA-resistant MT1-MMP expression (i) were plated on a type I collagen (gray) layer for 60 min and stained for F-actin (green), Tks5 (red), and DAPI (blue). Corresponding inverted images, with collagen shown in the right panels (collagen is pseudo-colored blue and Tks5 in red). Scale bar, 10 μ m. (j) Quantification of Tks5-positive invadopodia in MDA-MB-231 cells knocked down for MT1-MMP or mock-treated and rescued with the indicated MT1-MMP constructs (see Supplementary Figure 2a). The Y-axis is the ratio of the Tks5 area to the total cell area normalized to the mean value of corresponding Mock-treated cells (as percentage \pm SEM). n: number of cells analyzed; (n): number of independent experiments. Mann-Whitney tests.

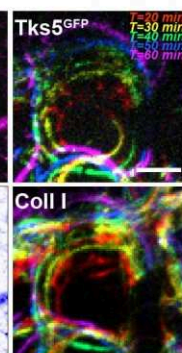
a MDA-MB-231 Tks5^{GFP} / 3D Collagen I



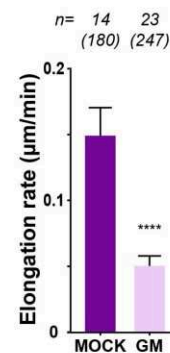
b Control



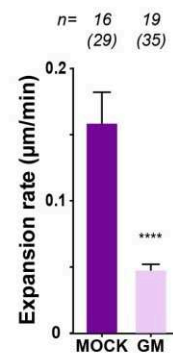
c



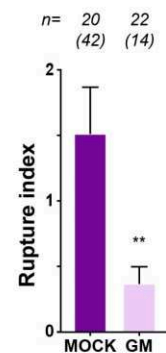
d



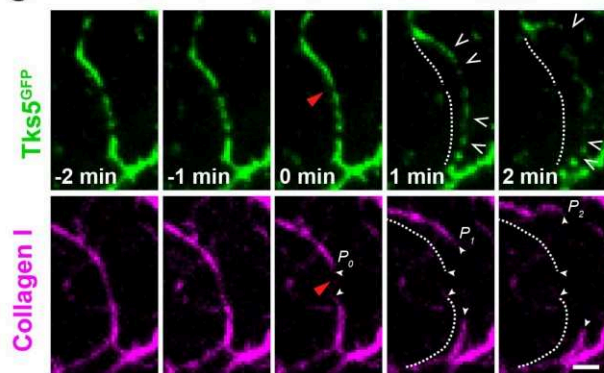
e



f



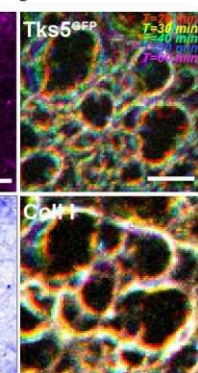
g



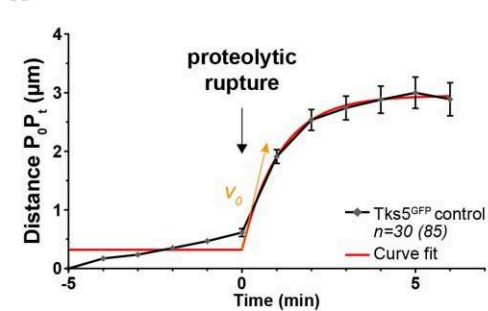
i

GM6001 (40μM)

j



h



k

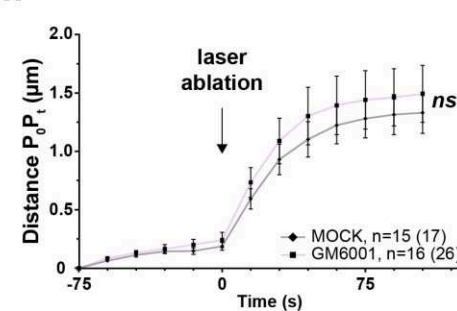


FIGURE 2

Figure 2. Force transmission and weakening of matrix counter-resistance by collagenolytic invadopodia. (a) Gallery of non-consecutive frames (time in hr:min) from a representative time-lapse sequence of Tks5^{GFP}-expressing MDA-MB-231 cells (green) embedded in a 3D-collagen gel (magenta) (see Movie 1). The bottom row shows a zoom-in of the boxed region for the GFP channel. Arrowheads point to Tks5^{GFP}-positive ring-like structures forming in association with constricting collagen fibers, which expand in size during cell penetration. *, nucleus position based on the absence of a GFP signal. The cell contour is shown. Scale bars, 10 μ m. (b) MDA-MB-231 cells expressing Tks5^{GFP} (green) were plated on top of a thin layer of type I collagen (magenta) and imaged over time. Images represent the first and last frames from a representative movie (time in hr:min, Movie 2). The bottom row shows the collagen layer in an inverted lookup table (pseudo-colored blue). Scale bar, 10 μ m. (c) Color-coded time-projections of five images made at 10-min intervals, corresponding to the boxed region in b, showing radial expansion of Tks5 invadopodia (upper image) and associated fiber (lower image) over time. Scale bar, 5 μ m. (d) Elongation rate of invadopodia along collagen fibers in cells treated with GM6001 (GM) compared to mock treatment. Data are presented as the mean \pm SEM from three independent experiments; Mann-Whitney test. n: number of cells; (n): number of invadopodia. (e) Radial invadopodia expansion rate in cells treated with GM6001 compared to mock treatment. Data are presented as the mean \pm SEM from three independent experiments; Mann-Whitney test. n: cell number; (n): invadopodia number. (f) Rupture index (*i.e.* rupture events/cell/hr) calculated in mock- and GM-treated cells. Data are presented as the mean \pm SEM from three independent experiments; Mann-Whitney test. n: cell number; (n): invadopodia number. (g) Gallery of consecutive frames from a time-lapse sequence of Tks5^{GFP}-expressing cells (green) plated on a type I collagen layer (magenta). The gallery shows an invadopodia/collagen-fiber ensemble undergoing collagenolytic rupture at time 0 (red arrowhead, see Movie 3). Rupture is followed by the elastic recoil of the invadopodia/collagen-fiber ensemble. The initial position of the invadopodia/collagen-fiber ensemble is shown by a dashed line and positions of the collagen fiber tips after rupture are indicated (lower row). White arrowheads point to regions of invadopodia disassembly (upper row). Time is indicated in min. Scale bar, 2 μ m. (h) Invadopodia/collagen-fiber tension. The distance between the position of the collagen fiber tip (P_t) and initial position (P_0) was calculated and plotted over time. The black curve represents the mean \pm SEM from 85 proteolytic rupture events aligned at rupture time point (t_0). n: number of cells analyzed from three independent experiments. The curve shows typical visco-elastic recoil after proteolytic rupture and was fitted to a “plateau followed by one-phase association” model (red). (i, j) MDA-MB-231 cells

were treated with the MMP-inhibitor GM6001 and analyzed as in panels b and c (see Movie 4).

(k) Displacement of an invadopodia/collagen-fiber ensemble before and after laser-ablation in mock- (gray) and GM-treated cells (pink) (see Movie 5). n: cell number; (n): invadopodia number from three independent experiments. Data were analyzed using two-way ANOVA with Sidak's multiple comparisons test for each time point.

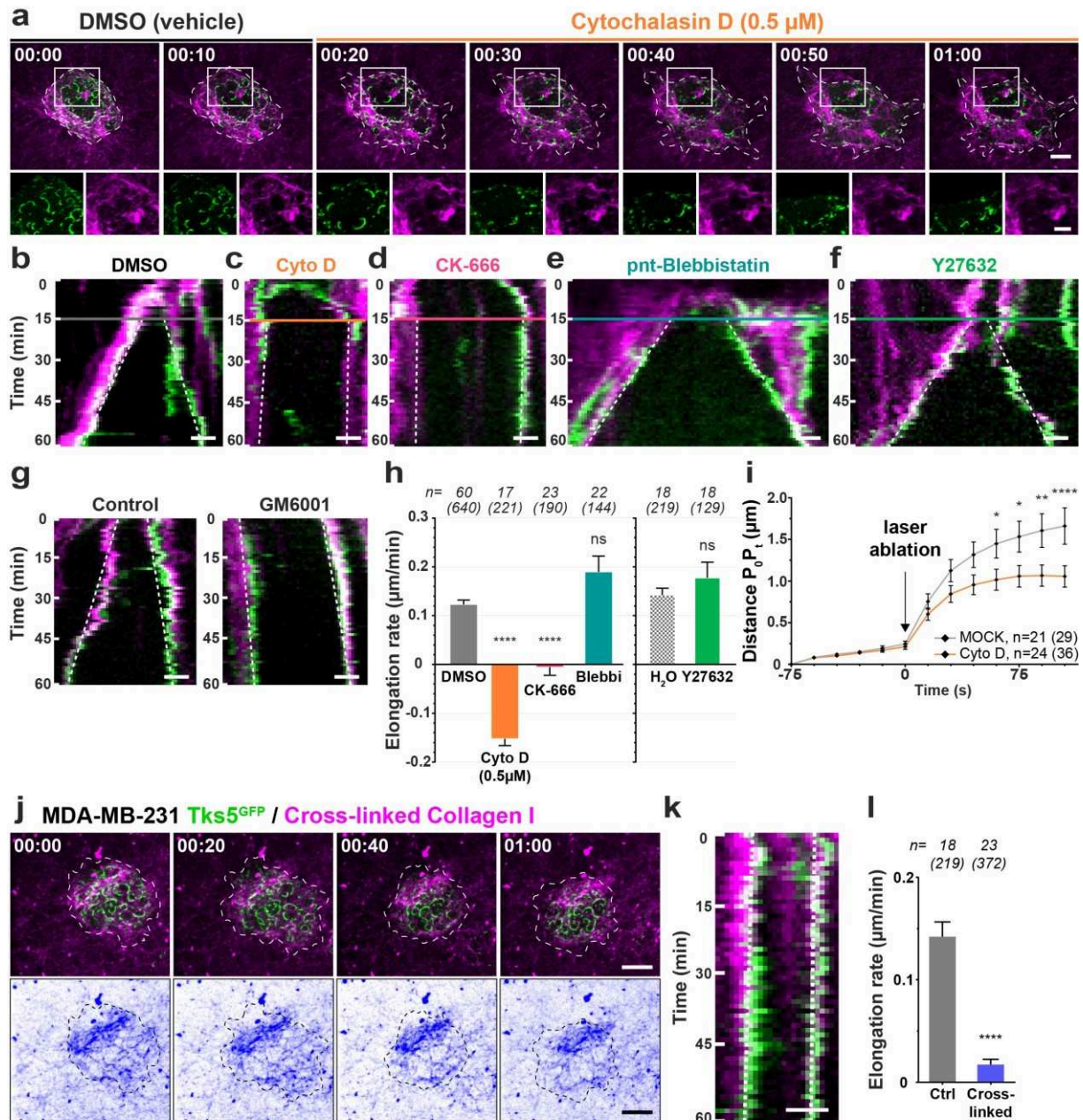


FIGURE 3

Figure 3. Invadopodial force production is powered by actin polymerization. (a) MDA-MB-231 cells expressing Tks5^{GFP} (green) were plated on a thin layer of type I collagen (magenta) and imaged over time. Cytochalasin D (0.5 μ M) was added 15 min after starting the time-lapse. Representative frames (time in h:min) show rapid disassembly following CytoD treatment and limited collagen-fiber remodeling (Movie 6). Scale bar, 10 μ m. The lower row represents separate channels in the boxed region. Scale bar, 5 μ m. (b–g) Kymograph analysis of radial expansion of an invadopodia/collagen-fiber ensemble upon drug addition (see Movies 4 and 6 to 9). Drugs were added 15 min after starting the time-lapse (see colored lines), except in panel g, in which GM was added at the beginning of the movie. Scale bars, 2 μ m. (h)

Quantification of the invadopodia elongation rate along collagen fibers in MDA-MB-231 cells treated with the indicated drugs. Data are presented as the means \pm SEM from three independent experiments (DMSO, 8 experiments). n: cell number; (n): invadopodia number. Kruskal-Wallis and Mann-Whitney (Y27632 vs. H₂O) tests. **(i)** Displacement of invadopodia/collagen-fiber ensemble over time before and after laser-ablation in CytoD (100 nM, orange) and mock-treated cells (gray). Curves represent the mean \pm SEM of 29 (Mock) and 36 (CytoD) curves aligned at rupture time-point (t_0). n: number of cells analyzed from three independent experiments. Two-way ANOVA with Sidak's multiple comparisons test for each time point. **(j)** Tks5^{GFP}-expressing cells were plated on crosslinked collagen (4% PFA, magenta) and analyzed by time-lapse microscopy. The gallery shows non-consecutive frames from a representative movie obtained from three independent experiments (time in hr:min, see Movie 10). The rigid collagen network is shown in the inverted images in the bottom row (pseudocolored blue). Scale bar: 10 μ m. **(k)** Kymograph analysis. Scale bar: 2 μ m. **(l)** Elongation rate of invadopodia in cells plated on crosslinked collagen. Data are presented as the mean \pm SEM from three independent experiments. n: cell number; (n): invadopodia number. Mann-Whitney test.

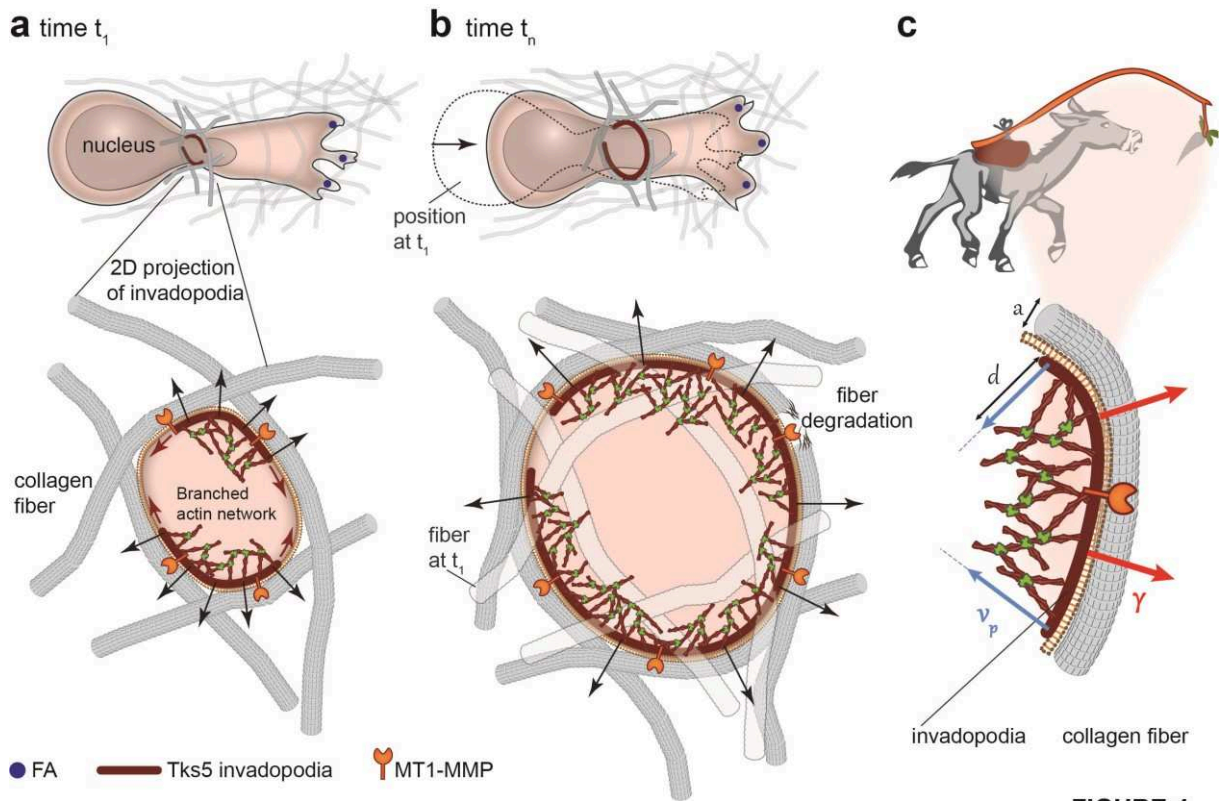
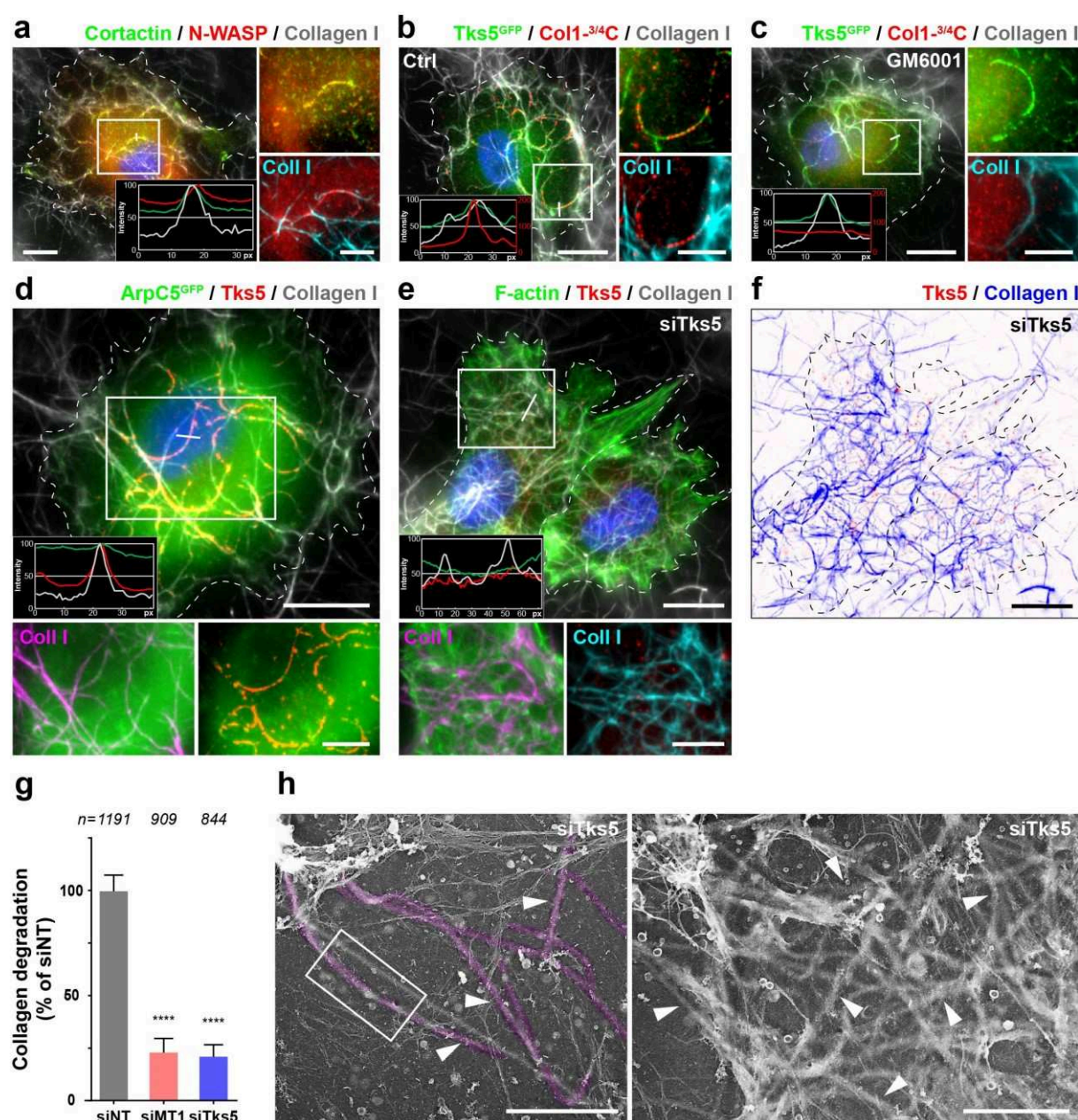


FIGURE 4

Figure 4. Actin assembly at proteolytic contacts drives ECM pore enlargement. (a, b) Confined migration of tumor cells through the dense 3D collagen network triggers formation of proteolytic contacts by recognition of collagen fibers by surface-exposed MT1-MMP. Invadopodial actin assembly pushes the plasma membrane away, resulting in matrix pore enlargement to promote cell invasion. **(c)** Upper panel: the overall propagative behavior of the invadopodia/collagen-fiber ensemble can be explained using the ‘donkey and the carrot’ metaphor, in which the donkey (invadopodium) is attracted to the carrot (ECM fiber) but the carrot moves away because of the donkey’s progression. MT1-MMP harbors collagen-binding ectodomains and a cytoplasmic tail that interacts with the invadopodial actin meshwork. Lower panel: sketch of the physical model representing the invadopodial actin filament meshwork. Due to the curvature of the invadopodia/collagen-fiber ensemble, filament density and shear stress in the actin meshwork and filament polymerization generate an outward pointing force that can further deform and displace the constricting fiber. The main parameters are depicted: a , collagen fiber diameter; d , thickness of the invadopodial actin meshwork; v_p , speed of inward actin polymerization; γ , resulting outward pointing normal force applied on the fiber.

Description of Additional Supplementary Files

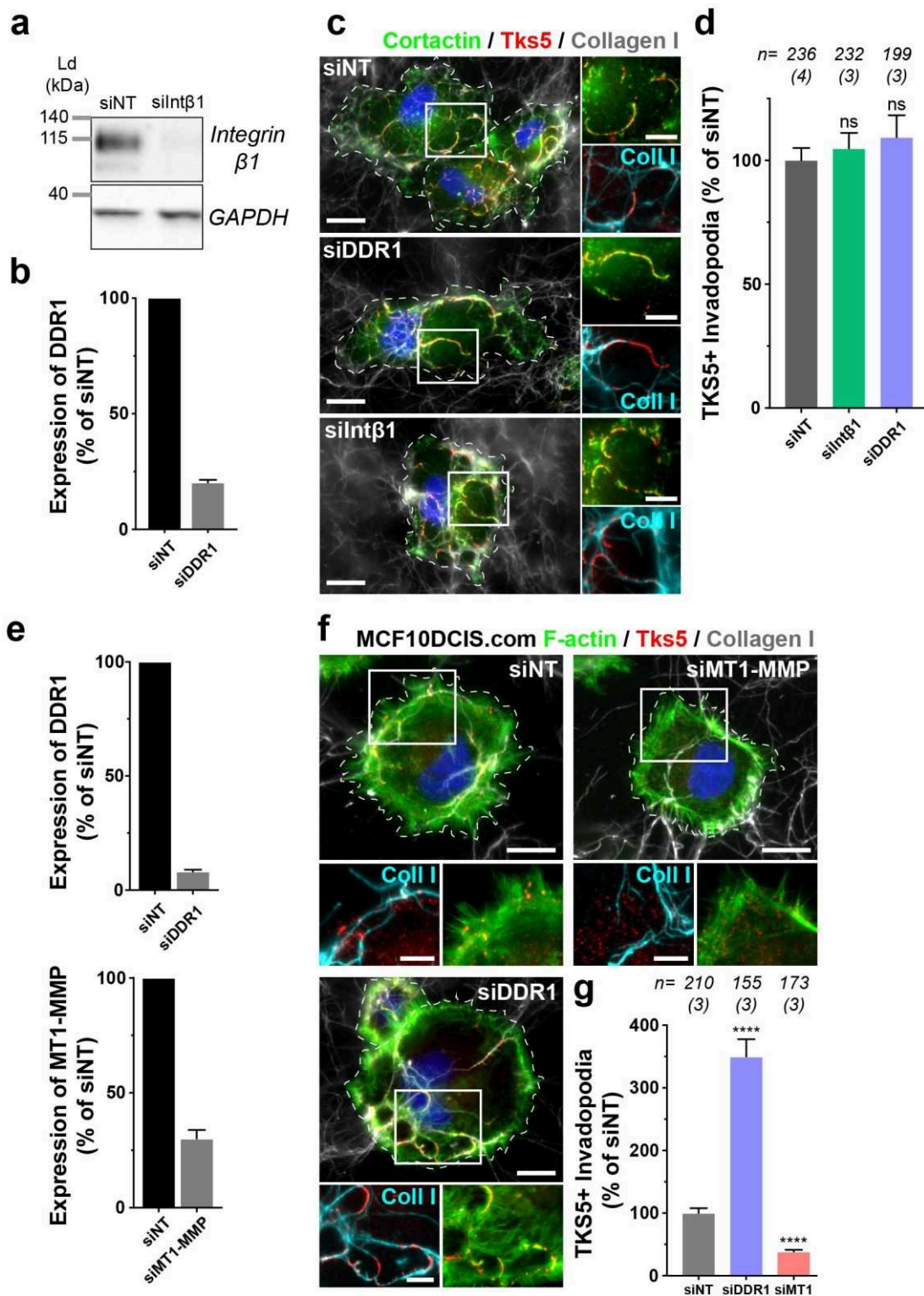


SUPPLEMENTARY FIGURE 1

Supplementary Figure 1. Invadopodia organization (supplementary figure to Figure 1).

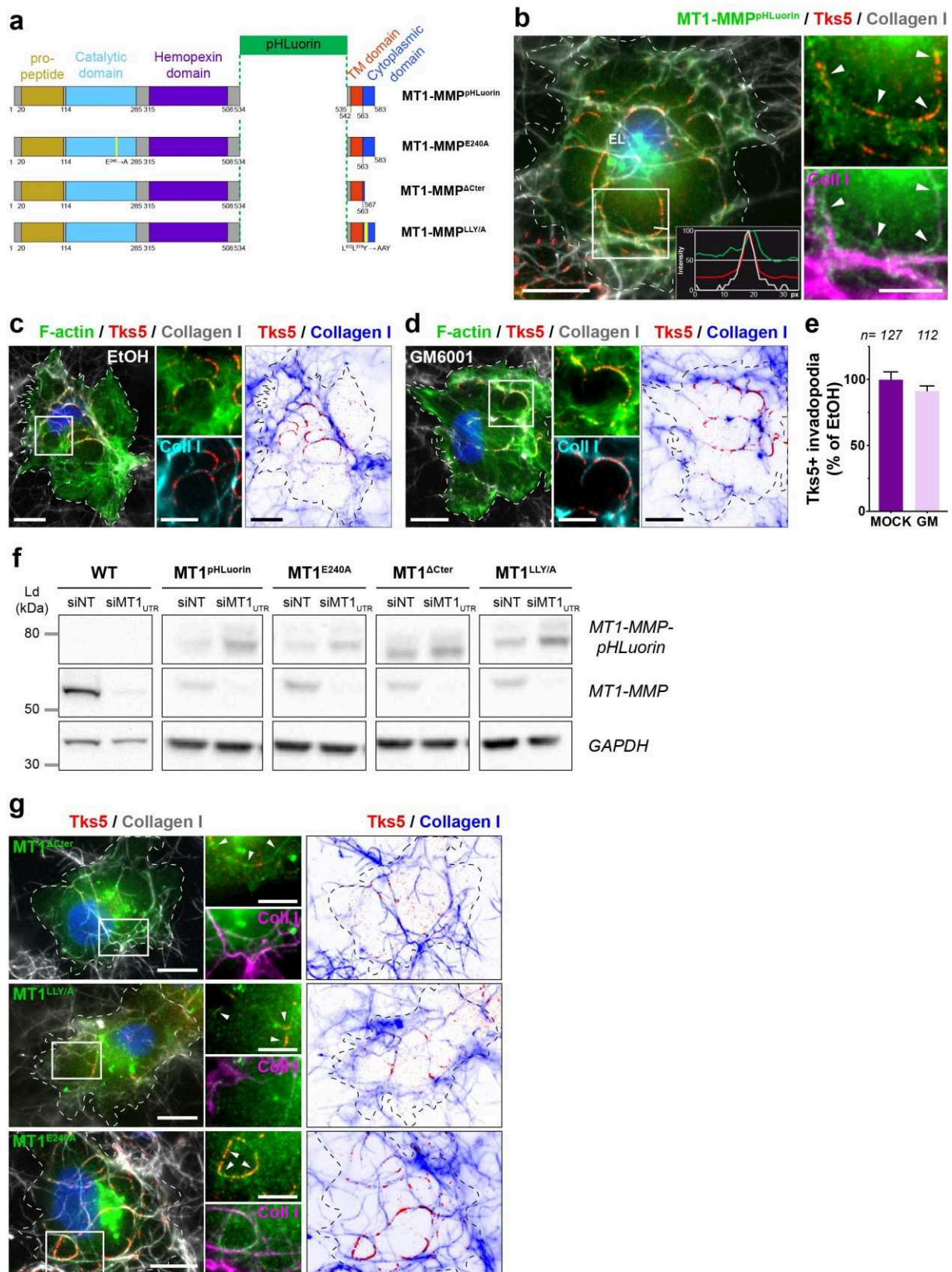
(a) MDA-MB-231 cells cultured on top of type I collagen (gray) were stained for Cortactin (green), N-WASP (red) and DAPI (blue). Normalized fluorescence intensity profiles along the white line are showed in the inset. Cell contour is shown. Scale bar, 10 μ m. Zoom-in of boxed region, scale bar, 5 μ m. (b) MDA-MB-231 cells expressing Tks5^{GFP} (green) cultured on a thin

collagen layer (gray) were stained for GFP (green), cleaved collagen neo-epitope (Col1- $\frac{3}{4}$ C, red) and DAPI (blue). Fluorescence intensity profiles along the white line are showed in the inset. Scale bar, 10 μ m. **(c)** Same as in (b) in GM6001-treated cells (40 μ M). **(d)** MDA-MB-231 cells expressing ARPC5^{GFP} were cultured on a layer of type I collagen (gray) and stained for GFP (green), Tks5 (red) and DAPI (blue) with lower panels showing separated channels. Normalized fluorescence intensity profiles along the white line are shown in the inset. Scale bar, 10 μ m; 5 μ m in zoom-in. **(e)** MDA-MB-231 cells silenced for Tks5 were plated on a layer of type I collagen (gray) and stained for F-actin (green), Tks5 (red) and DAPI (blue). Lower panels show separated channels. Intensity profiles along the white line are shown in the inset. **(f)** Same image using inverted lookup tables (collagen fibers in blue, Tks5-positive invadopodia in red). Scale bar; 10 μ m. **(g)** Pericellular collagenolysis by MDA-MB-231 cells treated with indicated siRNA measured as mean intensity of Col1- $\frac{3}{4}$ C signal per cell. Values for siNT-treated cells were set to 100%. n, number of cells analyzed from 3 independent experiments. Kruskal-Wallis test. **(h)** Enlarged PREM images of the cytoplasmic plasma membrane surface of unroofed MDA-MB-231 cells silenced for Tks5 and plated on type I collagen. Collagen fibers are pseudocolored magenta in the left-side image. Boxed region corresponds to zoom-in image in Figure 1g. Scale bars, 2 μ m.



RF_SUPPLEMENTARY FIGURE2

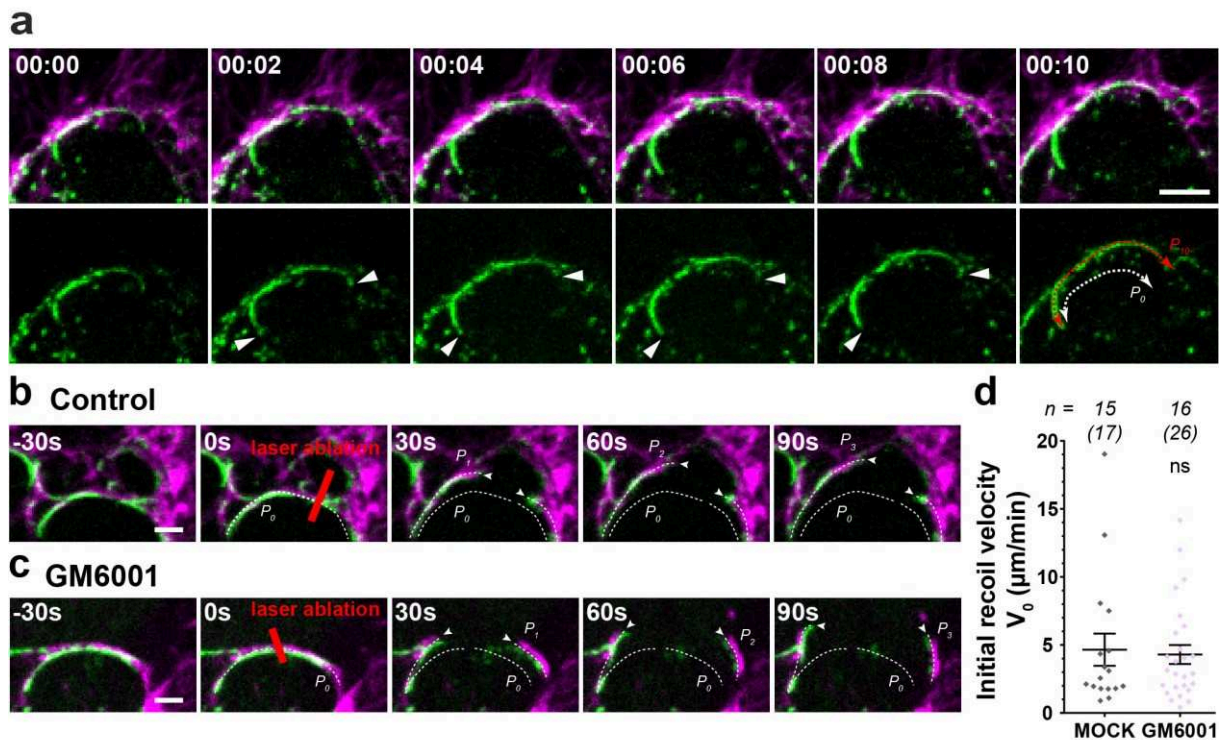
Supplementary Figure 2. DDR1 and integrin β 1 collagen receptors are not required for invadopodia formation (supplementary figure to Figure 1). (a) Representative immunoblotting analysis of integrin β 1 expression with GAPDH as loading control in MDA-MB-231 cells treated with non-targeting or integrin β 1 siRNA. (b) qPCR analysis of DDR1 mRNA expression in MDA-MB-231 cells treated with non-targeting or DDR1 siRNA. Y-axis indicates DDR1 expression normalized to mean value of siNT-treated cells (as percentage \pm SEM). (c) MDA-MB-231 cells treated with indicated siRNA were plated on a layer of type I collagen (gray) and stained for cortactin (green), Tks5 (red) and DAPI (blue). Right panels are zoom-in of the boxed regions showing separated channels. Scale bar: 10 μ m (5 μ m in zoom-in middle rows). (d) Quantification of Tks5-positive invadopodia in MDA-MB-231 cells treated with indicated siRNA plated on type I collagen. Y-axis indicates ratio of the Tks5 area to total cell area normalized to mean value of siNT-treated cells (as percentage \pm SEM). Kruskal-Wallis test. n: number of cells; (n): number of independent experiments. (e) qPCR analysis of DDR1 (top) and MT1-MMP (bottom) mRNA expression in MCF10DCIS.com cells treated with indicated siRNAs. Y-axis indicates DDR1 or MT1-MMP expression normalized to mean value of siNT-treated cells (as percentage \pm SEM). (f) MCF10DCIS.com cells treated with indicated siRNAs were plated on a layer of type I collagen (gray) and stained for F-actin (green), Tks5 (red) and DAPI (blue). Lower panels are zoom-in of the boxed regions showing separated channels. Scale bar: 10 μ m (5 μ m in zoom-in middle rows). (g) Quantification of Tks5-positive invadopodia in MCF10DCIS.com cells treated with indicated siRNA plated on type I collagen. Y-axis indicates ratio of Tks5 area to total cell area normalized to mean value of siNT-treated cells (as percentage \pm SEM). Kruskal-Wallis test. n: number of cells; (n): number of independent experiments.



SUPPLEMENTARY FIGURE 3

Supplementary Figure 3. MT1-MMP is the collagen receptor triggering invadopodia formation (supplementary figure to Figure 1). (a) Schematic representation of MT1-MMP^{pHLuorin} constructs used in rescue experiments. The different protein domains are colored and site of pHLuorin insertion is depicted. Constructs with E240/A mutation in the catalytic domain, cytoplasmic tail deletion Δ Cter (no C-terminus domain) and LLY/A mutation are shown with MT1-MMP amino acid numbering. (b) MDA-MB-231 cells expressing MT1-MMP^{pHLuorin} were cultured on a layer of type I collagen (gray), stained for GFP (green), Tks5 (red) and DAPI (blue). Right panels are zoom-in of the boxed region with separated channels. Full arrowheads point to surface MT1-MMP-pHLuorin associating with Tks5-positive invadopodia. Normalized fluorescence intensity profiles along the white line are shown in the inset. EL, perinuclear endolysosomes positive for MT1-MMP^{pHLuorin}. Cell contour is shown. Scale bar, 10 μ m; 5 μ m in zoom-in. (c, d) MDA-MB-231 cells mock-treated with ethanol vehicle (EtOH, panel c) or treated with GM6001 (40 μ M, panel d) were plated on a layer of type I collagen (gray) and stained for F-actin (green), Tks5 (red) and DAPI (blue). Middle rows are zoom-in of the boxed regions showing separated channels. Right rows are inverted lookup tables (collagen fibers in blue, Tks5-positive invadopodia in red). Scale bar: 10 μ m (5 μ m in zoom-in middle rows). (e) Quantification of Tks5-positive invadopodia in MDA-MB-231 mock- (EtOH) or GM-treated cells plated on type I collagen. Y-axis indicates ratio of Tks5 area to total cell area normalized to mean value of Mock-treated cells (as percentage \pm SEM). n number of cells analyzed from 3 independent experiments. Mann-Whitney test. (f) Cells were treated with siRNA against MT1-MMP 3' and 5' UTR sequences (siMT1_{UTR}, see Table S3) and transfected with indicated MT1-MMP^{pHLuorin} rescue constructs. Representative immunoblotting analysis of endogenous and pHLuorin-tagged MT1-MMP expression with GAPDH as loading control. (g) Cells treated with siMT1_{UTR} siRNAs and transfected with the indicated rescue constructs were plated on a layer of collagen (grey) and stained for F-actin

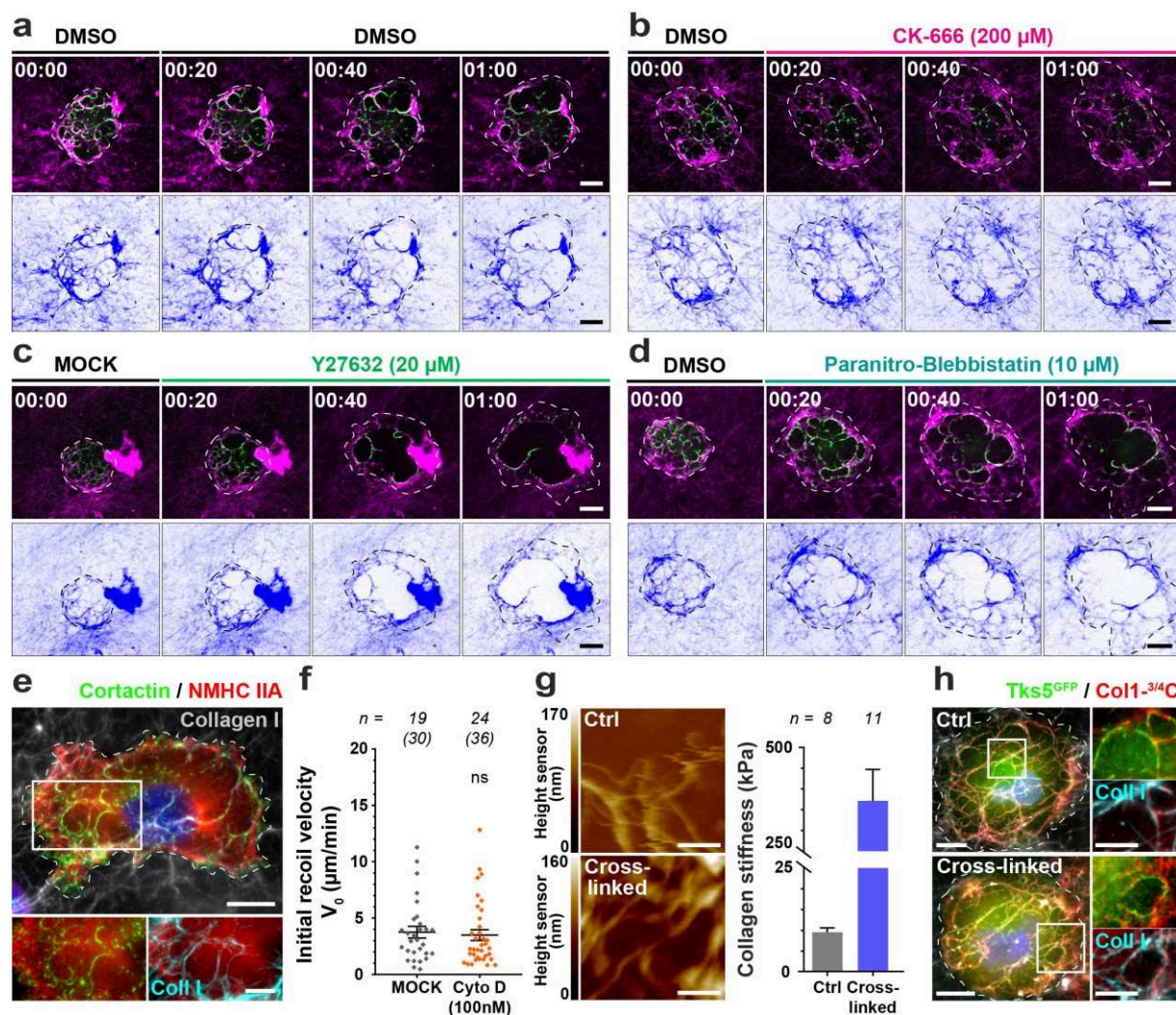
(green), Tks5 (red) and DAPI (blue). Middle panels are zoom-in of the boxed region with separated channels. Full arrowheads point to surface MT1-MMP-pHLuorin constructs associating with collagen fibers and/or Tks5-positive invadopodia. Right rows are inverted lookup tables (collagen fibers in blue, Tks5-positive invadopodia in red). Scale bars, 10 μm .



SUPPLEMENTARY FIGURE 4

Supplementary Figure 4. Force production is independent of MT1-MMP collagenolytic activity (supplementary figure to Figure 2). (a) Gallery of non-consecutive frames (time in hr:min) of a time-lapse sequence of MDA-MB-231 cells expressing Tks5^{GFP} (green) plated on top of type I collagen (magenta). Invadopodia elongation along the associated collagen fiber is indicated by arrowheads. Invadopodia length is indicated at time 0 and after 10 min with white and red dashed lines, respectively. Scale bar, 5 μm . (b-c) Galleries of nonconsecutive images showing Tks5^{GFP}-positive invadopodia in mock- (b) or GM6001-treated cells (c) overtime (see Movies 5 and 6). Laser ablation was performed at time 0 with the region of photo-ablation depicted in red. The position of the invadopodia tips after rupture is indicated with white arrowheads. The initial position of the invadopodia/collagen fiber ensemble (P_0) and positions after rupture (P_i) are indicated with dashed lines. Time is indicated in s. Scale bar, 2 μm . (d) Quantification of invadopodia initial recoil velocity after laser-induced rupture ablation in Mock- or GM-treated cells. The initial recoil velocity reflects the tension stored in the structure

prior rupture. Data are mean \pm SEM of 3 independent experiments. n, number of cells analyzed, (n) number of invadopodia. Mann-Whitney test.



SUPPLEMENTARY FIGURE 5

Supplementary Figure 5. Branched actin polymerization, not actomyosin activity is required for invadopodia force production (supplementary figure to Figure 3). (a-d) MDA-MB-231 cells expressing Tks5^{GFP} (green) were plated on a thin layer of type I collagen (magenta) and imaged overtime. Indicated drugs were added 15 min after starting the time-lapse. Non-consecutive frames from representative time sequences (see Movies 7 to 9) from three independent experiments are shown (time in hr:min). The collagen gel is shown in the bottom row using an inverted lookup table (collagen fibers pseudocolored blue). Scale bar; 10 μ m. (e) MDA-MB-231 cells cultured on a type I collagen layer (gray) were stained for Cortactin (green) to label invadopodia and non-muscle heavy chain of Myosin IIA (MHCIIA, red) and

DAPI (blue). Bottom panels are zoom-in of the boxed region with separated channels. **(f)** Quantification of invadopodia initial recoil velocity after laser-induced rupture in Mock- or CytoD-treated cells. Data are mean \pm SEM of 3 independent experiments. n, number of cells; (n) number of. Mann-Whitney test. **(g)** Quantification of collagen fiber stiffness in control or crosslinked (paraformaldehyde) collagen gels. Left panels are color-coded AFM height images of control and crosslinked collagens. Color-code scale is indicated. Scale bar: 1 μ m. Right panel shows Young's modulus determined for control and crosslinked collagen. Data are mean \pm SEM of 1 experiment. n, number of regions where stiffness was measured.

Supplementary Table 1. Experimental variables measured in this study.

Variable's name	Value (unit)	SEM	P-value	n (N)	Expt	Related Figure
<i>Tks5+ invadopodia (%)</i>						
siNT	100	4.3	-	250	3	Fig. 1j
siMT1	29.4	2.3	<0.0001	234	3	
siNT+MT1-MMP	100	6.6	-	117	4	
siMT1+MT1-MMP	109.5	8.0	0.7 (ns)	133	4	
siNT+MT1-MMP ^{ΔC}	100	7.0	-	109	4	
siMT1+MT1-MMP ^{ΔC}	43.65	4.1	<0.0001	134	4	
siNT+MT1-MMP ^{LLY/A}	100	5.6	-	107	3	
siMT1+MT1- MMP ^{LLY/A}	55.66	4.1	<0.0001	97	3	
<i>3D invadopodia diameter growth rate (μm/min)</i>						
	0.09	0.008	-	33 (64)	3	See text
<i>Invadopodia elongation rate (μm/min)</i>						
MOCK	0.15	0.02	-	14 (180)	3	Fig. 2d
GM6001	0.05	0.008	<0.0001	23 (247)	3	
<i>Invadopodia radial expansion rate (μm/min)</i>						
MOCK	0.16	0.02	-	16 (29)	3	Fig. 2e
GM6001	0.05	0.005	<0.0001	19 (35)	3	
<i>Invadopodia lifetime (min)</i>	41	1.7	-	34 (236)	2	See text
<i>Lifetime after rupture (min)</i>	8.6	0.9	-	16 (59)	3	See text
<i>Initial recoil velocity after rupture (μm/min)</i>	3.1	0.22	-	33 (85)	3	Fig. 2h
<i>Rupture index</i>						
MOCK	1.5	0.6	-	20 (42)	3	Fig. 2f
GM6001	0.4	0.1	0.007	22 (14)	3	
<i>Initial recoil velocity after laser ablation (μm/min)</i>						
MOCK	4.7	1.2	-	15 (17)	3	Fig. 2k
GM6001	4.3	0.7	0.9 (ns)	16 (26)	3	
<i>Invadopodia elongation rate (μm/min)</i>						
MOCK	0.12	0.008	-	60 (613)	8	Fig. 3h
Cytochalasin D (0.5 μM)	-0.15	0.01	<0.0001	17 (221)	3	
CK-666	-0.006	0.02	<0.0001	23 (190)	3	
Paranitro-blebbistatin	0.19	0.03	0.2 (ns)	22 (144)	2	
MOCK	0.14	0.03	-	18 (219)	3	
Y27632	0.18	0.01	0.8 (ns)	18 (129)	2	
<i>Initial recoil velocity after laser ablation (μm/min)</i>						
MOCK	3.7	0.5	-	19 (30)	3	Fig. 3i
Cytochalasin D (100 nM)	3.5	0.5	0.4 (ns)	24 (36)	3	

<i>Invadopodia elongation rate (μm/min)</i>						
MOCK	0.14	0.01	-	18 (219)	3	Fig. 31
Crosslinked collagen (4% PFA)	0.02	0.005	<0.0001	23 (372)	3	

N, number of cells; n, number of invadopodia.

Supplementary Table S2. siRNAs used in this study.

Gene targeted	Company	Reference	Type	Targeted Sequence
DDR1	Dharmacon	J-003111-12-0002	Pool of 2 individuals	5'-GGGACACCCUUUGCUGGUA-3'
		J-003111-15-0002		5'-AAGAGGAGCUGACGCUUCA-3'
ITGB1 (Integrin β1)	Dharmacon	L-004506-00-0005	Smartpool	5'-GUGCAGAGCCUUCAAUAAA-3'
				5'-GGUAGAAAGUCGGGACAAA-3'
				5'-UGAUAGAUCCAAUGGCUUA-3'
MMP14 (siMT1)	Dharmacon	L-004145-00-0005	Smartpool	5'-GGAUGGACACGGAGAAUUU-3'
				5'-GGAAACAAGUACUACCGUU-3'
				5'-GGUCUCAA AUGGCAACAUA-3'
				5'-GAUCAAGGCCAAUGUUCGA-3'
SH3PXD2A (siTKS5)	Dharmacon	L-006657-00-0005	Smartpool	5'-ACAAUAACCUCAAAGAUGU-3'
				5'-GGACGUAGCUGUGAAGAGA-3'
				5'-CGACGGAACUCCUCCUUUA-3'
				5'-GGAUAAGUUUCCCAUUGAA-3'
MMP14 (siMT1 _{UTR})	Qiagen	SI00071169	Pool of 3 siRNAs	5'-CACAAGGACUUUGCCUCUGAA-3'
		SI05042569		5'-CCCUCAGACCUCGCUGGUAAA-3'
		SI00071190		5'-GACAGCGGUCUAGGAAUUCAA-3'
Non-Targeting (NT)	Dharmacon	D-001810-01-05	Individual	5'-UGGUUUACAUGUCGACUAA-3'

Supplementary Table 3. Commercial antibodies used for this study

Antigen	Company	Reference	Assay	Dilution
Tks5	Novus Biological	NBP1-90454	IF	1/200
			WB	1/500
MT1-MMP	Millipore	3328	WB	1/1000
GAPDH	SantaCruz Biotechnology	sc-25778	WB	1/10000
Coll-3/4C	ImmunoGlobe GmbH	0217-050	IF	1/100
p34 (ARPC2B – Arp2/3 complex)	Millipore	07-227	IF	1/50
p16 (clone 323H3 – Arp2/3 complex)	SYSY company	305 011	IF	1/300
Cortactin	Millipore	05-180	IF	1/200
N-WASP	Cell signaling	4848S	IF	1/100
GFP	Abcam	ab13970	IF	1/2000
	Abcam	ab6556	IF	1/1000
Integrin β 1	Provided by C. Albiges-Rizo, IAB, Grenoble, France	NA	WB	1/500
Myosin II	Covance	PRB-440P	IF	1/500
IgG-mouse-Cy5	Invitrogen	A31571	IF	1/500
IgG-mouse-Cy3	Jackson ImmunoResearch	715-165-151	IF	1/500
IgG-mouse-A488	Molecular Probes	A21202	IF	1/500
IgG-mouse-Hrp	Jackson ImmunoResearch	115-035-062	WB	1/20000
IgG-rabbit-A488	Molecular Probes	A11034	IF	1/200
IgG-rabbit-Cy3	Jackson ImmunoResearch	711-165-152	IF	1/800
IgG-rabbit-Hrp	Jackson ImmunoResearch	111-035-045	WB	1/10000
IgG-rabbit-A488	Life Technologies	A11039	IF	1/300
Alexa Fluor 488 phalloidin	Molecular Probes	A12379	IF	1/400
Alexa Fluor 546 phalloidin	Molecular Probes	A22283	IF	1/200

Supplementary Table 4. Chemical reagents used in this study.

Reagent	Company	Reference	Vehicle	Concentration
paranitro-Blebbistatin	Optopharma	DR-N-111	DMSO	10 μ M
Y27632	Merck	688000	Water	20 μ M
Cytochalasin D	Merck (Sigma-aldrich)	C8273	DMSO	0.1 to 0.5 μ M
CK-666	Merck (Sigma-aldrich)	SML0006	DMSO	200 μ M
GM6001	Merck (Millipore)	CC1100	Ethanol	40 μ M
Hepatocyte growth factor (HGF)	PeproTech Inc.		Medium	20 ng/ml

Supplementary Movie 1. Ring-like Tks5-positive invadopodia during 3D collagen invasion. MDA-MB-231 cells expressing Tks5^{GFP} (green) were embedded in 3D fibrillar collagen-I (magenta) and analyzed by confocal spinning-disk microscopy. Images were taken every 10 min during 15 hr (time is in hr:min). Representative movie from three independent experiments. Asterisk: position of cell nucleus. Scale bar, 10 μ m.

Supplementary Movie 2. Collagenolytic invadopodia grow overtime and push collagen fibers away. MDA-MB-231 cells expressing Tks5^{GFP} (green) were plated on top of a thin type I collagen layer (magenta) and analyzed by confocal spinning-disk microscopy. Images were taken every min during 1 hr (time is in hr:min). Representative movie from three independent experiments. Asterisk: position of an unlabeled cell in the field. Scale bar, 10 μ m.

Supplementary Movie 3. Collagenolytic rupture of invadopodia/collagen fiber ensemble reveals typical visco-elastic movement. MDA-MB-231 cells expressing Tks5^{GFP} (green) were plated on top of a thin type I collagen layer (magenta) and analyzed by confocal spinning-disk microscopy. Boxed regions and corresponding insets document invadopodia/collagen fiber rupture events (pointed by red arrowheads) in separated channels. Images were taken every min during 1 hr (time is in hr:min). Representative movie from three independent experiments. Scale bar, 10 μ m.

Supplementary Movie 4. Inhibition of MMP proteolytic activity inhibits invadopodia expansion and elongation. MDA-MB-231 cells expressing Tks5^{GFP} (green) were treated with MMP-inhibitor GM6001 (40 μ M) and plated on top of a thin type I collagen layer (magenta) before analysis by confocal spinning-disk microscopy. Images were taken every min during 1 hr (time is in hr:min). Representative movie from three independent experiments. Asterisk: position of a cell with low Tks5^{GFP} expression in the field. Scale bar, 10 μ m.

Supplementary Movie 5. Laser-mediated rupture of invadopodia/collagen fiber ensemble. MDA-MB-231 cells expressing Tks5^{GFP} (green) Mock- or GM6001-treated (40 μ M) were

plated on top of a thin type I collagen layer (magenta) and analyzed by confocal spinning-disk microscopy. Photo-ablation was performed along the region shown in red. Images were taken every 15 s (time is in hr:min:s). Representative movie from three independent experiments. Scale bar: 5 μ m.

Supplementary Movie 6. Invadopodia force generation requires actin polymerization.

MDA-MB-231 cells expressing Tks5^{GFP} (green) were plated on top of a thin type I collagen layer (magenta) in DMSO-treated medium and analyzed by confocal spinning-disk microscopy. Cytochalasin D (0.5 μ M) was added 15 min after starting the time-lapse. Images were taken every min during 1 hr (time is in hr:min). Representative movie from three independent experiments. Scale bar, 10 μ m.

Supplementary Movie 7. Arp2/3 complex function is required for invadopodia-based force generation.

MDA-MB-231 cells expressing Tks5^{GFP} (green) were plated on top of a thin type I collagen layer (magenta) in DMSO-treated medium and analyzed by confocal spinning-disk microscopy. CK-666 (200 μ M) was added 15 min after starting the time-lapse. Images were taken every min during 1 hr (time is in hr:min). Representative movie from three independent experiments. Scale bar, 10 μ m.

Supplementary Movie 8. Invadopodia dynamics is not perturbed upon ROCK inhibition.

MDA-MB-231 cells expressing Tks5^{GFP} (green) were plated on top of a thin type I collagen layer (magenta) in complete medium and analyzed by confocal spinning-disk microscopy. Y27632 (20 μ M) was added 15 min after starting the time-lapse. Images were taken every min during 1 hr (time is in hr:min). Representative movie from three independent experiments. Scale bar, 10 μ m.

Supplementary Movie 9. Myosin II inhibition by blebbistatin does not affect invadopodia dynamics.

MDA-MB-231 cells expressing Tks5^{GFP} (green) were plated on top of a thin type I collagen layer (magenta) in DMSO-treated medium and analyzed by confocal spinning-disk

microscopy. Paranitro-Blebbistatin (10 μ M) was added 15 min after starting the time-lapse. Images were taken every min during 1 hr (time is in hr:min). Representative movie from three independent experiments. Scale bar, 10 μ m.

Supplementary Movie 10. Collagen crosslinking impairs invadopodia expansion. MDA-MB-231 cells expressing Tks5^{GFP} (green) were plated on top of a chemically (4% PFA) crosslinked type I collagen layer (magenta) and analyzed by confocal spinning-disk microscopy. Images were taken every min during 1 hr (time is in hr:min). Representative movie from three independent experiments. Asterisk: position of a cell with low Tks5^{GFP} expression in the field. Scale bar, 10 μ m.

Supplementary model to "Tumor cell invasion in fibrillar collagen
I is mediated by MT1-MMP-based force-producing proteolytic
contacts", by Ferrari et al.

I. MODEL HYPOTHESIS

We consider an ECM fiber in contact with the plasma membrane of a cell. Assuming in a first approximation small deformations of the fiber, we focus on in plane deformations. We denote by L the contact length and R the mean radius of curvature of the fiber. Following experimental results, we assume that actin nucleators are recruited at the membrane along the contact line with the ECM fiber, and trigger the polymerisation of an actin meshwork inwards in the cell at speed v_p . This actin meshwork can reach a steady state thickness d because of actin depolymerisation; this thickness can be estimated as $d = v_p/k_d$, where k_d is the actin depolymerisation rate. Following classical arguments of active gel theory [1–3], which provides a coarse grained description of actin meshworks, we describe at steady state the actin layer as a fluid of viscosity η , and we neglect actin/solvent friction forces in front of shear forces in the meshwork. We show below that curvature of the fiber induces a shear stress in the actin meshwork, which induces an outward pointing normal force on the fiber. This reads (per unit length):

$$\gamma \sim \frac{\eta v_p^2 a}{k_d R^2} \equiv \gamma_0 \frac{L^2}{R^2}, \quad (1)$$

where a denote the diameter of the ECM fiber. This normal force can be interpreted as an effective 2-dimensional pressure in the plane of deformation of the fiber, which tends to push the fiber along the out pointing normal; note that it scales as $\propto 1/R^2$ and therefore increases when deformation is increased.

In turn, the deformation of an ECM fiber as an energetic cost, due to the bending elasticity of the fiber. The corresponding bending energy is given by

$$E_b \sim \frac{kTl_p L}{2R^2} \equiv e_0 \frac{L^2}{R^2} \quad (2)$$

where k is the Boltzmann constant, T the temperature, and l_p the persistence length of the ECM fiber.

Last, tension τ in the fiber opposes fiber elongation and therefore deformation. For fiber bundles that are weakly cross-linked, as is expected for ECM fibres in the presence of proteolysis, the response to tension is expected to be viscoelastic ; at long time scales (larger than minutes) that are relevant to experimental observations, we therefore assume that tension is controlled by the viscous elongation of the ECM fiber, which is made possible

by the relative sliding of fibrils. Such expected viscous response in the presence of proteolysis implies in particular that at rest tension can be neglected.

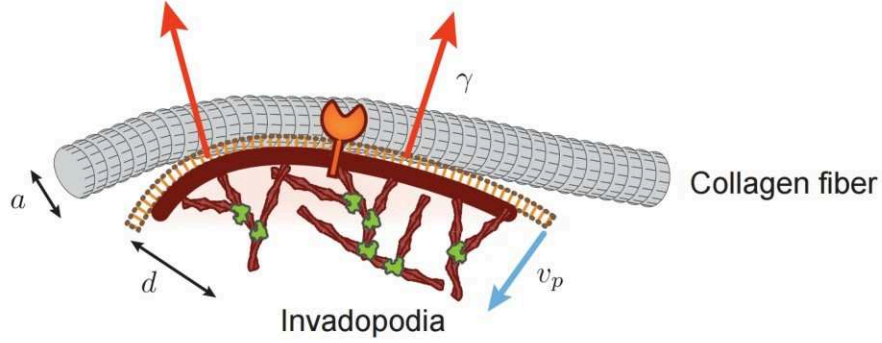


FIG. 1: Sketch of the model and main parameters.

II. EFFECTIVE ENERGY AND POLYMERISATION INDUCED BENDING

To analyse the competition between polymerisation forces, which tend to induce deformation, and bending energy, we assume that the contact length L is fixed and analyse deformations parametrised by R only. A total effective energy E_t can then be defined from $dE_t = dE_b - \gamma dA$, where dA is the area swept by an infinitesimal shape deformation of the fiber. Denoting by $x = L/R$ the normalised curvature, this leads to :

$$E_t/e_0 = x^2 + \alpha (x + \sin(x) - 2\text{Si}(x)), \quad (3)$$

where $\text{Si}(x)$ is the sine integral function. The shape of the effective energy is then critically controlled by the dimensionless parameter

$$\alpha = \frac{\gamma_0 L^2}{2e_0} = \frac{\eta v_p^2 a L}{k_d k T l_p}, \quad (4)$$

as shown in Fig.2 . For $\alpha \lesssim 10$ polymerisation forces are too weak to bend ECM fibers, and the effective energy is minimised for $x = 0$ only. For $\alpha \gtrsim 10$, the effective energy is non monotonic and displays a maximum for a critical curvature x_c and therefore a critical radius R_c . This shows that while the undeformed state ($x = 0$) is stable, beyond a critical deformation x_c , polymerisation forces overcome elastic forces and deform the fiber until it reaches a quasi circular shape. It is found that $R_c \sim \alpha L/10$, which shows that for

large polymerisation activity (α large), any small initial curvature is sufficient to trigger large deformation to a circular shape. Importantly, in the regime of deformation where polymerisation forces overcome elastic forces, force balance on the fiber is still satisfied because of dissipative forces, such as viscous elongation of the fiber described above or viscous drag with the environment. In absence of proteolysis, fiber elongation is limited and tension increases so that only small deformations are possible, even if polymerisation forces overcome elastic bending forces.

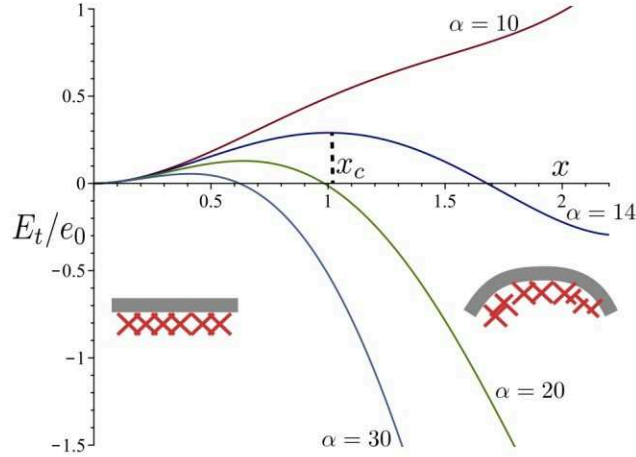


FIG. 2: Normalized effective energy as a function of the normalised curvature $x = L/R$, for different values of the critical parameter α .

III. ORDERS OF MAGNITUDE

The critical parameter α cannot be accurately determined from experiments. Orders of magnitudes can however be inferred from the literature[3, 4]. We take the following estimates: $\eta \sim 10^4$ Pa.s ; $v_p/k_d \sim 1\mu\text{m}$; $v_p \sim 1\mu\text{ms}^{-1}$; $a \sim 0.1\mu\text{m}$; $L \sim 10\mu\text{m}$; $kTl_p \lesssim 10^{-19} \text{ J.m}$. This shows that α can reach typical values of order 10 or larger, so that polymerisation forces are sufficient to bend ECM fibers.

IV. DERIVATION OF THE POLYMERISATION INDUCED FORCE

We consider radial coordinates in the plane of deformations ; the ECM fiber is delimited by the arc $r(\theta) = R$. By symmetry, we denote by $v_r \mathbf{u}_r$ the actin flow field, where \mathbf{u}_r is the

radial unit vector, and we neglect out of plane contributions. Boundary conditions at the ECM-membrane contact impose $v_r(R) = -v_p$; due to depolymerisation, the actin meshwork spans only the $R - d < r < R$ annular region. Force balance at the inner boundary then yields $\sigma_{rr}(R - d) = 0$. Neglecting pressure forces in the meshwork, as classically done [5–7], force balance reduces to

$$0 = \partial_r \sigma_{rr} + \frac{\sigma_{rr} - \sigma_{\theta\theta}}{r}, \quad (5)$$

where the components of the viscous stress tensor are given by $\sigma_{rr} = 2\eta\partial_r v_r$ and $\sigma_{\theta\theta} = 2\eta v_r/r$. This problem can be solved explicitly for the velocity field $v_r(r)$ and yields for the stress at the ECM membrane contact:

$$\sigma_{rr}(R) = -\frac{2\eta v_p}{R} \frac{\left(1 - \frac{(R-d)^2}{R^2}\right)}{\left(1 + \frac{(R-d)^2}{R^2}\right)} \underset{d \ll R}{\sim} -\frac{2\eta v_p d}{R^2}. \quad (6)$$

This yields in turn the force per unit length exerted on the ECM fiber, as given in Eq.(1).

Last, let us comment on force balance on the actin gel, which must be satisfied. In the case of a closed circular fiber, above described normal forces exerted in reaction by the fiber on the actin gel sum to 0 and force balance is satisfied. In the case of a finite arc shaped fiber, boundary conditions are necessary and require external forces at both ends of the fiber to balance the stress $\sigma_{\theta\theta}$; this ensures global force balance on the gel. Such boundary conditions could be due to friction forces of the gel along the fiber, or local interactions with other fibers.

-
- [1] K. Kruse, J. F. Joanny, F. Julicher, J. Prost, and K. Sekimoto, Physical Review Letters **92**, 078101 (2004).
 - [2] K. Kruse, J. F. Joanny, F. Julicher, J. Prost, and K. Sekimoto, European Physical Journal E **16**, 5 (2005).
 - [3] F. Julicher, K. Kruse, J. Prost, and J. F. Joanny, Physics Reports **449**, 3 (2007).
 - [4] A. C. Callan-Jones, J.-F. Joanny, and J. Prost, Physical Review Letters **100**, 258106 (2008).
 - [5] G. Salbreux, J. Prost, and J. F. Joanny, Phys Rev Lett **103**, 058102 (2009).
 - [6] M. Mayer, M. Depken, J. S. Bois, F. Jülicher, and S. W. Grill, Nature **467**, 617 (2010).
 - [7] V. Ruprecht, S. Wieser, A. Callan-Jones, M. Smutny, H. Morita, K. Sako, V. Barone, M. Ritsch-Marte, M. Sixt, R. Voituriez, et al., Cell **160**, 673 (2015).

Conclusions and discussion

1. Cancer cells engage MT1-MMP-based matrix proteolysis on-demand during confined migration

Over the last few years, several studies demonstrated that the stiffness and the deformability of cancer cells biggest organelle, the nucleus, were critical rate-limiting factors in cell migration. Accordingly, the mechanisms by which cancer cells deal with nuclear transmigration into narrow spaces encountered during invasion through adjacent tissues have drawn an increasing attention. Interactions of the nucleus with the cell cytoskeleton, which allow force transmission to the nucleus and determine its position, also strongly impacts cell migration. Our results reveal a novel “digest-on-demand” strategy used by invasive cancer cells to adapt to nucleus-confining 3D matrix environment (see **Article 1**, Infante et al., 2018). This adaptative response hinges on a strong polarization of cancer cells proteolytic machinery, composed of MT1-MMP-positive vesicles and invadopodia structures, in front of the nucleus in the direction of migration to proteolytically dissolve ECM fibers opposing to cell movement. This mechanism requires an intact link between the nucleus and the microtubules-centrosome system mediated by Nesprin-2 from the LINC complex and the dynein adaptor Lis1. Disruption of this connection impaired MT1-MMP endosomes polarization and invadopodia formation, thus affecting cell invasion. Altogether, our observations suggest that dynein motors located at the NE pulls the nucleus forward along microtubules and therefore contributes to nuclear deformation as a consequence of passive resistance opposed by constricting ECM fibers to cell movement (see **Figure 22**). A detailed discussion of the working model we proposed and its contribution to the current knowledge on cancer cell invasion is reported in a forum TiCB article presented in the **Annexe** section (Ferrari et al., 2019).

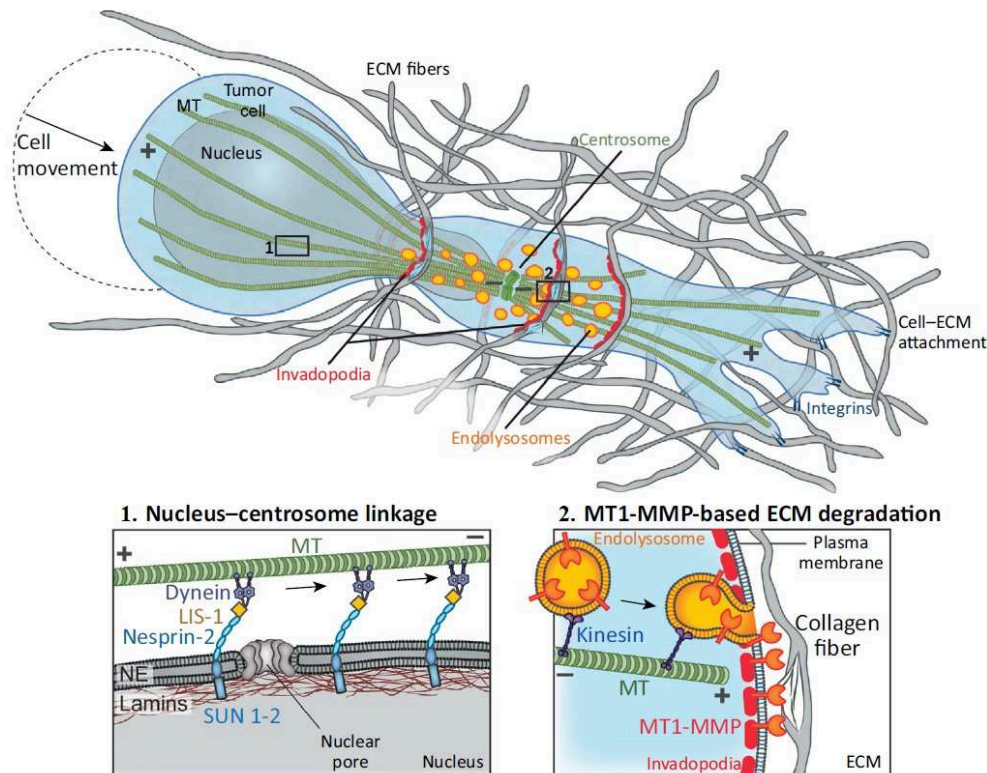


Figure 23: Model of invadopodia-, MT1-MMP-based matrix digest-on-demand response triggered by nuclear confinement during cancer invasion

During tumor cell invasion, nucleus movement is mediated by nucleus–MTs/centrosome linkage and nucleus frontward pulling by LINC complex interacting with dynein–Lis1 molecular motor (1). Confined migration through the dense 3D collagen network results in mechanical constraints applied on the nucleus by constricting matrix fibrils. Polarization of MT1-MMP-positive endosomes in front of the nucleus allow targeted delivery of MT1-MMP to invadopodia (2). Nucleus movement is then facilitated by localized invadopodia-based pericellular proteolysis of confining fibrils ahead of the nucleus. (1) Scheme of nucleus–cytoskeletal linkage through LINC complex components nesprin and SUN in association with lamins. Lis1 in complex with dynein associates to the NE depending on Nesprin-2 and is involved in nucleus–microtubule linkage and nucleus pulling. (2) Model of polarized surface-delivery of MT1-MMP from recycling endolysosomes. ECM, Extracellular matrix; LINC, linker of nucleoskeleton and cytoskeleton; MT, microtubule; NE, nuclear envelope.

Scheme based on Ferrari et al., Trends Cell Biol. (2019) 29(2), 93-96.

2. Mechanical nuclear stresses and their consequences in cancer cell invasion

Albeit this work and several converging studies point out the role of the nucleus in sensing mechanical constraints exerted by the surrounding environment, they also raise important questions in regard to the molecular mechanisms and the biological consequences of this mechanosensing (Cho et al., 2017; Graham and Burrridge, 2016).

2.1. *Mechanisms of nuclear deformation during migration*

As previously mentioned, the transmission of different mechanical stimuli to the nucleus involves well-described molecular components including cell cytoskeleton and the LINC

complex. In our model, the nucleus experiences pulling forces arising from dynein/dynactin activity at the nuclear surface along microtubules and counter-resistance forces from the matrix scaffold. If the latter is certainly conserved across different cell migration modes and only depends on ECM composition and mechanical properties, additional internal mechanisms based on perinuclear actin and actomyosin structures interacting with the LINC complex have been associated with nuclear deformation in invasive cells. Actomyosin-based contractile forces and actin polymerization applied on the NE enable the nucleus to squeeze through narrow spaces therefore promoting cell invasion in tissues (Lammerding and Wolf, 2016; Thiam et al., 2016; Thomas et al., 2015). Anterior actomyosin contractility can also use the nucleus as a piston to support 3D confined migration by increasing frontward hydrostatic pressure (Petrie et al., 2017, 2014). Even though this mechanism has been recently reported as an adaptation of cancer cells to low MMP activity, whether higher pressure in front of the nucleus could induce MT1-MMP-positive endo-lysosomes frontward polarization is an interesting possibility to explore. Further work will be needed to determine how cancer cells integrate and potentially switch between these different mechanisms as well as their biological relevance in metastasis.

2.2. Nuclear mechanosensing during 3D migration

Downstream signalling cascades by which the nucleus integrates and transforms physical tension into biologically relevant signals within the nucleoplasm remain largely unknown. Most of the mechanisms that have been proposed involve the regulation of genes expression mediated by changes in chromatin organization or activation of transcription factors among others (Fedorchak et al., 2014). In the context of confined migration however, engagement of cellular pools of MT1-MMP-positive vesicles or formation of invadopodia structures are rapid responses most likely incompatible with *de novo* protein synthesis time-scale. Several recent studies have revealed novel signalling pathways implicated in nucleus mechanosensing including phosphorylation as well as conformational changes of nuclear proteins such as lamins or emerin, while modulation of nuclear pore complexes activity and therefore cytoplasm-nucleus exchanges may also be involved (Buxboim et al., 2014; Cho et al., 2017; Guilluy et al., 2014; Ihalaenen et al., 2015). Future work will be needed to assess whether and how these pathways contribute in nuclear responses to physical tension particularly during migration. Alternatively, we can speculate that increased tension in the microtubule network due to dynein motor activity could in itself regulate invadopodia formation as microtubules may regulate stiffness-sensitive migration by affecting actin-based protrusion dynamics as recently reported (Prah et al., 2018).

Additionally, the microtubule-centrosome-nucleus axis has recently been proposed to determine the path of least resistance (*i.e.* with larger pore size) during confined migration in ameboid dendritic cells with the nucleus front positioning serving as a mechanical sensor (Renkawitz et al., 2019). Although the molecular mechanisms underlying nuclear mechanical guidance in dendritic cells remain to be determined, it presumably dispenses cells to use matrix proteolysis or at least promote cell migration under low proteolytic activity regime. By contrast, mesenchymal-type cells display a strong polarization of the centrosome-microtubule system in the front that is required for directed cell migration (Infante et al., 2018; Prentice-Mott et al., 2016; Zhang et al., 2014). This mesenchymal centrosome and cell-body-first configuration may not allow sampling for larger pore size, but is likely to support the pericellular proteolysis path-generating strategy we observed as an alternative strategy (Infante et al., 2018).

2.3. NE integrity during confined migration and role of MT1-MMP

Recent reports have shown that mechanical stress applied on the nucleus during migration in confining environments can result in loss of NE integrity as a consequence of extensive nuclear deformations (Denais et al., 2016; Irianto et al., 2017a; Pfeifer et al., 2018; Raab et al., 2016). Transient NE ruptures cause uncontrolled bi-directional exchanges of components from the cytoplasm and the nucleoplasm upon cell migration into sub-micrometric constrictions. It is exemplified by leakage of nuclear NLS (Nuclear localization sequence)-GFP construct into the cytoplasm and entry of cytoplasmic GFP-cGAS (cyclic guanosine monophosphate–adenosinemonophosphate (GMP-AMP) synthase) construct into the nucleus. Although NE ruptures are rapidly repaired by the ESCRT-III complex, accumulation of γ H2AX and 53-BP1-positive nuclear foci, DNA double-strand break marker and DNA damage repair (DDR) machinery component respectively, indicates that DNA damages are generated during constricting migration and induce the DDR response (Denais et al., 2016; Raab et al., 2016). Disruption of both DDR response and NE repair mediated by the ESCRT-III-based machinery strongly correlates with a drop of survival in cells passing through constrictions, while affecting the ESCRT-III complex only slowed down NE resealing (Raab et al., 2016). In accordance with previous reports, depletion of lamins A/C proteins increased cell death during confined migration, which is further enhanced in case of inhibition of NE resealing machinery (Denais et al., 2016; Harada et al., 2014; Raab et al., 2016). The molecular mechanisms mediating DNA damage during constricted cell migration remain unclear. One possibility is that exposure of the nuclear content to cytoplasmic proteins including nucleases may trigger DNA damage by enzymatic reactions (Denais et al., 2016; Raab et al., 2016). A second emerging hypothesis

proposes that leakage of nuclear DNA repair factors away through NE ruptures may delay the DDR response thus increasing accumulation of DNA damage as well as genomic alterations and chromosomal copy-number changes (Irianto et al., 2017a, 2017b). Correspondingly, the consequences of migration-induced DNA damage are a matter of debate and the fact that repetitive NE rupture could contribute to genomic instability, thus representing a mutation-invasion mechanism potentially explaining tumor heterogeneity is a possibility that remains to be tested *in vivo* (Isermann and Lammerding, 2017; Pfeifer et al., 2017).

Interestingly, the occurrence of NE breakages is significantly enhanced upon inhibition of MMP activity in cells migrating into dense collagen (Denais et al., 2016). It is therefore tempting to speculate that MT1-MMP has a protective effect on cells nuclei during confined migration by reducing ECM-mediated mechanical stress. In line with these findings, we and others have shown that treatment with a pharmacological inhibitor of MMPs correlates with increased nuclear deformations in invasive cells (Infante et al., 2018; Wolf et al., 2013). Another evidence of MT1-MMP acting as a functional shield to diminish nuclear constraints came from the study of MT1-MMP-deficient mice that exhibit important changes resulting in increased cell senescence, including modification of cell metabolism and alterations of cell cytoskeleton and nuclear lamina (Gutiérrez-Fernández et al., 2015). Most notably, abnormal nuclear morphology, with herniations and blebs in the nuclear lamina, was observed in fibroblasts of these mice and was associated with increased DNA damage (Gutiérrez-Fernández et al., 2015). However, recent observations in mice with conditional MT1-MMP KO in the mammary gland did not confirm the senescence phenotype in mammary epithelial cell (Feinberg et al., 2018). Possibly, these observations support the idea that ECM proteolysis by MT1-MMP is essential to maintain nucleus and genome integrity in cells. In the context of migration, MT1-MMP may thus play both a pro-invasive role by clearing a path to favor invasion in the dense ECM, and a protectory role to limit ECM-mediated physical assaults to promote DNA damage-free migration and/or cell survival. Additionally, MT1-MMP could serve in response to other stresses including metabolic stress which frequently occurs during cancer progression, and could degrade the ECM scaffold to provide external nutrients to cancer cells in case of low nutrient supply (Olivares et al., 2017; *Colombero and Chavrier, pers. comm.*).

2.4. Mechanical and functional interplay between invadopodia and the nucleus

MT1-MMP-based matrix degradation occurs at specific ECM contact sites termed invadopodia that represent cancer cells degrading units. We observed invadopodia forming in

front of the nucleus in the direction of migration in cells invading dense collagen gels (Infante et al., 2018). Inhibition of dynein/dynactin activity, disruption of the LINC complex or modulation of nuclear stiffness by silencing lamin A/C proteins consistently reduce invadopodia formation along ECM fibers in cells plated on top of a thick fibrillar collagen layer (Infante et al., 2018). It may be questionable whether in this 2.5D system cancer cells experience mechanical constraints from the ECM scaffold but we still observed cells and even sometimes the nucleus squeezing in free interstices between fibrils as well as physical remodeling of the extracellular environment by cells pulling and pushing schemes. Together, these data demonstrate that an intact link between the nucleus and cell cytoskeleton is required for invadopodia formation and suggest that invadopodia is part of the adaptive response of cancer cells to nuclear confinement. However, how mechanical stimuli from the ECM induce invadopodia formation along constricting fibers is unknown and is of great importance to understand the mechanisms of cancer progression and metastasis formation.

Interestingly, a previous study reported no effect on invadopodia formation or function when interfering with the LINC complex by silencing either SUN 1 or Nesprin 2 proteins (Revach et al., 2015). This divergence with our data may be explained by differences in cell types used (melanoma cells versus breast carcinoma and fibrosarcoma cells in our study), and in matrix composition (a stiff 2D denatured collagen or gelatin, in contrast to fibrillar collagen in our study). Hence, whether the nucleus and invadopodia structures are functionally connected in this situation remain to be determined. The authors also documented a direct effect of invadopodia on the structure of the nucleus whereby actin polymerization in invadopodia triggers outward protrusion in the ECM but also actin bundles elongating inward to the nucleus to form nuclear indentations (Revach et al., 2015). They proposed that this mechanism, where the nucleus, serving as a rigid support, exerts counteracting forces that enable invadopodia to generate sufficient ECM penetrating force. Potential mechanisms enabling force production in invadopodia are discussed in more details in subsequent sections.

3. Invadopodia are self-assembling and force-producing proteolytic structures

As part of cancer cells pro-invasive tools allowing ECM degradation and perforation of tissue barriers including basement membranes (BMs), invadopodia have been extensively studied over the last decade. Most of the studies however have been performed on cancer cells plated on 2D gelatin (*i.e.* denatured collagen) as a substrate, which poorly mimic BM and is not comparable to the fibrillar collagen network observed in connective tissues. In this classical

model, invadopodia consists of an F-actin-rich membrane protrusion elongating into the substrate. Even though some studies also observed that, similar to podosomes, the actin core can be surrounded by an adhesive ring containing actomyosin filaments and integrins connected to the substrate, this remains largely debated in the case of invadopodia. Recent work conducted on cancer cells plated on a thin fibrillar collagen layer has led to the discovery of elongated invadopodia forming along collagen fiber and comprising similar core components with classical invadopodia (Juin et al., 2014, 2012; Monteiro et al., 2013). Based on these findings and our immunofluorescence, electron microscopy and live-imaging analysis, we proposed a new paradigm for invadopodia as self-assembling structures that combine actin-driven force generation and matrix-degrading capacities to enlarge pre-existing matrix pores and promote cell and nuclear movement (see **Article 2, Ferrari et al., submitted**). These collagenolytic invadopodia differ from their punctate counterparts in morphology, dynamics, and mechanisms of formation and function.

3.1. Collagen receptors in invadopodia formation

Although several collagen receptors have been proposed to trigger invadopodia formation, with conflicting results, our results indicate that MT1-MMP could be the long-sought initiator of collagenolytic invadopodia formation. We showed that integrins binding to collagen (*i.e.* $\beta 1$ and 3 subunits) are not required for invadopodia formation along collagen fibers (**Ferrari et al., submitted** and **data not shown**) as opposed to invadopodia forming on gelatin but also on high-density fibrillar collagen (Artym et al., 2015; Destaing et al., 2010). This may reflect differences in the composition, topology as well as mechanical properties of the matrix scaffold as gelatin and highly-dense collagen are stiffer than fibrillar collagen. Most unexpected, the DDR1 collagen receptor that has been involved in linear invadopodia formation along collagen fibers, seems to suppress invadopodia formation in the two breast cancer cell lines we tested (Juin et al., 2014; **Ferrari et al., submitted**). Surprisingly, invasive MDA-MB-231 breast cancer cells, in which DDR1 was initially demonstrated as the collagen receptor mediating linear invadopodia formation, expressed extremely low levels of DDR1, as reported by others (Hansen et al., 2006; Takai et al., 2018; Valiathan et al., 2012). A rational explanation for this discrepancy is still lacking and slight differences between collagen polymerization, with very sparse collagen fibers versus a denser collagen layer in our study, or divergences in the cell lines used, could possibly explicate these conflicting results. Furthermore, DDR1 expression has generally been associated with an epithelial phenotype and was shown to decrease upon induction of epithelial to mesenchymal transition in breast cancer cells (Koh et

al., 2015). Finally, DDR1 binds only to fibrillar collagen and not to denatured collagen (*i.e.* gelatin) and thus cannot be involved in the formation of invadopodia on gelatin (Leitinger, 2011). Altogether, these results do not support a prominent role for DDR1 in mediating formation of invadopodia pro-invasive structures. Additional experiments, not shown in our manuscript, further suggest a direct suppressor role for DDR1 in invadopodia formation, as expression of a DDR1-GFP construct in MDA-MB-231 cells triggers a significant reduction of these structures along collagen fibers. Multiple downstream signalling pathways including those of Src kinase, phosphatases such as SHP-1/2, as well as Rho GTPases, have been connected to DDR1 activation, depending or not on its kinase activity (Leitinger, 2014). Interestingly, DDR1 co-localizes with myosin II, is excluded from collagenolytic invadopodia (**Ferrari et al., submitted**), and has been functionally associated with cell contraction, a process we think is antagonist to invadopodia function (**see below** and Huang et al., 2009; Meyer Zum Gottesberge and Hansen, 2014; Staudinger et al., 2013). In addition, a recent report showed that in Mardin–Darby canine kidney (MDCK) cells, DDR1 suppresses Cdc42 activity, an essential component of invadopodia structures that contributes to the activation of actin polymerization (Yeh et al., 2009). How these different mechanisms relate with our findings and others is currently unknown and further experiments are needed to clarify the role of DDR1 in invadopodia formation.

3.2. MT1-MMP in invadopodia: from cover to cover

We showed that MT1-MMP acts both as an initiator, potentially through binding to collagen and as an effector, by its matrix-degrading activity but important questions regarding the precise signalling cascade leading to functional collagenolytic invadopodia are still to be answered. MT1-MMP has a small 20 amino-acid long cytoplasmic tail, with several protein binding and signalling motifs. Most notably a motif composed of two leucine and one tyrosine residues has been shown to be required for both F-actin and AP-2 clathrin adaptor complex binding to the cytoplasmic tail of MT1-MMP (Remacle et al., 2003; Uekita et al., 2001). We further showed that mutation of these two leucine residues into alanine affected the ability of cells to form invadopodia based on detection of Tks5 along collagen fibers. Remarkably, recent observations of a specific alignment of clathrin-coated lattices along matrix fibers were reported in MDA-MB-231 cells plated on collagen (Elkhatib et al., 2017). These structures formed rapidly in contact with collagen fibers mediated by integrin β 1 but declined after 30 to 60 min. The authors concluded that these structures were undergoing “frustrated” endocytosis and predominantly acted in cell adhesion to the matrix during migration. More work is required to

determine whether these AP-2 adaptor complex based structures are involved in invadopodia formation. However, our preliminary results indicate that integrin $\beta 1$ receptor associates with collagen fibers but segregates from Tks5-positive invadopodia; furthermore, AP-2 depletion does not seem to affect the formation of collagenolytic invadopodia (**data not shown**).

Our observation that F-actin-binding to MT1-MMP via the LLY motif is remarkable as actin polymerization is essential for invadopodia formation and activity. Whether this process may compete with AP-2 binding to the same “LL” motif in the MT1-MMP cytosolic tail is unknown but studying the interplay between these two mechanisms may bring important insights into invadopodia formation and regulation (Uekita et al., 2001). Additionally, understanding how the minimal invadopodia actin polymerization module, consisting of Cdc42, N-WASP and Arp2/3 complex can be recruited consequently to MT1-MMP engagement with collagen fibers will be of paramount importance. Unpublished work from Anna Zagryazhskaya-Masson, a postdoc in the lab, who studied the interactome of Tks5 in MDA-MB-231 cells plated on fibrillar collagen demonstrated that Tks5 directly interacts with FGD1, a Cdc42-specific GEF necessary for invadopodia formation and function (**Anna Zagryazhskaya-Masson et al, *in prep.***). She further showed that Tks5 was associated, possibly through its N-terminal PX domain, with PI(3,4)P₂ accumulation along collagen fibers, while PI(4,5)P₂ was not enriched in invadopodia (Abram et al., 2003; Sharma et al., 2013). Therefore, lipid-modifying enzymes, *i.e.* kinases and phosphatases involved in the formation of these phosphoinositides, may also play a critical role in invadopodia formation. Altogether, these results define a model whereby MT1-MMP engagement with collagen fibers and Tks5 recruitment, possibly involving PI(3,4)P₂ production, drives invadopodia formation and actin polymerization. Whether and how these signalling events are coordinated and regulated together are the next steps toward a complete understanding of how cancer cells form invadopodia at matrix contact sites.

By contrast, MT1-MMP does not seem to act as a mediator of podosome formation in non-cancer cells like macrophages, even though studies describing podosomes in normal cells plated on fibrillar collagen are rare. Either way, this all-in-one formula depicting invadopodia as self-assembling structures may be of paramount importance to develop new pharmacological approaches to target cancer cell invasion as solely inhibiting MT1-MMP catalytic activity have been unsuccessful in clinics so far.

3.3. Force production in invadosomes

Another interesting feature of collagenolytic invadopodia based on our findings is their ability to produce forces that are transmitted to the matrix scaffold. Podosomes and

invadopodia, together known as invadosomes, have been assumed to produce forces owing to their membrane protrusive capacity. In addition, several studies have shown that invadosomes are involved in sensing the matrix stiffness potentially through force production, although experimental evidences and more specifically direct measurements of forces produced by these structures were lacking (Albiges-Rizo et al., 2009; Alexander et al., 2008; Parekh and Weaver, 2016; van den Dries et al., 2014). Recently, an original experimental set-up allowed to quantify forces produced by podosomes and applied on the underlying substrate (Labernadie et al., 2014). In this study, the authors plated human macrophages on a thin formvar elastic membrane and measured nanoscale deformations of the membrane by atomic force microscopy to deduct the protrusive forces built by podosomes. Actin polymerization in the podosome core was required for protrusion and therefore force production, as well as actomyosin-based contraction as pharmacological inhibition with cytochalasin D or blebbistatin significantly reduced formvar membrane deformations (Labernadie et al., 2014). The authors further proposed a model whereby actomyosin filaments in the podosome adhesion ring support actin polymerization at the core to generate an outward protrusive force, similar to protrusive forces generated in the lamellipodium at the migration front (Bouissou et al., 2017; Labernadie et al., 2014) (see **Figure 23**). Although providing interesting insights in podosomes force generation, it remains to be proved that this mechanism can be used to perforate more physiological substrates including BMs, and how it fits with the classical protrusive invadopodia as it is not clear whether myosin is present in these structures or not (Alexander et al., 2008).

Contrasting with podosomes in macrophages, myosin II does not localize in invadopodia forming along collagen fibers and actomyosin contractility was not required for invadopodia-based force generation (*Ferrari et al., submitted*). Instead, actin polymerization alone was able to produce enough force to deform and push curved collagen fibers. To our knowledge, collagenolytic invadopodia are the first non-protrusive expanding ring-like actin structures identified to date, since most equivalent structures (*i.e.* actin rings observed during cell division or wound closure) are contractile. With the help of our collaborator S. Vassilopoulos, who generated the first electron microscopy images of the collagenolytic invadopodia, we described, with previously unreachable resolution, the exquisite organization of the invadopodial actin cytoskeleton. Based on this description, we further contacted a theoretician physicist, R. Voituriez, who developed a theoretical model to understand how actin polymerization in invadopodia ring-like structures could isotropically spread away collagen fibers. His model predicts that for any sufficient initial curvature, outward forces generated by shear stress in the polymerizing actin network due to its curvature would overcome matrix fiber elasticity and

further deform the fiber (see **Figure 23**). In other words, due to the curvature of the collagen fiber, the density of actin filaments increases as the distance of the filaments to the plasma membrane/collagen fiber interface increases. As a direct consequence of increased density, friction against each other causes actin filaments to counteract polymerization forces, which ultimately generate a force directed orthogonally toward the matrix fiber. The importance of the topology of both the substrate and the actin network makes this model noticeably different from classical protrusive models, including the lamellipodium. In these, the actin retrograde flow induced by actin polymerization against the plasma membrane is counterbalanced by both contractile actomyosin filaments located just behind the front edge, and focal adhesions (FAs) that serve as a physical anchor to actin filaments. In the end, this generates an outward force leading to membrane deformation and protrusion (Dolati et al., 2018; Prass et al., 2006; Zimmermann et al., 2012).

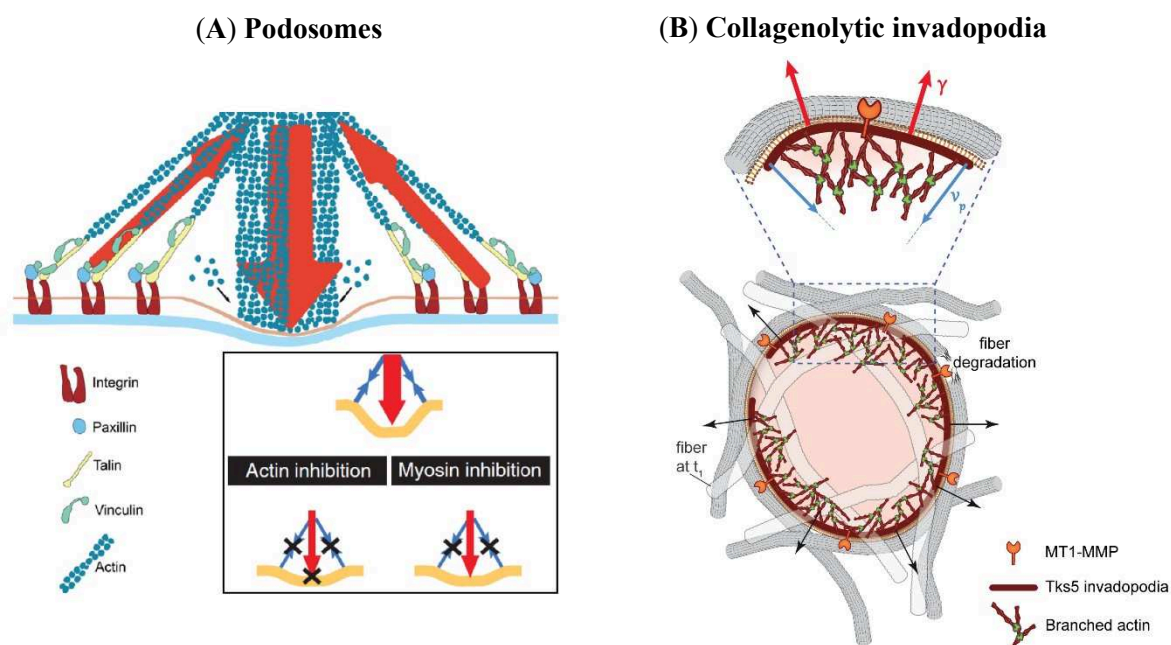


Figure 24: Schematic representation of force production in podosomes and collagenolytic invadopodia

(A) Protein organization and force generation in podosomes. At the core, F-actin polymerization drives protrusion forces against the substrate (central arrow) together with counteracting traction forces in the adhesive ring (lateral arrows), transmitted to the substrate by talin and vincullin. Upon myosin II or actin polymerization inhibition, podosome protrusion forces are diminished, leading to smaller deformations of the substrate.

(B) Surface-exposed MT1-MMP initiates invadopodia formation along collagen fibers during migration. Matrix degradation and force production at invadopodia result in matrix pore enlargement in an acto-myosin independent manner. We proposed a physical model whereby, due to the collagen fiber curvature, inward actin polymerization at invadopodia produced an outward pointing force that can further deform and displace the constricting fiber. The main parameters are depicted: v_p , speed of inward actin polymerization; γ , resulting outward pointing normal force applied on the fiber.

Schemes adapted from Bouissou et al., ASC Nano (2017) 11(4), 4028-40, and Ferrari et al, submitted.

Furthermore, as MT1-MMP both binds to the polymerized actin filament network through its cytoplasmic tail (LLY motif), and to collagen fibers via its hemopexin domain, it can function like a trans-membrane connector between the advancing actin network and the collagen fibers. In a way, this is similar to the donkey and the carrot metaphor where the stick preserves a constant proximity, yet at a certain distance, between the animal and the food (see *Ferrari et al., submitted*). In this sense MT1-MMP could maintain the polymerizing actin network against the collagen fiber and continuously move its activating signals (that remain to be completely determined, see **above**) with the displacement of the matrix fibril. Consequently, it could also explain the rather limited (around 200-300 nm) thickness of the actin network, as activation signals are maintained in contact with the plasma membrane. Finally, MT1-MMP-mediated collagen proteolysis further potentiate force production against matrix fibers presumably by increasing their compliance (*i.e.* diminution of the energy required to bend the fiber). More specifically, to degrade collagen fibers, it is thought that MT1-MMP hemopexin domain first unwind collagen triple helix, before its catalytic domain cleaves it (Chung et al., 2004; Gioia et al., 2007). This activity could also contribute to inter- and intra-fibrils sliding and further explain how actin polymerization at invadopodia could extensively expand collagen matrix pores. In addition, a recent report has shown that collagenolysis is enhanced when collagen fibers are sustaining mechanical load (Adhikari et al., 2011). In our system, this could represent a potential auto-amplificatory loop between actin-based force production and MT1-MMP-mediated collagen proteolysis at invadopodia.

Hence, our results point out that the topology of the matrix scaffold is critical to determine whether forces can be produced at invadopodia or not. This may have important consequences in both invadopodia biology and more generally in our view of how cells produce forces. Additional work will thus be required to decipher whether other cellular force-producing structures can respond to substrate topology and if similar topologies result in comparable effects. Furthermore, it would be fascinating to assess if, similar to what has been shown recently in the lamellipodium, force production by actin polymerization at invadopodia could adapt to the load (*i.e.* matrix compliance in our system) (Mueller et al., 2017). Although we showed that for extremely stiff substrate induced by PFA crosslinking, invadopodia-based force generation cannot compensate matrix rigidity, an intriguing possibility is that it could adapt for more subtle changes.

Additionally, interesting results obtained in *Caenorhabditis elegans* development showed that forces based on actin polymerization at invadosome structures drive basement membrane perforation by the anchor cell (Cáceres et al., 2018; Sherwood and Plastino, 2018). This process

resembles podosomes force production as deformation of the BM could be observed prior perforation, but whether actomyosin activity is required remains to be determined (Cáceres et al., 2018). An interesting possibility is that similar to collagenolytic invadopodia and subsequent to BM primary perforation, the actin machinery may distribute and produce forces along the edges of the hole to promote pore enlargement without membrane protrusion. Consequently, future experiments following Tks5 and actin dynamics in live during BM breaching would be needed to test this hypothesis.

3.4. *Integration of invadopodia-based force production to cell invasion mechanisms*

Cell adhesion to the ECM, which is critical to pull and push forward the cell body during 3D migration, is mediated by integrin receptors and FAs, and requires an intact matrix scaffold. An intriguing question raised by our work is how cancer cells determine whether a matrix fiber can be used for adhesion and traction to support cell movement, or whether proteolytic cleavage and/or force-based displacement is needed when it opposes cell movement. We and others observed that in migrating cells, invadopodia formed close to the nucleus and were rather segregated away from more peripheral FAs (**data not shown** and Friedl and Wolf, 2009). These structures result from distinct ECM receptors, respectively MT1-MMP for invadopodia and integrins for FAs (**data not shown** and *Ferrari et al., submitted*). Although they provide a molecular basis for the observed differences, these results do not clarify how cancer cells can regionalize these structures on the same collagen scaffold. A possible explanation may arise from the fact that FAs tend to apply pulling forces to collagen fibers, thus aligning them, while invadopodia stem and produce force on curved fibers to subsequently degrade and push them away. It is therefore tempting to speculate that invasive cells can somehow assimilate the topology of the matrix scaffold as an information to regionalize different pro-invasive structures. Formation of FAs would then frequently occur on untouched collagen fibers ahead of the cell body where invadopodia would form less or be less stable because of the fibers alignment induced by FAs. On the other hand, the advancing cell body and nucleus may bend and deform proximal collagen fibers thereby generating an optimal scaffold to form force-producing invadopodia. Future work will be required to assess the contribution of this particular tug-of-war mechanism based on matrix scaffold topology, in the compartmentalization of adhesive/pulling and degradative/pushing regions in invasive cells.

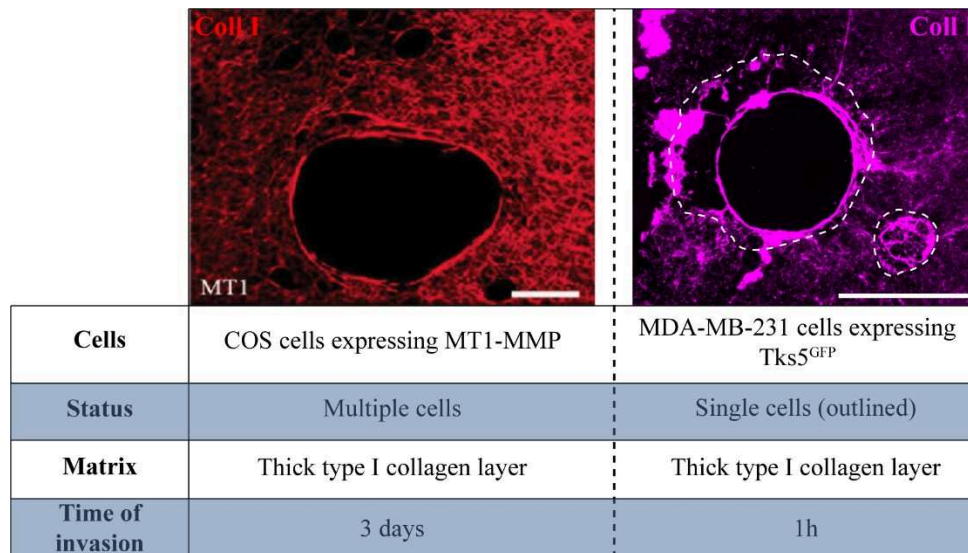


Figure 25: Could collagen remodeling of single cells be integrated at a multicellular level?

Confocal images of labelled-collagen in different experimental systems showing comparable collagen fibers remodeling at roughly equivalent scales (scale bars: 50 μ m).

Left: Images of collagen fibers after 3 days of incubation with multiple COS cells expressing MT1-MMP. **Right:** Images of collagen fibers after 2h of incubation with single MDA-MB-231 cells (cell edges depicted by white dashed lines).

Important spreading of underneath collagen fibers into a large matrix-free pore and fibrils bundling at the edges seem to be generated in both assays. This suggests that invadopodia-based matrix degradation/pushing forces may be a multicellular integrated process to promote cell invasion.

Images adapted from Li et al., Mol. Biol. Cell (2008) 19(8), 3221-3233, and Ferrari et al., submitted.

Similarly, another more distantly related issue raised by our work is whether and how matrix adhesion and matrix clearance mechanisms can be coordinated during the collective movement of epithelial cancer cells. Previous works have shown that cancer cells can use pre-existing proteolytic tracks or tunnels formed by preceding cells within the ECM scaffold to migrate in a protease-independent manner (Kraning-Rush et al., 2013; Wolf et al., 2007). If proteolytic tracks formed by matrix degradation are likely to be permanent, whether matrix pores enlargement by invadopodia-mediated pushing forces can last enough to be used by following invasive cells is an interesting possibility to explore in future work. Laser ablation experiments and observations of weak collagen fibers relaxation following invadopodia disassembly upon cytochalasin D treatment constitute the first evidences of long-lasting deformations and suggest that matrix fibers remodeling by invadopodia follow a viscoelastic regime whereby perpetual changes in collagen fibers structure are induced. Intriguingly, images showing matrix fibers remodeling by groups of cells invading into a thick collagen gel, which were published some years ago are similar to our own images of collagen remodeling by single invasive MDA-MB-231 cell, yet with slightly different dimensions (Li et al., 2008; **Ferrari et**

al., submitted)(see **Figure 24**). Altogether, these results suggest the possibility that invadopodia pushing and degrading collagen activity may be integrated at a collective or even supracellular level by carcinoma cells. It would also reinforce the idea that cancer cells display important plasticity and may re-use individual mechanisms of cell invasion to contribute to multicellular invasion depending on the environmental context.

4. Concluding remarks

Beside genetic and environmental factors, biophysical interactions of cancer cells with the microenvironment have tremendous impact on cancer progression. Based on our work, showed that cancer cells respond to physical constraints induced by the matrix during migration in a physiological fibrillar collagen network, by polarizing their proteolytic machinery based on MT1-MMP and invadopodia in front of the nucleus. We further showed that this MT1-MMP/invadopodia axis dissolve, by matrix degradation, and spread away, by force generation, constricting collagen fibers to reduce mechanical stress applied on the nucleus thereby promoting cell invasion. Our results reveal a comprehensive framework characterizing the conditions by which cancer cells engage their proteolytic machinery during confined migration. It also defines a new paradigm for invadopodia contribution in cancer cells 3D invasion as both degrading and force-producing structures. Overall, our findings should open new roads for biomechanical manipulation of invadopodia function in the context of targeted cancer therapy, as most of the attempts to treat cancer by inhibiting tumor cell migration and dissemination have been unsuccessful so far.

References

- Abram, C.L., Seals, D.F., Pass, I., Salinsky, D., Maurer, L., Roth, T.M., Courtneidge, S.A., 2003. The adaptor protein fish associates with members of the ADAMs family and localizes to podosomes of Src-transformed cells. *J. Biol. Chem.* 278, 16844–16851. <https://doi.org/10.1074/jbc.M300267200>
- Adhikari, A.S., Chai, J., Dunn, A.R., 2011. Mechanical load induces a 100-fold increase in the rate of collagen proteolysis by MMP-1. *J. Am. Chem. Soc.* 133, 1686–1689. <https://doi.org/10.1021/ja109972p>
- Akhmanova, A., Hoogenraad, C.C., 2015. Microtubule minus-end-targeting proteins. *Curr. Biol.* 25, R162–171. <https://doi.org/10.1016/j.cub.2014.12.027>
- Akhmanova, A., Steinmetz, M.O., 2015. Control of microtubule organization and dynamics: two ends in the limelight. *Nature Reviews Molecular Cell Biology* 16, 711–726. <https://doi.org/10.1038/nrm4084>
- Albiges-Rizo, C., Destaing, O., Fourcade, B., Planus, E., Block, M.R., 2009. Actin machinery and mechanosensitivity in invadopodia, podosomes and focal adhesions. *J. Cell. Sci.* 122, 3037–3049. <https://doi.org/10.1242/jcs.052704>
- Albrechtsen, R., Stautz, D., Sanjay, A., Kveiborg, M., Wewer, U.M., 2011. Extracellular engagement of ADAM12 induces clusters of invadopodia with localized ectodomain shedding activity. *Exp. Cell Res.* 317, 195–209. <https://doi.org/10.1016/j.yexcr.2010.10.003>
- Alexander, N.R., Branch, K.M., Parekh, A., Clark, E.S., Iwueke, I.C., Guelcher, S.A., Weaver, A.M., 2008. Extracellular matrix rigidity promotes invadopodia activity. *Curr Biol* 18, 1295–1299. <https://doi.org/10.1016/j.cub.2008.07.090>
- Annabi, B., Lachambre, M., Bousquet-Gagnon, N., Pagé, M., Gingras, D., Béliveau, R., 2001. Localization of membrane-type 1 matrix metalloproteinase in caveolae membrane domains. *Biochem. J.* 353, 547–553.
- Annabi, B., Thibeault, S., Moumdjian, R., Béliveau, R., 2004. Hyaluronan cell surface binding is induced by type I collagen and regulated by caveolae in glioma cells. *J. Biol. Chem.* 279, 21888–21896. <https://doi.org/10.1074/jbc.M313694200>
- Antoku, S., Zhu, R., Kutscheidt, S., Fackler, O.T., Gundersen, G.G., 2015. Reinforcing the LINC complex connection to actin filaments: the role of FHOD1 in TAN line formation and nuclear movement. *Cell Cycle* 14, 2200–2205. <https://doi.org/10.1080/15384101.2015.1053665>
- Artym, V.V., 2016. Preparation of High-Density Fibrillar Collagen Matrices That Mimic Desmoplastic Tumor Stroma. *Curr Protoc Cell Biol* 70, 10.19.1–10.19.11. <https://doi.org/10.1002/0471143030.cb1019s70>
- Artym, V.V., Swatkoski, S., Matsumoto, K., Campbell, C.B., Petrie, R.J., Dimitriadis, E.K., Li, X., Mueller, S.C., Bugge, T.H., Gucek, M., Yamada, K.M., 2015. Dense fibrillar collagen is a potent inducer of invadopodia via a specific signaling network. *J. Cell Biol.* 208, 331–350. <https://doi.org/10.1083/jcb.201405099>
- Artym, V.V., Zhang, Y., Seillier-Moiseiwitsch, F., Yamada, K.M., Mueller, S.C., 2006. Dynamic Interactions of Cortactin and Membrane Type 1 Matrix Metalloproteinase at Invadopodia: Defining the Stages of Invadopodia Formation and Function. *Cancer Res* 66, 3034–3043. <https://doi.org/10.1158/0008-5472.CAN-05-2177>
- Attieh, Y., Vignjevic, D.M., 2016. The hallmarks of CAFs in cancer invasion. *Eur. J. Cell Biol.* 95, 493–502. <https://doi.org/10.1016/j.ejcb.2016.07.004>
- Aureille, J., Belaadi, N., Guilluy, C., 2017. Mechanotransduction via the nuclear envelope: a distant reflection of the cell surface. *Curr. Opin. Cell Biol.* 44, 59–67. <https://doi.org/10.1016/j.ceb.2016.10.003>
- Ayala, I., Baldassarre, M., Giacchetti, G., Caldieri, G., Tetè, S., Luini, A., Buccione, R., 2008. Multiple regulatory inputs converge on cortactin to control invadopodia biogenesis and extracellular matrix degradation. *J Cell Sci* 121, 369–378. <https://doi.org/10.1242/jcs.008037>

- Ayala, I., Giacchetti, G., Caldieri, G., Attanasio, F., Marigliò, S., Tetè, S., Polishchuk, R., Castronovo, V., Buccione, R., 2009. Faciogenital dysplasia protein Fgd1 regulates invadopodia biogenesis and extracellular matrix degradation and is up-regulated in prostate and breast cancer. *Cancer Res.* 69, 747–752. <https://doi.org/10.1158/0008-5472.CAN-08-1980>
- Ayres, C.E., Jha, B.S., Sell, S.A., Bowlin, G.L., Simpson, D.G., 2010. Nanotechnology in the design of soft tissue scaffolds: innovations in structure and function. *Wiley Interdiscip Rev Nanomed Nanobiotechnol* 2, 20–34. <https://doi.org/10.1002/wnan.55>
- Badowski, C., Pawlak, G., Grichine, A., Chabadel, A., Oddou, C., Jurdic, P., Pfaff, M., Albigès-Rizo, C., Block, M.R., 2008. Paxillin phosphorylation controls invadopodia/podosomes spatiotemporal organization. *Mol. Biol. Cell* 19, 633–645. <https://doi.org/10.1091/mbc.e06-01-0088>
- Baldassarre, M., Pompeo, A., Beznoussenko, G., Castaldi, C., Cortellino, S., McNiven, M.A., Luini, A., Buccione, R., 2003. Dynamin participates in focal extracellular matrix degradation by invasive cells. *Mol. Biol. Cell* 14, 1074–1084. <https://doi.org/10.1091/mbc.E02-05-0308>
- Baldassarre, T., Watt, K., Truesdell, P., Meens, J., Schneider, M.M., Sengupta, S.K., Craig, A.W., 2015. Endophilin A2 Promotes TNBC Cell Invasion and Tumor Metastasis. *Mol. Cancer Res.* 13, 1044–1055. <https://doi.org/10.1158/1541-7786.MCR-14-0573>
- Banerjee, I., Zhang, J., Moore-Morris, T., Pfeiffer, E., Buchholz, K.S., Liu, A., Ouyang, K., Stroud, M.J., Gerace, L., Evans, S.M., McCulloch, A., Chen, J., 2014. Targeted ablation of nesprin 1 and nesprin 2 from murine myocardium results in cardiomyopathy, altered nuclear morphology and inhibition of the biomechanical gene response. *PLoS Genet.* 10, e1004114. <https://doi.org/10.1371/journal.pgen.1004114>
- Barbouri, D., Afratis, N., Gialeli, C., Vynios, D.H., Theocharis, A.D., Karamanos, N.K., 2014. Syndecans as modulators and potential pharmacological targets in cancer progression. *Front Oncol* 4, 4. <https://doi.org/10.3389/fonc.2014.00004>
- Barker, H.E., Cox, T.R., Erler, J.T., 2012. The rationale for targeting the LOX family in cancer. *Nat. Rev. Cancer* 12, 540–552. <https://doi.org/10.1038/nrc3319>
- Barthel, S.R., Gavino, J.D., Descheny, L., Dimitroff, C.J., 2007. Targeting selectins and selectin ligands in inflammation and cancer. *Expert Opin Ther Targets* 11, 1473–1491. <https://doi.org/10.1517/14728222.11.11.1473>
- Battaglia, C., Mayer, U., Aumailley, M., Timpl, R., 1992. Basement-membrane heparan sulfate proteoglycan binds to laminin by its heparan sulfate chains and to nidogen by sites in the protein core. *Eur. J. Biochem.* 208, 359–366.
- Beaty, B.T., Condeelis, J., 2014. Digging a little deeper: the stages of invadopodium formation and maturation. *Eur. J. Cell Biol.* 93, 438–444. <https://doi.org/10.1016/j.ejcb.2014.07.003>
- Beaty, B.T., Sharma, V.P., Bravo-Cordero, J.J., Simpson, M.A., Eddy, R.J., Koleske, A.J., Condeelis, J., 2013. $\beta 1$ integrin regulates Arg to promote invadopodial maturation and matrix degradation. *Mol. Biol. Cell* 24, 1661–1675, S1–11. <https://doi.org/10.1091/mbc.E12-12-0908>
- Bedard, K., Krause, K.-H., 2007. The NOX family of ROS-generating NADPH oxidases: physiology and pathophysiology. *Physiol. Rev.* 87, 245–313. <https://doi.org/10.1152/physrev.00044.2005>
- Beghein, E., Devriese, D., Van Hoey, E., Gettemans, J., 2018. Cortactin and fascin-1 regulate extracellular vesicle release by controlling endosomal trafficking or invadopodia formation and function. *Sci Rep* 8, 15606. <https://doi.org/10.1038/s41598-018-33868-z>
- Bell, E.S., Lammerding, J., 2016. Causes and consequences of nuclear envelope alterations in tumour progression. *Eur. J. Cell Biol.* 95, 449–464. <https://doi.org/10.1016/j.ejcb.2016.06.007>
- Bella, J., 2016. Collagen structure: new tricks from a very old dog. *Biochem. J.* 473, 1001–1025. <https://doi.org/10.1042/BJ20151169>
- Bendas, G., Borsig, L., 2012. Cancer cell adhesion and metastasis: selectins, integrins, and the inhibitory potential of heparins. *Int J Cell Biol* 2012, 676731. <https://doi.org/10.1155/2012/676731>
- Beningo, K.A., Hamao, K., Dembo, M., Wang, Y.-L., Hosoya, H., 2006. Traction forces of fibroblasts are regulated by the Rho-dependent kinase but not by the myosin light chain kinase. *Arch. Biochem. Biophys.* 456, 224–231. <https://doi.org/10.1016/j.abb.2006.09.025>
- Benton, G., Crooke, E., George, J., 2009. Laminin-1 induces E-cadherin expression in 3-dimensional cultured breast cancer cells by inhibiting DNA methyltransferase 1 and reversing promoter methylation status. *FASEB J.* 23, 3884–3895. <https://doi.org/10.1096/fj.08-128702>

- Bergert, M., Chandradoss, S.D., Desai, R.A., Paluch, E., 2012. Cell mechanics control rapid transitions between blebs and lamellipodia during migration. *Proc. Natl. Acad. Sci. U.S.A.* 109, 14434–14439. <https://doi.org/10.1073/pnas.1207968109>
- Bergert, M., Erzberger, A., Desai, R.A., Aspalter, I.M., Oates, A.C., Charras, G., Salbreux, G., Paluch, E.K., 2015. Force transmission during adhesion-independent migration. *Nat. Cell Biol.* 17, 524–529. <https://doi.org/10.1038/ncb3134>
- Bhuwania, R., Cornfine, S., Fang, Z., Krüger, M., Luna, E.J., Linder, S., 2012. Supervillin couples myosin-dependent contractility to podosomes and enables their turnover. *J. Cell. Sci.* 125, 2300–2314. <https://doi.org/10.1242/jcs.100032>
- Bianconi, D., Unseld, M., Prager, G.W., 2016. Integrins in the Spotlight of Cancer. *Int J Mol Sci* 17. <https://doi.org/10.3390/ijms17122037>
- Blackburn, D.G., 1992. Convergent Evolution of Viviparity, Matrotrophy, and Specializations for Fetal Nutrition in Reptiles and Other Vertebrates. *Integr Comp Biol* 32, 313–321. <https://doi.org/10.1093/icb/32.2.313>
- Blanchoin, L., Boujemaa-Paterski, R., Sykes, C., Plastino, J., 2014. Actin dynamics, architecture, and mechanics in cell motility. *Physiol. Rev.* 94, 235–263. <https://doi.org/10.1152/physrev.00018.2013>
- Blavier, L., Lazaryev, A., Dorey, F., Shackelford, G.M., DeClerck, Y.A., 2006. Matrix metalloproteinases play an active role in Wnt1-induced mammary tumorigenesis. *Cancer Res.* 66, 2691–2699. <https://doi.org/10.1158/0008-5472.CAN-05-2919>
- Blouw, B., Patel, M., Iizuka, S., Abdullah, C., You, W.K., Huang, X., Li, J.-L., Diaz, B., Stallcup, W.B., Courtneidge, S.A., 2015. The invadopodia scaffold protein Tks5 is required for the growth of human breast cancer cells in vitro and in vivo. *PLoS ONE* 10, e0121003. <https://doi.org/10.1371/journal.pone.0121003>
- Bonnans, C., Chou, J., Werb, Z., 2014. Remodelling the extracellular matrix in development and disease. *Nat. Rev. Mol. Cell Biol.* 15, 786–801. <https://doi.org/10.1038/nrm3904>
- Bouchet, B.P., Akhmanova, A., 2017. Microtubules in 3D cell motility. *J. Cell. Sci.* 130, 39–50. <https://doi.org/10.1242/jcs.189431>
- Bouissou, A., Proag, A., Bourg, N., Pingris, K., Cabriel, C., Balor, S., Mangeat, T., Thibault, C., Vieu, C., Dupuis, G., Fort, E., Lévêque-Fort, S., Maridonneau-Parini, I., Poincloux, R., 2017. Podosome Force Generation Machinery: A Local Balance between Protrusion at the Core and Traction at the Ring. *ACS Nano* 11, 4028–4040. <https://doi.org/10.1021/acsnano.7b00622>
- Boyd, N.F., Lockwood, G.A., Martin, L.J., Knight, J.A., Byng, J.W., Yaffe, M.J., Tritchler, D.L., 1998. Mammographic densities and breast cancer risk. *Breast Dis* 10, 113–126.
- Bradley, W.D., Koleske, A.J., 2009. Regulation of cell migration and morphogenesis by Abl-family kinases: emerging mechanisms and physiological contexts. *J. Cell. Sci.* 122, 3441–3454. <https://doi.org/10.1242/jcs.039859>
- Bravo-Cordero, J.J., Cordani, M., Soriano, S.F., Díez, B., Muñoz-Agudo, C., Casanova-Acebes, M., Boullosa, C., Guadamillas, M.C., Ezkurdia, I., González-Pisano, D., Del Pozo, M.A., Montoya, M.C., 2016. A novel high-content analysis tool reveals Rab8-driven cytoskeletal reorganization through Rho GTPases, calpain and MT1-MMP. *J. Cell. Sci.* 129, 1734–1749. <https://doi.org/10.1242/jcs.174920>
- Bravo-Cordero, J.J., Marrero-Díaz, R., Megías, D., Genís, L., García-Grande, A., García, M.A., Arroyo, A.G., Montoya, M.C., 2007. MT1-MMP proinvasive activity is regulated by a novel Rab8-dependent exocytic pathway. *EMBO J.* 26, 1499–1510. <https://doi.org/10.1038/sj.emboj.7601606>
- Briskin, C., Park, S., Vass, T., Lydon, J.P., O'Malley, B.W., Weinberg, R.A., 1998. A paracrine role for the epithelial progesterone receptor in mammary gland development. *Proc. Natl. Acad. Sci. U.S.A.* 95, 5076–5081.
- Brisson, L., Gillet, L., Calaghan, S., Besson, P., Le Guennec, J.-Y., Roger, S., Gore, J., 2011. Na(V)1.5 enhances breast cancer cell invasiveness by increasing NHE1-dependent H(+) efflux in caveolae. *Oncogene* 30, 2070–2076. <https://doi.org/10.1038/onc.2010.574>
- Brodsky, B., Persikov, A.V., 2005. Molecular structure of the collagen triple helix. *Adv. Protein Chem.* 70, 301–339. [https://doi.org/10.1016/S0065-3233\(05\)70009-7](https://doi.org/10.1016/S0065-3233(05)70009-7)

- Bronsert, P., Enderle-Ammour, K., Bader, M., Timme, S., Kuehs, M., Csanadi, A., Kayser, G., Kohler, I., Bausch, D., Hoepfner, J., Hopt, U.T., Keck, T., Stickeler, E., Passlick, B., Schilling, O., Reiss, C.P., Vashist, Y., Brabletz, T., Berger, J., Lotz, J., Olesch, J., Werner, M., Wellner, U.F., 2014. Cancer cell invasion and EMT marker expression: a three-dimensional study of the human cancer-host interface. *J. Pathol.* 234, 410–422. <https://doi.org/10.1002/path.4416>
- Buccione, R., Caldieri, G., Ayala, I., 2009. Invadopodia: specialized tumor cell structures for the focal degradation of the extracellular matrix. *Cancer Metastasis Rev.* 28, 137–149. <https://doi.org/10.1007/s10555-008-9176-1>
- Burger, K.L., Learman, B.S., Boucherle, A.K., Sirintrapun, S.J., Isom, S., Díaz, B., Courtneidge, S.A., Seals, D.F., 2014. Src-dependent Tks5 phosphorylation regulates invadopodia-associated invasion in prostate cancer cells. *Prostate* 74, 134–148. <https://doi.org/10.1002/pros.22735>
- Burgess, S.A., Yu, S., Walker, M.L., Hawkins, R.J., Chalovich, J.M., Knight, P.J., 2007. Structures of smooth muscle myosin and heavy meromyosin in the folded, shutdown state. *J. Mol. Biol.* 372, 1165–1178. <https://doi.org/10.1016/j.jmb.2007.07.014>
- Burgstaller, G., Gimona, M., 2005. Podosome-mediated matrix resorption and cell motility in vascular smooth muscle cells. *Am. J. Physiol. Heart Circ. Physiol.* 288, H3001–3005. <https://doi.org/10.1152/ajpheart.01002.2004>
- Burkhardt, L., Grob, T.J., Hermann, I., Burandt, E., Choschzick, M., Jänicke, F., Müller, V., Bokemeyer, C., Simon, R., Sauter, G., Wilczak, W., Lebeau, A., 2010. Gene amplification in ductal carcinoma in situ of the breast. *Breast Cancer Res. Treat.* 123, 757–765. <https://doi.org/10.1007/s10549-009-0675-8>
- Buschman, M.D., Bromann, P.A., Cejudo-Martin, P., Wen, F., Pass, I., Courtneidge, S.A., 2009. The novel adaptor protein Tks4 (SH3PXD2B) is required for functional podosome formation. *Mol. Biol. Cell* 20, 1302–1311. <https://doi.org/10.1091/mbc.e08-09-0949>
- Butcher, D.T., Alliston, T., Weaver, V.M., 2009. A tense situation: forcing tumour progression. *Nat. Rev. Cancer* 9, 108–122. <https://doi.org/10.1038/nrc2544>
- Buxboim, A., Swift, J., Irianto, J., Spinler, K.R., Dingal, P.C.D.P., Athirasala, A., Kao, Y.-R.C., Cho, S., Harada, T., Shin, J.-W., Discher, D.E., 2014. Matrix elasticity regulates lamin-A/C phosphorylation and turnover with feedback to actomyosin. *Curr. Biol.* 24, 1909–1917. <https://doi.org/10.1016/j.cub.2014.07.001>
- Cáceres, R., Bojanala, N., Kelley, L.C., Dreier, J., Manzi, J., Di Federico, F., Chi, Q., Risler, T., Testa, I., Sherwood, D.R., Plastino, J., 2018. Forces drive basement membrane invasion in *Caenorhabditis elegans*. *Proc. Natl. Acad. Sci. U.S.A.* 115, 11537–11542. <https://doi.org/10.1073/pnas.1808760115>
- Cagnet, S., Faraldo, M.M., Kreft, M., Sonnenberg, A., Raymond, K., Glukhova, M.A., 2014. Signaling events mediated by $\alpha 3 \beta 1$ integrin are essential for mammary tumorigenesis. *Oncogene* 33, 4286–4295. <https://doi.org/10.1038/onc.2013.391>
- Calle, Y., Carragher, N.O., Thrasher, A.J., Jones, G.E., 2006. Inhibition of calpain stabilises podosomes and impairs dendritic cell motility. *J. Cell. Sci.* 119, 2375–2385. <https://doi.org/10.1242/jcs.02939>
- Calle, Y., Jones, G.E., Jagger, C., Fuller, K., Blundell, M.P., Chow, J., Chambers, T., Thrasher, A.J., 2004. WASp deficiency in mice results in failure to form osteoclast sealing zones and defects in bone resorption. *Blood* 103, 3552–3561. <https://doi.org/10.1182/blood-2003-04-1259>
- Campeau, P.M., Foulkes, W.D., Tischkowitz, M.D., 2008. Hereditary breast cancer: new genetic developments, new therapeutic avenues. *Hum. Genet.* 124, 31–42. <https://doi.org/10.1007/s00439-008-0529-1>
- Campellone, K.G., Welch, M.D., 2010. A nucleator arms race: cellular control of actin assembly. *Nat. Rev. Mol. Cell Biol.* 11, 237–251. <https://doi.org/10.1038/nrm2867>
- Candiello, J., Balasubramani, M., Schreiber, E.M., Cole, G.J., Mayer, U., Halfter, W., Lin, H., 2007. Biomechanical properties of native basement membranes. *FEBS J.* 274, 2897–2908. <https://doi.org/10.1111/j.1742-4658.2007.05823.x>
- Cao, J., Kozarekar, P., Pavlaki, M., Chiarelli, C., Bahou, W.F., Zucker, S., 2004. Distinct Roles for the Catalytic and Hemopexin Domains of Membrane Type 1-Matrix Metalloproteinase in Substrate Degradation and Cell Migration. *J. Biol. Chem.* 279, 14129–14139. <https://doi.org/10.1074/jbc.M312120200>

- Carpenter, P.M., Dao, A.V., Arain, Z.S., Chang, M.K., Nguyen, H.P., Arain, S., Wang-Rodriguez, J., Kwon, S.-Y., Wilczynski, S.P., 2009. Motility induction in breast carcinoma by mammary epithelial laminin 332 (laminin 5). *Mol. Cancer Res.* 7, 462–475. <https://doi.org/10.1158/1541-7786.MCR-08-0148>
- Case, L.B., Waterman, C.M., 2015. Integration of actin dynamics and cell adhesion by a three-dimensional, mechanosensitive molecular clutch. *Nat. Cell Biol.* 17, 955–963. <https://doi.org/10.1038/ncb3191>
- Castagnino, A., Castro-Castro, A., Irondelle, M., Guichard, A., Lodillinsky, C., Fuhrmann, L., Vacher, S., Agüera-González, S., Zagryazhskaya-Masson, A., Romao, M., El Kesrouani, C., Noegel, A.A., Dubois, T., Raposo, G., Bear, J.E., Clemen, C.S., Vincent-Salomon, A., Bièche, I., Chavrier, P., 2018. Coronin 1C promotes triple-negative breast cancer invasiveness through regulation of MT1-MMP traffic and invadopodia function. *Oncogene* 37, 6425–6441. <https://doi.org/10.1038/s41388-018-0422-x>
- Castro-Castro, A., Janke, C., Montagnac, G., Paul-Gilloteaux, P., Chavrier, P., 2012. ATAT1/MEC-17 acetyltransferase and HDAC6 deacetylase control a balance of acetylation of alpha-tubulin and cortactin and regulate MT1-MMP trafficking and breast tumor cell invasion. *Eur. J. Cell Biol.* 91, 950–960. <https://doi.org/10.1016/j.ejcb.2012.07.001>
- Castro-Castro, A., Marchesin, V., Monteiro, P., Lodillinsky, C., Rossé, C., Chavrier, P., 2016. Cellular and Molecular Mechanisms of MT1-MMP-Dependent Cancer Cell Invasion. *Annu. Rev. Cell Dev. Biol.* 32, 555–576. <https://doi.org/10.1146/annurev-cellbio-111315-125227>
- Castro-Sanchez, L., Soto-Guzman, A., Navarro-Tito, N., Martinez-Orozco, R., Salazar, E.P., 2010. Native type IV collagen induces cell migration through a CD9 and DDR1-dependent pathway in MDA-MB-231 breast cancer cells. *Eur. J. Cell Biol.* 89, 843–852. <https://doi.org/10.1016/j.ejcb.2010.07.004>
- Cathcart, J.M., Banach, A., Liu, A., Chen, J., Goligorsky, M., Cao, J., 2016. Interleukin-6 increases matrix metalloproteinase-14 (MMP-14) levels via down-regulation of p53 to drive cancer progression. *Oncotarget* 7, 61107–61120. <https://doi.org/10.18632/oncotarget.11243>
- Cejudo-Martin, P., Yuen, A., Vlahovich, N., Lock, P., Courtneidge, S.A., Díaz, B., 2014. Genetic disruption of the sh3pxd2a gene reveals an essential role in mouse development and the existence of a novel isoform of tks5. *PLoS ONE* 9, e107674. <https://doi.org/10.1371/journal.pone.0107674>
- Chabadel, A., Bañón-Rodríguez, I., Cluet, D., Rudkin, B.B., Wehrle-Haller, B., Genot, E., Jurdic, P., Anton, I.M., Saltel, F., 2007. CD44 and beta3 integrin organize two functionally distinct actin-based domains in osteoclasts. *Mol. Biol. Cell* 18, 4899–4910. <https://doi.org/10.1091/mbc.e07-04-0378>
- Chambliss, A.B., Khatau, S.B., Erdenberger, N., Robinson, D.K., Hodzic, D., Longmore, G.D., Wirtz, D., 2013. The LINC-anchored actin cap connects the extracellular milieu to the nucleus for ultrafast mechanotransduction. *Sci Rep* 3, 1087. <https://doi.org/10.1038/srep01087>
- Chan, C.E., Odde, D.J., 2008. Traction dynamics of filopodia on compliant substrates. *Science* 322, 1687–1691. <https://doi.org/10.1126/science.1163595>
- Chancellor, T.J., Lee, J., Thodeti, C.K., Lele, T., 2010. Actomyosin tension exerted on the nucleus through nesprin-1 connections influences endothelial cell adhesion, migration, and cyclic strain-induced reorientation. *Biophys. J.* 99, 115–123. <https://doi.org/10.1016/j.bpj.2010.04.011>
- Chang, W., Antoku, S., Östlund, C., Worman, H.J., Gundersen, G.G., 2015. Linker of nucleoskeleton and cytoskeleton (LINC) complex-mediated actin-dependent nuclear positioning orients centrosomes in migrating myoblasts. *Nucleus* 6, 77–88. <https://doi.org/10.1080/19491034.2015.1004947>
- Chang, Y.-C., Nalbant, P., Birkenfeld, J., Chang, Z.-F., Bokoch, G.M., 2008. GEF-H1 couples nocodazole-induced microtubule disassembly to cell contractility via RhoA. *Mol. Biol. Cell* 19, 2147–2153. <https://doi.org/10.1091/mbc.e07-12-1269>
- Charras, G., Paluch, E., 2008. Blebs lead the way: how to migrate without lamellipodia. *Nat. Rev. Mol. Cell Biol.* 9, 730–736. <https://doi.org/10.1038/nrm2453>
- Charrier, S., Stockholm, D., Seye, K., Opolon, P., Taveau, M., Gross, D.-A., Bucher-Laurent, S., Delenda, C., Vainchenker, W., Danos, O., Galy, A., 2005. A lentiviral vector encoding the

- human Wiskott-Aldrich syndrome protein corrects immune and cytoskeletal defects in WASP knockout mice. *Gene Ther.* 12, 597–606. <https://doi.org/10.1038/sj.gt.3302440>
- Chaudhuri, O., Koshy, S.T., Branco da Cunha, C., Shin, J.-W., Verbeke, C.S., Allison, K.H., Mooney, D.J., 2014. Extracellular matrix stiffness and composition jointly regulate the induction of malignant phenotypes in mammary epithelium. *Nat Mater* 13, 970–978. <https://doi.org/10.1038/nmat4009>
- Chen, W.T., 1989. Proteolytic activity of specialized surface protrusions formed at rosette contact sites of transformed cells. *J. Exp. Zool.* 251, 167–185. <https://doi.org/10.1002/jez.1402510206>
- Chen, W.T., Olden, K., Bernard, B.A., Chu, F.F., 1984. Expression of transformation-associated protease(s) that degrade fibronectin at cell contact sites. *The Journal of Cell Biology* 98, 1546–1555. <https://doi.org/10.1083/jcb.98.4.1546>
- Chen, Z., Borek, D., Padrick, S.B., Gomez, T.S., Metlagel, Z., Ismail, A.M., Umetani, J., Billadeau, D.D., Otwinowski, Z., Rosen, M.K., 2010. Structure and control of the actin regulatory WAVE complex. *Nature* 468, 533–538. <https://doi.org/10.1038/nature09623>
- Chevalier, C., Collin, G., Descamps, S., Touaitahuata, H., Simon, V., Reymond, N., Fernandez, L., Milhiet, P.-E., Georget, V., Urbach, S., Lasorsa, L., Orsetti, B., Boissière-Michot, F., Lopez-Crapez, E., Theillet, C., Roche, S., Benistant, C., 2016. TOM1L1 drives membrane delivery of MT1-MMP to promote ERBB2-induced breast cancer cell invasion. *Nat Commun* 7, 10765. <https://doi.org/10.1038/ncomms10765>
- Chiang, S.P.H., Cabrera, R.M., Segall, J.E., 2016. Tumor cell intravasation. *Am J Physiol Cell Physiol* 311, C1–C14. <https://doi.org/10.1152/ajpcell.00238.2015>
- Cho, S., Irianto, J., Discher, D.E., 2017. Mechanosensing by the nucleus: From pathways to scaling relationships. *J. Cell Biol.* <https://doi.org/10.1083/jcb.201610042>
- Chou, S.-Y., Hsu, K.-S., Otsu, W., Hsu, Y.-C., Luo, Y.-C., Yeh, C., Shehab, S.S., Chen, J., Shieh, V., He, G., Marean, M.B., Felsen, D., Ding, A., Poppas, D.P., Chuang, J.-Z., Sung, C.-H., 2016. CLIC4 regulates apical exocytosis and renal tube luminogenesis through retromer- and actin-mediated endocytic trafficking. *Nat Commun* 7, 10412. <https://doi.org/10.1038/ncomms10412>
- Christiansen, D.L., Huang, E.K., Silver, F.H., 2000. Assembly of type I collagen: fusion of fibril subunits and the influence of fibril diameter on mechanical properties. *Matrix Biol.* 19, 409–420.
- Chung, L., Dinakarpanian, D., Yoshida, N., Lauer-Fields, J.L., Fields, G.B., Visse, R., Nagase, H., 2004. Collagenase unwinds triple-helical collagen prior to peptide bond hydrolysis. *EMBO J.* 23, 3020–3030. <https://doi.org/10.1038/sj.emboj.7600318>
- Clark, A.G., Vignjevic, D.M., 2015. Modes of cancer cell invasion and the role of the microenvironment. *Curr. Opin. Cell Biol.* 36, 13–22. <https://doi.org/10.1016/j.ceb.2015.06.004>
- Clark, E.S., Weaver, A.M., 2008. A new role for cortactin in invadopodia: regulation of protease secretion. *Eur. J. Cell Biol.* 87, 581–590. <https://doi.org/10.1016/j.ejcb.2008.01.008>
- Clark, E.S., Whigham, A.S., Yarbrough, W.G., Weaver, A.M., 2007. Cortactin is an essential regulator of matrix metalloproteinase secretion and extracellular matrix degradation in invadopodia. *Cancer Res.* 67, 4227–4235. <https://doi.org/10.1158/0008-5472.CAN-06-3928>
- Cockburn, J.J.B., Hesketh, S.J., Mulhair, P., Thomsen, M., O’Connell, M.J., Way, M., 2018. Insights into Kinesin-1 Activation from the Crystal Structure of KLC2 Bound to JIP3. *Structure* 26, 1486–1498.e6. <https://doi.org/10.1016/j.str.2018.07.011>
- Cojoc, D., Difato, F., Ferrari, E., Shahapure, R.B., Laishram, J., Righi, M., Di Fabrizio, E.M., Torre, V., 2007. Properties of the Force Exerted by Filopodia and Lamellipodia and the Involvement of Cytoskeletal Components. *PLoS One* 2. <https://doi.org/10.1371/journal.pone.0001072>
- Collin, O., Na, S., Chowdhury, F., Hong, M., Shin, M.E., Wang, F., Wang, N., 2008. Self-organized podosomes are dynamic mechanosensors. *Curr. Biol.* 18, 1288–1294. <https://doi.org/10.1016/j.cub.2008.07.046>
- Collins, V.P., Loeffler, R.K., Tivey, H., 1956. Observations on growth rates of human tumors. *Am J Roentgenol Radium Ther Nucl Med* 76, 988–1000.
- Conklin, M.W., Eickhoff, J.C., Riching, K.M., Pehlke, C.A., Eliceiri, K.W., Provenzano, P.P., Friedl, A., Keely, P.J., 2011. Aligned collagen is a prognostic signature for survival in human breast carcinoma. *Am. J. Pathol.* 178, 1221–1232. <https://doi.org/10.1016/j.ajpath.2010.11.076>

- Conti, M.A., Adelstein, R.S., 2008. Nonmuscle myosin II moves in new directions. *J. Cell. Sci.* 121, 11–18. <https://doi.org/10.1242/jcs.007112>
- Courtneidge, S.A., 2012. Cell migration and invasion in human disease: the Tks adaptor proteins. *Biochem. Soc. Trans.* 40, 129–132. <https://doi.org/10.1042/BST20110685>
- Cowden Dahl, K.D., Symowicz, J., Ning, Y., Gutierrez, E., Fishman, D.A., Adley, B.P., Stack, M.S., Hudson, L.G., 2008. Matrix metalloproteinase 9 is a mediator of epidermal growth factor-dependent e-cadherin loss in ovarian carcinoma cells. *Cancer Res.* 68, 4606–4613. <https://doi.org/10.1158/0008-5472.CAN-07-5046>
- Cowell, C.F., Weigelt, B., Sakr, R.A., Ng, C.K.Y., Hicks, J., King, T.A., Reis-Filho, J.S., 2013. Progression from ductal carcinoma in situ to invasive breast cancer: revisited. *Mol Oncol* 7, 859–869. <https://doi.org/10.1016/j.molonc.2013.07.005>
- Cox, T.R., Erler, J.T., 2011. Remodeling and homeostasis of the extracellular matrix: implications for fibrotic diseases and cancer. *Dis Model Mech* 4, 165–178. <https://doi.org/10.1242/dmm.004077>
- Cruz-Acuña, R., García, A.J., 2017. Synthetic hydrogels mimicking basement membrane matrices to promote cell-matrix interactions. *Matrix Biol.* 57–58, 324–333. <https://doi.org/10.1016/j.matbio.2016.06.002>
- Cukierman, E., Pankov, R., Stevens, D.R., Yamada, K.M., 2001. Taking cell-matrix adhesions to the third dimension. *Science* 294, 1708–1712. <https://doi.org/10.1126/science.1064829>
- Cupesi, M., Yoshioka, J., Gannon, J., Kudinova, A., Stewart, C.L., Lammerding, J., 2010. Attenuated hypertrophic response to pressure overload in a lamin A/C haploinsufficiency mouse. *J. Mol. Cell. Cardiol.* 48, 1290–1297. <https://doi.org/10.1016/j.yjmcc.2009.10.024>
- Curado, F., Spuul, P., Egaña, I., Rottiers, P., Daubon, T., Veillat, V., Duhamel, P., Leclercq, A., Gontier, E., Génot, E., 2014. ALK5 and ALK1 play antagonistic roles in transforming growth factor β -induced podosome formation in aortic endothelial cells. *Mol. Cell. Biol.* 34, 4389–4403. <https://doi.org/10.1128/MCB.01026-14>
- Daubon, T., Buccione, R., Génot, E., 2011. The Aarskog-Scott syndrome protein Fgd1 regulates podosome formation and extracellular matrix remodeling in transforming growth factor β -stimulated aortic endothelial cells. *Mol. Cell. Biol.* 31, 4430–4441. <https://doi.org/10.1128/MCB.05474-11>
- David-Pfeuty, T., Singer, S.J., 1980. Altered distributions of the cytoskeletal proteins vinculin and alpha-actinin in cultured fibroblasts transformed by Rous sarcoma virus. *PNAS* 77, 6687–6691. <https://doi.org/10.1073/pnas.77.11.6687>
- Davidson, P.M., Denais, C., Bakshi, M.C., Lammerding, J., 2014. Nuclear deformability constitutes a rate-limiting step during cell migration in 3-D environments. *Cell Mol Bioeng* 7, 293–306. <https://doi.org/10.1007/s12195-014-0342-y>
- Davidson, P.M., Lammerding, J., 2014. Broken nuclei – lamins, nuclear mechanics, and disease. *Trends in Cell Biology* 24, 247–256. <https://doi.org/10.1016/j.tcb.2013.11.004>
- De Franceschi, N., Hamidi, H., Alanko, J., Sahgal, P., Ivaska, J., 2015. Integrin traffic - the update. *J. Cell. Sci.* 128, 839–852. <https://doi.org/10.1242/jcs.161653>
- De Vos, W.H., Houben, F., Kamps, M., Malhas, A., Verheyen, F., Cox, J., Manders, E.M.M., Verstraeten, V.L.R.M., van Steensel, M.A.M., Marcelis, C.L.M., van den Wijngaard, A., Vaux, D.J., Ramaekers, F.C.S., Broers, J.L.V., 2011. Repetitive disruptions of the nuclear envelope invoke temporary loss of cellular compartmentalization in laminopathies. *Hum. Mol. Genet.* 20, 4175–4186. <https://doi.org/10.1093/hmg/ddr344>
- Denais, C.M., Gilbert, R.M., Isermann, P., McGregor, A.L., te Lindert, M., Weigelin, B., Davidson, P.M., Friedl, P., Wolf, K., Lammerding, J., 2016. Nuclear envelope rupture and repair during cancer cell migration. *Science* 352, 353–358. <https://doi.org/10.1126/science.aad7297>
- Dent, R., Trudeau, M., Pritchard, K.I., Hanna, W.M., Kahn, H.K., Sawka, C.A., Lickley, L.A., Rawlinson, E., Sun, P., Narod, S.A., 2007. Triple-negative breast cancer: clinical features and patterns of recurrence. *Clin. Cancer Res.* 13, 4429–4434. <https://doi.org/10.1158/1078-0432.CCR-06-3045>
- Deryugina, E.I., Ratnikov, B., Monosov, E., Postnova, T.I., DiScipio, R., Smith, J.W., Strongin, A.Y., 2001. MT1-MMP initiates activation of pro-MMP-2 and integrin $\alpha v \beta 3$ promotes maturation of MMP-2 in breast carcinoma cells. *Exp. Cell Res.* 263, 209–223. <https://doi.org/10.1006/excr.2000.5118>

- Deryugina, E.I., Ratnikov, B.I., Postnova, T.I., Rozanov, D.V., Strongin, A.Y., 2002. Processing of integrin $\alpha(v)$ subunit by membrane type 1 matrix metalloproteinase stimulates migration of breast carcinoma cells on vitronectin and enhances tyrosine phosphorylation of focal adhesion kinase. *J. Biol. Chem.* 277, 9749–9756. <https://doi.org/10.1074/jbc.M110269200>
- Desmarais, V., Yamaguchi, H., Oser, M., Soon, L., Mouneimne, G., Sarmiento, C., Eddy, R., Condeelis, J., 2009. N-WASP and cortactin are involved in invadopodium-dependent chemotaxis to EGF in breast tumor cells. *Cell Motil. Cytoskeleton* 66, 303–316. <https://doi.org/10.1002/cm.20361>
- Destaing, O., Ferguson, S.M., Grichine, A., Oddou, C., De Camilli, P., Albiges-Rizo, C., Baron, R., 2013. Essential function of dynamin in the invasive properties and actin architecture of v-Src induced podosomes/invadosomes. *PLoS ONE* 8, e77956. <https://doi.org/10.1371/journal.pone.0077956>
- Destaing, O., Planus, E., Bouvard, D., Oddou, C., Badowski, C., Bossy, V., Raducanu, A., Fourcade, B., Albiges-Rizo, C., Block, M.R., 2010. $\beta 1A$ integrin is a master regulator of invadosome organization and function. *Mol. Biol. Cell* 21, 4108–4119. <https://doi.org/10.1091/mbc.E10-07-0580>
- Destaing, O., Saltel, F., G  minard, J.-C., Jurdic, P., Bard, F., 2003. Podosomes display actin turnover and dynamic self-organization in osteoclasts expressing actin-green fluorescent protein. *Mol. Biol. Cell* 14, 407–416. <https://doi.org/10.1091/mbc.e02-07-0389>
- Devarajan, E., Song, Y.-H., Krishnappa, S., Alt, E., 2012. Epithelial-mesenchymal transition in breast cancer lines is mediated through PDGF-D released by tissue-resident stem cells. *Int. J. Cancer* 131, 1023–1031. <https://doi.org/10.1002/ijc.26493>
- Di Martino, J., Paysan, L., Gest, C., Lagr  e, V., Juin, A., Saltel, F., Moreau, V., 2014. Cdc42 and Tks5: a minimal and universal molecular signature for functional invadosomes. *Cell Adh Migr* 8, 280–292.
- Diaz, B., Shani, G., Pass, I., Anderson, D., Quintavalle, M., Courtneidge, S.A., 2009. Tks5-dependent, nox-mediated generation of reactive oxygen species is necessary for invadopodia formation. *Sci Signal* 2, ra53. <https://doi.org/10.1126/scisignal.2000368>
- D  az, B., Yuen, A., Iizuka, S., Higashiyama, S., Courtneidge, S.A., 2013a. Notch increases the shedding of HB-EGF by ADAM12 to potentiate invadopodia formation in hypoxia. *J. Cell Biol.* 201, 279–292. <https://doi.org/10.1083/jcb.201209151>
- D  az, B., Yuen, A., Iizuka, S., Higashiyama, S., Courtneidge, S.A., 2013b. Notch increases the shedding of HB-EGF by ADAM12 to potentiate invadopodia formation in hypoxia. *J. Cell Biol.* 201, 279–292. <https://doi.org/10.1083/jcb.201209151>
- Dolati, S., Kage, F., Mueller, J., M  sken, M., Kirchner, M., Dittmar, G., Sixt, M., Rottner, K., Falcke, M., 2018. On the relation between filament density, force generation, and protrusion rate in mesenchymal cell motility. *Mol. Biol. Cell* 29, 2674–2686. <https://doi.org/10.1091/mbc.E18-02-0082>
- Dorfleutner, A., Cho, Y., Vincent, D., Cunnick, J., Lin, H., Weed, S.A., Stehlik, C., Flynn, D.C., 2008. Phosphorylation of AFAP-110 affects podosome lifespan in A7r5 cells. *J. Cell. Sci.* 121, 2394–2405. <https://doi.org/10.1242/jcs.026187>
- Doyle, A.D., Carvajal, N., Jin, A., Matsumoto, K., Yamada, K.M., 2015. Local 3D matrix microenvironment regulates cell migration through spatiotemporal dynamics of contractility-dependent adhesions. *Nat Commun* 6, 8720. <https://doi.org/10.1038/ncomms9720>
- Doyle, A.D., Yamada, K.M., 2016. Mechanosensing via cell-matrix adhesions in 3D microenvironments. *Exp. Cell Res.* 343, 60–66. <https://doi.org/10.1016/j.yexcr.2015.10.033>
- Dufour, A., Sampson, N.S., Zucker, S., Cao, J., 2008. Role of the hemopexin domain of matrix metalloproteinases in cell migration. *J. Cell. Physiol.* 217, 643–651. <https://doi.org/10.1002/jcp.21535>
- Dujardin, D.L., Barnhart, L.E., Stehman, S.A., Gomes, E.R., Gundersen, G.G., Vallee, R.B., 2003. A role for cytoplasmic dynein and LIS1 in directed cell movement. *J Cell Biol* 163, 1205–1211. <https://doi.org/10.1083/jcb.200310097>
- Dzamba, B.J., DeSimone, D.W., 2018. Extracellular Matrix (ECM) and the Sculpting of Embryonic Tissues. *Curr. Top. Dev. Biol.* 130, 245–274. <https://doi.org/10.1016/bs.ctdb.2018.03.006>
- Eckert, J.J., Fleming, T.P., 2008. Tight junction biogenesis during early development. *Biochim. Biophys. Acta* 1778, 717–728. <https://doi.org/10.1016/j.bbamem.2007.09.031>

- Eckert, M.A., Lwin, T.M., Chang, A.T., Kim, J., Danis, E., Ohno-Machado, L., Yang, J., 2011. Twist1-induced invadopodia formation promotes tumor metastasis. *Cancer Cell* 19, 372–386. <https://doi.org/10.1016/j.ccr.2011.01.036>
- Eckert, M.A., Santiago-Medina, M., Lwin, T.M., Kim, J., Courtneidge, S.A., Yang, J., 2017. ADAM12 induction by Twist1 promotes tumor invasion and metastasis via regulation of invadopodia and focal adhesions. *J. Cell. Sci.* 130, 2036–2048. <https://doi.org/10.1242/jcs.198200>
- Edwards, M., Zwolak, A., Schafer, D.A., Sept, D., Dominguez, R., Cooper, J.A., 2014. Capping protein regulators fine-tune actin assembly dynamics. *Nat. Rev. Mol. Cell Biol.* 15, 677–689. <https://doi.org/10.1038/nrm3869>
- Egeblad, M., Rasch, M.G., Weaver, V.M., 2010. Dynamic interplay between the collagen scaffold and tumor evolution. *Curr. Opin. Cell Biol.* 22, 697–706. <https://doi.org/10.1016/j.ceb.2010.08.015>
- Ehrbar, M., Sala, A., Lienemann, P., Ranga, A., Mosiewicz, K., Bittermann, A., Rizzi, S.C., Weber, F.E., Lutolf, M.P., 2011. Elucidating the role of matrix stiffness in 3D cell migration and remodeling. *Biophys. J.* 100, 284–293. <https://doi.org/10.1016/j.bpj.2010.11.082>
- Elkhatib, N., Bresteau, E., Baschieri, F., Rioja, A.L., van Niel, G., Vassilopoulos, S., Montagnac, G., 2017. Tubular clathrin/AP-2 lattices pinch collagen fibers to support 3D cell migration. *Science* 356. <https://doi.org/10.1126/science.aal4713>
- Elosegui-Artola, A., Oria, R., Chen, Y., Kosmalska, A., Pérez-González, C., Castro, N., Zhu, C., Trepats, X., Roca-Cusachs, P., 2016. Mechanical regulation of a molecular clutch defines force transmission and transduction in response to matrix rigidity. *Nat. Cell Biol.* 18, 540–548. <https://doi.org/10.1038/ncb3336>
- Endo, K., Takino, T., Miyamori, H., Kinsen, H., Yoshizaki, T., Furukawa, M., Sato, H., 2003. Cleavage of syndecan-1 by membrane type matrix metalloproteinase-1 stimulates cell migration. *J. Biol. Chem.* 278, 40764–40770. <https://doi.org/10.1074/jbc.M306736200>
- Engl, W., Arasi, B., Yap, L.L., Thiery, J.P., Viasnoff, V., 2014. Actin dynamics modulate mechanosensitive immobilization of E-cadherin at adherens junctions. *Nat. Cell Biol.* 16, 587–594. <https://doi.org/10.1038/ncb2973>
- Engler, A.J., Sen, S., Sweeney, H.L., Discher, D.E., 2006. Matrix elasticity directs stem cell lineage specification. *Cell* 126, 677–689. <https://doi.org/10.1016/j.cell.2006.06.044>
- English, J.L., Kassiri, Z., Koskivirta, I., Atkinson, S.J., Di Grappa, M., Soloway, P.D., Nagase, H., Vuorio, E., Murphy, G., Khokha, R., 2006. Individual Timp deficiencies differentially impact pro-MMP-2 activation. *J. Biol. Chem.* 281, 10337–10346. <https://doi.org/10.1074/jbc.M512009200>
- Erler, J.T., Bennewith, K.L., Nicolau, M., Dornhöfer, N., Kong, C., Le, Q.-T., Chi, J.-T.A., Jeffrey, S.S., Giaccia, A.J., 2006. Lysyl oxidase is essential for hypoxia-induced metastasis. *Nature* 440, 1222–1226. <https://doi.org/10.1038/nature04695>
- Eroles, P., Bosch, A., Pérez-Fidalgo, J.A., Lluch, A., 2012. Molecular biology in breast cancer: intrinsic subtypes and signaling pathways. *Cancer Treat. Rev.* 38, 698–707. <https://doi.org/10.1016/j.ctrv.2011.11.005>
- Etienne-Manneville, S., 2013. Microtubules in cell migration. *Annu. Rev. Cell Dev. Biol.* 29, 471–499. <https://doi.org/10.1146/annurev-cellbio-101011-155711>
- Etienne-Manneville, S., 2010. From signaling pathways to microtubule dynamics: the key players. *Current Opinion in Cell Biology, Cell structure and dynamics* 22, 104–111. <https://doi.org/10.1016/j.ceb.2009.11.008>
- Etienne-Manneville, S., Hall, A., 2001. Integrin-mediated activation of Cdc42 controls cell polarity in migrating astrocytes through PKC ζ . *Cell* 106, 489–498.
- Fang, M., Yuan, J., Peng, C., Li, Y., 2014. Collagen as a double-edged sword in tumor progression. *Tumour Biol.* 35, 2871–2882. <https://doi.org/10.1007/s13277-013-1511-7>
- Fedorchak, G.R., Kaminski, A., Lammerding, J., 2014. Cellular mechanosensing: getting to the nucleus of it all. *Prog. Biophys. Mol. Biol.* 115, 76–92. <https://doi.org/10.1016/j.pbiomolbio.2014.06.009>
- Feinberg, T.Y., Zheng, H., Liu, R., Wicha, M.S., Yu, S.M., Weiss, S.J., 2018. Divergent Matrix-Remodeling Strategies Distinguish Developmental from Neoplastic Mammary Epithelial Cell Invasion Programs. *Dev. Cell* 47, 145–160.e6. <https://doi.org/10.1016/j.devcel.2018.08.025>

- Ferrari, R., Infante, E., Chavrier, P., 2019. Nucleus-Invadopodia Duo During Cancer Invasion. *Trends Cell Biol.* 29, 93–96. <https://doi.org/10.1016/j.tcb.2018.11.006>
- Fraley, S.I., Feng, Y., Krishnamurthy, R., Kim, D.-H., Celedon, A., Longmore, G.D., Wirtz, D., 2010. A distinctive role for focal adhesion proteins in three-dimensional cell motility. *Nat Cell Biol* 12, 598–604. <https://doi.org/10.1038/ncb2062>
- Fraley, S.I., Wu, P.-H., He, L., Feng, Y., Krishnamurthy, R., Longmore, G.D., Wirtz, D., 2015. Three-dimensional matrix fiber alignment modulates cell migration and MT1-MMP utility by spatially and temporally directing protrusions. *Sci Rep* 5, 14580. <https://doi.org/10.1038/srep14580>
- Frantz, C., Stewart, K.M., Weaver, V.M., 2010. The extracellular matrix at a glance. *J. Cell. Sci.* 123, 4195–4200. <https://doi.org/10.1242/jcs.023820>
- Friedl, P., Alexander, S., 2011. Cancer Invasion and the Microenvironment: Plasticity and Reciprocity. *Cell* 147, 992–1009. <https://doi.org/10.1016/j.cell.2011.11.016>
- Friedl, P., Gilmour, D., 2009. Collective cell migration in morphogenesis, regeneration and cancer. *Nat. Rev. Mol. Cell Biol.* 10, 445–457. <https://doi.org/10.1038/nrm2720>
- Friedl, P., Wolf, K., 2010. Plasticity of cell migration: a multiscale tuning model. *J. Cell Biol.* 188, 11–19. <https://doi.org/10.1083/jcb.200909003>
- Friedl, P., Wolf, K., 2009. Proteolytic interstitial cell migration: a five-step process. *Cancer Metastasis Rev.* 28, 129–135. <https://doi.org/10.1007/s10555-008-9174-3>
- Friedl, P., Wolf, K., Lammerding, J., 2011. Nuclear mechanics during cell migration. *Current Opinion in Cell Biology, Cell structure and dynamics* 23, 55–64. <https://doi.org/10.1016/j.ceb.2010.10.015>
- Frittoli, E., Palamidessi, A., Marighetti, P., Confalonieri, S., Bianchi, F., Malinverno, C., Mazzarol, G., Viale, G., Martin-Padura, I., Garré, M., Parazzoli, D., Mattei, V., Cortellino, S., Bertalot, G., Di Fiore, P.P., Scita, G., 2014. A RAB5/RAB4 recycling circuitry induces a proteolytic invasive program and promotes tumor dissemination. *J. Cell Biol.* 206, 307–328. <https://doi.org/10.1083/jcb.201403127>
- Fu, H.-L., Sohail, A., Valiathan, R.R., Wasinski, B.D., Kumarasiri, M., Mahasenan, K.V., Bernardo, M.M., Tokmina-Roszyk, D., Fields, G.B., Mobashery, S., Fridman, R., 2013a. Shedding of discoidin domain receptor 1 by membrane-type matrix metalloproteinases. *J. Biol. Chem.* 288, 12114–12129. <https://doi.org/10.1074/jbc.M112.409599>
- Fu, H.-L., Valiathan, R.R., Arkwright, R., Sohail, A., Mihai, C., Kumarasiri, M., Mahasenan, K.V., Mobashery, S., Huang, P., Agarwal, G., Fridman, R., 2013b. Discoidin domain receptors: unique receptor tyrosine kinases in collagen-mediated signaling. *J. Biol. Chem.* 288, 7430–7437. <https://doi.org/10.1074/jbc.R112.444158>
- Furmaniak-Kazmierczak, E., Crawley, S.W., Carter, R.L., Maurice, D.H., Côté, G.P., 2007. Formation of extracellular matrix-digesting invadopodia by primary aortic smooth muscle cells. *Circ. Res.* 100, 1328–1336. <https://doi.org/10.1161/CIRCRESAHA.106.147744>
- Gálvez, B.G., Matías-Román, S., Yáñez-Mó, M., Vicente-Manzanares, M., Sánchez-Madrid, F., Arroyo, A.G., 2004. Caveolae are a novel pathway for membrane-type 1 matrix metalloproteinase traffic in human endothelial cells. *Mol. Biol. Cell* 15, 678–687. <https://doi.org/10.1091/mbc.e03-07-0516>
- García, E., Machesky, L.M., Jones, G.E., Antón, I.M., 2014. WIP is necessary for matrix invasion by breast cancer cells. *Eur. J. Cell Biol.* 93, 413–423. <https://doi.org/10.1016/j.ejcb.2014.07.008>
- Garrod, D., Chidgey, M., 2008. Desmosome structure, composition and function. *Biochim. Biophys. Acta* 1778, 572–587. <https://doi.org/10.1016/j.bbamem.2007.07.014>
- Gawden-Bone, C., Zhou, Z., King, E., Prescott, A., Watts, C., Lucocq, J., 2010. Dendritic cell podosomes are protrusive and invade the extracellular matrix using metalloproteinase MMP-14. *J. Cell. Sci.* 123, 1427–1437. <https://doi.org/10.1242/jcs.056515>
- Genot, E., Daubon, T., Sorrentino, V., Buccione, R., 2012. FGD1 as a central regulator of extracellular matrix remodelling--lessons from faciogenital dysplasia. *J. Cell. Sci.* 125, 3265–3270. <https://doi.org/10.1242/jcs.093419>
- Génot, E., Gligorijevic, B., 2014. Invadosomes in their natural habitat. *Eur. J. Cell Biol.* 93, 367–379. <https://doi.org/10.1016/j.ejcb.2014.10.002>
- Gherssi, G., Zhao, Q., Salamone, M., Yeh, Y., Zucker, S., Chen, W.-T., 2006. The protease complex consisting of dipeptidyl peptidase IV and seprase plays a role in the migration and invasion of

- human endothelial cells in collagenous matrices. *Cancer Res.* 66, 4652–4661. <https://doi.org/10.1158/0008-5472.CAN-05-1245>
- Giampieri, S., Manning, C., Hooper, S., Jones, L., Hill, C.S., Sahai, E., 2009. Localized and reversible TGFbeta signalling switches breast cancer cells from cohesive to single cell motility. *Nat. Cell Biol.* 11, 1287–1296. <https://doi.org/10.1038/ncb1973>
- Gianni, D., Diaz, B., Taulet, N., Fowler, B., Courtneidge, S.A., Bokoch, G.M., 2009. Novel p47(phox)-related organizers regulate localized NADPH oxidase 1 (Nox1) activity. *Sci Signal* 2, ra54. <https://doi.org/10.1126/scisignal.2000370>
- Gianni, D., Taulet, N., DerMardirossian, C., Bokoch, G.M., 2010a. c-Src-mediated phosphorylation of NoxA1 and Tks4 induces the reactive oxygen species (ROS)-dependent formation of functional invadopodia in human colon cancer cells. *Mol. Biol. Cell* 21, 4287–4298. <https://doi.org/10.1091/mbc.E10-08-0685>
- Gianni, D., Taulet, N., Zhang, H., DerMardirossian, C., Kister, J., Martinez, L., Roush, W.R., Brown, S.J., Bokoch, G.M., Rosen, H., 2010b. A novel and specific NADPH oxidase-1 (Nox1) small-molecule inhibitor blocks the formation of functional invadopodia in human colon cancer cells. *ACS Chem. Biol.* 5, 981–993. <https://doi.org/10.1021/cb100219n>
- Gierke, S., Wittmann, T., 2012. EB1-recruited microtubule +TIP complexes coordinate protrusion dynamics during 3D epithelial remodeling. *Curr. Biol.* 22, 753–762. <https://doi.org/10.1016/j.cub.2012.02.069>
- Gilles, C., Polette, M., Seiki, M., Birembaut, P., Thompson, E.W., 1997. Implication of collagen type I-induced membrane-type 1-matrix metalloproteinase expression and matrix metalloproteinase-2 activation in the metastatic progression of breast carcinoma. *Lab. Invest.* 76, 651–660.
- Gillet, L., Roger, S., Besson, P., Lecaille, F., Gore, J., Bougnoux, P., Lalmanach, G., Le Guennec, J.-Y., 2009. Voltage-gated Sodium Channel Activity Promotes Cysteine Cathepsin-dependent Invasiveness and Colony Growth of Human Cancer Cells. *J. Biol. Chem.* 284, 8680–8691. <https://doi.org/10.1074/jbc.M806891200>
- Gimona, M., Buccione, R., Courtneidge, S.A., Linder, S., 2008. Assembly and biological role of podosomes and invadopodia. *Curr. Opin. Cell Biol.* 20, 235–241. <https://doi.org/10.1016/j.ceb.2008.01.005>
- Gioia, M., Monaco, S., Fasciglione, G.F., Coletti, A., Modesti, A., Marini, S., Coletta, M., 2007. Characterization of the mechanisms by which gelatinase A, neutrophil collagenase, and membrane-type metalloproteinase MMP-14 recognize collagen I and enzymatically process the two alpha-chains. *J. Mol. Biol.* 368, 1101–1113. <https://doi.org/10.1016/j.jmb.2007.02.076>
- Glasheen, B.M., Kabra, A.T., Page-McCaw, A., 2009. Distinct functions for the catalytic and hemopexin domains of a Drosophila matrix metalloproteinase. *Proc. Natl. Acad. Sci. U.S.A.* 106, 2659–2664. <https://doi.org/10.1073/pnas.0804171106>
- Glentis, A., Gurchenkov, V., Matic Vignjevic, D., 2014. Assembly, heterogeneity, and breaching of the basement membranes. *Cell Adh Migr* 8, 236–245.
- Glentis, A., Oertle, P., Mariani, P., Chikina, A., El Marjou, F., Attieh, Y., Zaccarini, F., Lae, M., Loew, D., Dingli, F., Sirven, P., Schoumacher, M., Gurchenkov, B.G., Plodinec, M., Vignjevic, D.M., 2017. Cancer-associated fibroblasts induce metalloprotease-independent cancer cell invasion of the basement membrane. *Nat Commun* 8, 924. <https://doi.org/10.1038/s41467-017-00985-8>
- Gligorijevic, B., Bergman, A., Condeelis, J., 2014. Multiparametric classification links tumor microenvironments with tumor cell phenotype. *PLoS Biol.* 12, e1001995. <https://doi.org/10.1371/journal.pbio.1001995>
- Gligorijevic, B., Wyckoff, J., Yamaguchi, H., Wang, Y., Roussos, E.T., Condeelis, J., 2012. N-WASP-mediated invadopodium formation is involved in intravasation and lung metastasis of mammary tumors. *J. Cell. Sci.* 125, 724–734. <https://doi.org/10.1242/jcs.092726>
- Goetz, J.G., Minguet, S., Navarro-Lérida, I., Lazcano, J.J., Samaniego, R., Calvo, E., Tello, M., Osteso-Ibáñez, T., Pellinen, T., Echarrí, A., Cerezo, A., Klein-Szanto, A.J.P., Garcia, R., Keely, P.J., Sánchez-Mateos, P., Cukierman, E., Del Pozo, M.A., 2011. Biomechanical remodeling of the microenvironment by stromal caveolin-1 favors tumor invasion and metastasis. *Cell* 146, 148–163. <https://doi.org/10.1016/j.cell.2011.05.040>
- Goudarzi, M., Banisch, T.U., Mobin, M.B., Maghelli, N., Tarbashevich, K., Strate, I., van den Berg, J., Blaser, H., Bandemer, S., Paluch, E., Bakkers, J., Tolić-Nørrelykke, I.M., Raz, E., 2012.

- Identification and regulation of a molecular module for bleb-based cell motility. *Dev. Cell* 23, 210–218. <https://doi.org/10.1016/j.devcel.2012.05.007>
- Graham, D.M., Burridge, K., 2016. Mechanotransduction and nuclear function. *Curr. Opin. Cell Biol.* 40, 98–105. <https://doi.org/10.1016/j.ceb.2016.03.006>
- Granger, E., McNee, G., Allan, V., Woodman, P., 2014. The role of the cytoskeleton and molecular motors in endosomal dynamics. *Semin Cell Dev Biol* 31, 20–29. <https://doi.org/10.1016/j.semcdb.2014.04.011>
- Greco, M.R., Antelmi, E., Busco, G., Guerra, L., Rubino, R., Casavola, V., Reshkin, S.J., Cardone, R.A., 2014. Protease activity at invadopodial focal digestive areas is dependent on NHE1-driven acidic pH. *Oncol. Rep.* 31, 940–946. <https://doi.org/10.3892/or.2013.2923>
- Green, K.J., Getsios, S., Troyanovsky, S., Godsel, L.M., 2010. Intercellular junction assembly, dynamics, and homeostasis. *Cold Spring Harb Perspect Biol* 2, a000125. <https://doi.org/10.1101/cshperspect.a000125>
- Grigore, A.D., Jolly, M.K., Jia, D., Farach-Carson, M.C., Levine, H., 2016. Tumor Budding: The Name is EMT. Partial EMT. *J Clin Med* 5. <https://doi.org/10.3390/jcm5050051>
- Gritsenko, P.G., Ilina, O., Friedl, P., 2012. Interstitial guidance of cancer invasion. *J. Pathol.* 226, 185–199. <https://doi.org/10.1002/path.3031>
- Gudjonsson, T., Adriance, M.C., Sternlicht, M.D., Petersen, O.W., Bissell, M.J., 2005. Myoepithelial cells: their origin and function in breast morphogenesis and neoplasia. *J Mammary Gland Biol Neoplasia* 10, 261–272. <https://doi.org/10.1007/s10911-005-9586-4>
- Guilluy, C., Osborne, L.D., Van Landeghem, L., Sharek, L., Superfine, R., Garcia-Mata, R., Burridge, K., 2014. Isolated nuclei adapt to force and reveal a mechanotransduction pathway in the nucleus. *Nat. Cell Biol.* 16, 376–381. <https://doi.org/10.1038/ncb2927>
- Guilluy, C., Swaminathan, V., Garcia-Mata, R., O'Brien, E.T., Superfine, R., Burridge, K., 2011. The Rho GEFs LARG and GEF-H1 regulate the mechanical response to force on integrins. *Nat. Cell Biol.* 13, 722–727. <https://doi.org/10.1038/ncb2254>
- Guinebreière, J.M., Menet, E., Tardivon, A., Cherel, P., Vanel, D., 2005. Normal and pathological breast, the histological basis. *Eur J Radiol* 54, 6–14. <https://doi.org/10.1016/j.ejrad.2004.11.020>
- Gunasinghe, N.P.A.D., Wells, A., Thompson, E.W., Hugo, H.J., 2012. Mesenchymal-epithelial transition (MET) as a mechanism for metastatic colonisation in breast cancer. *Cancer Metastasis Rev.* 31, 469–478. <https://doi.org/10.1007/s10555-012-9377-5>
- Gundersen, G.G., Worman, H.J., 2013. Nuclear positioning. *Cell* 152, 1376–1389. <https://doi.org/10.1016/j.cell.2013.02.031>
- Gutiérrez-Fernández, A., Soria-Valles, C., Osorio, F.G., Gutiérrez-Abril, J., Garabaya, C., Aguirre, A., Fueyo, A., Fernández-García, M.S., Puente, X.S., López-Otín, C., 2015. Loss of MT1-MMP causes cell senescence and nuclear defects which can be reversed by retinoic acid. *EMBO J.* <https://doi.org/10.15252/embj.201490594>
- Haaksma, C.J., Schwartz, R.J., Tomasek, J.J., 2011. Myoepithelial cell contraction and milk ejection are impaired in mammary glands of mice lacking smooth muscle alpha-actin. *Biol. Reprod.* 85, 13–21. <https://doi.org/10.1095/biolreprod.110.090639>
- Haas, T.L., Stitelman, D., Davis, S.J., Apte, S.S., Madri, J.A., 1999. Egr-1 mediates extracellular matrix-driven transcription of membrane type 1 matrix metalloproteinase in endothelium. *J. Biol. Chem.* 274, 22679–22685.
- Hamidi, H., Ivaska, J., 2018. Every step of the way: integrins in cancer progression and metastasis. *Nat. Rev. Cancer* 18, 533–548. <https://doi.org/10.1038/s41568-018-0038-z>
- Han, J., Luo, T., Gu, Y., Li, G., Jia, W., Luo, M., 2009. Cathepsin K regulates adipocyte differentiation: possible involvement of type I collagen degradation. *Endocr. J.* 56, 55–63.
- Han, W., Chen, S., Yuan, W., Fan, Q., Tian, J., Wang, X., Chen, L., Zhang, X., Wei, W., Liu, R., Qu, J., Jiao, Y., Austin, R.H., Liu, L., 2016. Oriented collagen fibers direct tumor cell intravasation. *Proc. Natl. Acad. Sci. U.S.A.* 113, 11208–11213. <https://doi.org/10.1073/pnas.1610347113>
- Hanahan, D., Weinberg, R.A., 2011. Hallmarks of cancer: the next generation. *Cell* 144, 646–674. <https://doi.org/10.1016/j.cell.2011.02.013>
- Hangai, M., Kitaya, N., Xu, J., Chan, C.K., Kim, J.J., Werb, Z., Ryan, S.J., Brooks, P.C., 2002. Matrix Metalloproteinase-9-Dependent Exposure of a Cryptic Migratory Control Site in Collagen is Required before Retinal Angiogenesis. *Am J Pathol* 161, 1429–1437.

- Hansen, C., Greengard, P., Nairn, A.C., Andersson, T., Vogel, W.F., 2006. Phosphorylation of DARPP-32 regulates breast cancer cell migration downstream of the receptor tyrosine kinase DDR1. *Exp. Cell Res.* 312, 4011–4018. <https://doi.org/10.1016/j.yexcr.2006.09.003>
- Harada, T., Swift, J., Irianto, J., Shin, J.-W., Spinler, K.R., Athirasala, A., Diegmiller, R., Dingal, P.C.D.P., Ivanovska, I.L., Discher, D.E., 2014. Nuclear lamin stiffness is a barrier to 3D migration, but softness can limit survival. *J. Cell Biol.* 204, 669–682. <https://doi.org/10.1083/jcb.201308029>
- Harbour, M.E., Breusegem, S.Y., Seaman, M.N.J., 2012. Recruitment of the endosomal WASH complex is mediated by the extended “tail” of Fam21 binding to the retromer protein Vps35. *Biochem. J.* 442, 209–220. <https://doi.org/10.1042/BJ20111761>
- Harbour, M.E., Breusegem, S.Y.A., Antrobus, R., Freeman, C., Reid, E., Seaman, M.N.J., 2010. The cargo-selective retromer complex is a recruiting hub for protein complexes that regulate endosomal tubule dynamics. *J. Cell. Sci.* 123, 3703–3717. <https://doi.org/10.1242/jcs.071472>
- Harper, K.L., Sosa, M.S., Entenberg, D., Hosseini, H., Cheung, J.F., Nobre, R., Avivar-Valderas, A., Nagi, C., Girmius, N., Davis, R.J., Farias, E.F., Condeelis, J., Klein, C.A., Aguirre-Ghiso, J.A., 2016. Mechanism of early dissemination and metastasis in Her2⁺ mammary cancer. *Nature*. <https://doi.org/10.1038/nature20609>
- Hartman, M.A., Spudich, J.A., 2012. The myosin superfamily at a glance. *J Cell Sci* 125, 1627–1632. <https://doi.org/10.1242/jcs.094300>
- Hatch, E.M., Hetzer, M.W., 2016. Nuclear envelope rupture is induced by actin-based nucleus confinement. *J. Cell Biol.* 215, 27–36. <https://doi.org/10.1083/jcb.201603053>
- Hawkins, P.T., Stephens, L.R., 2016. Emerging evidence of signalling roles for PI(3,4)P₂ in Class I and II PI3K-regulated pathways. *Biochem. Soc. Trans.* 44, 307–314. <https://doi.org/10.1042/BST20150248>
- Heissler, S.M., Sellers, J.R., 2016. Kinetic Adaptations of Myosins for their Diverse Cellular Functions. *Traffic* 17, 839–859. <https://doi.org/10.1111/tra.12388>
- Henriet, E., Sala, M., Abou Hammoud, A., Tuariiionoa, A., Di Martino, J., Ros, M., Saltel, F., 2018. Multitasking discoidin domain receptors are involved in several and specific hallmarks of cancer. *Cell Adh Migr* 12, 363–377. <https://doi.org/10.1080/19336918.2018.1465156>
- Hernandez, M., Patzig, J., Mayoral, S.R., Costa, K.D., Chan, J.R., Casaccia, P., 2016. Mechanostimulation Promotes Nuclear and Epigenetic Changes in Oligodendrocytes. *J. Neurosci.* 36, 806–813. <https://doi.org/10.1523/JNEUROSCI.2873-15.2016>
- Herschkowitz, J.I., Simin, K., Weigman, V.J., Mikaelian, I., Usary, J., Hu, Z., Rasmussen, K.E., Jones, L.P., Assefnia, S., Chandrasekharan, S., Backlund, M.G., Yin, Y., Khramtsov, A.I., Bastein, R., Quackenbush, J., Glazer, R.I., Brown, P.H., Green, J.E., Kopelovich, L., Furth, P.A., Palazzo, J.P., Olopade, O.I., Bernard, P.S., Churchill, G.A., Van Dyke, T., Perou, C.M., 2007. Identification of conserved gene expression features between murine mammary carcinoma models and human breast tumors. *Genome Biol.* 8, R76. <https://doi.org/10.1186/gb-2007-8-5-r76>
- Holmbeck, K., Bianco, P., Caterina, J., Yamada, S., Kromer, M., Kuznetsov, S.A., Mankani, M., Robey, P.G., Poole, A.R., Pidoux, I., Ward, J.M., Birkedal-Hansen, H., 1999. MT1-MMP-deficient mice develop dwarfism, osteopenia, arthritis, and connective tissue disease due to inadequate collagen turnover. *Cell* 99, 81–92.
- Holmes, D.F., Lu, Y., Starborg, T., Kadler, K.E., 2018. Collagen Fibril Assembly and Function. *Curr. Top. Dev. Biol.* 130, 107–142. <https://doi.org/10.1016/bs.ctdb.2018.02.004>
- Hong, I.-K., Byun, H.-J., Lee, J., Jin, Y.-J., Wang, S.-J., Jeoung, D.-I., Kim, Y.-M., Lee, H., 2014. The tetraspanin CD81 protein increases melanoma cell motility by up-regulating metalloproteinase MT1-MMP expression through the pro-oncogenic Akt-dependent Sp1 activation signaling pathways. *J. Biol. Chem.* 289, 15691–15704. <https://doi.org/10.1074/jbc.M113.534206>
- Hoshino, D., Branch, K.M., Weaver, A.M., 2013. Signaling inputs to invadopodia and podosomes. *J. Cell. Sci.* 126, 2979–2989. <https://doi.org/10.1242/jcs.079475>
- Hoshino, D., Koshikawa, N., Suzuki, T., Quaranta, V., Weaver, A.M., Seiki, M., Ichikawa, K., 2012. Establishment and validation of computational model for MT1-MMP dependent ECM degradation and intervention strategies. *PLoS Comput. Biol.* 8, e1002479. <https://doi.org/10.1371/journal.pcbi.1002479>

- Hosseini, H., Obradović, M.M.S., Hoffmann, M., Harper, K.L., Sosa, M.S., Werner-Klein, M., Nanduri, L.K., Werno, C., Ehrl, C., Maneck, M., Patwary, N., Haunschild, G., Gužvić, M., Reimelt, C., Grauvogl, M., Eichner, N., Weber, F., Hartkopf, A.D., Taran, F.-A., Brucker, S.Y., Fehm, T., Rack, B., Buchholz, S., Spang, R., Meister, G., Aguirre-Ghiso, J.A., Klein, C.A., 2016. Early dissemination seeds metastasis in breast cancer. *Nature*. <https://doi.org/10.1038/nature20785>
- Hotary, K., Allen, E., Punturieri, A., Yana, I., Weiss, S.J., 2000. Regulation of cell invasion and morphogenesis in a three-dimensional type I collagen matrix by membrane-type matrix metalloproteinases 1, 2, and 3. *J. Cell Biol.* 149, 1309–1323.
- Hotary, K., Li, X.-Y., Allen, E., Stevens, S.L., Weiss, S.J., 2006. A cancer cell metalloprotease triad regulates the basement membrane transmigration program. *Genes Dev.* 20, 2673–2686. <https://doi.org/10.1101/gad.1451806>
- Hotary, K.B., Allen, E.D., Brooks, P.C., Datta, N.S., Long, M.W., Weiss, S.J., 2003. Membrane type I matrix metalloproteinase usurps tumor growth control imposed by the three-dimensional extracellular matrix. *Cell* 114, 33–45.
- Hovey, R.C., Aimo, L., 2010. Diverse and active roles for adipocytes during mammary gland growth and function. *J Mammary Gland Biol Neoplasia* 15, 279–290. <https://doi.org/10.1007/s10911-010-9187-8>
- Howard, B.A., Gusterson, B.A., 2000. Human breast development. *J Mammary Gland Biol Neoplasia* 5, 119–137.
- Huang, Y., Arora, P., McCulloch, C.A., Vogel, W.F., 2009. The collagen receptor DDR1 regulates cell spreading and motility by associating with myosin IIA. *J. Cell. Sci.* 122, 1637–1646. <https://doi.org/10.1242/jcs.046219>
- Huebner, R.J., Ewald, A.J., 2014. Cellular foundations of mammary tubulogenesis. *Semin. Cell Dev. Biol.* 31, 124–131. <https://doi.org/10.1016/j.semcdb.2014.04.019>
- Hugo, H., Ackland, M.L., Blick, T., Lawrence, M.G., Clements, J.A., Williams, E.D., Thompson, E.W., 2007. Epithelial--mesenchymal and mesenchymal--epithelial transitions in carcinoma progression. *J. Cell. Physiol.* 213, 374–383. <https://doi.org/10.1002/jcp.21223>
- Humbert, P.O., Dow, L.E., Russell, S.M., 2006. The Scribble and Par complexes in polarity and migration: friends or foes? *Trends Cell Biol.* 16, 622–630. <https://doi.org/10.1016/j.tcb.2006.10.005>
- Humphries, J.D., Byron, A., Humphries, M.J., 2006. Integrin ligands at a glance. *J. Cell. Sci.* 119, 3901–3903. <https://doi.org/10.1242/jcs.03098>
- Huovila, A.-P.J., Turner, A.J., Peltö-Huikko, M., Kärkkäinen, I., Ortiz, R.M., 2005. Shedding light on ADAM metalloproteinases. *Trends Biochem. Sci.* 30, 413–422. <https://doi.org/10.1016/j.tibs.2005.05.006>
- Huttenlocher, A., Horwitz, A.R., 2011. Integrins in cell migration. *Cold Spring Harb Perspect Biol* 3, a005074. <https://doi.org/10.1101/cshperspect.a005074>
- Ihalainen, T.O., Aires, L., Herzog, F.A., Schwartlander, R., Moeller, J., Vogel, V., 2015. Differential basal-to-apical accessibility of lamin A/C epitopes in the nuclear lamina regulated by changes in cytoskeletal tension. *Nat Mater.* <https://doi.org/10.1038/nmat4389>
- Iizuka, S., Abdullah, C., Buschman, M.D., Diaz, B., Courtneidge, S.A., 2016. The role of Tks adaptor proteins in invadopodia formation, growth and metastasis of melanoma. *Oncotarget*. <https://doi.org/10.18632/oncotarget.12954>
- Infante, E., Castagnino, A., Ferrari, R., Monteiro, P., Agüera-González, S., Paul-Gilloteaux, P., Domingues, M.J., Maiuri, P., Raab, M., Shanahan, C.M., Baffet, A., Piel, M., Gomes, E.R., Chavrier, P., 2018. LINC complex-Lis1 interplay controls MT1-MMP matrix digest-on-demand response for confined tumor cell migration. *Nat Commun* 9, 2443. <https://doi.org/10.1038/s41467-018-04865-7>
- Ingman, W.V., Wyckoff, J., Gouon-Evans, V., Condeelis, J., Pollard, J.W., 2006. Macrophages promote collagen fibrillogenesis around terminal end buds of the developing mammary gland. *Dev. Dyn.* 235, 3222–3229. <https://doi.org/10.1002/dvdy.20972>
- Inman, J.L., Robertson, C., Mott, J.D., Bissell, M.J., 2015. Mammary gland development: cell fate specification, stem cells and the microenvironment. *Development* 142, 1028–1042. <https://doi.org/10.1242/dev.087643>

- Insua-Rodríguez, J., Oskarsson, T., 2016. The extracellular matrix in breast cancer. *Adv. Drug Deliv. Rev.* 97, 41–55. <https://doi.org/10.1016/j.addr.2015.12.017>
- Iqbal, Z., Cejudo-Martin, P., de Brouwer, A., van der Zwaag, B., Ruiz-Lozano, P., Scimia, M.C., Lindsey, J.D., Weinreb, R., Albrecht, B., Megarbane, A., Alanay, Y., Ben-Neriah, Z., Amenduni, M., Artuso, R., Veltman, J.A., van Beusekom, E., Oudakker, A., Millán, J.L., Hennekam, R., Hamel, B., Courtneidge, S.A., van Bokhoven, H., 2010. Disruption of the podosome adaptor protein TKS4 (SH3PXD2B) causes the skeletal dysplasia, eye, and cardiac abnormalities of Frank-Ter Haar Syndrome. *Am. J. Hum. Genet.* 86, 254–261. <https://doi.org/10.1016/j.ajhg.2010.01.009>
- Irianto, J., Xia, Y., Pfeifer, C.R., Athirasala, A., Ji, J., Alvey, C., Tewari, M., Bennett, R., Harding, S.M., Liu, A., Greenberg, R.A., Discher, D.E., 2017a. DNA damage follows repair factor depletion and portends genome variation in cancer cells after pore migration. *Curr Biol* 27, 210–223. <https://doi.org/10.1016/j.cub.2016.11.049>
- Irianto, J., Xia, Y., Pfeifer, C.R., Greenberg, R.A., Discher, D.E., 2017b. As a Nucleus Enters a Small Pore, Chromatin Stretches and Maintains Integrity, Even with DNA Breaks. *Biophys. J.* 112, 446–449. <https://doi.org/10.1016/j.bpj.2016.09.047>
- Isermann, P., Lammerding, J., 2017. Consequences of a tight squeeze: Nuclear envelope rupture and repair. *Nucleus* 8, 268–274. <https://doi.org/10.1080/19491034.2017.1292191>
- Isermann, P., Lammerding, J., 2013. Nuclear Mechanics and Mechanotransduction in Health and Disease. *Curr Biol* 23. <https://doi.org/10.1016/j.cub.2013.11.009>
- Itoh, Y., 2015. Membrane-type matrix metalloproteinases: Their functions and regulations. *Matrix Biol.* 44–46, 207–223. <https://doi.org/10.1016/j.matbio.2015.03.004>
- Itoh, Y., Ito, N., Nagase, H., Evans, R.D., Bird, S.A., Seiki, M., 2006. Cell surface collagenolysis requires homodimerization of the membrane-bound collagenase MT1-MMP. *Mol. Biol. Cell* 17, 5390–5399. <https://doi.org/10.1091/mbc.e06-08-0740>
- Itoh, Y., Ito, N., Nagase, H., Seiki, M., 2008. The second dimer interface of MT1-MMP, the transmembrane domain, is essential for ProMMP-2 activation on the cell surface. *J. Biol. Chem.* 283, 13053–13062. <https://doi.org/10.1074/jbc.M709327200>
- Itoh, Y., Palmisano, R., Anilkumar, N., Nagase, H., Miyawaki, A., Seiki, M., 2011. Dimerization of MT1-MMP during cellular invasion detected by fluorescence resonance energy transfer. *Biochem. J.* 440, 319–326. <https://doi.org/10.1042/BJ20110424>
- Itoh, Y., Seiki, M., 2006. MT1-MMP: a potent modifier of pericellular microenvironment. *J. Cell. Physiol.* 206, 1–8. <https://doi.org/10.1002/jcp.20431>
- Jahed, Z., Shams, H., Mehrbod, M., Mofrad, M.R.K., 2014. Mechanotransduction pathways linking the extracellular matrix to the nucleus. *Int Rev Cell Mol Biol* 310, 171–220. <https://doi.org/10.1016/B978-0-12-800180-6.00005-0>
- Jeannot, P., Besson, A., 2017. Cortactin function in invadopodia. *Small GTPases* 1–15. <https://doi.org/10.1080/21541248.2017.1405773>
- Jevnikar, Z., Mirković, B., Fonović, U.P., Zidar, N., Švajger, U., Kos, J., 2012. Three-dimensional invasion of macrophages is mediated by cysteine cathepsins in protrusive podosomes. *Eur. J. Immunol.* 42, 3429–3441. <https://doi.org/10.1002/eji.201242610>
- Jiang, A., Lehti, K., Wang, X., Weiss, S.J., Keski-Oja, J., Pei, D., 2001. Regulation of membrane-type matrix metalloproteinase 1 activity by dynamin-mediated endocytosis. *Proc. Natl. Acad. Sci. U.S.A.* 98, 13693–13698. <https://doi.org/10.1073/pnas.241293698>
- Johnson, J.L., Pillai, S., Pernazza, D., Sebt, S.M., Lawrence, N.J., Chellappan, S.P., 2012. Regulation of matrix metalloproteinase genes by E2F transcription factors: Rb-Raf-1 interaction as a novel target for metastatic disease. *Cancer Res.* 72, 516–526. <https://doi.org/10.1158/0008-5472.CAN-11-2647>
- Joosten, B., Willemse, M., Fransen, J., Cambi, A., van den Dries, K., 2018. Super-Resolution Correlative Light and Electron Microscopy (SR-CLEM) Reveals Novel Ultrastructural Insights Into Dendritic Cell Podosomes. *Front Immunol* 9, 1908. <https://doi.org/10.3389/fimmu.2018.01908>
- Jorrich, M.H., Shih, W., Yamada, S., 2013. Myosin IIA deficient cells migrate efficiently despite reduced traction forces at cell periphery. *Biol Open* 2, 368–372. <https://doi.org/10.1242/bio.20133707>

- Juin, A., Billottet, C., Moreau, V., Destaing, O., Albiges-Rizo, C., Rosenbaum, J., Génot, E., Saltel, F., 2012. Physiological type I collagen organization induces the formation of a novel class of linear invadosomes. *Mol. Biol. Cell* 23, 297–309. <https://doi.org/10.1091/mbc.E11-07-0594>
- Juin, A., Di Martino, J., Leitinger, B., Henriët, E., Gary, A.-S., Paysan, L., Bomo, J., Baffet, G., Gauthier-Rouvière, C., Rosenbaum, J., Moreau, V., Saltel, F., 2014. Discoidin domain receptor 1 controls linear invadosome formation via a Cdc42-Tuba pathway. *J. Cell Biol.* 207, 517–533. <https://doi.org/10.1083/jcb.201404079>
- Kajiho, H., Kajiho, Y., Frittoli, E., Confalonieri, S., Bertalot, G., Viale, G., Di Fiore, P.P., Oldani, A., Garre, M., Beznoussenko, G.V., Palamidessi, A., Vecchi, M., Chavrier, P., Perez, F., Scita, G., 2016. RAB2A controls MT1-MMP endocytic and E-cadherin polarized Golgi trafficking to promote invasive breast cancer programs. *EMBO Rep.* 17, 1061–1080. <https://doi.org/10.15252/embr.201642032>
- Kalluri, R., 2003. Basement membranes: structure, assembly and role in tumour angiogenesis. *Nat. Rev. Cancer* 3, 422–433. <https://doi.org/10.1038/nrc1094>
- Kalluri, R., Weinberg, R.A., 2009. The basics of epithelial-mesenchymal transition. *J. Clin. Invest.* 119, 1420–1428. <https://doi.org/10.1172/JCI39104>
- Kedinger, M., Lefebvre, O., Duluc, I., Freund, J.N., Simon-Assmann, P., 1998. Cellular and molecular partners involved in gut morphogenesis and differentiation. *Philos. Trans. R. Soc. Lond., B, Biol. Sci.* 353, 847–856. <https://doi.org/10.1098/rstb.1998.0249>
- Kedrin, D., Gligorijevic, B., Wyckoff, J., Verkhusha, V.V., Condeelis, J., Segall, J.E., van Rheenen, J., 2008. Intravital imaging of metastatic behavior through a mammary imaging window. *Nat. Methods* 5, 1019–1021. <https://doi.org/10.1038/nmeth.1269>
- Kelley, L.C., Lohmer, L.L., Hagedorn, E.J., Sherwood, D.R., 2014. Traversing the basement membrane in vivo: A diversity of strategies. *J. Cell Biol.* 204, 291–302. <https://doi.org/10.1083/jcb.201311112>
- Keren, K., Pincus, Z., Allen, G.M., Barnhart, E.L., Marriott, G., Mogilner, A., Theriot, J.A., 2008. Mechanism of shape determination in motile cells. *Nature* 453, 475–480. <https://doi.org/10.1038/nature06952>
- Kessenbrock, K., Plaks, V., Werb, Z., 2010. Matrix Metalloproteinases: Regulators of the Tumor Microenvironment. *Cell* 141, 52–67. <https://doi.org/10.1016/j.cell.2010.03.015>
- Kessenbrock, K., Wang, C.-Y., Werb, Z., 2015. Matrix metalloproteinases in stem cell regulation and cancer. *Matrix Biol.* <https://doi.org/10.1016/j.matbio.2015.01.022>
- Khaket, T.P., Kwon, T.K., Kang, S.C., 2019. Cathepsins: Potent regulators in carcinogenesis. *Pharmacol. Ther.* <https://doi.org/10.1016/j.pharmthera.2019.02.003>
- Khoshnoodi, J., Pedchenko, V., Hudson, B.G., 2008. Mammalian collagen IV. *Microsc. Res. Tech.* 71, 357–370. <https://doi.org/10.1002/jemt.20564>
- Kim, D., Jung, J., You, E., Ko, P., Oh, S., Rhee, S., 2016. mDial regulates breast cancer invasion by controlling membrane type 1-matrix metalloproteinase localization. *Oncotarget* 7, 17829–17843. <https://doi.org/10.18632/oncotarget.7429>
- Kim, D.-H., Wirtz, D., 2015. Cytoskeletal tension induces the polarized architecture of the nucleus. *Biomaterials* 48, 161–172. <https://doi.org/10.1016/j.biomaterials.2015.01.023>
- Kirkbride, K.C., Sung, B.H., Sinha, S., Weaver, A.M., 2011. Cortactin: a multifunctional regulator of cellular invasiveness. *Cell Adh Migr* 5, 187–198.
- Kirmse, R., Otto, H., Ludwig, T., 2011. Interdependency of cell adhesion, force generation and extracellular proteolysis in matrix remodeling. *J. Cell. Sci.* 124, 1857–1866. <https://doi.org/10.1242/jcs.079343>
- Klein, C.A., 2009. Parallel progression of primary tumours and metastases. *Nat. Rev. Cancer* 9, 302–312. <https://doi.org/10.1038/nrc2627>
- Kleinman, H.K., Martin, G.R., 2005. Matrigel: basement membrane matrix with biological activity. *Semin. Cancer Biol.* 15, 378–386. <https://doi.org/10.1016/j.semcancer.2005.05.004>
- Knopf, J.D., Tholen, S., Koczorowska, M.M., De Wever, O., Biniowski, M.L., Schilling, O., 2015. The stromal cell-surface protease fibroblast activation protein- α localizes to lipid rafts and is recruited to invadopodia. *Biochim. Biophys. Acta* 1853, 2515–2525. <https://doi.org/10.1016/j.bbamcr.2015.07.013>

- Koh, M., Woo, Y., Valiathan, R.R., Jung, H.Y., Park, S.Y., Kim, Y.N., Kim, H.-R.C., Fridman, R., Moon, A., 2015. Discoidin domain receptor 1 is a novel transcriptional target of ZEB1 in breast epithelial cells undergoing H-Ras-induced epithelial to mesenchymal transition. *Int. J. Cancer* 136, E508-520. <https://doi.org/10.1002/ijc.29154>
- Kolb, T., Maass, K., Hergt, M., Aebi, U., Herrmann, H., 2011. Lamin A and lamin C form homodimers and coexist in higher complex forms both in the nucleoplasmic fraction and in the lamina of cultured human cells. *Nucleus* 2, 425–433. <https://doi.org/10.4161/nucl.2.5.17765>
- Komori, K., Nonaka, T., Okada, A., Kinoh, H., Hayashita-Kinoh, H., Yoshida, N., Yana, I., Seiki, M., 2004. Absence of mechanical allodynia and Abeta-fiber sprouting after sciatic nerve injury in mice lacking membrane-type 5 matrix metalloproteinase. *FEBS Lett.* 557, 125–128.
- Kovar, D.R., Pollard, T.D., 2004. Insertional assembly of actin filament barbed ends in association with formins produces piconewton forces. *Proc. Natl. Acad. Sci. U.S.A.* 101, 14725–14730. <https://doi.org/10.1073/pnas.0405902101>
- Kraning-Rush, C.M., Carey, S.P., Lampi, M.C., Reinhart-King, C.A., 2013. Microfabricated collagen tracks facilitate single cell metastatic invasion in 3D. *Integr Biol (Camb)* 5, 606–616. <https://doi.org/10.1039/c3ib20196a>
- Kusuma, N., Denoyer, D., Eble, J.A., Redvers, R.P., Parker, B.S., Pelzer, R., Anderson, R.L., Pouliot, N., 2012. Integrin-dependent response to laminin-511 regulates breast tumor cell invasion and metastasis. *Int. J. Cancer* 130, 555–566. <https://doi.org/10.1002/ijc.26018>
- Labernadie, A., Bouissou, A., Delobelle, P., Balor, S., Voituriez, R., Proag, A., Fourquaux, I., Thibault, C., Vieu, C., Poincloux, R., Charrière, G.M., Maridonneau-Parini, I., 2014. Protrusion force microscopy reveals oscillatory force generation and mechanosensing activity of human macrophage podosomes. *Nat Commun* 5, 5343. <https://doi.org/10.1038/ncomms6343>
- Lafleur, M.A., Mercuri, F.A., Ruangpanit, N., Seiki, M., Sato, H., Thompson, E.W., 2006. Type I collagen abrogates the clathrin-mediated internalization of membrane type 1 matrix metalloproteinase (MT1-MMP) via the MT1-MMP hemopexin domain. *J. Biol. Chem.* 281, 6826–6840. <https://doi.org/10.1074/jbc.M513084200>
- Lagoutte, E., Villeneuve, C., Lafanechère, L., Wells, C.M., Jones, G.E., Chavrier, P., Rossé, C., 2016. LIMK Regulates Tumor-Cell Invasion and Matrix Degradation Through Tyrosine Phosphorylation of MT1-MMP. *Sci Rep* 6, 24925. <https://doi.org/10.1038/srep24925>
- Lammerding, J., Fong, L.G., Ji, J.Y., Reue, K., Stewart, C.L., Young, S.G., Lee, R.T., 2006. Lamins A and C but not lamin B1 regulate nuclear mechanics. *J. Biol. Chem.* 281, 25768–25780. <https://doi.org/10.1074/jbc.M513511200>
- Lammerding, J., Wolf, K., 2016. Nuclear envelope rupture: Actin fibers are putting the squeeze on the nucleus. *J. Cell Biol.* 215, 5–8. <https://doi.org/10.1083/jcb.201609102>
- Lamouille, S., Xu, J., Derynck, R., 2014. Molecular mechanisms of epithelial-mesenchymal transition. *Nat. Rev. Mol. Cell Biol.* 15, 178–196. <https://doi.org/10.1038/nrm3758>
- Lauffenburger, D.A., Horwitz, A.F., 1996. Cell migration: a physically integrated molecular process. *Cell* 84, 359–369.
- Lawson, C.D., Ridley, A.J., 2018. Rho GTPase signaling complexes in cell migration and invasion. *J. Cell Biol.* 217, 447–457. <https://doi.org/10.1083/jcb.201612069>
- Le, H.Q., Ghatak, S., Yeung, C.-Y.C., Tellkamp, F., Günschmann, C., Dieterich, C., Yeroslaviz, A., Habermann, B., Pombo, A., Niessen, C.M., Wickström, S.A., 2016. Mechanical regulation of transcription controls Polycomb-mediated gene silencing during lineage commitment. *Nat. Cell Biol.* 18, 864–875. <https://doi.org/10.1038/ncb3387>
- Leckband, D.E., de Rooij, J., 2014. Cadherin adhesion and mechanotransduction. *Annu. Rev. Cell Dev. Biol.* 30, 291–315. <https://doi.org/10.1146/annurev-cellbio-100913-013212>
- Lee, Y.-H., Albig, A.R., Regner, M., Schiemann, B.J., Schiemann, W.P., 2008. Fibulin-5 initiates epithelial-mesenchymal transition (EMT) and enhances EMT induced by TGF-beta in mammary epithelial cells via a MMP-dependent mechanism. *Carcinogenesis* 29, 2243–2251. <https://doi.org/10.1093/carcin/bgn199>
- Leitinger, B., 2014. Discoidin domain receptor functions in physiological and pathological conditions. *Int Rev Cell Mol Biol* 310, 39–87. <https://doi.org/10.1016/B978-0-12-800180-6.00002-5>
- Leitinger, B., 2011. Transmembrane collagen receptors. *Annu. Rev. Cell Dev. Biol.* 27, 265–290. <https://doi.org/10.1146/annurev-cellbio-092910-154013>

- Leitinger, B., 2003. Molecular analysis of collagen binding by the human discoidin domain receptors, DDR1 and DDR2. Identification of collagen binding sites in DDR2. *J. Biol. Chem.* 278, 16761–16769. <https://doi.org/10.1074/jbc.M301370200>
- Leong, H.S., Robertson, A.E., Stoletov, K., Leith, S.J., Chin, C.A., Chien, A.E., Hague, M.N., Ablack, A., Carmine-Simmen, K., McPherson, V.A., Postenka, C.O., Turley, E.A., Courtneidge, S.A., Chambers, A.F., Lewis, J.D., 2014. Invadopodia are required for cancer cell extravasation and are a therapeutic target for metastasis. *Cell Rep* 8, 1558–1570. <https://doi.org/10.1016/j.celrep.2014.07.050>
- Levental, K.R., Yu, H., Kass, L., Lakins, J.N., Egeblad, M., Erler, J.T., Fong, S.F.T., Csiszar, K., Giaccia, A., Weninger, W., Yamauchi, M., Gasser, D.L., Weaver, V.M., 2009. Matrix crosslinking forces tumor progression by enhancing integrin signaling. *Cell* 139, 891–906. <https://doi.org/10.1016/j.cell.2009.10.027>
- Li, A., Dawson, J.C., Forero-Vargas, M., Spence, H.J., Yu, X., König, I., Anderson, K., Machesky, L.M., 2010. The actin-bundling protein fascin stabilizes actin in invadopodia and potentiates protrusive invasion. *Curr. Biol.* 20, 339–345. <https://doi.org/10.1016/j.cub.2009.12.035>
- Li, C.M.-C., Chen, G., Dayton, T.L., Kim-Kiselak, C., Hoersch, S., Whittaker, C.A., Bronson, R.T., Beer, D.G., Winslow, M.M., Jacks, T., 2013. Differential Tks5 isoform expression contributes to metastatic invasion of lung adenocarcinoma. *Genes Dev.* 27, 1557–1567. <https://doi.org/10.1101/gad.222745.113>
- Li, X.-Y., Ota, I., Yana, I., Sabeh, F., Weiss, S.J., 2008. Molecular dissection of the structural machinery underlying the tissue-invasive activity of membrane type-1 matrix metalloproteinase. *Mol. Biol. Cell* 19, 3221–3233. <https://doi.org/10.1091/mbc.E08-01-0016>
- Li, Y., Kucsu, C., Banach, A., Zhang, Q., Pulkoski-Gross, A., Kim, D., Liu, J., Roth, E., Li, E., Shroyer, K.R., Denoya, P.I., Zhu, X., Chen, L., Cao, J., 2015. miR-181a-5p Inhibits Cancer Cell Migration and Angiogenesis via Downregulation of Matrix Metalloproteinase-14. *Cancer Res.* 75, 2674–2685. <https://doi.org/10.1158/0008-5472.CAN-14-2875>
- Lin, C.-Y., Tsai, P.-H., Kandaswami, C.C., Lee, P.-P., Huang, C.-J., Hwang, J.-J., Lee, M.-T., 2011. Matrix metalloproteinase-9 cooperates with transcription factor Snail to induce epithelial-mesenchymal transition. *Cancer Sci.* 102, 815–827. <https://doi.org/10.1111/j.1349-7006.2011.01861.x>
- Linder, S., 2007. The matrix corroded: podosomes and invadopodia in extracellular matrix degradation. *Trends Cell Biol.* 17, 107–117. <https://doi.org/10.1016/j.tcb.2007.01.002>
- Linder, S., Nelson, D., Weiss, M., Aepfelbacher, M., 1999. Wiskott-Aldrich syndrome protein regulates podosomes in primary human macrophages. *Proc. Natl. Acad. Sci. U.S.A.* 96, 9648–9653.
- Linder, S., Scita, G., 2015. RABGTPases in MT1-MMP trafficking and cell invasion: Physiology versus pathology. *Small GTPases* 6, 145–152. <https://doi.org/10.4161/21541248.2014.985484>
- Linder, S., Wiesner, C., 2016. Feel the force: Podosomes in mechanosensing. *Exp. Cell Res.* 343, 67–72. <https://doi.org/10.1016/j.yexcr.2015.11.026>
- Linder, S., Wiesner, C., Himmel, M., 2011. Degrading devices: invadosomes in proteolytic cell invasion. *Annu. Rev. Cell Dev. Biol.* 27, 185–211. <https://doi.org/10.1146/annurev-cellbio-092910-154216>
- Liu, J., Yue, P., Artym, V.V., Mueller, S.C., Guo, W., 2009. The role of the exocyst in matrix metalloproteinase secretion and actin dynamics during tumor cell invadopodia formation. *Mol. Biol. Cell* 20, 3763–3771. <https://doi.org/10.1091/mbc.e08-09-0967>
- Liu, J.-J., 2017. Regulation of dynein-dynactin-driven vesicular transport. *Traffic* 18, 336–347. <https://doi.org/10.1111/tra.12475>
- Liu, L., Luo, Q., Sun, J., Song, G., 2016. Nucleus and nucleus-cytoskeleton connections in 3D cell migration. *Exp. Cell Res.* <https://doi.org/10.1016/j.yexcr.2016.09.001>
- Livne, A., Geiger, B., 2016. The inner workings of stress fibers - from contractile machinery to focal adhesions and back. *J. Cell. Sci.* 129, 1293–1304. <https://doi.org/10.1242/jcs.180927>
- Lizárraga, F., Poincloux, R., Romao, M., Montagnac, G., Dez, G.L., Bonne, I., Rigail, G., Raposo, G., Chavrier, P., 2009. Diaphanous-Related Formins Are Required for Invadopodia Formation and Invasion of Breast Tumor Cells. *Cancer Res* 69, 2792–2800. <https://doi.org/10.1158/0008-5472.CAN-08-3709>

- Lloyd-Lewis, B., Harris, O.B., Watson, C.J., Davis, F.M., 2017. Mammary Stem Cells: Premise, Properties, and Perspectives. *Trends Cell Biol.* 27, 556–567. <https://doi.org/10.1016/j.tcb.2017.04.001>
- Lodillinsky, C., Infante, E., Guichard, A., Chaligné, R., Fuhrmann, L., Cyrta, J., Irondelle, M., Lagoutte, E., Vacher, S., Bonsang-Kitzis, H., Glukhova, M., Rey, F., Bièche, I., Vincent-Salomon, A., Chavrier, P., 2015. p63/MT1-MMP axis is required for in situ to invasive transition in basal-like breast cancer. *Oncogene*. <https://doi.org/10.1038/onc.2015.87>
- Lombardi, M.L., Lammerding, J., 2011. Keeping the LINC: the importance of nucleocytoplasmic coupling in intracellular force transmission and cellular function. *Biochem. Soc. Trans.* 39, 1729–1734. <https://doi.org/10.1042/BST20110686>
- Lorentzen, A., Bamber, J., Sadok, A., Elson-Schwab, I., Marshall, C.J., 2011. An ezrin-rich, rigid uropod-like structure directs movement of amoeboid blebbing cells. *J. Cell. Sci.* 124, 1256–1267. <https://doi.org/10.1242/jcs.074849>
- Lu, P., Takai, K., Weaver, V.M., Werb, Z., 2011. Extracellular matrix degradation and remodeling in development and disease. *Cold Spring Harb Perspect Biol* 3. <https://doi.org/10.1101/cshperspect.a005058>
- Lucas, J.T., Salimath, B.P., Slomiany, M.G., Rosenzweig, S.A., 2010. Regulation of invasive behavior by vascular endothelial growth factor is HIF1-dependent. *Oncogene* 29, 4449–4459. <https://doi.org/10.1038/onc.2010.185>
- Lucero, H.A., Kagan, H.M., 2006. Lysyl oxidase: an oxidative enzyme and effector of cell function. *Cell. Mol. Life Sci.* 63, 2304–2316. <https://doi.org/10.1007/s00018-006-6149-9>
- Luxton, G.W.G., Gomes, E.R., Folker, E.S., Vintinner, E., Gundersen, G.G., 2010. Linear arrays of nuclear envelope proteins harness retrograde actin flow for nuclear movement. *Science* 329, 956–959. <https://doi.org/10.1126/science.1189072>
- Luxton, G.W.G., Gundersen, G.G., 2011. Orientation and Function of the Nuclear-Centrosomal Axis During Cell Migration. *Curr Opin Cell Biol* 23, 579–588. <https://doi.org/10.1016/j.ceb.2011.08.001>
- Lv, Z.-D., Kong, B., Li, J.-G., Qu, H.-L., Wang, X.-G., Cao, W.-H., Liu, X.-Y., Wang, Y., Yang, Z.-C., Xu, H.-M., Wang, H.-B., 2013. Transforming growth factor- β 1 enhances the invasiveness of breast cancer cells by inducing a Smad2-dependent epithelial-to-mesenchymal transition. *Oncol. Rep.* 29, 219–225. <https://doi.org/10.3892/or.2012.2111>
- Macias, H., Hinck, L., 2012. Mammary gland development. *Wiley Interdiscip Rev Dev Biol* 1, 533–557. <https://doi.org/10.1002/wdev.35>
- Macpherson, I.R., Rainero, E., Mitchell, L.E., van den Berghe, P.V.E., Speirs, C., Dozynkiewicz, M.A., Chaudhary, S., Kalna, G., Edwards, J., Timpson, P., Norman, J.C., 2014. CLIC3 controls recycling of late endosomal MT1-MMP and dictates invasion and metastasis in breast cancer. *J. Cell. Sci.* 127, 3893–3901. <https://doi.org/10.1242/jcs.135947>
- Mader, C.C., Oser, M., Magalhaes, M.A.O., Bravo-Cordero, J.J., Condeelis, J., Koleske, A.J., Gil-Henn, H., 2011. An EGFR-Src-Arg-cortactin pathway mediates functional maturation of invadopodia and breast cancer cell invasion. *Cancer Res.* 71, 1730–1741. <https://doi.org/10.1158/0008-5472.CAN-10-1432>
- Madsen, C.D., Sahai, E., 2010. Cancer dissemination--lessons from leukocytes. *Dev. Cell* 19, 13–26. <https://doi.org/10.1016/j.devcel.2010.06.013>
- Magalhaes, M.A.O., Larson, D.R., Mader, C.C., Bravo-Cordero, J.J., Gil-Henn, H., Oser, M., Chen, X., Koleske, A.J., Condeelis, J., 2011. Cortactin phosphorylation regulates cell invasion through a pH-dependent pathway. *J. Cell Biol.* 195, 903–920. <https://doi.org/10.1083/jcb.201103045>
- Majkowska, I., Shitomi, Y., Ito, N., Gray, N.S., Itoh, Y., 2017. Discoidin domain receptor 2 mediates collagen-induced activation of membrane-type 1 matrix metalloproteinase in human fibroblasts. *J. Biol. Chem.* 292, 6633–6643. <https://doi.org/10.1074/jbc.M116.770057>
- Malhotra, G.K., Zhao, X., Band, H., Band, V., 2010. Histological, molecular and functional subtypes of breast cancers. *Cancer Biol Ther* 10, 955–960. <https://doi.org/10.4161/cbt.10.10.13879>
- Malik, R., Lelkes, P.I., Cukierman, E., 2015. Biomechanical and biochemical remodeling of stromal extracellular matrix in cancer. *Trends Biotechnol.* 33, 230–236. <https://doi.org/10.1016/j.tibtech.2015.01.004>

- Mandal, S., Johnson, K.R., Wheelock, M.J., 2008. TGF-beta induces formation of F-actin cores and matrix degradation in human breast cancer cells via distinct signaling pathways. *Exp. Cell Res.* 314, 3478–3493. <https://doi.org/10.1016/j.yexcr.2008.09.013>
- Marchesin, V., Castro-Castro, A., Lodillinsky, C., Castagnino, A., Cyrt, J., Bonsang-Kitzis, H., Fuhrmann, L., Irondelle, M., Infante, E., Montagnac, G., Rey, F., Vincent-Salomon, A., Chavrier, P., 2015. ARF6-JIP3/4 regulate endosomal tubules for MT1-MMP exocytosis in cancer invasion. *J. Cell Biol.* 211, 339–358. <https://doi.org/10.1083/jcb.201506002>
- Marchisio, P.C., Cirillo, D., Teti, A., Zamboni-Zallone, A., Tarone, G., 1987. Rous sarcoma virus-transformed fibroblasts and cells of monocytic origin display a peculiar dot-like organization of cytoskeletal proteins involved in microfilament-membrane interactions. *Experimental Cell Research* 169, 202–214. [https://doi.org/10.1016/0014-4827\(87\)90238-2](https://doi.org/10.1016/0014-4827(87)90238-2)
- Mason, B.N., Starchenko, A., Williams, R.M., Bonassar, L.J., Reinhart-King, C.A., 2013. Tuning three-dimensional collagen matrix stiffness independently of collagen concentration modulates endothelial cell behavior. *Acta Biomater* 9, 4635–4644. <https://doi.org/10.1016/j.actbio.2012.08.007>
- Mattila, P.K., Lappalainen, P., 2008. Filopodia: molecular architecture and cellular functions. *Nat. Rev. Mol. Cell Biol.* 9, 446–454. <https://doi.org/10.1038/nrm2406>
- Maugis, B., Brugués, J., Nassoy, P., Guillen, N., Sens, P., Amblard, F., 2010. Dynamic instability of the intracellular pressure drives bleb-based motility. *J. Cell. Sci.* 123, 3884–3892. <https://doi.org/10.1242/jcs.065672>
- McAtee, C.O., Barycki, J.J., Simpson, M.A., 2014. Emerging roles for hyaluronidase in cancer metastasis and therapy. *Adv. Cancer Res.* 123, 1–34. <https://doi.org/10.1016/B978-0-12-800092-2.00001-0>
- McCaffrey, L.M., Macara, I.G., 2012. Signaling pathways in cell polarity. *Cold Spring Harb Perspect Biol* 4. <https://doi.org/10.1101/cshperspect.a009654>
- McGregor, A.L., Hsia, C.-R., Lammerding, J., 2016. Squish and squeeze-the nucleus as a physical barrier during migration in confined environments. *Curr. Opin. Cell Biol.* 40, 32–40. <https://doi.org/10.1016/j.ceb.2016.01.011>
- McKee, K.K., Harrison, D., Capizzi, S., Yurchenco, P.D., 2007. Role of laminin terminal globular domains in basement membrane assembly. *J. Biol. Chem.* 282, 21437–21447. <https://doi.org/10.1074/jbc.M702963200>
- McLachlan, E., Shao, Q., Laird, D.W., 2007. Connexins and gap junctions in mammary gland development and breast cancer progression. *J. Membr. Biol.* 218, 107–121. <https://doi.org/10.1007/s00232-007-9052-x>
- Md Hashim, N.F., Nicholas, N.S., Dart, A.E., Kiriakidis, S., Paleolog, E., Wells, C.M., 2013. Hypoxia-induced invadopodia formation: a role for β -PIX. *Open Biol* 3, 120159. <https://doi.org/10.1098/rsob.120159>
- Mecham, R.P., 2012. Overview of extracellular matrix. *Curr Protoc Cell Biol* Chapter 10, Unit 10.1. <https://doi.org/10.1002/0471143030.cb1001s57>
- Meddens, M.B.M., Pandzic, E., Slotman, J.A., Guillet, D., Joosten, B., Mennens, S., Paardekooper, L.M., Houtsmuller, A.B., van den Dries, K., Wiseman, P.W., Cambi, A., 2016. Actomyosin-dependent dynamic spatial patterns of cytoskeletal components drive mesoscale podosome organization. *Nat Commun* 7, 13127. <https://doi.org/10.1038/ncomms13127>
- Meyer Zum Gottesberge, A.M., Hansen, S., 2014. The collagen receptor DDR1 co-localizes with the non-muscle myosin IIA in mice inner ear and contributes to the cytoarchitecture and stability of motile cells. *Cell Tissue Res.* 358, 729–736. <https://doi.org/10.1007/s00441-014-2009-3>
- Mickel, W., Münster, S., Jawerth, L.M., Vader, D.A., Weitz, D.A., Sheppard, A.P., Mecke, K., Fabry, B., Schröder-Turk, G.E., 2008. Robust pore size analysis of filamentous networks from three-dimensional confocal microscopy. *Biophys. J.* 95, 6072–6080. <https://doi.org/10.1529/biophysj.108.135939>
- Miller, M.-C., Manning, H.B., Jain, A., Troeberg, L., Dudhia, J., Essex, D., Sandison, A., Seiki, M., Nanchahal, J., Nagase, H., Itoh, Y., 2009. Membrane type 1 matrix metalloproteinase is a crucial promoter of synovial invasion in human rheumatoid arthritis. *Arthritis Rheum.* 60, 686–697. <https://doi.org/10.1002/art.24331>

- Miller, P.M., Folkmann, A.W., Maia, A.R.R., Efimova, N., Efimov, A., Kaverina, I., 2009. Golgi-derived CLASP-dependent microtubules control Golgi organization and polarized trafficking in motile cells. *Nat. Cell Biol.* 11, 1069–1080. <https://doi.org/10.1038/ncb1920>
- Mogilner, A., Oster, G., 2003. Polymer motors: pushing out the front and pulling up the back. *Curr. Biol.* 13, R721–733.
- Montagnac, G., Meas-Yedid, V., Irondelle, M., Castro-Castro, A., Franco, M., Shida, T., Nachury, M.V., Benmerah, A., Olivo-Marin, J.-C., Chavrier, P., 2013. ?TAT1 catalyzes microtubule acetylation at clathrin-coated pits. *Nature* 502, 567–570. <https://doi.org/10.1038/nature12571>
- Montagnac, G., Sibarita, J.-B., Loubéry, S., Daviet, L., Romao, M., Raposo, G., Chavrier, P., 2009. ARF6 Interacts with JIP4 to control a motor switch mechanism regulating endosome traffic in cytokinesis. *Curr. Biol.* 19, 184–195. <https://doi.org/10.1016/j.cub.2008.12.043>
- Monteiro, P., Rossé, C., Castro-Castro, A., Irondelle, M., Lagoutte, E., Paul-Gilloteaux, P., Desnos, C., Formstecher, E., Darchen, F., Perrais, D., Gautreau, A., Hertzog, M., Chavrier, P., 2013. Endosomal WASH and exocyst complexes control exocytosis of MT1-MMP at invadopodia. *J Cell Biol* 203, 1063–1079. <https://doi.org/10.1083/jcb.201306162>
- Moreau, V., Tatin, F., Varon, C., Génot, E., 2003. Actin can reorganize into podosomes in aortic endothelial cells, a process controlled by Cdc42 and RhoA. *Mol. Cell. Biol.* 23, 6809–6822.
- Moreno-Bueno, G., Cubillo, E., Sarrió, D., Peinado, H., Rodríguez-Pinilla, S.M., Villa, S., Bolós, V., Jordá, M., Fabra, A., Portillo, F., Palacios, J., Cano, A., 2006. Genetic profiling of epithelial cells expressing E-cadherin repressors reveals a distinct role for Snail, Slug, and E47 factors in epithelial-mesenchymal transition. *Cancer Res.* 66, 9543–9556. <https://doi.org/10.1158/0008-5472.CAN-06-0479>
- Morrison, C.J., Overall, C.M., 2006. TIMP independence of matrix metalloproteinase (MMP)-2 activation by membrane type 2 (MT2)-MMP is determined by contributions of both the MT2-MMP catalytic and hemopexin C domains. *J. Biol. Chem.* 281, 26528–26539. <https://doi.org/10.1074/jbc.M603331200>
- Moshfegh, Y., Bravo-Cordero, J.J., Miskolci, V., Condeelis, J., Hodgson, L., 2014. A Trio-Rac1-Pak1 signalling axis drives invadopodia disassembly. *Nat. Cell Biol.* 16, 574–586. <https://doi.org/10.1038/ncb2972>
- Mouw, J.K., Ou, G., Weaver, V.M., 2014. Extracellular matrix assembly: a multiscale deconstruction. *Nat. Rev. Mol. Cell Biol.* 15, 771–785. <https://doi.org/10.1038/nrm3902>
- Mrkonjic, S., Destaing, O., Albiges-Rizo, C., 2017. Mechanotransduction pulls the strings of matrix degradation at invadosome. *Matrix Biol.* 57–58, 190–203. <https://doi.org/10.1016/j.matbio.2016.06.007>
- Mueller, J., Szep, G., Nemethova, M., de Vries, I., Lieber, A.D., Winkler, C., Kruse, K., Small, J.V., Schmeiser, C., Keren, K., Hauschild, R., Sixt, M., 2017. Load Adaptation of Lamellipodial Actin Networks. *Cell* 171, 188–200.e16. <https://doi.org/10.1016/j.cell.2017.07.051>
- Mueller, S.C., Gherzi, G., Akiyama, S.K., Sang, Q.X., Howard, L., Pineiro-Sanchez, M., Nakahara, H., Yeh, Y., Chen, W.T., 1999. A novel protease-docking function of integrin at invadopodia. *J. Biol. Chem.* 274, 24947–24952.
- Mukhopadhyay, U.K., Mooney, P., Jia, L., Eves, R., Raptis, L., Mak, A.S., 2010. Doubles game: Src-Stat3 versus p53-PTEN in cellular migration and invasion. *Mol. Cell. Biol.* 30, 4980–4995. <https://doi.org/10.1128/MCB.00004-10>
- Muller, P.A.J., Caswell, P.T., Doyle, B., Iwanicki, M.P., Tan, E.H., Karim, S., Lukashchuk, N., Gillespie, D.A., Ludwig, R.L., Gosselin, P., Cromer, A., Brugge, J.S., Sansom, O.J., Norman, J.C., Vousden, K.H., 2009. Mutant p53 drives invasion by promoting integrin recycling. *Cell* 139, 1327–1341. <https://doi.org/10.1016/j.cell.2009.11.026>
- Muncie, J.M., Weaver, V.M., 2018. The Physical and Biochemical Properties of the Extracellular Matrix Regulate Cell Fate. *Curr. Top. Dev. Biol.* 130, 1–37. <https://doi.org/10.1016/bs.ctdb.2018.02.002>
- Murphy, D.A., Courtneidge, S.A., 2011. The “ins” and “outs” of podosomes and invadopodia: characteristics, formation and function. *Nat. Rev. Mol. Cell Biol.* 12, 413–426. <https://doi.org/10.1038/nrm3141>
- Murphy, D.A., Diaz, B., Bromann, P.A., Tsai, J.H., Kawakami, Y., Maurer, J., Stewart, R.A., Izpisua-Belmonte, J.C., Courtneidge, S.A., 2011. A Src-Tks5 pathway is required for neural crest cell

- migration during embryonic development. *PLoS ONE* 6, e22499. <https://doi.org/10.1371/journal.pone.0022499>
- Nabeshima, K., Inoue, T., Shimao, Y., Kataoka, H., Kono, M., 1999. Cohort migration of carcinoma cells: differentiated colorectal carcinoma cells move as coherent cell clusters or sheets. *Histol. Histopathol.* 14, 1183–1197. <https://doi.org/10.14670/HH-14.1183>
- Nagase, H., Visse, R., Murphy, G., 2006. Structure and function of matrix metalloproteinases and TIMPs. *Cardiovasc. Res.* 69, 562–573. <https://doi.org/10.1016/j.cardiores.2005.12.002>
- Nakamura, I., Pilkington, M.F., Lakkakorpi, P.T., Lipfert, L., Sims, S.M., Dixon, S.J., Rodan, G.A., Duong, L.T., 1999. Role of alpha(v)beta(3) integrin in osteoclast migration and formation of the sealing zone. *J. Cell. Sci.* 112 (Pt 22), 3985–3993.
- Nakamura, Takahiro, Sakai, K., Nakamura, Toshikazu, Matsumoto, K., 2011. Hepatocyte growth factor twenty years on: Much more than a growth factor. *J. Gastroenterol. Hepatol.* 26 Suppl 1, 188–202. <https://doi.org/10.1111/j.1440-1746.2010.06549.x>
- Nance, J., Zallen, J.A., 2011. Elaborating polarity: PAR proteins and the cytoskeleton. *Development* 138, 799–809. <https://doi.org/10.1242/dev.053538>
- Narumiya, S., Tanji, M., Ishizaki, T., 2009. Rho signaling, ROCK and mDia1, in transformation, metastasis and invasion. *Cancer Metastasis Rev.* 28, 65–76. <https://doi.org/10.1007/s10555-008-9170-7>
- Nishiuchi, R., Takagi, J., Hayashi, M., Ido, H., Yagi, Y., Sanzen, N., Tsuji, T., Yamada, M., Sekiguchi, K., 2006. Ligand-binding specificities of laminin-binding integrins: a comprehensive survey of laminin-integrin interactions using recombinant alpha3beta1, alpha6beta1, alpha7beta1 and alpha6beta4 integrins. *Matrix Biol.* 25, 189–197. <https://doi.org/10.1016/j.matbio.2005.12.001>
- Nuhn, J.A.M., Perez, A.M., Schneider, I.C., 2018. Contact guidance diversity in rotationally aligned collagen matrices. *Acta Biomater* 66, 248–257. <https://doi.org/10.1016/j.actbio.2017.11.039>
- O'Brien, P., O'Connor, B.F., 2008. Seprase: an overview of an important matrix serine protease. *Biochim. Biophys. Acta* 1784, 1130–1145. <https://doi.org/10.1016/j.bbapap.2008.01.006>
- Oikawa, T., Itoh, T., Takenawa, T., 2008. Sequential signals toward podosome formation in NIH-src cells. *J. Cell Biol.* 182, 157–169. <https://doi.org/10.1083/jcb.200801042>
- Oldberg, A., Kalamajski, S., Salnikov, A.V., Stuhr, L., Mörgelin, M., Reed, R.K., Heldin, N.-E., Rubin, K., 2007. Collagen-binding proteoglycan fibromodulin can determine stroma matrix structure and fluid balance in experimental carcinoma. *Proc. Natl. Acad. Sci. U.S.A.* 104, 13966–13971. <https://doi.org/10.1073/pnas.0702014104>
- Olivares, O., Mayers, J.R., Gouirand, V., Torrence, M.E., Gicquel, T., Borge, L., Lac, S., Roques, J., Lavaut, M.-N., Berthezène, P., Rubis, M., Secq, V., Garcia, S., Moutardier, V., Lombardo, D., Iovanna, J.L., Tomasini, R., Guillaumond, F., Vander Heiden, M.G., Vasseur, S., 2017. Collagen-derived proline promotes pancreatic ductal adenocarcinoma cell survival under nutrient limited conditions. *Nat Commun* 8, 16031. <https://doi.org/10.1038/ncomms16031>
- Orimo, A., Weinberg, R.A., 2006. Stromal fibroblasts in cancer: a novel tumor-promoting cell type. *Cell Cycle* 5, 1597–1601. <https://doi.org/10.4161/cc.5.15.3112>
- Oser, M., Condeelis, J., 2009. The cofilin activity cycle in lamellipodia and invadopodia. *J. Cell. Biochem.* 108, 1252–1262. <https://doi.org/10.1002/jcb.22372>
- Oser, M., Mader, C.C., Gil-Henn, H., Magalhaes, M., Bravo-Cordero, J.J., Koleske, A.J., Condeelis, J., 2010. Specific tyrosine phosphorylation sites on cortactin regulate Nck1-dependent actin polymerization in invadopodia. *J. Cell. Sci.* 123, 3662–3673. <https://doi.org/10.1242/jcs.068163>
- Oser, M., Yamaguchi, H., Mader, C.C., Bravo-Cordero, J.J., Arias, M., Chen, X., Desmarais, V., van Rheenen, J., Koleske, A.J., Condeelis, J., 2009. Cortactin regulates cofilin and N-WASp activities to control the stages of invadopodium assembly and maturation. *J. Cell Biol.* 186, 571–587. <https://doi.org/10.1083/jcb.200812176>
- Osiak, A.-E., Zenner, G., Linder, S., 2005. Subconfluent endothelial cells form podosomes downstream of cytokine and RhoGTPase signaling. *Exp. Cell Res.* 307, 342–353. <https://doi.org/10.1016/j.yexcr.2005.03.035>
- Oskarsson, T., Acharyya, S., Zhang, X.H.-F., Vanharanta, S., Tavazoie, S.F., Morris, P.G., Downey, R.J., Manova-Todorova, K., Brogi, E., Massagué, J., 2011. Breast cancer cells produce tenascin C as a metastatic niche component to colonize the lungs. *Nat. Med.* 17, 867–874. <https://doi.org/10.1038/nm.2379>

- Osmanagic-Myers, S., Dechat, T., Foisner, R., 2015. Lamins at the crossroads of mechanosignaling. *Genes Dev.* 29, 225–237. <https://doi.org/10.1101/gad.255968.114>
- Osmani, N., Peglion, F., Chavrier, P., Etienne-Manneville, S., 2010. Cdc42 localization and cell polarity depend on membrane traffic. *J. Cell Biol.* 191, 1261–1269. <https://doi.org/10.1083/jcb.201003091>
- Ota, I., Li, X.-Y., Hu, Y., Weiss, S.J., 2009. Induction of a MT1-MMP and MT2-MMP-dependent basement membrane transmigration program in cancer cells by Snail1. *Proc. Natl. Acad. Sci. U.S.A.* 106, 20318–20323. <https://doi.org/10.1073/pnas.0910962106>
- Page-McCaw, A., Ewald, A.J., Werb, Z., 2007. Matrix metalloproteinases and the regulation of tissue remodelling. *Nat. Rev. Mol. Cell Biol.* 8, 221–233. <https://doi.org/10.1038/nrm2125>
- Paluch, E.K., Raz, E., 2013. The role and regulation of blebs in cell migration. *Curr Opin Cell Biol* 25, 582–590. <https://doi.org/10.1016/j.ceb.2013.05.005>
- Pan, B., Guo, J., Liao, Q., Zhao, Y., 2018. $\beta 1$ and $\beta 3$ integrins in breast, prostate and pancreatic cancer: A novel implication. *Oncol Lett* 15, 5412–5416. <https://doi.org/10.3892/ol.2018.8076>
- Pandya, P., Orgaz, J.L., Sanz-Moreno, V., 2017. Modes of invasion during tumour dissemination. *Mol Oncol* 11, 5–27. <https://doi.org/10.1002/1878-0261.12019>
- Papageorgis, P., Lambert, A.W., Ozturk, S., Gao, F., Pan, H., Manne, U., Alekseyev, Y.O., Thiagalingam, A., Abdolmaleky, H.M., Lenburg, M., Thiagalingam, S., 2010. Smad signaling is required to maintain epigenetic silencing during breast cancer progression. *Cancer Res.* 70, 968–978. <https://doi.org/10.1158/0008-5472.CAN-09-1872>
- Parekh, A., Ruppender, N.S., Branch, K.M., Sewell-Loftin, M.K., Lin, J., Boyer, P.D., Candiello, J.E., Merryman, W.D., Guelcher, S.A., Weaver, A.M., 2011. Sensing and modulation of invadopodia across a wide range of rigidities. *Biophys. J.* 100, 573–582. <https://doi.org/10.1016/j.bpj.2010.12.3733>
- Parekh, A., Weaver, A.M., 2016. Regulation of invadopodia by mechanical signaling. *Exp. Cell Res.* 343, 89–95. <https://doi.org/10.1016/j.yexcr.2015.10.038>
- Parker, J.S., Mullins, M., Cheang, M.C.U., Leung, S., Voduc, D., Vickery, T., Davies, S., Fauron, C., He, X., Hu, Z., Quackenbush, J.F., Stijleman, I.J., Palazzo, J., Marron, J.S., Nobel, A.B., Mardis, E., Nielsen, T.O., Ellis, M.J., Perou, C.M., Bernard, P.S., 2009. Supervised risk predictor of breast cancer based on intrinsic subtypes. *J. Clin. Oncol.* 27, 1160–1167. <https://doi.org/10.1200/JCO.2008.18.1370>
- Parsons, J.T., Horwitz, A.R., Schwartz, M.A., 2010. Cell adhesion: integrating cytoskeletal dynamics and cellular tension. *Nat. Rev. Mol. Cell Biol.* 11, 633–643. <https://doi.org/10.1038/nrm2957>
- Parton, R.G., del Pozo, M.A., 2013. Caveolae as plasma membrane sensors, protectors and organizers. *Nat. Rev. Mol. Cell Biol.* 14, 98–112. <https://doi.org/10.1038/nrm3512>
- Parvani, J.G., Galliher-Beckley, A.J., Schieman, B.J., Schieman, W.P., 2013. Targeted inactivation of $\beta 1$ integrin induces $\beta 3$ integrin switching, which drives breast cancer metastasis by TGF- β . *Mol. Biol. Cell* 24, 3449–3459. <https://doi.org/10.1091/mbc.E12-10-0776>
- Patel, S., Homaei, A., El-Seedi, H.R., Akhtar, N., 2018. Cathepsins: Proteases that are vital for survival but can also be fatal. *Biomed. Pharmacother.* 105, 526–532. <https://doi.org/10.1016/j.biopha.2018.05.148>
- Paterson, E.K., Courtneidge, S.A., 2017. Invadosomes are coming: new insights into function and disease relevance. *FEBS J.* <https://doi.org/10.1111/febs.14123>
- Paul, A.S., Pollard, T.D., 2009. Review of the mechanism of processive actin filament elongation by formins. *Cell Motil. Cytoskeleton* 66, 606–617. <https://doi.org/10.1002/cm.20379>
- Paul, N.R., Allen, J.L., Chapman, A., Morlan-Mairal, M., Zindy, E., Jacquemet, G., Fernandez del Ama, L., Ferizovic, N., Green, D.M., Howe, J.D., Ehler, E., Hurlstone, A., Caswell, P.T., 2015a. $\alpha 5 \beta 1$ integrin recycling promotes Arp2/3-independent cancer cell invasion via the formin FHOD3. *J. Cell Biol.* 210, 1013–1031. <https://doi.org/10.1083/jcb.201502040>
- Paul, N.R., Jacquemet, G., Caswell, P.T., 2015b. Endocytic Trafficking of Integrins in Cell Migration. *Curr. Biol.* 25, R1092–1105. <https://doi.org/10.1016/j.cub.2015.09.049>
- Paz, H., Pathak, N., Yang, J., 2014. Invading one step at a time: the role of invadopodia in tumor metastasis. *Oncogene* 33, 4193–4202. <https://doi.org/10.1038/onc.2013.393>
- Pecci, A., Ma, X., Savoia, A., Adelstein, R.S., 2018. MYH9: Structure, functions and role of non-muscle myosin IIA in human disease. *Gene* 664, 152–167. <https://doi.org/10.1016/j.gene.2018.04.048>

- Pein, M., Oskarsson, T., 2015. Microenvironment in metastasis: roadblocks and supportive niches. *Am. J. Physiol., Cell Physiol.* 309, C627–638. <https://doi.org/10.1152/ajpcell.00145.2015>
- Peinado, H., Portillo, F., Cano, A., 2004. Transcriptional regulation of cadherins during development and carcinogenesis. *Int. J. Dev. Biol.* 48, 365–375. <https://doi.org/10.1387/ijdb.041794hp>
- Peláez, R., Morales, X., Salvo, E., Garasa, S., Ortiz de Solórzano, C., Martínez, A., Larrayoz, I.M., Rouzaut, A., 2017. $\beta 3$ integrin expression is required for invadopodia-mediated ECM degradation in lung carcinoma cells. *PLoS ONE* 12, e0181579. <https://doi.org/10.1371/journal.pone.0181579>
- Pellikainen, J.M., Ropponen, K.M., Kataja, V.V., Kellokoski, J.K., Eskelinen, M.J., Kosma, V.-M., 2004. Expression of matrix metalloproteinase (MMP)-2 and MMP-9 in breast cancer with a special reference to activator protein-2, HER2, and prognosis. *Clin. Cancer Res.* 10, 7621–7628. <https://doi.org/10.1158/1078-0432.CCR-04-1061>
- Perentes, J.Y., Kirkpatrick, N.D., Nagano, S., Smith, E.Y., Shaver, C.M., Sgroi, D., Garkavtsev, I., Munn, L.L., Jain, R.K., Boucher, Y., 2011. Cancer cell-associated MT1-MMP promotes blood vessel invasion and distant metastasis in triple-negative mammary tumors. *Cancer Res.* 71, 4527–4538. <https://doi.org/10.1158/0008-5472.CAN-10-4376>
- Perou, C.M., Sørli, T., Eisen, M.B., van de Rijn, M., Jeffrey, S.S., Rees, C.A., Pollack, J.R., Ross, D.T., Johnsen, H., Akslen, L.A., Fluge, Ø., Pergamenschikov, A., Williams, C., Zhu, S.X., Lønning, P.E., Børresen-Dale, A.-L., Brown, P.O., Botstein, D., 2000. Molecular portraits of human breast tumours. *Nature* 406, 747–752. <https://doi.org/10.1038/35021093>
- Petrella, B.L., Lohi, J., Brinckerhoff, C.E., 2005. Identification of membrane type-1 matrix metalloproteinase as a target of hypoxia-inducible factor-2 α in von Hippel-Lindau renal cell carcinoma. *Oncogene* 24, 1043–1052. <https://doi.org/10.1038/sj.onc.1208305>
- Petrie, R.J., Gavara, N., Chadwick, R.S., Yamada, K.M., 2012. Nonpolarized signaling reveals two distinct modes of 3D cell migration. *J Cell Biol* 197, 439–455. <https://doi.org/10.1083/jcb.201201124>
- Petrie, R.J., Harlin, H.M., Korsak, L.I.T., Yamada, K.M., 2017. Activating the nuclear piston mechanism of 3D migration in tumor cells. *J Cell Biol* 216, 93–100. <https://doi.org/10.1083/jcb.201605097>
- Petrie, R.J., Koo, H., Yamada, K.M., 2014. Generation of compartmentalized pressure by a nuclear piston governs cell motility in a 3D matrix. *Science* 345, 1062–1065. <https://doi.org/10.1126/science.1256965>
- Petrie, R.J., Yamada, K.M., 2016. Multiple mechanisms of 3D migration: the origins of plasticity. *Curr. Opin. Cell Biol.* 42, 7–12. <https://doi.org/10.1016/j.ceb.2016.03.025>
- Petropoulos, C., Oddou, C., Emadali, A., Hiriart-Bryant, E., Boyault, C., Faurobert, E., Vande Pol, S., Kim-Kaneyama, J.-R., Kraut, A., Coute, Y., Block, M., Albiges-Rizo, C., Destaing, O., 2016. Roles of paxillin family members in adhesion and ECM degradation coupling at invadosomes. *J. Cell Biol.* 213, 585–599. <https://doi.org/10.1083/jcb.201510036>
- Pfeifer, C.R., Alvey, C.M., Irianto, J., Discher, D.E., 2017. Genome variation across cancers scales with tissue stiffness - an invasion-mutation mechanism and implications for immune cell infiltration. *Curr Opin Syst Biol* 2, 103–114. <https://doi.org/10.1016/j.coisb.2017.04.005>
- Pfeifer, C.R., Xia, Y., Zhu, K., Liu, D., Irianto, J., García, V.M.M., Millán, L.M.S., Niese, B., Harding, S., Deviri, D., Greenberg, R.A., Discher, D.E., 2018. Constricted migration increases DNA damage and independently represses cell cycle. *Mol Biol Cell* 29, 1948–1962. <https://doi.org/10.1091/mbc.E18-02-0079>
- Pignatelli, J., Tumbarello, D.A., Schmidt, R.P., Turner, C.E., 2012. Hic-5 promotes invadopodia formation and invasion during TGF- β -induced epithelial-mesenchymal transition. *J. Cell Biol.* 197, 421–437. <https://doi.org/10.1083/jcb.201108143>
- Pinner, S., Sahai, E., 2008. Imaging amoeboid cancer cell motility in vivo. *J Microsc* 231, 441–445. <https://doi.org/10.1111/j.1365-2818.2008.02056.x>
- Plotnikov, S.V., Pasapera, A.M., Sabass, B., Waterman, C.M., 2012. Force fluctuations within focal adhesions mediate ECM-rigidity sensing to guide directed cell migration. *Cell* 151, 1513–1527. <https://doi.org/10.1016/j.cell.2012.11.034>
- Pocha, S.M., Knust, E., 2013. Complexities of Crumbs function and regulation in tissue morphogenesis. *Curr. Biol.* 23, R289–293. <https://doi.org/10.1016/j.cub.2013.03.001>

- Poincloux, R., Lizárraga, F., Chavrier, P., 2009. Matrix invasion by tumour cells: a focus on MT1-MMP trafficking to invadopodia. *J Cell Sci* 122, 3015–3024. <https://doi.org/10.1242/jcs.034561>
- Polette, M., Gilles, C., de Bentzmann, S., Gruenert, D., Tournier, J.M., Birembaut, P., 1998. Association of fibroblastoid features with the invasive phenotype in human bronchial cancer cell lines. *Clin. Exp. Metastasis* 16, 105–112.
- Pollard, T.D., 2016. Actin and Actin-Binding Proteins. *Cold Spring Harb Perspect Biol* 8. <https://doi.org/10.1101/cshperspect.a018226>
- Pollard, T.D., Borisy, G.G., 2003. Cellular motility driven by assembly and disassembly of actin filaments. *Cell* 112, 453–465.
- Polyak, K., Kalluri, R., 2010. The role of the microenvironment in mammary gland development and cancer. *Cold Spring Harb Perspect Biol* 2, a003244. <https://doi.org/10.1101/cshperspect.a003244>
- Poola, I., DeWitty, R.L., Marshalleck, J.J., Bhatnagar, R., Abraham, J., Leffall, L.D., 2005. Identification of MMP-1 as a putative breast cancer predictive marker by global gene expression analysis. *Nat. Med.* 11, 481–483. <https://doi.org/10.1038/nm1243>
- Pourfarhangi, K.E., Bergman, A., Gligorijevic, B., 2018. ECM Cross-Linking Regulates Invadopodia Dynamics. *Biophys. J.* 114, 1455–1466. <https://doi.org/10.1016/j.bpj.2018.01.027>
- Prahl, L.S., Bangasser, P.F., Stopfer, L.E., Hemmat, M., White, F.M., Rosenfeld, S.S., Odde, D.J., 2018. Microtubule-Based Control of Motor-Clutch System Mechanics in Glioma Cell Migration. *Cell Rep* 25, 2591–2604.e8. <https://doi.org/10.1016/j.celrep.2018.10.101>
- Prass, M., Jacobson, K., Mogilner, A., Radmacher, M., 2006. Direct measurement of the lamellipodial protrusive force in a migrating cell. *J. Cell Biol.* 174, 767–772. <https://doi.org/10.1083/jcb.200601159>
- Prentice-Mott, H.V., Meroz, Y., Carlson, A., Levine, M.A., Davidson, M.W., Irimia, D., Charras, G.T., Mahadevan, L., Shah, J.V., 2016. Directional memory arises from long-lived cytoskeletal asymmetries in polarized chemotactic cells. *Proc. Natl. Acad. Sci. U.S.A.* 113, 1267–1272. <https://doi.org/10.1073/pnas.1513289113>
- Provenzano, P.P., Eliceiri, K.W., Campbell, J.M., Inman, D.R., White, J.G., Keely, P.J., 2006. Collagen reorganization at the tumor-stromal interface facilitates local invasion. *BMC Med* 4, 38. <https://doi.org/10.1186/1741-7015-4-38>
- Provenzano, P.P., Inman, D.R., Eliceiri, K.W., Knittel, J.G., Yan, L., Rueden, C.T., White, J.G., Keely, P.J., 2008. Collagen density promotes mammary tumor initiation and progression. *BMC Med* 6, 11. <https://doi.org/10.1186/1741-7015-6-11>
- Ra, H.-J., Parks, W.C., 2007. Control of matrix metalloproteinase catalytic activity. *Matrix Biol.* 26, 587–596. <https://doi.org/10.1016/j.matbio.2007.07.001>
- Raab, M., Gentili, M., de Belly, H., Thiam, H.R., Vargas, P., Jimenez, A.J., Lautenschlaeger, F., Voituriez, R., Lennon-Duménil, A.M., Manel, N., Piel, M., 2016. ESCRT III repairs nuclear envelope ruptures during cell migration to limit DNA damage and cell death. *Science* 352, 359–362. <https://doi.org/10.1126/science.aad7611>
- Radisky, D.C., Levy, D.D., Littlepage, L.E., Liu, H., Nelson, C.M., Fata, J.E., Leake, D., Godden, E.L., Albertson, D.G., Nieto, M.A., Werb, Z., Bissell, M.J., 2005. Rac1b and reactive oxygen species mediate MMP-3-induced EMT and genomic instability. *Nature* 436, 123–127. <https://doi.org/10.1038/nature03688>
- Rajadurai, C.V., Havrylov, S., Zaoui, K., Vaillancourt, R., Stuble, M., Naujokas, M., Zuo, D., Tremblay, M.L., Park, M., 2012. Met receptor tyrosine kinase signals through a cortactin-Gab1 scaffold complex, to mediate invadopodia. *J. Cell. Sci.* 125, 2940–2953. <https://doi.org/10.1242/jcs.100834>
- Ramirez, N.E., Zhang, Z., Madamanchi, A., Boyd, K.L., O'Rear, L.D., Nashabi, A., Li, Z., Dupont, W.D., Zijlstra, A., Zutter, M.M., 2011. The $\alpha_2\beta_1$ integrin is a metastasis suppressor in mouse models and human cancer. *J. Clin. Invest.* 121, 226–237. <https://doi.org/10.1172/JCI42328>
- Rammal, H., Saby, C., Magnien, K., Van-Gulick, L., Garnotel, R., Buache, E., El Btaouri, H., Jeannesson, P., Morjani, H., 2016. Discoidin Domain Receptors: Potential Actors and Targets in Cancer. *Front Pharmacol* 7, 55. <https://doi.org/10.3389/fphar.2016.00055>

- Ray, A., Lee, O., Win, Z., Edwards, R.M., Alford, P.W., Kim, D.-H., Provenzano, P.P., 2017. Anisotropic forces from spatially constrained focal adhesions mediate contact guidance directed cell migration. *Nat Commun* 8, 14923. <https://doi.org/10.1038/ncomms14923>
- Razidlo, G.L., Schroeder, B., Chen, J., Billadeau, D.D., McNiven, M.A., 2014. Vav1 as a central regulator of invadopodia assembly. *Curr. Biol.* 24, 86–93. <https://doi.org/10.1016/j.cub.2013.11.013>
- Reed, J.R., Schwertfeger, K.L., 2010. Immune cell location and function during post-natal mammary gland development. *J Mammary Gland Biol Neoplasia* 15, 329–339. <https://doi.org/10.1007/s10911-010-9188-7>
- Remacle, A., Murphy, G., Roghi, C., 2003. Membrane type I-matrix metalloproteinase (MT1-MMP) is internalised by two different pathways and is recycled to the cell surface. *J. Cell. Sci.* 116, 3905–3916. <https://doi.org/10.1242/jcs.00710>
- Ren, F., Tang, R., Zhang, X., Madushi, W.M., Luo, D., Dang, Y., Li, Z., Wei, K., Chen, G., 2015. Overexpression of MMP Family Members Functions as Prognostic Biomarker for Breast Cancer Patients: A Systematic Review and Meta-Analysis. *PLoS ONE* 10, e0135544. <https://doi.org/10.1371/journal.pone.0135544>
- Renkawitz, J., Kopf, A., Stopp, J., de Vries, I., Driscoll, M.K., Merrin, J., Hauschild, R., Welf, E.S., Danuser, G., Fiolka, R., Sixt, M., 2019. Nuclear positioning facilitates amoeboid migration along the path of least resistance. *Nature*. <https://doi.org/10.1038/s41586-019-1087-5>
- Revach, O.-Y., Weiner, A., Rechav, K., Sabanay, I., Livne, A., Geiger, B., 2015. Mechanical interplay between invadopodia and the nucleus in cultured cancer cells. *Sci Rep* 5, 9466. <https://doi.org/10.1038/srep09466>
- Rhee, S., Jiang, H., Ho, C.-H., Grinnell, F., 2007. Microtubule function in fibroblast spreading is modulated according to the tension state of cell-matrix interactions. *Proc. Natl. Acad. Sci. U.S.A.* 104, 5425–5430. <https://doi.org/10.1073/pnas.0608030104>
- Ridley, A.J., Schwartz, M.A., Burridge, K., Firtel, R.A., Ginsberg, M.H., Borisy, G., Parsons, J.T., Horwitz, A.R., 2003. Cell migration: integrating signals from front to back. *Science* 302, 1704–1709. <https://doi.org/10.1126/science.1092053>
- Rikimaru, A., Komori, K., Sakamoto, T., Ichise, H., Yoshida, N., Yana, I., Seiki, M., 2007. Establishment of an MT4-MMP-deficient mouse strain representing an efficient tracking system for MT4-MMP/MMP-17 expression in vivo using beta-galactosidase. *Genes Cells* 12, 1091–1100. <https://doi.org/10.1111/j.1365-2443.2007.01110.x>
- Rodriguez-Boulán, E., Macara, I.G., 2014. Organization and execution of the epithelial polarity programme. *Nat. Rev. Mol. Cell Biol.* 15, 225–242. <https://doi.org/10.1038/nrm3775>
- Rohani, M.G., Parks, W.C., 2015. Matrix remodeling by MMPs during wound repair. *Matrix Biology*. <https://doi.org/10.1016/j.matbio.2015.03.002>
- Rossé, C., Lodillinsky, C., Fuhrmann, L., Nourieh, M., Monteiro, P., Irondele, M., Lagoutte, E., Vacher, S., Waharte, F., Paul-Gilloteaux, P., Romao, M., Sengmanivong, L., Linch, M., van Lint, J., Raposo, G., Vincent-Salomon, A., Bièche, I., Parker, P.J., Chavrier, P., 2014. Control of MT1-MMP transport by atypical PKC during breast-cancer progression. *Proc. Natl. Acad. Sci. U.S.A.* 111, E1872–1879. <https://doi.org/10.1073/pnas.1400749111>
- Rosso, F., Marino, G., Giordano, A., Barbarisi, M., Parmeggiani, D., Barbarisi, A., 2005. Smart materials as scaffolds for tissue engineering. *J. Cell. Physiol.* 203, 465–470. <https://doi.org/10.1002/jcp.20270>
- Rottiers, P., Saltel, F., Daubon, T., Chaigne-Delalande, B., Tridon, V., Billottet, C., Reuzeau, E., Génot, E., 2009. TGFbeta-induced endothelial podosomes mediate basement membrane collagen degradation in arterial vessels. *J. Cell. Sci.* 122, 4311–4318. <https://doi.org/10.1242/jcs.057448>
- Rouiller, I., Xu, X.-P., Amann, K.J., Egile, C., Nickell, S., Nicastro, D., Li, R., Pollard, T.D., Volkmann, N., Hanein, D., 2008. The structural basis of actin filament branching by the Arp2/3 complex. *J. Cell Biol.* 180, 887–895. <https://doi.org/10.1083/jcb.200709092>
- Roux, K.J., Crisp, M.L., Liu, Q., Kim, D., Kozlov, S., Stewart, C.L., Burke, B., 2009. Nesprin 4 is an outer nuclear membrane protein that can induce kinesin-mediated cell polarization. *Proc. Natl. Acad. Sci. U.S.A.* 106, 2194–2199. <https://doi.org/10.1073/pnas.0808602106>
- Rowe, R.G., Li, X.-Y., Hu, Y., Saunders, T.L., Virtanen, I., Garcia de Herreros, A., Becker, K.-F., Ingvarsen, S., Engelholm, L.H., Bommer, G.T., Fearon, E.R., Weiss, S.J., 2009. Mesenchymal

- cells reactivate Snail1 expression to drive three-dimensional invasion programs. *J. Cell Biol.* 184, 399–408. <https://doi.org/10.1083/jcb.200810113>
- Rowe, R.G., Weiss, S.J., 2009. Navigating ECM barriers at the invasive front: the cancer cell-stroma interface. *Annu. Rev. Cell Dev. Biol.* 25, 567–595. <https://doi.org/10.1146/annurev.cellbio.24.110707.175315>
- Rowe, R.G., Weiss, S.J., 2008. Breaching the basement membrane: who, when and how? *Trends Cell Biol.* 18, 560–574. <https://doi.org/10.1016/j.tcb.2008.08.007>
- Rupp, P.A., Visconti, R.P., Czirók, A., Cheres, D.A., Little, C.D., 2008. Matrix metalloproteinase 2-integrin $\alpha(v)\beta3$ binding is required for mesenchymal cell invasive activity but not epithelial locomotion: a computational time-lapse study. *Mol. Biol. Cell* 19, 5529–5540. <https://doi.org/10.1091/mbc.e07-05-0480>
- Sabeh, F., Fox, D., Weiss, S.J., 2010. Membrane-type I matrix metalloproteinase-dependent regulation of rheumatoid arthritis synoviocyte function. *J. Immunol.* 184, 6396–6406. <https://doi.org/10.4049/jimmunol.0904068>
- Sabeh, F., Ota, I., Holmbeck, K., Birkedal-Hansen, H., Soloway, P., Balbin, M., Lopez-Otin, C., Shapiro, S., Inada, M., Krane, S., Allen, E., Chung, D., Weiss, S.J., 2004. Tumor cell traffic through the extracellular matrix is controlled by the membrane-anchored collagenase MT1-MMP. *J Cell Biol* 167, 769–781. <https://doi.org/10.1083/jcb.200408028>
- Sabeh, F., Shimizu-Hirota, R., Weiss, S.J., 2009. Protease-dependent versus -independent cancer cell invasion programs: three-dimensional amoeboid movement revisited. *J. Cell Biol.* 185, 11–19. <https://doi.org/10.1083/jcb.200807195>
- Sahai, E., Marshall, C.J., 2003. Differing modes of tumour cell invasion have distinct requirements for Rho/ROCK signalling and extracellular proteolysis. *Nat. Cell Biol.* 5, 711–719. <https://doi.org/10.1038/ncb1019>
- Saini, P., Courtneidge, S.A., 2018. Tks adaptor proteins at a glance. *J. Cell. Sci.* 131. <https://doi.org/10.1242/jcs.203661>
- Sakai, K., Nakamura, T., Suzuki, Y., Imizu, T., Matsumoto, K., 2011. 3-D collagen-dependent cell surface expression of MT1-MMP and MMP-2 activation regardless of integrin $\beta1$ function and matrix stiffness. *Biochem. Biophys. Res. Commun.* 412, 98–103. <https://doi.org/10.1016/j.bbrc.2011.07.050>
- Sakurai-Yageta, M., Recchi, C., Le Dez, G., Sibarita, J.-B., Daviet, L., Camonis, J., D'Souza-Schorey, C., Chavrier, P., 2008. The interaction of IQGAP1 with the exocyst complex is required for tumor cell invasion downstream of Cdc42 and RhoA. *J. Cell Biol.* 181, 985–998. <https://doi.org/10.1083/jcb.200709076>
- Saltel, F., Chabadel, A., Bonnelye, E., Jurdic, P., 2008. Actin cytoskeletal organisation in osteoclasts: a model to decipher transmigration and matrix degradation. *Eur. J. Cell Biol.* 87, 459–468. <https://doi.org/10.1016/j.ejcb.2008.01.001>
- Sander, L.M., 2014. Modeling contact guidance and invasion by cancer cells. *Cancer Res.* 74, 4588–4596. <https://doi.org/10.1158/0008-5472.CAN-13-3294>
- Sanders, M.E., Schuyler, P.A., Dupont, W.D., Page, D.L., 2005. The natural history of low-grade ductal carcinoma in situ of the breast in women treated by biopsy only revealed over 30 years of long-term follow-up. *Cancer* 103, 2481–2484. <https://doi.org/10.1002/cncr.21069>
- Sanz-Moreno, V., Gadea, G., Ahn, J., Paterson, H., Marra, P., Pinner, S., Sahai, E., Marshall, C.J., 2008. Rac activation and inactivation control plasticity of tumor cell movement. *Cell* 135, 510–523. <https://doi.org/10.1016/j.cell.2008.09.043>
- Sato, H., Takino, T., Okada, Y., Cao, J., Shinagawa, A., Yamamoto, E., Seiki, M., 1994. A matrix metalloproteinase expressed on the surface of invasive tumour cells. *Nature* 370, 61–65. <https://doi.org/10.1038/370061a0>
- Sato, T., Mushiake, S., Kato, Y., Sato, K., Sato, M., Takeda, N., Ozono, K., Miki, K., Kubo, Y., Tsuji, A., Harada, R., Harada, A., 2007. The Rab8 GTPase regulates apical protein localization in intestinal cells. *Nature* 448, 366–369. <https://doi.org/10.1038/nature05929>
- Saunders, L.R., McClay, D.R., 2014. Sub-circuits of a gene regulatory network control a developmental epithelial-mesenchymal transition. *Development* 141, 1503–1513. <https://doi.org/10.1242/dev.101436>

- Schedin, P., Keely, P.J., 2011. Mammary Gland ECM Remodeling, Stiffness, and Mechanosignaling in Normal Development and Tumor Progression. *Cold Spring Harb Perspect Biol* 3. <https://doi.org/10.1101/cshperspect.a003228>
- Schmidt-Kittler, O., Ragg, T., Daskalakis, A., Granzow, M., Ahr, A., Blankenstein, T.J.F., Kaufmann, M., Diebold, J., Arnholdt, H., Muller, P., Bischoff, J., Harich, D., Schlimok, G., Riethmuller, G., Eils, R., Klein, C.A., 2003. From latent disseminated cells to overt metastasis: genetic analysis of systemic breast cancer progression. *Proc. Natl. Acad. Sci. U.S.A.* 100, 7737–7742. <https://doi.org/10.1073/pnas.1331931100>
- Schoumacher, M., Glentis, A., Gurchenkov, V.V., Vignjevic, D.M., 2013. Basement membrane invasion assays: native basement membrane and chemoinvasion assay. *Methods Mol. Biol.* 1046, 133–144. https://doi.org/10.1007/978-1-62703-538-5_8
- Schoumacher, M., Goldman, R.D., Louvard, D., Vignjevic, D.M., 2010. Actin, microtubules, and vimentin intermediate filaments cooperate for elongation of invadopodia. *J. Cell Biol.* 189, 541–556. <https://doi.org/10.1083/jcb.200909113>
- Schreiber, K.H., Kennedy, B.K., 2013. When lamins go bad: nuclear structure and disease. *Cell* 152, 1365–1375. <https://doi.org/10.1016/j.cell.2013.02.015>
- Seals, D.F., Azucena, E.F., Pass, I., Tesfay, L., Gordon, R., Woodrow, M., Resau, J.H., Courtneidge, S.A., 2005. The adaptor protein Tks5/Fish is required for podosome formation and function, and for the protease-driven invasion of cancer cells. *Cancer Cell* 7, 155–165. <https://doi.org/10.1016/j.ccr.2005.01.006>
- Seals, D.F., Courtneidge, S.A., 2003. The ADAMs family of metalloproteases: multidomain proteins with multiple functions. *Genes Dev.* 17, 7–30. <https://doi.org/10.1101/gad.1039703>
- Seano, G., Chiaverina, G., Gagliardi, P.A., di Blasio, L., Puliafito, A., Bouvard, C., Sessa, R., Tarone, G., Sorokin, L., Helley, D., Jain, R.K., Serini, G., Bussolino, F., Primo, L., 2014. Endothelial podosome rosettes regulate vascular branching in tumour angiogenesis. *Nat. Cell Biol.* 16, 931–941. <https://doi.org/10.1038/ncb3036>
- Sekiguchi, R., Yamada, K.M., 2018. Basement Membranes in Development and Disease. *Curr. Top. Dev. Biol.* 130, 143–191. <https://doi.org/10.1016/bs.ctdb.2018.02.005>
- Sharma, V.P., Eddy, R., Entenberg, D., Kai, M., Gertler, F.B., Condeelis, J., 2013. Tks5 and SHIP2 regulate invadopodium maturation, but not initiation, in breast carcinoma cells. *Curr. Biol.* 23, 2079–2089. <https://doi.org/10.1016/j.cub.2013.08.044>
- Shay, G., Lynch, C.C., Fingleton, B., 2015. Moving targets: Emerging roles for MMPs in cancer progression and metastasis. *Matrix Biol.* 44–46, 200–206. <https://doi.org/10.1016/j.matbio.2015.01.019>
- Sherwood, D.R., Plastino, J., 2018. Invading, Leading and Navigating Cells in *Caenorhabditis elegans*: Insights into Cell Movement in Vivo. *Genetics* 208, 53–78. <https://doi.org/10.1534/genetics.117.300082>
- Shi, J., Son, M.-Y., Yamada, S., Szabova, L., Kahan, S., Chrysovergis, K., Wolf, L., Surmak, A., Holmbeck, K., 2008. Membrane-type MMPs enable extracellular matrix permissiveness and mesenchymal cell proliferation during embryogenesis. *Dev. Biol.* 313, 196–209. <https://doi.org/10.1016/j.ydbio.2007.10.017>
- Shields, M.A., Dangi-Garimella, S., Redig, A.J., Munshi, H.G., 2012. Biochemical role of the collagen-rich tumour microenvironment in pancreatic cancer progression. *Biochem. J.* 441, 541–552. <https://doi.org/10.1042/BJ20111240>
- Shih, W., Yamada, S., 2010. Myosin IIA dependent retrograde flow drives 3D cell migration. *Biophys. J.* 98, L29–31. <https://doi.org/10.1016/j.bpj.2010.02.028>
- Shimada, T., Nakamura, H., Ohuchi, E., Fujii, Y., Murakami, Y., Sato, H., Seiki, M., Okada, Y., 1999. Characterization of a truncated recombinant form of human membrane type 3 matrix metalloproteinase. *Eur. J. Biochem.* 262, 907–914.
- Shiomi, T., Lemaître, V., D'Armiento, J., Okada, Y., 2010. Matrix metalloproteinases, a disintegrin and metalloproteinases, and a disintegrin and metalloproteinases with thrombospondin motifs in non-neoplastic diseases. *Pathol. Int.* 60, 477–496. <https://doi.org/10.1111/j.1440-1827.2010.02547.x>
- Shutova, M.S., Svitkina, T.M., 2018. Mammalian nonmuscle myosin II comes in three flavors. *Biochem. Biophys. Res. Commun.* 506, 394–402. <https://doi.org/10.1016/j.bbrc.2018.03.103>

- Sibony-Benyamini, H., Gil-Henn, H., 2012. Invadopodia: the leading force. *Eur. J. Cell Biol.* 91, 896–901. <https://doi.org/10.1016/j.ejcb.2012.04.001>
- Smith-Pearson, P.S., Greuber, E.K., Yogalingam, G., Pendergast, A.M., 2010. Abl kinases are required for invadopodia formation and chemokine-induced invasion. *J. Biol. Chem.* 285, 40201–40211. <https://doi.org/10.1074/jbc.M110.147330>
- Soofi, S.S., Last, J.A., Liliensiek, S.J., Nealey, P.F., Murphy, C.J., 2009. The elastic modulus of Matrigel as determined by atomic force microscopy. *J. Struct. Biol.* 167, 216–219. <https://doi.org/10.1016/j.jsb.2009.05.005>
- Sosa, B.A., Kutay, U., Schwartz, T.U., 2013. Structural insights into LINC complexes. *Current Opinion in Structural Biology, Theory and simulation / Macromolecular assemblies* 23, 285–291. <https://doi.org/10.1016/j.sbi.2013.03.005>
- Sounni, N.E., Dehne, K., van Kempen, L., Egeblad, M., Affara, N.I., Cuevas, I., Wiesen, J., Junankar, S., Korets, L., Lee, J., Shen, J., Morrison, C.J., Overall, C.M., Krane, S.M., Werb, Z., Boudreau, N., Coussens, L.M., 2010. Stromal regulation of vessel stability by MMP14 and TGFbeta. *Dis Model Mech* 3, 317–332. <https://doi.org/10.1242/dmm.003863>
- Spuul, P., Daubon, T., Pitter, B., Alonso, F., Fremaux, I., Kramer, Ij., Montanez, E., Génot, E., 2016. VEGF-A/Notch-Induced Podosomes Proteolyse Basement Membrane Collagen-IV during Retinal Sprouting Angiogenesis. *Cell Rep* 17, 484–500. <https://doi.org/10.1016/j.celrep.2016.09.016>
- Starke, J., Wehrle-Haller, B., Friedl, P., 2014. Plasticity of the actin cytoskeleton in response to extracellular matrix nanostructure and dimensionality. *Biochem. Soc. Trans.* 42, 1356–1366. <https://doi.org/10.1042/BST20140139>
- Starr, D.A., Fridolfsson, H.N., 2010. Interactions between nuclei and the cytoskeleton are mediated by SUN-KASH nuclear-envelope bridges. *Annu. Rev. Cell Dev. Biol.* 26, 421–444. <https://doi.org/10.1146/annurev-cellbio-100109-104037>
- Staudinger, L.A., Spano, S.J., Lee, W., Coelho, N., Rajshankar, D., Bendeck, M.P., Moriarty, T., McCulloch, C.A., 2013. Interactions between the discoidin domain receptor 1 and beta1 integrin regulate attachment to collagen. *Biol Open* 2, 1148–1159. <https://doi.org/10.1242/bio.20135090>
- Stautz, D., Sanjay, A., Hansen, M.T., Albrechtsen, R., Wewer, U.M., Kveiborg, M., 2010. ADAM12 localizes with c-Src to actin-rich structures at the cell periphery and regulates Src kinase activity. *Exp. Cell Res.* 316, 55–67. <https://doi.org/10.1016/j.yexcr.2009.09.017>
- Stautz, D., Wewer, U.M., Kveiborg, M., 2012. Functional analysis of a breast cancer-associated mutation in the intracellular domain of the metalloprotease ADAM12. *PLoS ONE* 7, e37628. <https://doi.org/10.1371/journal.pone.0037628>
- Steffen, A., Le Dez, G., Poincloux, R., Recchi, C., Nassoy, P., Rottner, K., Galli, T., Chavrier, P., 2008. MT1-MMP-dependent invasion is regulated by TI-VAMP/VAMP7. *Curr. Biol.* 18, 926–931. <https://doi.org/10.1016/j.cub.2008.05.044>
- Stehbens, S., Wittmann, T., 2012. Targeting and transport: how microtubules control focal adhesion dynamics. *J. Cell Biol.* 198, 481–489. <https://doi.org/10.1083/jcb.201206050>
- Sternlicht, M.D., Werb, Z., 2001. How matrix metalloproteinases regulate cell behavior. *Annu. Rev. Cell Dev. Biol.* 17, 463–516. <https://doi.org/10.1146/annurev.cellbio.17.1.463>
- Stingl, J., Caldas, C., 2007. Molecular heterogeneity of breast carcinomas and the cancer stem cell hypothesis. *Nat. Rev. Cancer* 7, 791–799. <https://doi.org/10.1038/nrc2212>
- Strongin, A.Y., Collier, I., Bannikov, G., Marmer, B.L., Grant, G.A., Goldberg, G.I., 1995. Mechanism of cell surface activation of 72-kDa type IV collagenase. Isolation of the activated form of the membrane metalloprotease. *J. Biol. Chem.* 270, 5331–5338.
- Strutz, F., Zeisberg, M., Ziyadeh, F.N., Yang, C.-Q., Kalluri, R., Müller, G.A., Neilson, E.G., 2002. Role of basic fibroblast growth factor-2 in epithelial-mesenchymal transformation. *Kidney Int.* 61, 1714–1728. <https://doi.org/10.1046/j.1523-1755.2002.00333.x>
- Stylli, S.S., Stacey, T.T.I., Verhagen, A.M., Xu, S.S., Pass, I., Courtneidge, S.A., Lock, P., 2009. Nck adaptor proteins link Tks5 to invadopodia actin regulation and ECM degradation. *J. Cell. Sci.* 122, 2727–2740. <https://doi.org/10.1242/jcs.046680>
- Suenaga, N., Mori, H., Itoh, Y., Seiki, M., 2005. CD44 binding through the hemopexin-like domain is critical for its shedding by membrane-type 1 matrix metalloproteinase. *Oncogene* 24, 859–868. <https://doi.org/10.1038/sj.onc.1208258>

- Sugiyama, N., Varjosalo, M., Meller, P., Lohi, J., Chan, K.M., Zhou, Z., Alitalo, K., Taipale, J., Keski-Oja, J., Lehti, K., 2010. FGF receptor-4 (FGFR4) polymorphism acts as an activity switch of a membrane type 1 matrix metalloproteinase-FGFR4 complex. *Proc. Natl. Acad. Sci. U.S.A.* 107, 15786–15791. <https://doi.org/10.1073/pnas.0914459107>
- Sun, Z., Guo, S.S., Fässler, R., 2016. Integrin-mediated mechanotransduction. *J. Cell Biol.* 215, 445–456. <https://doi.org/10.1083/jcb.201609037>
- Svitkina, T., 2018. The Actin Cytoskeleton and Actin-Based Motility. *Cold Spring Harb Perspect Biol* 10. <https://doi.org/10.1101/cshperspect.a018267>
- Svitkina, T.M., Borisy, G.G., 1999. Arp2/3 complex and actin depolymerizing factor/cofilin in dendritic organization and treadmilling of actin filament array in lamellipodia. *J. Cell Biol.* 145, 1009–1026.
- Swaminathan, V., Fischer, R.S., Waterman, C.M., 2016. The FAK-Arp2/3 interaction promotes leading edge advance and haptosensing by coupling nascent adhesions to lamellipodia actin. *Mol. Biol. Cell* 27, 1085–1100. <https://doi.org/10.1091/mbc.E15-08-0590>
- Swaminathan, V., Waterman, C.M., 2016. The molecular clutch model for mechanotransduction evolves. *Nat. Cell Biol.* 18, 459–461. <https://doi.org/10.1038/ncb3350>
- Swift, J., Ivanovska, I.L., Buxboim, A., Harada, T., Dingal, P.C.D.P., Pinter, J., Pajeroski, J.D., Spinler, K.R., Shin, J.-W., Tewari, M., Rehfeldt, F., Speicher, D.W., Discher, D.E., 2013. Nuclear lamin-A scales with tissue stiffness and enhances matrix-directed differentiation. *Science* 341, 1240104. <https://doi.org/10.1126/science.1240104>
- Szabova, L., Chrysovergis, K., Yamada, S.S., Holmbeck, K., 2008. MT1-MMP is required for efficient tumor dissemination in experimental metastatic disease. *Oncogene* 27, 3274–3281. <https://doi.org/10.1038/sj.onc.1210982>
- Tabdanov, E.D., Puram, V., Zhovmer, A., Provenzano, P.P., 2018. Microtubule-Actomyosin Mechanical Cooperation during Contact Guidance Sensing. *Cell Rep* 25, 328–338.e5. <https://doi.org/10.1016/j.celrep.2018.09.030>
- Takai, K., Drain, A.P., Lawson, D.A., Littlepage, L.E., Karpuj, M., Kessenbrock, K., Le, A., Inoue, K., Weaver, V.M., Werb, Z., 2018. Discoidin domain receptor 1 (DDR1) ablation promotes tissue fibrosis and hypoxia to induce aggressive basal-like breast cancers. *Genes Dev.* 32, 244–257. <https://doi.org/10.1101/gad.301366.117>
- Tarone, G., Cirillo, D., Giancotti, F.G., Comoglio, P.M., Marchisio, P.C., 1985. Rous sarcoma virus-transformed fibroblasts adhere primarily at discrete protrusions of the ventral membrane called podosomes. *Exp. Cell Res.* 159, 141–157.
- Tatti, O., Vehviläinen, P., Lehti, K., Keski-Oja, J., 2008. MT1-MMP releases latent TGF-beta1 from endothelial cell extracellular matrix via proteolytic processing of LTBP-1. *Exp. Cell Res.* 314, 2501–2514. <https://doi.org/10.1016/j.yexcr.2008.05.018>
- Teschendorff, A.E., Caldas, C., 2009. The breast cancer somatic “muta-ome”: tackling the complexity. *Breast Cancer Res.* 11, 301. <https://doi.org/10.1186/bcr2236>
- Thiam, H.-R., Vargas, P., Carpi, N., Crespo, C.L., Raab, M., Terriac, E., King, M.C., Jacobelli, J., Alberts, A.S., Stradal, T., Lennon-Dumenil, A.-M., Piel, M., 2016. Perinuclear Arp2/3-driven actin polymerization enables nuclear deformation to facilitate cell migration through complex environments. *Nat Commun* 7. <https://doi.org/10.1038/ncomms10997>
- Thiery, J.P., Acloque, H., Huang, R.Y.J., Nieto, M.A., 2009. Epithelial-mesenchymal transitions in development and disease. *Cell* 139, 871–890. <https://doi.org/10.1016/j.cell.2009.11.007>
- Thomas, D.G., Yenepalli, A., Denais, C.M., Rape, A., Beach, J.R., Wang, Y.-L., Schiemann, W.P., Baskaran, H., Lammerding, J., Egelhoff, T.T., 2015. Non-muscle myosin IIB is critical for nuclear translocation during 3D invasion. *J. Cell Biol.* 210, 583–594. <https://doi.org/10.1083/jcb.201502039>
- Tochowicz, A., Goettig, P., Evans, R., Visse, R., Shitomi, Y., Palmisano, R., Ito, N., Richter, K., Maskos, K., Franke, D., Svergun, D., Nagase, H., Bode, W., Itoh, Y., 2011. The dimer interface of the membrane type 1 matrix metalloproteinase hemopexin domain: crystal structure and biological functions. *J. Biol. Chem.* 286, 7587–7600. <https://doi.org/10.1074/jbc.M110.178434>
- Tojkander, S., Gateva, G., Lappalainen, P., 2012. Actin stress fibers--assembly, dynamics and biological roles. *J. Cell. Sci.* 125, 1855–1864. <https://doi.org/10.1242/jcs.098087>

- Tokui, N., Yoneyama, M.S., Hatakeyama, S., Yamamoto, H., Koie, T., Saitoh, H., Yamaya, K., Funyu, T., Nakamura, T., Ohyama, C., Tsuboi, S., 2014. Extravasation during bladder cancer metastasis requires cortactin-mediated invadopodia formation. *Mol Med Rep* 9, 1142–1146. <https://doi.org/10.3892/mmr.2014.1965>
- Toy, K.A., Valiathan, R.R., Núñez, F., Kidwell, K.M., Gonzalez, M.E., Fridman, R., Kleer, C.G., 2015. Tyrosine kinase discoidin domain receptors DDR1 and DDR2 are coordinately deregulated in triple-negative breast cancer. *Breast Cancer Res. Treat.* 150, 9–18. <https://doi.org/10.1007/s10549-015-3285-7>
- Trichet, L., Le Digabel, J., Hawkins, R.J., Vedula, S.R.K., Gupta, M., Ribault, C., Hersen, P., Voituriez, R., Ladoux, B., 2012. Evidence of a large-scale mechanosensing mechanism for cellular adaptation to substrate stiffness. *Proc. Natl. Acad. Sci. U.S.A.* 109, 6933–6938. <https://doi.org/10.1073/pnas.1117810109>
- Tsai, J.-W., Bremner, K.H., Vallee, R.B., 2007. Dual subcellular roles for LIS1 and dynein in radial neuronal migration in live brain tissue. *Nat. Neurosci.* 10, 970–979. <https://doi.org/10.1038/nn1934>
- Tsai, J.-W., Lian, W.-N., Kemal, S., Kriegstein, A.R., Vallee, R.B., 2010. Kinesin 3 and cytoplasmic dynein mediate interkinetic nuclear migration in neural stem cells. *Nat. Neurosci.* 13, 1463–1471. <https://doi.org/10.1038/nn.2665>
- Tu, C., Ortega-Cava, C.F., Chen, G., Fernandes, N.D., Cavallo-Medved, D., Sloane, B.F., Band, V., Band, H., 2008. Lysosomal cathepsin B participates in the podosome-mediated extracellular matrix degradation and invasion via secreted lysosomes in v-Src fibroblasts. *Cancer Res.* 68, 9147–9156. <https://doi.org/10.1158/0008-5472.CAN-07-5127>
- Turunen, S.P., Tatti-Bugaeva, O., Lehti, K., 2017. Membrane-type matrix metalloproteases as diverse effectors of cancer progression. *Biochim Biophys Acta Mol Cell Res* 1864, 1974–1988. <https://doi.org/10.1016/j.bbamcr.2017.04.002>
- Tzanakakis, G., Kavasi, R.-M., Voudouri, K., Berdiaki, A., Spyridaki, I., Tsatsakis, A., Nikitovic, D., 2018. Role of the extracellular matrix in cancer-associated epithelial to mesenchymal transition phenomenon. *Dev. Dyn.* 247, 368–381. <https://doi.org/10.1002/dvdy.24557>
- Uekita, T., Itoh, Y., Yana, I., Ohno, H., Seiki, M., 2001. Cytoplasmic tail-dependent internalization of membrane-type 1 matrix metalloproteinase is important for its invasion-promoting activity. *J. Cell Biol.* 155, 1345–1356. <https://doi.org/10.1083/jcb.200108112>
- Uematsu, J., Nishizawa, Y., Hirako, Y., Kitamura, K., Usukura, J., Miyata, T., Owaribe, K., 2005. Both type-I hemidesmosomes and adherens-type junctions contribute to the cell-substratum adhesion system in myoepithelial cells. *Eur. J. Cell Biol.* 84, 407–415. <https://doi.org/10.1016/j.ejcb.2005.01.001>
- Unsworth, A., Anderson, R., Britt, K., 2014. Stromal fibroblasts and the immune microenvironment: partners in mammary gland biology and pathology? *J Mammary Gland Biol Neoplasia* 19, 169–182. <https://doi.org/10.1007/s10911-014-9326-8>
- Valcourt, U., Kowanzet, M., Niimi, H., Heldin, C.-H., Moustakas, A., 2005. TGF-beta and the Smad signaling pathway support transcriptomic reprogramming during epithelial-mesenchymal cell transition. *Mol. Biol. Cell* 16, 1987–2002. <https://doi.org/10.1091/mbc.e04-08-0658>
- Valiathan, R.R., Marco, M., Leitinger, B., Kleer, C.G., Fridman, R., 2012. DISCOIDIN DOMAIN RECEPTOR TYROSINE KINASES: NEW PLAYERS IN CANCER PROGRESSION. *Cancer Metastasis Rev* 31, 295–321. <https://doi.org/10.1007/s10555-012-9346-z>
- Van Audenhove, I., Denert, M., Boucherie, C., Pieters, L., Cornelissen, M., Gettemans, J., 2016. Fascin Rigidity and L-plastin Flexibility Cooperate in Cancer Cell Invadopodia and Filopodia. *J. Biol. Chem.* 291, 9148–9160. <https://doi.org/10.1074/jbc.M115.706937>
- van den Dries, K., Bolomini-Vittori, M., Cambi, A., 2014. Spatiotemporal organization and mechanosensory function of podosomes. *Cell Adh Migr* 8, 268–272.
- van den Dries, K., Meddens, M.B.M., de Keijzer, S., Shekhar, S., Subramaniam, V., Figdor, C.G., Cambi, A., 2013. Interplay between myosin IIA-mediated contractility and actin network integrity orchestrates podosome composition and oscillations. *Nat Commun* 4, 1412. <https://doi.org/10.1038/ncomms2402>

- Van Goethem, E., Guiet, R., Balor, S., Charrière, G.M., Poincloux, R., Labrousse, A., Maridonneau-Parini, I., Le Cabec, V., 2011. Macrophage podosomes go 3D. *Eur. J. Cell Biol.* 90, 224–236. <https://doi.org/10.1016/j.ejcb.2010.07.011>
- Van Goethem, E., Poincloux, R., Gauffre, F., Maridonneau-Parini, I., Le Cabec, V., 2010. Matrix architecture dictates three-dimensional migration modes of human macrophages: differential involvement of proteases and podosome-like structures. *J. Immunol.* 184, 1049–1061. <https://doi.org/10.4049/jimmunol.0902223>
- van Helvert, S., Storm, C., Friedl, P., 2018. Mechanoreciprocity in cell migration. *Nat. Cell Biol.* 20, 8–20. <https://doi.org/10.1038/s41556-017-0012-0>
- van Hinsbergh, V.W.M., Engelse, M.A., Quax, P.H.A., 2006. Pericellular proteases in angiogenesis and vasculogenesis. *Arterioscler. Thromb. Vasc. Biol.* 26, 716–728. <https://doi.org/10.1161/01.ATV.0000209518.58252.17>
- Vargas, J.D., Hatch, E.M., Anderson, D.J., Hetzer, M.W., 2012. Transient nuclear envelope rupturing during interphase in human cancer cells. *Nucleus* 3, 88–100. <https://doi.org/10.4161/nucl.18954>
- Vicente-Manzanares, M., Ma, X., Adelstein, R.S., Horwitz, A.R., 2009. Non-muscle myosin II takes centre stage in cell adhesion and migration. *Nat Rev Mol Cell Biol* 10, 778–790. <https://doi.org/10.1038/nrm2786>
- Vicente-Manzanares, M., Zareno, J., Whitmore, L., Choi, C.K., Horwitz, A.F., 2007. Regulation of protrusion, adhesion dynamics, and polarity by myosins IIA and IIB in migrating cells. *J. Cell Biol.* 176, 573–580. <https://doi.org/10.1083/jcb.200612043>
- Vidal-Quadras, M., Holst, M.R., Francis, M.K., Larsson, E., Hachimi, M., Yau, W.-L., Peränen, J., Martín-Belmonte, F., Lundmark, R., 2017. Endocytic turnover of Rab8 controls cell polarization. *J. Cell. Sci.* 130, 1147–1157. <https://doi.org/10.1242/jcs.195420>
- Vignjevic, D., Kojima, S., Aratyn, Y., Danciu, O., Svitkina, T., Borisy, G.G., 2006. Role of fascin in filopodial protrusion. *J. Cell Biol.* 174, 863–875. <https://doi.org/10.1083/jcb.200603013>
- Vinogradova, T., Miller, P.M., Kaverina, I., 2009. Microtubule Network Asymmetry in Motile Cells: Role of Golgi-derived Array. *Cell Cycle* 8, 2168–2174.
- Vizovišek, M., Fonović, M., Turk, B., 2019. Cysteine cathepsins in extracellular matrix remodeling: Extracellular matrix degradation and beyond. *Matrix Biol.* 75–76, 141–159. <https://doi.org/10.1016/j.matbio.2018.01.024>
- Vogel, W., Gish, G.D., Alves, F., Pawson, T., 1997. The discoidin domain receptor tyrosine kinases are activated by collagen. *Mol. Cell* 1, 13–23.
- Vracko, R., Strandness, D.E., 1967. Basal lamina of abdominal skeletal muscle capillaries in diabetics and nondiabetics. *Circulation* 35, 690–700.
- Vuoriluoto, K., Högnäs, G., Meller, P., Lehti, K., Ivaska, J., 2011. Syndecan-1 and -4 differentially regulate oncogenic K-ras dependent cell invasion into collagen through $\alpha 2 \beta 1$ integrin and MT1-MMP. *Matrix Biol.* 30, 207–217. <https://doi.org/10.1016/j.matbio.2011.03.003>
- Walker, C., Mojares, E., Del Río Hernández, A., 2018. Role of Extracellular Matrix in Development and Cancer Progression. *Int J Mol Sci* 19. <https://doi.org/10.3390/ijms19103028>
- Wang, N., Tytell, J.D., Ingber, D.E., 2009. Mechanotransduction at a distance: mechanically coupling the extracellular matrix with the nucleus. *Nat. Rev. Mol. Cell Biol.* 10, 75–82. <https://doi.org/10.1038/nrm2594>
- Watson, C.J., Khaled, W.T., 2008. Mammary development in the embryo and adult: a journey of morphogenesis and commitment. *Development* 135, 995–1003. <https://doi.org/10.1242/dev.005439>
- Weaver, A.M., 2008. Cortactin in tumor invasiveness. *Cancer Lett.* 265, 157–166. <https://doi.org/10.1016/j.canlet.2008.02.066>
- Wellings, S.R., Jensen, H.M., 1973. On the origin and progression of ductal carcinoma in the human breast. *J. Natl. Cancer Inst.* 50, 1111–1118.
- Wiesner, C., Faix, J., Himmel, M., Bentzien, F., Linder, S., 2010. KIF5B and KIF3A/KIF3B kinesins drive MT1-MMP surface exposure, CD44 shedding, and extracellular matrix degradation in primary macrophages. *Blood* 116, 1559–1569. <https://doi.org/10.1182/blood-2009-12-257089>
- Wiesner, C., Le-Cabec, V., El Azzouzi, K., Maridonneau-Parini, I., Linder, S., 2014. Podosomes in space: macrophage migration and matrix degradation in 2D and 3D settings. *Cell Adh Migr* 8, 179–191.

- Wilhelmsen, K., Litjens, S.H.M., Kuikman, I., Tshimbalanga, N., Janssen, H., van den Bout, I., Raymond, K., Sonnenberg, A., 2005. Nesprin-3, a novel outer nuclear membrane protein, associates with the cytoskeletal linker protein plectin. *J. Cell Biol.* 171, 799–810. <https://doi.org/10.1083/jcb.200506083>
- Will, H., Atkinson, S.J., Butler, G.S., Smith, B., Murphy, G., 1996. The soluble catalytic domain of membrane type 1 matrix metalloproteinase cleaves the propeptide of progelatinase A and initiates autoproteolytic activation. Regulation by TIMP-2 and TIMP-3. *J. Biol. Chem.* 271, 17119–17123.
- Williams, K.C., Coppelino, M.G., 2011. Phosphorylation of membrane type 1-matrix metalloproteinase (MT1-MMP) and its vesicle-associated membrane protein 7 (VAMP7)-dependent trafficking facilitate cell invasion and migration. *J. Biol. Chem.* 286, 43405–43416. <https://doi.org/10.1074/jbc.M111.297069>
- Williams, K.C., McNeilly, R.E., Coppelino, M.G., 2014. SNAP23, Syntaxin4, and vesicle-associated membrane protein 7 (VAMP7) mediate trafficking of membrane type 1-matrix metalloproteinase (MT1-MMP) during invadopodium formation and tumor cell invasion. *Mol. Biol. Cell* 25, 2061–2070. <https://doi.org/10.1091/mbc.E13-10-0582>
- Williams, T.M., Medina, F., Badano, I., Hazan, R.B., Hutchinson, J., Muller, W.J., Chopra, N.G., Scherer, P.E., Pestell, R.G., Lisanti, M.P., 2004. Caveolin-1 gene disruption promotes mammary tumorigenesis and dramatically enhances lung metastasis in vivo. Role of Cav-1 in cell invasiveness and matrix metalloproteinase (MMP-2/9) secretion. *J. Biol. Chem.* 279, 51630–51646. <https://doi.org/10.1074/jbc.M409214200>
- Willis, A.L., Sabeh, F., Li, X.-Y., Weiss, S.J., 2013. Extracellular matrix determinants and the regulation of cancer cell invasion stratagems. *J Microsc* 251, 250–260. <https://doi.org/10.1111/jmi.12064>
- Wisdom, K.M., Adebawale, K., Chang, J., Lee, J.Y., Nam, S., Desai, R., Rossen, N.S., Rafat, M., West, R.B., Hodgson, L., Chaudhuri, O., 2018. Matrix mechanical plasticity regulates cancer cell migration through confining microenvironments. *Nat Commun* 9, 4144. <https://doi.org/10.1038/s41467-018-06641-z>
- Wolf, K., Friedl, P., 2011. Extracellular matrix determinants of proteolytic and non-proteolytic cell migration. *Trends in Cell Biology* 21, 736–744. <https://doi.org/10.1016/j.tcb.2011.09.006>
- Wolf, K., Mazo, I., Leung, H., Engelke, K., von Andrian, U.H., Deryugina, E.I., Strongin, A.Y., Bröcker, E.-B., Friedl, P., 2003. Compensation mechanism in tumor cell migration: mesenchymal-amoeboid transition after blocking of pericellular proteolysis. *J. Cell Biol.* 160, 267–277. <https://doi.org/10.1083/jcb.200209006>
- Wolf, K., te Lindert, M., Krause, M., Alexander, S., te Riet, J., Willis, A.L., Hoffman, R.M., Figdor, C.G., Weiss, S.J., Friedl, P., 2013. Physical limits of cell migration: Control by ECM space and nuclear deformation and tuning by proteolysis and traction force. *J Cell Biol* 201, 1069–1084. <https://doi.org/10.1083/jcb.201210152>
- Wolf, K., Wu, Y.I., Liu, Y., Geiger, J., Tam, E., Overall, C., Stack, M.S., Friedl, P., 2007. Multi-step pericellular proteolysis controls the transition from individual to collective cancer cell invasion. *Nat. Cell Biol.* 9, 893–904. <https://doi.org/10.1038/ncb1616>
- Wu, J., Kent, I.A., Shekhar, N., Chancellor, T.J., Mendonca, A., Dickinson, R.B., Lele, T.P., 2014. Actomyosin pulls to advance the nucleus in a migrating tissue cell. *Biophys. J.* 106, 7–15. <https://doi.org/10.1016/j.bpj.2013.11.4489>
- Wu, X., Gan, B., Yoo, Y., Guan, J.-L., 2005. FAK-mediated src phosphorylation of endophilin A2 inhibits endocytosis of MT1-MMP and promotes ECM degradation. *Dev. Cell* 9, 185–196. <https://doi.org/10.1016/j.devcel.2005.06.006>
- Xu, J., Lamouille, S., Derynck, R., 2009. TGF-beta-induced epithelial to mesenchymal transition. *Cell Res.* 19, 156–172. <https://doi.org/10.1038/cr.2009.5>
- Yamaguchi, H., Lorenz, M., Kempiak, S., Sarmiento, C., Coniglio, S., Symons, M., Segall, J., Eddy, R., Miki, H., Takenawa, T., Condeelis, J., 2005. Molecular mechanisms of invadopodium formation: the role of the N-WASP-Arp2/3 complex pathway and cofilin. *J. Cell Biol.* 168, 441–452. <https://doi.org/10.1083/jcb.200407076>
- Yamaguchi, H., Takeo, Y., Yoshida, S., Kouchi, Z., Nakamura, Y., Fukami, K., 2009. Lipid rafts and caveolin-1 are required for invadopodia formation and extracellular matrix degradation by

- human breast cancer cells. *Cancer Res.* 69, 8594–8602. <https://doi.org/10.1158/0008-5472.CAN-09-2305>
- Yamaguchi, H., Yoshida, S., Muroi, E., Yoshida, N., Kawamura, M., Kouchi, Z., Nakamura, Y., Sakai, R., Fukami, K., 2011. Phosphoinositide 3-kinase signaling pathway mediated by p110 α regulates invadopodia formation. *J. Cell Biol.* 193, 1275–1288. <https://doi.org/10.1083/jcb.201009126>
- Yana, I., Weiss, S.J., 2000. Regulation of membrane type-1 matrix metalloproteinase activation by proprotein convertases. *Mol. Biol. Cell* 11, 2387–2401. <https://doi.org/10.1091/mbc.11.7.2387>
- Yang, C., Svitkina, T., 2011. Filopodia initiation: focus on the Arp2/3 complex and formins. *Cell Adh Migr* 5, 402–408. <https://doi.org/10.4161/cam.5.5.16971>
- Yang, H., Guan, L., Li, S., Jiang, Y., Xiong, N., Li, L., Wu, C., Zeng, H., Liu, Y., 2016. Mechanosensitive caveolin-1 activation-induced PI3K/Akt/mTOR signaling pathway promotes breast cancer motility, invadopodia formation and metastasis in vivo. *Oncotarget* 7, 16227–16247. <https://doi.org/10.18632/oncotarget.7583>
- Yang, J., Weinberg, R.A., 2008. Epithelial-mesenchymal transition: at the crossroads of development and tumor metastasis. *Dev. Cell* 14, 818–829. <https://doi.org/10.1016/j.devcel.2008.05.009>
- Yang, N., Mosher, R., Seo, S., Beebe, D., Friedl, A., 2011. Syndecan-1 in breast cancer stroma fibroblasts regulates extracellular matrix fiber organization and carcinoma cell motility. *Am. J. Pathol.* 178, 325–335. <https://doi.org/10.1016/j.ajpath.2010.11.039>
- Yang, Y., Motte, S., Kaufman, L.J., 2010. Pore size variable type I collagen gels and their interaction with glioma cells. *Biomaterials* 31, 5678–5688. <https://doi.org/10.1016/j.biomaterials.2010.03.039>
- Yeh, Y.-C., Wang, C.-Z., Tang, M.-J., 2009. Discoidin domain receptor 1 activation suppresses α 2 β 1 integrin-dependent cell spreading through inhibition of Cdc42 activity. *J. Cell. Physiol.* 218, 146–156. <https://doi.org/10.1002/jcp.21578>
- Yu, J., Lei, K., Zhou, M., Craft, C.M., Xu, G., Xu, T., Zhuang, Y., Xu, R., Han, M., 2011. KASH protein Syne-2/Nesprin-2 and SUN proteins SUN1/2 mediate nuclear migration during mammalian retinal development. *Hum. Mol. Genet.* 20, 1061–1073. <https://doi.org/10.1093/hmg/ddq549>
- Yu, X., Zech, T., McDonald, L., Gonzalez, E.G., Li, A., Macpherson, I., Schwarz, J.P., Spence, H., Futó, K., Timpson, P., Nixon, C., Ma, Y., Anton, I.M., Visegrády, B., Insall, R.H., Oien, K., Blyth, K., Norman, J.C., Machesky, L.M., 2012. N-WASP coordinates the delivery and F-actin-mediated capture of MT1-MMP at invasive pseudopods. *J Cell Biol* 199, 527–544. <https://doi.org/10.1083/jcb.201203025>
- Yurchenco, P.D., 2011. Basement Membranes: Cell Scaffoldings and Signaling Platforms. *Cold Spring Harb Perspect Biol* 3. <https://doi.org/10.1101/cshperspect.a004911>
- Zambonin-Zallone, A., Teti, A., Carano, A., Marchisio, P.C., 1988. The distribution of podosomes in osteoclasts cultured on bone laminae: effect of retinol. *J. Bone Miner. Res.* 3, 517–523. <https://doi.org/10.1002/jbmr.5650030507>
- Zarzyska, J.M., 2014. Two faces of TGF- β 1 in breast cancer. *Mediators Inflamm.* 2014, 141747. <https://doi.org/10.1155/2014/141747>
- Zhang, J., Guo, W.-H., Wang, Y.-L., 2014. Microtubules stabilize cell polarity by localizing rear signals. *Proc. Natl. Acad. Sci. U.S.A.* 111, 16383–16388. <https://doi.org/10.1073/pnas.1410533111>
- Zhang, K., Corsa, C.A., Ponik, S.M., Prior, J.L., Piwnica-Worms, D., Eliceiri, K.W., Keely, P.J., Longmore, G.D., 2013. The collagen receptor discoidin domain receptor 2 stabilizes SNAIL1 to facilitate breast cancer metastasis. *Nat. Cell Biol.* 15, 677–687. <https://doi.org/10.1038/ncb2743>
- Zhang, X., Lei, K., Yuan, X., Wu, X., Zhuang, Y., Xu, T., Xu, R., Han, M., 2009. SUN1/2 and Syne/Nesprin-1/2 Complexes Connect Centrosome to the Nucleus during Neurogenesis and Neuronal Migration in Mice. *Neuron* 64, 173–187. <https://doi.org/10.1016/j.neuron.2009.08.018>
- Zhao, H., Sohail, A., Sun, Q., Shi, Q., Kim, S., Mobashery, S., Fridman, R., 2008. Identification and role of the homodimerization interface of the glycosylphosphatidylinositol-anchored membrane type 6 matrix metalloproteinase (MMP25). *J. Biol. Chem.* 283, 35023–35032. <https://doi.org/10.1074/jbc.M806553200>

- Zhu, J., 2010. Bioactive modification of poly(ethylene glycol) hydrogels for tissue engineering. *Biomaterials* 31, 4639–4656. <https://doi.org/10.1016/j.biomaterials.2010.02.044>
- Zimmermann, J., Brunner, C., Enculescu, M., Goegler, M., Ehrlicher, A., Käs, J., Falcke, M., 2012. Actin filament elasticity and retrograde flow shape the force-velocity relation of motile cells. *Biophys. J.* 102, 287–295. <https://doi.org/10.1016/j.bpj.2011.12.023>
- Zuo, Q.-F., Cao, L.-Y., Yu, T., Gong, L., Wang, L.-N., Zhao, Y.-L., Xiao, B., Zou, Q.-M., 2015. MicroRNA-22 inhibits tumor growth and metastasis in gastric cancer by directly targeting MMP14 and Snail. *Cell Death Dis* 6, e2000. <https://doi.org/10.1038/cddis.2015.297>

Annexe

Nucleus-invadopodia duo during cancer invasion

Robin Ferrari ¹, Elvira Infante ² and Philippe Chavrier ^{1, *}

¹ Institut Curie, PSL Research University, CNRS, UMR 144, 26 rue d'Ulm, F-75005, Paris, France

² Department of Physics, King's College London, WC2R 2LS, London, UK

* Corresponding authors, e-mail: philippe.chavrier@curie.fr

Published in Trends in Cell Biology: February 2019.

Forum

Nucleus–Invadopodia Duo During Cancer Invasion

Robin Ferrari,¹ Elvira Infante,^{1,2} and Philippe Chavrier^{1,*}

Matrix proteolysis mediated by MT1-MMP facilitates the invasive migration of tumor cells in dense tissues, which otherwise get trapped in the matrix because of limited nuclear deformability. A digest-on-demand response has been identified, which requires nucleus–microtubule linkage through the LINC complex and triggers MT1-MMP surface-exposure to facilitate nucleus movement.

Introduction

During their metastatic journey, tumor cells migrate through dense and complex 3D microenvironments within connective tissues. For carcinoma cells deriving from epithelial tumors, dissemination starts by breaching the 0.1–1- μ m thick basement membrane (BM) made of laminins, cross-linked type IV collagen, and proteoglycans that surround epithelial tissues. BM transmigration signals the transition from *in situ* to more aggressive infiltrating carcinomatous lesions; then invasive cells can disseminate, mostly in cohorts, through interstitial tissues consisting of bundles of type I collagen-rich fibrils interspaced with discontinuities. A salient feature of tumor cell invasion in confining environments is that it requires extensive nuclear deformation to squeeze the bulky and stiff nucleus through constricting pores within the tissue matrix [1]. Recent studies, which are detailed in Box 1, revealed that nuclear deformations during constricted migration can lead to nuclear envelope (NE) rupture, with potential

consequences for genome stability and tumor progression [2–5]. In addition, it has been shown that when the pore size of the matrix meshwork is below the deformability of nucleus, then cell movement stops [1]. It is also established that surface-exposed membrane-type (i.e., trans-membrane) matrix metalloproteinases (MT-MMPs) can enlarge the pores in the matrix [1,6]. Altogether, these findings have raised important questions as to whether and how the matrix proteolysis machinery of cancer cells can scale with the level of confinement by the matrix, and what is the influence of nuclear deformation and mechanosensing to this response and to the invasive potential of tumor cells.

Nucleus Pulling and Pushing Schemes Generate Nuclear Deformation During Confined Migration

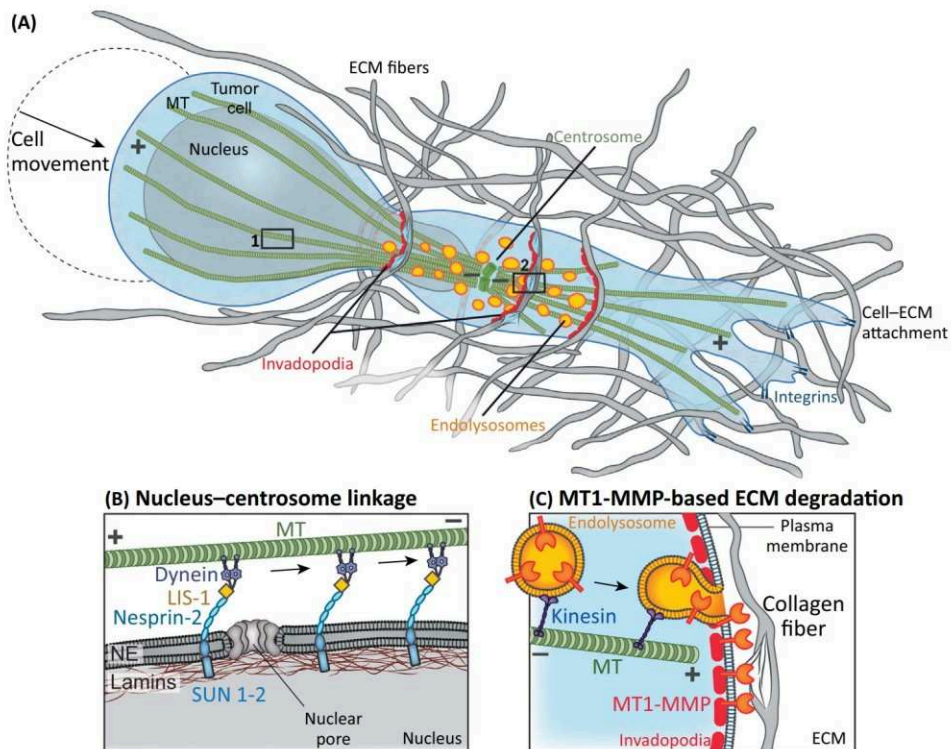
Deformability and mechanical stability of the nucleus depends on nuclear lamina proteins lamin-A and B (LMNA, -B), which form a viscoelastic proteinaceous network underneath the inner nuclear membrane. Nuclear stiffness scales with LMNA levels: LMNA overexpression impedes transmigration by augmenting nuclear rigidity, while reducing LMNA levels increases invasion speed in 3D reconstituted matrix [1,2,7]. Thus, nuclear stiffness and limited nuclear deformability have been identified as restrictive factors

that impede cell migration in confined environments [1,2]. Interestingly, a gradient of LMNA expression, decreasing from the core to the invasive front of tumor xenografts, has been reported and LMNA-deficient tumors have a growth advantage [2,5]. The downside is that nuclear resistance to mechanical insults drops with LMNA deficiency and repeated passages across constrictions can lead to cell death as a failure to repair consequent NE rupture and DNA damage [2–5] (Box 1).

Nuclear deformation reflects the pulling and pushing schemes by tumor cells to move their nucleus across constrictions. As during cell migration in 2D, integrin-based adhesion to surrounding collagen fibers and actomyosin-based contractility produce traction forces that can propel the nucleus forward through constraining spaces ([8] and references herein). Additionally, pulling forces can result from dynein and kinesin molecular motors attached to the nuclear surface and moving the nucleus along the microtubule network [9]. Proteins responsible for nucleocytoskeleton attachment and motor association to the surface of the nucleus belong to the linker of nucleoskeleton and cytoskeleton (LINC) complex. This complex consists in SUN and nesprin proteins, which span the inner and outer nuclear membrane, respectively, and interact through SUN domain

Box 1. Mechanical Stress on the Nucleus in Cancer

Cells are submitted to compressive forces during physiological and disease conditions. Tumor growth can generate compressive forces due to overgrowth and confinement by the tissue environment. In addition, cancer cells are submitted to elastic deformations of the cell body and bulky nucleus as they invade across interstitial spaces during metastatic spread [6]. Recent studies reported that extensive nuclear deformation could result in local NE rupture, which can be rapidly repaired [3,4]. Leakage of nuclear DNA repair factors, as well as transient exposure of nuclear DNA to cytoplasmic nucleases such as three-prime repair exonuclease (TREX)1, can lead to DNA damage and double-strand breaks, as indicated by appearance of foci of DNA damage repair marker γ -H2AX [3,4,15]. Sensitivity of tumor cells to mechanical nuclear stress somehow scales with LMNA levels. Genomic analysis of cancer cell lines following repeated cycles of migration through small microfabricated rigid pores revealed that NE rupture can lead to genomic alterations and chromosomal copy-number changes [15]. Altogether, repetitive nuclear rupture could contribute to cancer progression by favoring genomic instability and chromosomal rearrangements, an idea that remains to be experimentally tested.



Trends in Cell Biology

Figure 1. Model of Invadopodia-, MT1-MMP-Based Matrix Digest-on-Demand Response Triggered upon Nucleus Confinement During Cancer Invasion. (A) Confined migration of tumor cells through the dense 3D collagen network results in nucleus confinement by constricting collagen fibrils. Nucleus-microtubule/centrosome linkage and nucleus pulling is mediated by LINC complex interacting with dynein-Lis1 molecular motor. Cortical anchoring of microtubules is required for centrosome and MT1-MMP-positive endosome positioning and for targeted delivery of MT1-MMP to invadopodia. Nucleus movement is facilitated by localized invadopodia-based pericellular proteolysis of confining fibrils ahead of the nucleus. (B) Scheme of nucleus-cytoskeletal linkage through LINC complex components nesprin and SUN in association with lamins. Lis1 in complex with dynein associates to the NE depending on Nesprin-2 and is involved in nucleus-microtubule linkage and nucleus pulling (adapted from [7]). (C) Model of polarized surface-delivery of MT1-MMP from recycling endolysosomes (adapted from [11]). ECM, Extracellular matrix; LINC, linker of nucleoskeleton and cytoskeleton; MT, microtubule; NE, nuclear envelope.

and the carboxy-terminal Klarsicht, ANC-1, Syne Homology (KASH) domain of nesprins in the intermembrane space. Nesprin-2 was reported to be required for recruitment of LIS1, a regulatory protein of dynein motor function, to the cytoplasmic face of the nucleus in invasive MDA-MB-231 breast tumor cells [7]. In humans, LIS1 deficiency leads to lissencephaly (smooth brain) due to severe cortical neuron migration and positioning defects caused by impaired dynein-dependent nucleokinesis. It was recently found that LINC complex and LIS1 mediate nucleo-centrosome linkage and

centrosome positioning ahead of the nucleus [7]. These observations suggest that Nesprin-2 and LIS1 contribute to pulling forces exerted on the nucleus by dynein moving along microtubules to support nucleus movement through confining environments, generating nuclear deformation (Figure 1).

Invadopodia Mediate MT1-MMP-Based Matrix Degradation by Cancer Cells

Membrane-anchored MT1-MMP (aka MMP14) is the sword arm of the collagenolytic program of carcinoma cells.

Using the intraductal mammary gland xenograft model, it was reported that silencing of MT1-MMP impairs the ability of ductal carcinoma in *in situ* tumor xenografts to progress into infiltrating lesions, providing validation for the prominence of MT1-MMP for BM transmigration by breast cancer cells *in vivo* [10]. MT1-MMP has also been implicated in invasive migration of mesenchymal cells through the fibrous interstitial type I collagen network, in the infiltration of vascular and lymphatic compartments, and in extravasation during metastasis. Inhibition of MT1-MMP function can evoke

protease-independent programs of cancer cells, which can switch to contractility-driven ameboid movement or use the nucleus as a piston to propel the cell ahead [6,8]. Moreover, in support of a major role during cancer dissemination, MT1-MMP is linked to malignancy of multiple tumor types, including lung, gastric, colon, breast, and cervical carcinomas, gliomas, and melanomas. MT1-MMP is accumulated and spatially restricted to invadopodia that correspond to actin-based plasmalemmal subdomains, which combine membrane protrusive and matrix proteolytic functions to promote cancer cell invasion and metastasis [11]. Invadopodia form dynamically in association with constricting matrix fibers and can vary in shape and possibly in composition, depending on extracellular matrix (ECM) topology and components [12].

Nuclear Confinement Triggers Polarized MT1-MMP/Invadopodia-Based Matrix Degradation Ahead of the Nucleus

Contrasting with gel-like pseudopodial protrusions that can squeeze through narrow pores between matrix fibers, the nucleus has limited deformability (experimentally estimated to be ~10% of original nuclear cross section) [1]. When nuclear deformability limit is reached, cell migration physically stops as the nucleus becomes entrapped in the fibrous matrix network [1,7]. It is well established that pericellular collagenolysis by MMPs can modulate restricting environmental conditions by widening ECM pores [1]. Recent studies demonstrated that MMP inhibition during confined migration of tumor cells in dense collagen environment leads to increased nuclear deformation and mechanical rupture of the NE [1,3]. However, how mechanical input from the ECM microenvironment triggers the invadopodial response is unknown and of paramount importance in light of data

showing that the biomechanical properties of the microenvironment have major impact on cancer progression [13].

Recent work in breast cancer cells revealed that surface exposure of MT1-MMP and pericellular collagenolysis are adaptive responses, which are switched off under low nucleus confinement, while decreased matrix pore size or increased nuclear stiffness trigger the collagenolytic program [7]. MT1-MMP is known to recycle from endolysosomal compartments to invadopodia in metastatic breast cancer cells [11]. It was found that MT1-MMP-storage endolysosomal compartments distribute ahead of the nucleus with a centrosome-centered polarization optimal to fuel MT1-MMP delivery to invadopodia forming at the nuclear anterior zone (Figure 1C) [7]. The polarization of MT1-MMP-secretory compartments and the assembly of functional invadopodia require integrity of nucleo-microtubule linkage, depending on the LINC complex and LIS1 functionality (Figure 1B) [7]. Thus, a working model is that tension generated by dynein motor, along the microtubule network through NE and cell cortex anchoring, pulls the nucleus forward for movement; extra tension on trapped nucleus through constricting ECM fibrils triggers formation of proteolytically active invadopodia and dissolution of the confining fibrils to open the way for nucleus migration during confined invasion of tumor cells (Figure 1).

This model raises several questions. One question is how migrating cells negotiating changing environments recognize nucleus-constricting fibers and degrade them, while ECM fibrils involved in integrin-based adhesion and cell movement at the cell front are spared from degradation? One possible mechanism for segregation of specialized degradation and adhesion contact zones is that distinct collagenic receptors selectively

trigger assembly of peripheral focal adhesions to mediate traction force generation, and invadopodia, ahead of the nucleus. While beta1 and -3 integrin receptors are classically involved in cell-collagen adhesion, receptors mediating invadopodia formation in association with collagen fibers remain poorly defined and need to be identified. Another conundrum is how mechanical constraints on the nucleus can trigger invadopodia formation and MT1-MMP delivery. As tumor cells have constantly to adapt to changes in the matrix environment, these responses have to happen on a fast time-scale, too fast for genetic regulation. Several studies revealed the ability of the nucleus to sense and respond to forces supporting the emerging concept of nuclear mechanotransduction [14]. Nuclear mechanosignaling effectors have been recently identified, including the nuclear membrane protein emerin, which can contribute to nucleo-centrosome linkage and mediates the response to tensional force applied to the nucleus in relation with LINC complex and LMNA function [14]. Therefore, a possible mechanism to be further explored is that nuclear tension and mechanosignaling can control the recycling machinery ensuring MT1-MMP delivery to invadopodia. These observations also highlight the possibility of targeting the machinery linking nuclear tension with MT1-MMP surface delivery as a new therapeutic road to target cancer metastasis.

Acknowledgements

The authors thank Alessia Castagnino and Pedro Monteiro for helpful discussion and Agnieszka Kawska (<http://www.IlluScientia.com>) for artwork. The authors apologize to all investigators whose work could not be cited due to space constraints. This work was supported by grants from Fondation ARC (PGA1-RF20170205408) and Worldwide Cancer Research (Grant 16-1235) to P.C. and by institutional support from Institut Curie and Centre National pour la Recherche Scientifique (CNRS).

¹Institut Curie, PSL Research University, CNRS, UMR 144, 26 rue d'Ulm, F-75005, Paris, France

²Current address: Department of Physics, King's College London, WC2R 2LS, London, UK

*Correspondence: philippe.chavier@curie.fr (P. Chavier).
<https://doi.org/10.1016/j.tcb.2018.11.006>

References

1. Wolf, K. *et al.* (2013) Physical limits of cell migration: control by ECM space and nuclear deformation and tuning by proteolysis and traction force. *J. Cell Biol.* 201, 1069–1084
2. Harada, T. *et al.* (2014) Nuclear lamin stiffness is a barrier to 3D migration, but softness can limit survival. *J. Cell Biol.* 204, 669–682
3. Denais, C.M. *et al.* (2016) Nuclear envelope rupture and repair during cancer cell migration. *Science* 352, 353–358
4. Raab, M. *et al.* (2016) ESCRT III repairs nuclear envelope ruptures during cell migration to limit DNA damage and cell death. *Science* 352, 359–362
5. Bell, E.S. and Lammerding, J. (2016) Causes and consequences of nuclear envelope alterations in tumour progression. *Eur. J. Cell Biol.* 95, 449–464
6. Wolf, K. and Friedl, P. (2011) Extracellular matrix determinants of proteolytic and non-proteolytic cell migration. *Trends Cell Biol.* 21, 736–744
7. Infante, E. *et al.* (2018) LINC complex-Lis1 interplay controls MT1-MMP matrix digest-on-demand response for confined tumor cell migration. *Nat. Commun.* 9, 2443
8. Petrie, R.J. *et al.* (2017) Activating the nuclear piston mechanism of 3D migration in tumor cells. *J. Cell Biol.* 216, 93–100
9. Bone, C.R. and Starr, D.A. (2016) Nuclear migration events throughout development. *J. Cell Sci.* 129, 1951–1961
10. Lodillinsky, C. *et al.* (2016) p63/MT1-MMP axis is required for *in situ* to invasive transition in basal-like breast cancer. *Oncogene* 35, 344–357
11. Castro-Castro, A. *et al.* (2016) Cellular and molecular mechanisms of MT1-MMP-dependent cancer cell invasion. *Annu. Rev. Cell Dev. Biol.* 32, 555–576
12. Artym, V.V. *et al.* (2015) Dense fibrillar collagen is a potent inducer of invadopodia via a specific signaling network. *J. Cell Biol.* 208, 331–350
13. Kai, F. *et al.* (2016) Force matters: biomechanical regulation of cell invasion and migration in disease. *Trends Cell Biol.* 26, 486–497
14. Aureille, J. *et al.* (2017) Mechanotransduction via the nuclear envelope: a distant reflection of the cell surface. *Curr. Opin. Cell Biol.* 44, 59–67
15. Irianto, J. *et al.* (2017) DNA damage follows repair factor depletion and portends genome variation in cancer cells after pore migration. *Curr. Biol.* 27, 210–223

Caractérisation de l'axe invadopodes/MT1-MMP au cours de l'invasion des cellules cancéreuses de sein

Résumé :

La formation de métastases est la principale cause de mortalité associée aux cancers. Les cellules tumorales métastatiques traversent différentes barrières physiques constituées de matrices extracellulaires (MEC), incluant la membrane basale et le collagène fibrillaire de type I. La migration cellulaire dans ces environnements denses est limitée par la rigidité du noyau et peut nécessiter la protéolyse de la MEC par des métalloprotéinases (MMPs), dont la protéase transmembranaire MT1-MMP, au niveau de structures d'actine nommées invadopodes. Les mécanismes d'adaptation aux signaux mécaniques extérieurs mis en jeu par les cellules invasives afin de former des invadopodes et dégrader la matrice restent mal connus. Au cours de mon projet de thèse, j'ai montré que les cellules concentrent MT1-MMP et dégradent la matrice en formant des invadopodes à l'avant du noyau dans le sens de la migration. Cette réponse adaptative dépend de la taille des pores matriciels ainsi que de la rigidité du noyau, suggérant que les cellules sont capables de répondre aux contraintes physiques de l'environnement, via la dégradation « à la demande » des composants de la MEC qui s'opposent au mouvement. Par ailleurs, j'ai montré que la polymérisation d'actine au sein des invadopodes génère des forces de poussée transmises aux fibres de collagène, qui, combinées à la dégradation des fibres par MT1-MMP, permettent l'agrandissement des pores matriciels. L'ensemble de mes travaux a mis en évidence un nouveau mécanisme d'action des invadopodes conjuguant production de forces par l'actine et dégradation de la matrice par MT1-MMP, afin de faciliter l'invasion tumorale.

Mots clés : Cancer, invasion, MT1-MMP, invadopodes, noyau

Characterization of the MT1-MMP/invadopodia axis during breast cancer cell invasion

Abstract :

Tumor invasion and distant metastasis are leading causes of cancer-related death. Cancer invasive program requires tumor cells to transmigrate through the basement membrane and invade through type I fibrous collagen networks, which act as physical barriers opposing cell movement. Cancer cell migration into constricting pores is limited by nuclear stiffness and deformability and necessitates proteolytic remodeling of extracellular matrix (ECM) components by metalloproteinases (MMPs). In particular, membrane-tethered 1 (MT1)-MMP exocytosis in specialized actin-rich structures called invadopodia allows pericellular proteolysis to widen matrix pores and facilitate nuclear transmigration. However, whether and how invasive cells coordinate mechanical cues from the environment with invadopodia formation, localization and function in matrix degradation is unknown. In my PhD work, I showed that confined migration into fibrillar collagen networks triggers polarization of MT1-MMP storage compartments and invadopodia-based pericellular collagenolysis in front of the nucleus. Modulation of either matrix pore size or nuclear stiffness interferes with this adaptive response indicating that invasive cells adapt MT1-MMP-mediated ECM proteolysis to matrix confinement levels in a “digest-on-demand” strategy. I further showed that actin polymerization in invadopodia structures produced forces which are transmitted to and push aside the underlying collagen fibers enabling matrix pore widening. Overall, these findings define a new role for invadopodia as proteolytic contacts that combine actin-driven force production and matrix-cleavage activity to facilitate path clearance for invasion.

Keywords : Cancer, invasion, MT1-MMP, invadopodia, nucleus